Evaluation of reduced oxygen display and storage of watercolours

Jacob Llewellyn Thomas

UCL

The Bartlett School of Graduate Studies

Doctoral Thesis

I, Jacob Llewellyn Thomas confirm that the work presented in this Thesis is my own. Where information has been derived from other sources, I confirm that this has been indicated in the Thesis.

Jacob Llewellyn Thomas

Abstract

Reduced-oxygen display and storage, through the limitation of oxidative processes, can enhance the preservation of works on paper. By limiting photo-oxidative processes, access to objects can be increased, allowing their display at higher light levels and/or for longer periods. Published research indicates that most artists' materials will either benefit from or suffer no detrimental effect from reduced-oxygen environments. However, some colourants have been found to undergo accelerated change in the absence of oxygen. Therefore, evaluation of benefits to heritage objects prior to reduced-oxygen treatment is required.

The Anoxic Frames Project at Tate, of which this Thesis is an outcome, aimed to develop reduced-oxygen framing solutions, test their efficacy, identify materials that undergo accelerated change in a reduced-oxygen environment and develop methods to identify candidate objects for anoxic storage. The scope of my research at Tate and for this Thesis was limited to 19th-century watercolour drawings, with a focus on J.M.W. Turner. My research contributed to several publications, conference papers, posters, reproduction of a 19th-century paper, a prototype reaction cell and was, in part, patented.

This Thesis presents: a literature review of both the behaviour of artists' materials in zero oxygen (anoxia) and of analytical methods; a technical study leading to the reproduction of a paper used by Turner; analytical studies of the photo-reactivity of madder lakes and Prussian blues; the design and testing of a prototype reaction cell for *operando* spectroscopy studies of heritage materials; an outline of the field of heritage degradomics; the application of heritage degradomics with advanced chemometric methods to evaluate the headspace profiles of watercolours aged in both anoxia and room atmosphere. The Thesis concludes with an evaluation of reduced-oxygen treatment, and a proposal of how heritage institutions can both select objects suitable for reduced-oxygen storage and display and implement low-cost reduced-oxygen cassettes in their display practice.

For Joyce

Acknowledgements

There are too many people whom I would like to thank for their good sense, advice, encouragement and assistance, such that I cannot give details about how each has contributed in a larger or smaller way to the completion of my PhD. What I have done is listed them by alphabetical order (first names only). The persons on this list know what they have done to help me, and they know that I am grateful. That is enough.

Anna, Bronwyn, Charlotte, Danijela, Dave, Elina, Helen, Henry, Irena, Jana, John, Joyce, Julia, Kevin, Leslie, Linda, Louise, Manca, Matija, Max née Deborah, May, Monse, Nick, Nikos, Paper Conservation, the Pauls, Piers, Rachel, Sam, Sarah, Stephen, Sven, Tim, Tim, Tom, Tomasz, Valentine and Will

Some people need to be mentioned again, but with more details.

I would like to thank: *Matija Strlič*, my PhD supervisor at UCL, *May Cassar*, my subsidiary PhD supervisor at UCL, and *Joyce H. Townsend*, my line manager at Tate; without your guidance and patience this PhD would never have come to be.

I must also acknowledge the work of several interns who worked on the Anoxic Frames Project (AFP) at Tate: *Charlotte Caspers, Monse Pis Marcos, Anna Brookes* and *Sarah Styler*. Without Charlotte's expertise in historically informed reconstructions and her willingness to grind pigments and prepare paint outs, my sample set would never have been feasible. Under Charlotte's guidance Monse and Anna helped in the preparation of some of the watercolour paints used in this research. Sarah conducted ATR-FTIR measurements of the pigment library collected as part of the AFP.

I would like to acknowledge *COST Action D42, EnviART* for supporting my short term scientific mission (STSM) to the University of Ljubljana. I would like to thank *Irena Cigić Kralj* for hosting my STSM and *Manca Mozetic* and *Danijela Pucko Mencigar* at the University of Ljubljana for conducting the viscometry measurements for me.

I would like to acknowledge the *Department for Business, Innovation & Skills* (BIS) for funding this research through their *Public Sector Research Exploitation Fund* (PSRE) grant system.

To finish, I would like to thank *Maud* and *Æthel*, respectively my wife and baby daughter. Maud's support and Æthel's eminent and subsequent birth have kept my nose to the grind stone.

Table of Contents

Table of Figures

Chapter 1 A Review of Anoxia

1.1 Introduction

Oxygen-free (anoxic) storage and display have been proposed as a means to limit display-associated damage of an object. Empirical experiments at Tate demonstrated the potential of anoxia by generating visually clearly distinguishable samples photodegraded in anoxia and in room atmosphere, Figure 1. This early experiment demonstrated the potential for anoxic display in limiting light degradation of sensitive materials found in contemporary art and served as part of the pilot study used in the pursuit of further research funding (1). The results indicate that anoxic display could be used to extend display time and significantly increase light levels with little to no effect on the visual impact of light sensitive objects such as works of art on paper (WOP).[1]
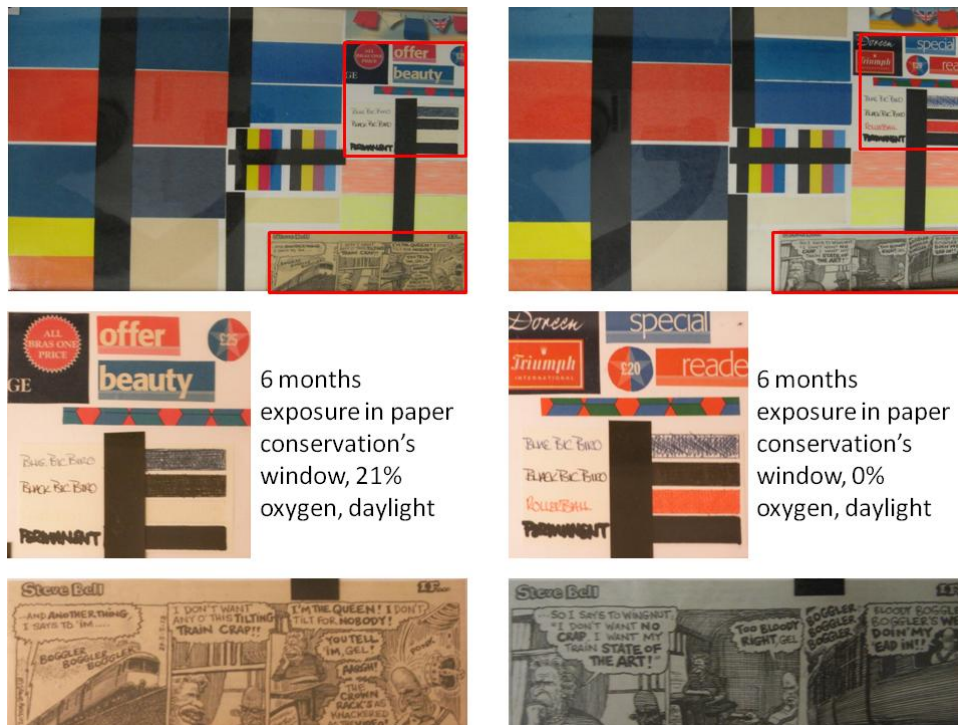
Figure 1 Two collages (with excerpted details) of light-sensitive materials prepared by member of the Tate Paper Conservation Section. Both were exposed in the paper conservation studio's windows for six months. The collage on the left was exposed in room atmosphere, while the collage on the right was exposed in an early anoxic frame prepared from Perspex and Escal adhered with Beva adhesive. Anoxia was established using Ageless RPK and confirmed with an Ageless Eye.

---

[1] The acronym WOP is in common usage at Tate and other heritage institutions in the UK. I am well aware of the other usage of the same acronym, but I decided it better to comply with Tate's usage than create a new acronym for works of art on paper.

These results generated significant interest within Tate and other heritage institutions; however, the technique has not been widely adopted for the display of heritage objects. This reticence stems from the fact that anoxic display, while benefiting most colourants (2, 3), has a negative impact on some artists' pigments, particularly Prussian blue (4-7), raising a spectre of unforeseeable complications and catastrophic outcomes with the adoption of a new display method, and it has resulted in a "wait and see" attitude at most institutions. It seems that institutions were waiting for the following questions to be answered:

1. Is anoxic display and storage safe?
2. How do I determine if an object should go into anoxic display/storage?
3. What are the effects (beneficial and detrimental) of anoxic display and storage?
4. How should anoxic framing be implemented?
5. Once implemented, how can one monitor the condition of an object in anoxic display/storage?

The Anoxic Frames Project (AFP) at Tate aimed to address these questions and to develop a marketable anoxic framing solution for WOP and other heritage objects that are sensitive to photo-oxidation. My research for this Thesis was a significant portion of the AFP, and as such it was targeted to address the project's research questions and goals. I was given much latitude in how I chose to address the projects' questions, and this allowed me to develop concepts and prototype reaction cells that were not anticipated at the time that the AFP project proposal was written. My roles within the AFP through this Thesis research were as follows:

- To conduct a literature review to begin to address question 1. A full version of this review has been accepted for publication in *Studies in Conservation* (3), and a condensed version is presented in Chapter 1.

- Chemiluminometry (CL), Chapter 5 and published in *Polymer Degradation and Stability* (8); viscometry, Chapter 5; x-ray absorption spectroscopy (XAS), Chapter 6; and headspace-gas chromatography-mass spectrometry (HS-GC-MS) with multivariate analysis, Chapter 7, were used to gain a better understanding of the degradation pathways of the pigment/binding media/paper substrate system and to address question 1 and question 3. A by-product of this work was the development of the concept of heritage degradomics which has been introduced in *Analytical Chemistry (9).*

- To further develop the anoxic frame design and oxygen monitoring method to address question 4 and elements of question 5, Chapter 9.

- To develop an *operando* reaction cell termed 'Heritage Degradomics Reactor' (HDR) that can be used to conduct complex accelerated degradation experiments with control of light, temperature and atmosphere and monitoring with UV-Vis-NIR spectroscopy and gas phase analysis, Chapter 8. The HDR can be used to evaluate the degradation of materials as well as heritage objects under modified atmospheres, and as such address question 2.

- And to develop a method that can be used to evaluate and monitor the condition of an object in a modified atmosphere using HS-GC-MS Chapter 7.

1.1.1 Evaluation of Modified Atmospheres[2]

One of the goals of the Anoxic Frames Project (AFP) at Tate was to develop methods that could be used to evaluate the effect of modified atmosphere display and storage on WOP, but the benefits received by a particular object are subtle and difficult to translate into a simple expression of "lifetime extension". This is due to the fact that the different elements of a WOP benefit to different extents and thus the overall degradation of a WOP in modified atmosphere will qualitatively proceed differently than from the same WOP in ambient atmosphere.

Because the visual impact is arguably the most important factor with respect to a WOP, and the fading of colourants results in the most easily distinguishable change in the visual impact of a WOP, evaluation of the light fastness of applied colourants under modified atmospheres has been the focus of much research (3) that demonstrates that oxygen-free display and storage limits the fading of many colourants, but some colourants have been found to fade at the same rate or even faster in anoxia, see Section 1.3, for a review on this topic. However, standard light fastness testing methods require large samples, and are therefore not applicable to WOP. To circumvent this limitation, micro-fadeometry was developed by Whitmore as a means to micro-destructively evaluate the light fastness of colourants in a WOP (10). This technique was successfully used to evaluate the effect of anoxia on heritage objects, and is the focus of the PhD Thesis of Andrew Lerwill (11). While further research is needed, it seems that the micro-fadeometry results generally agree with the previously published results of bulk fading work, and therefore the method can be used with some confidence to evaluate the effect of modified atmospheres on heritage objects.

The degradation of the paper substrate must also be considered because it can lead to changes in visual impact and long-term stability of a WOP. Research by Major (12) and later Arney (13-15) has shown that during thermal-degradation experiments the rate of degradation of paper is reduced for samples in nitrogen indicating a reduction in autoxidation processes. Later work has shown that irradiation of samples of paper with and without colourants in an oxygen-free environment led to a reduced production of peroxides and subsequent loss of degree of polymerisation (DP) of the paper substrate (8, 16-18), thus demonstrating that anoxia has the potential to limit photo-oxidation of paper as well, see the Section 1.3, for a review on this topic. What is missing is a means to non- or micro-destructively evaluate the effect of anoxia on the paper

---

[2] N.B. The term 'modified atmosphere' is widely used in the food and pharmaceutical packaging industry. It is applied to any atmosphere that has been purposefully changed within an enclosure (blister pack, bottle, bag, carton, shipping container, etc. to enhance the preservation/stability of the product contained therein. As such it can be applied to a variety of variables: relative humidity (RH), oxygen concentration, introduction, reduction and/or exclusion of a specific gases or gas blends (e.g. ethylene). In terms of this research it is used to refer solely to oxygen concentration as efforts were made to keep the RH levels constant between sample types.

substrate of a WOP. Measurement of the DP of a WOP before and after display could be used, but viscometry, the standard method, requires a large sample of paper (19, 20), and even size exclusion chromatography (SEC) still requires micro-sampling (21, 22). Therefore these methods cannot be applied to a WOP. Near Infra Red (NIR) spectroscopic methods have been developed to evaluate the condition of many types of paper found in library and archive collections (23-26), but artists papers and the effect of binding media and pigments on the spectra were not included in the training set that was used to construct the models used by the SurveNIR instrument, therefore, this method, though non-destructive is not usable until models are developed for WOP.

But even when aesthetic merits are excluded a WOP is more than a sum of its parts. They are composite materials. Each component (paper substrate, binding medium, colourant etc.) has a particular reactivity, and, in addition to exogenous factors (light, heat, pollution, and oxygen concentration) the endogenous degradation products of each component (as well as the components themselves) have the potential to affect the degradation of every other component. Therefore, WOP are best thought of as a dynamic system that can be influenced, rather than static objects that can be put into stasis. By changing a parameter, *i.e.* oxygen concentration, the system is influenced and this can in turn result in changes to the rates of change of materials in the WOP, however the changes will vary from material to material thus resulting in differential change of the object's appearance or visual impact.[3]

Figure 2 *Duniquoich Hill, with Inveraray Castle and Loch Fyne; Figures on the Shore and in Boat*, **J.M.W. Turner, Tate, D03635, circa 1801-1810 © Tate 2011. This painting is one of a series that show extensive access-associated damage due to display in standard atmosphere. The arrows indicated sections where the indigo blue of the sky and water is totally lost except where protected by the passepartout.**

---

[3] It must be noted here that differential change occurs during standard museum practice; that is some colourants in a WOP fade faster than other colourants resulting in the loss of a colour. This loss is accepted because it lies upon the "normal" degradation vector of the object. If anoxia is applied the object will continue to change but it will be on a different vector than that which is known to be the "normal" ageing of an object resulting in a new differential change to the object's appearance.

The situation is perhaps best exemplified by the watercolour drawing *Duniquoich Hill, with Inveraray Castle and Loch Fyne; Figures on the Shore and in Boat*, J.M.W. Turner, Tate, D03635, Figure 2. In this watercolour drawing the sky and water were rendered in indigo and Prussian blue respectively. In the image the extent of the light damage is readily apparent. Since the object entered the national collection, display in normal atmosphere has resulted in the total loss of the indigo except where it was covered by the passepartout, however the darker blues of the shadows rendered in inorganic blues have remained unchanged.

Hypothetically, if the object were displayed under the same light conditions but in an anoxic frame, then the indigo would have been saved and, if not allowed to revert, the Prussian blue would have slightly faded. The fading and loss of organic colourants, which in this case represent a significant proportion of the painting, are seen as regrettable but normal occurrence, but the (temporary and effectively totally reversible) fading of Prussian blue, which is used sparingly in this and many paintings, is often considered to be impermissible damage because it deviates from the patterns of normal ageing imprinted in our minds.[4] Overcoming this imprinted pattern is as much part of evaluation of the effect of anoxic framing, as is understanding of the chemistry behind the changes themselves.

1.2 A Brief Review of Paper Degradation

Before reviewing anoxic research and the effect of anoxia on WOP a brief and very general review of paper degradation is presented here. For a more comprehensive review of carbohydrate chemistry, readers are directed to Sinnott's excellent *Carbohydrate Chemistry and Biochemistry* (27), and for a heritage science-focused review of paper degradation please see *Ageing and Stabilisation of Paper* (28).

Paper degradation is a complex system of competing reactions, and the exact mechanism for a unique object cannot be defined (29). However, in museums the reaction pathways can broadly be defined as hydrolytic, biodegradative and (photo) oxidative. Which reaction type(s) dominate the degradation system depends on a multitude of exogenous and endogenous factors as outlined in Schematic 1 (30, 31).

---

[4] I have not conducted a controlled survey of museum professionals, but this statement is based on my 6 years of experience working on projects related to the anoxic display of WOPs within heritage institutions in the UK and Poland. However, I have spent many hours in meetings and discussions with curators and conservators regarding this issue, and this point always comes up when I propose to put an object from the collection into anoxic display.
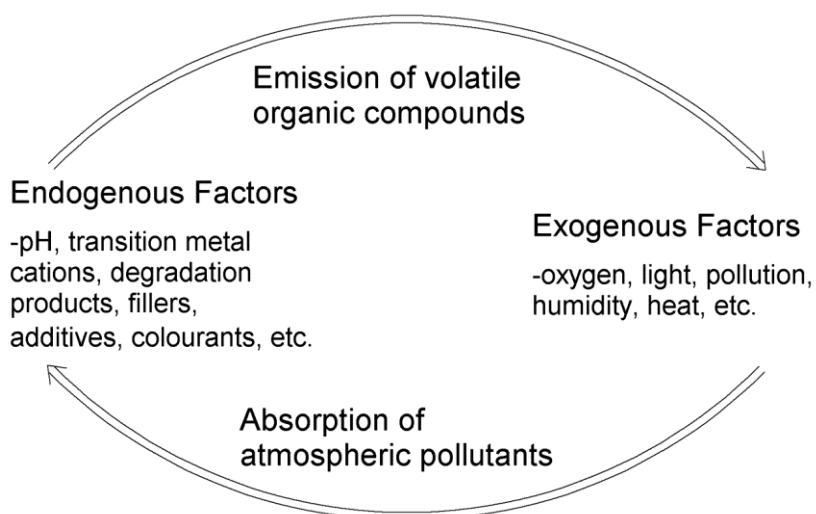
Schematic 1 Interrelation of endogenous and exogenous factors leading to the degradation of a WOP.

1.2.1 Hydrolysis

In an acidic environment hydrolysis occurs when a hydronium ion reacts with the glycosidic oxygen making the bond unstable leading to the breaking of the glycosidic bond between monomer units. This yields two smaller macromolecular units and leads to loss of the degree of polymerisation of the macromolecular matrix, Schematic 2.
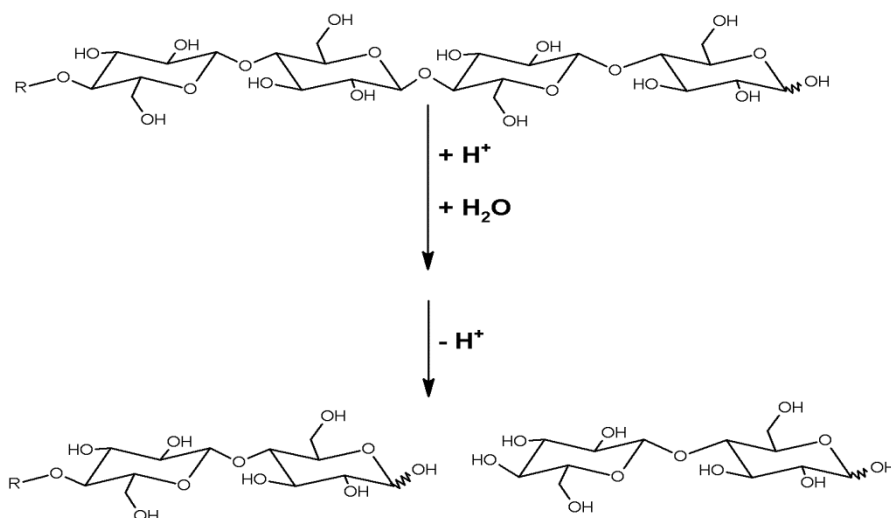
Schematic 2 Acid catalysed hydrolysis of cellulose.

Hydrolysis will not be discussed in this review except in regard to the autocatalytic link between acids produced during oxidation and hydrolysis in an enclosed environment (32-34). For an in-depth review of hydrolysis of cellulose see (35).

1.2.2 Biodegradation

Biodegradation of cellulose requires the presence of a living organism. Typically the degradation is mechanical in the case of higher organisms such as insects, or enzyme-mediated hydrolytic in the case of micro-organisms such as fungi and bacteria. The effect of anoxia on biodegradation will be discussed below.

1.2.3 Photodegradation and Autoxidation

Direct photolysis of cellulose can be ignored in a museum setting as it requires wavelengths shorter than 280-310 nm (16).

Oxidation of paper is a complex process with pathways and end-products influenced by pre-oxidised functionalities on the cellulosic structure, presence of metal ions and pH of the system (31, 36, 37). With regard to the mechanism of oxidation, molecular oxygen is a non-specific oxidant, and autoxidation of various species in paper by molecular oxygen proceeds through radical pathways (38-40). The Bolland-Gee scheme for autoxidation of hydrocarbons can be used to describe the process, Schematic 3. Oxidation is influenced by multiple factors, including: pH, presence of transition metal ions, presence of aldehyde groups, presence of sizing agents and the presence of lignin and other non-cellulosic fractions (39-41).
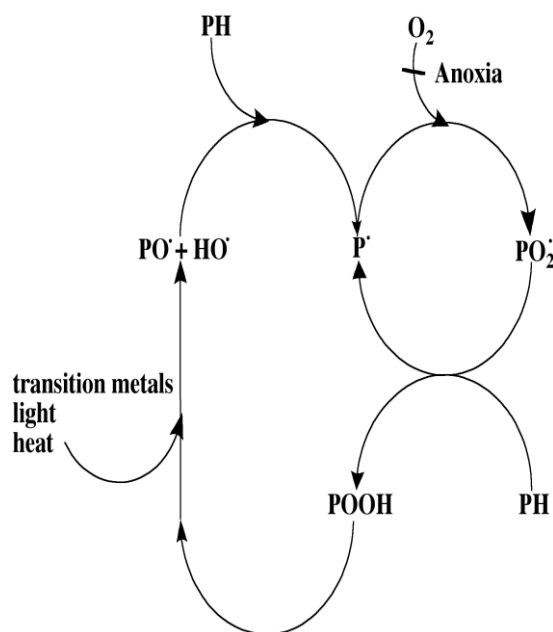
Schematic 3 The Bolland-Gee reaction scheme indicating where anoxia can lead to an interruption in its propagation. In the above schematic, "P" represents polymer, *e.g.* cellulose.

Photo-oxidation of lignocellulosic material can proceed through many different pathways, radical and otherwise. Near-UV and visible light can also initiate photo-oxidation of hemicelluloses, lignin and amorphous regions of cellulose, or cause oxidation of various species through photosensitizing intermediaries such as dyes or transition metal ions, which might be adsorbed on the cellulose fibre or

applied as pigments, or triplet photosensitisers such as titanium dioxide (TiO$_2$) or zinc oxide (ZnO), which can be present as bulking agents, pigments, or residues from deacidification processes (42-46).

$$—CH_2CH_2\overset{*}{C}CH_2CH_2CH_2— \longrightarrow —CH_2CH_2\dot{C} + —CH_2CH_2\dot{C}H_2$$
$$\underset{O}{\|} \qquad\qquad \underset{O}{\|}$$
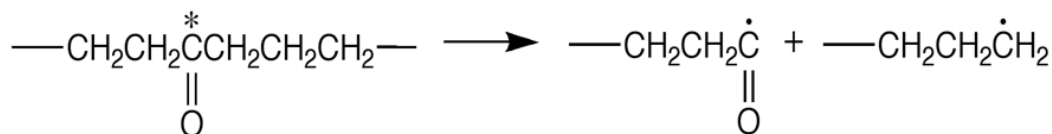
Schematic 4 Norrish type 1 mechanism. The photo-excited (*) triplet state carbonyl decomposes by α-scission into two radicals that can undergo further reactions with the polymer substrate.

$$—CH_2CH_2\overset{*}{C}CH_2CH_2CH_2— \longrightarrow —CH_2CH_2\dot{C}CH_2CH_2\dot{C}H—$$
$$\underset{O}{\|} \qquad\qquad \underset{OH}{|}$$

$$—CH_2CH_2CCH_3 + —C=CH_2$$
$$\underset{O}{\|} \qquad \underset{H}{|}$$
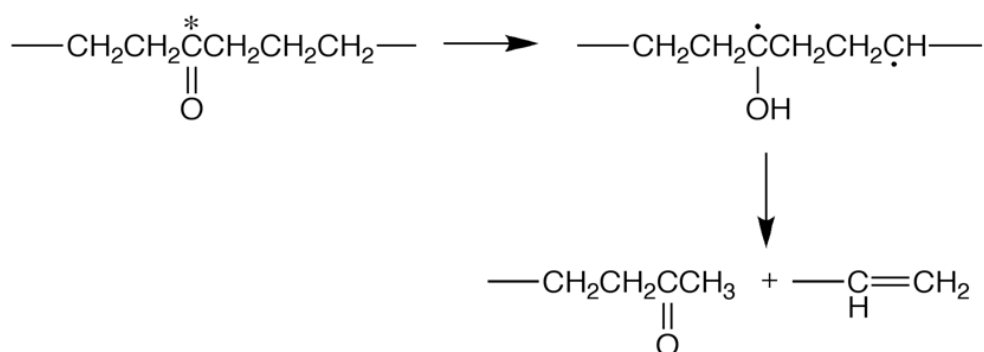
Schematic 5 Norrish type 2 mechanism. The photo-excited (*) triplet state carbonyl decomposes by β-scission into an alkyl ketone and an alkene, potentially leading to colour change and VOC accumulation.

Additionally pre-oxidized functionalities on the cellulose structure and coloured degradation products (47, 48), and chromophores, absorb light in the visible region and through Norrish type reactions, Schematics 4 and 5, which can produce radicals that feed into the Bolland-Gee reaction scheme, or be further oxidized to the carboxyl leukoform and participate in hydrolysis of the cellulose substrate creating an autocatalytic loop, Schematic 6 (32, 49-51).
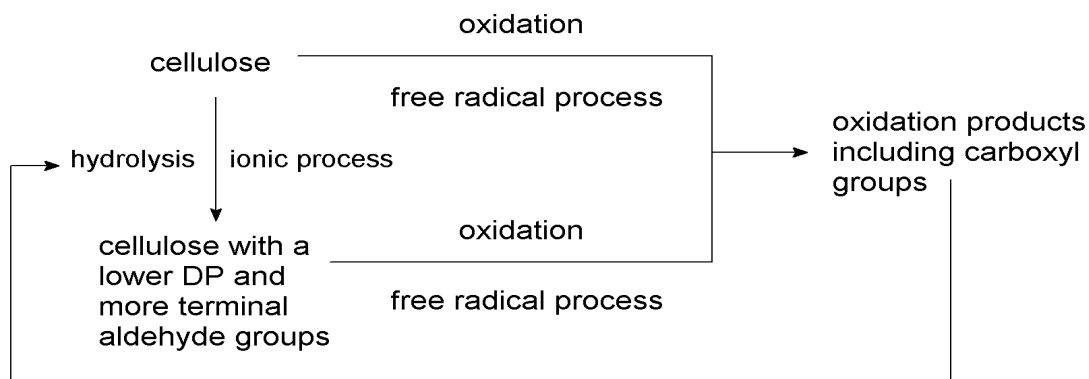
Schematic 6 A simplified schematic indicating the connection between oxidative and hydrolytic degradation of cellulose.

1.3 A Review of Anoxic Research

Strictly speaking anoxia is the total absence of oxygen. In practice, particularly with regard to conservation, anoxia can be treated as an extreme form of hypoxia or low oxygen. Often, anoxia has been assumed in heritage applications, as the actual oxygen concentration in an anoxic enclosure is not measured, or anoxia is defined as the lower detection limit of the method used to measure oxygen concentration. This leads to a certain unknown variability and difficulties in comparing inter-laboratory results. With regard to this review, all conditions stated in the literature as being 'anoxic' will be treated as such.

1.3.1 A Brief History of Anoxia

1.3.1.1 19th Century

The mid-19th century saw the first research into the effect of anoxia on artists' materials. The most frequent citation in English language conservation literature is the Russell and Abney 1888 report on *Action of Light on Watercolours* (52). Despite its age, this report is one of the most thorough with regard to the effect of light source, wavelength dependence of fading, the effect of humidity, pollution, and anoxia (by gas displacement or vacuum) on traditional pigments in gum medium. The key result of the research is a list of pigments used by artists of the period, and their photostability under various conditions. The report's findings can be summarised:

- Most pigments fade by oxidative pathways in the presence of water and are thus protected in anoxia, achieved through vacuum or by dry gas displacement,
- Some pigments exhibit more rapid colour change in vacuum or under moist hydrogen,
- Higher energy photons (near UV through blue) are the most damaging for pigments,
- In colourant mixtures which undergo no chemical interaction, the most fugitive component will fade leaving the stable colour relatively unchanged,
- Most pigments follow the reciprocity rule (53)[5].

In addition to the above-mentioned report several other researchers were active in this period. Chevreul published a memoir on the effect of anoxia on turmeric, annatto, and Prussian blue in 1837 (54); Church published a treatise on the chemistry of paints and painting in 1892; and Richardson presented research to the British Association Meeting in 1888 where he defined two classes of pigments, those that fade by oxidation in the presence of light, air and moisture, and those that fade by reduction independent of air and sometimes moisture (55).

---

[5] The rule of reciprocity in the fading of colourants states that there is a linear relationship between the rate of fading and the intensity of the irradiation; thus a ten-fold increase in light intensity will result in a ten-fold increase in the rate of colour change, or rather it will take 1/10 of the time to induce the same degree of change.

A consequence of the Russell and Abney Report was the filing by W. S. Simpson of the first patent for an anoxic frame (No. 6556-1892) (55). The design relies upon asbestos and putty seals to maintain low vacuum passively, and seems to have had a single application to a painting by J.M.W. Turner at the South Kensington Museum (now the Victoria and Albert Museum, where the painting has remained in the same enclosure since the 1890s) (55). This application is the earliest recorded instance of anoxic framing of an art object.

1.3.1.2 Early to Mid-20th Century

There is little more published anoxic research until the mid-20th century. There are several studies on the light fastness and chemistry of various organic dyes,[6] and a paper about the effect of oxygen and moisture on leather (56), but no further development or applications of anoxic display methods until 1951-52 when the parchment-based American Charters of Freedom were placed in hermetically sealed, humidified, helium-filled cases (57, 58). Whilst not art on paper, the anoxic cases for these objects deserve mention as they served as the state of the art for fifty years. The report published by NBS (now NIST) lucidly outlines the requirements and challenges of any anoxic frame design:

- aesthetics of the design and display,
- method of anoxia,
- humidity levels,
- mounting materials and methods,
- monitoring, light levels,
- seal integrity.

That these cases still contained helium after fifty years of near constant display is a testament to the efficacy of their elegant design (57, 58).

1.3.1.3 Mid to Late 20th Century

The latter half of the 20th century was a period of increased interest in the degradation mechanisms of many materials. Of particular interest are studies into the degradation of paper and colourants under various conditions, with several significant publications comparing accelerated degradation under oxygen-containing and inert atmospheres that serve as the basis for current anoxic research (12-15, 59-63).

In recent decades there has been an increased interest in the heritage sector in the application of hypoxia and anoxia to collections and objects, with several meetings devoted to the subject. Methods adopted from modern food packaging technologies, where modified atmosphere de-infestation, shipping, and storage are now common practice (64), were investigated, exploiting oxygen scavengers and flexible oxygen barrier materials. Though it should be noted that modified atmosphere food packaging is a short-term (days to

---

[6] Browsing any textile or dye related journal from the period (*e.g. Journal of the Society of Dyers and Colourists)* yields numerous examples.

months) application, and modified atmosphere storage and display of heritage objects is a long-term (years to decades) application; as a result the philosophy, aesthetic, and applications differ greatly.

In the late 1980s the use of CO_2 fumigation for pest control was proposed (65). Later research focused on evaluation of modified atmospheres for de-infestation (66), and on the construction of an anoxic display case for an Egyptian mummy (67) and evaluation of the effect of anoxia on biodeterioration of museum objects (68, 69). The Getty Conservation Institute has published two books on the application of anoxia for pest control in museums (67, 70), and a review of anoxic display cases (71). Kenjo researched reduced oxygen atmospheres for pigments used in traditional Japanese paintings and prevent fungal growth (61, 62, 72, 73).

Another application of anoxia is fire prevention by hypoxic, reduced-oxygen, conditions. Nitrogen or pre-mixed hypoxic air is fed into a defined space until the percent oxygen reaches the desired level, typically <16%. Hypoxic storage for library and archive materials has been adopted by several large institutions, for example the British Library's automated low-oxygen storage facility (74). The use of hypoxic venting has also been studied for applications in historic buildings. Historic Scotland and Riksantikvaren, the Norwegian Directorate for Cultural Heritage, commissioned a report on the method in support of the COST Action C17, *Built Heritage: Fire Loss to Historic Buildings* (75).

From the mid-1990s to the present, several patents have been filed for anoxic frames, cases, etc. and companies offering anoxic services to the cultural sector have been established. These patents and services are often marketed as being a universal solution (76)**.** Conservation literature is not so confident about the universal applicability, utility, or safety of anoxic storage and display, and several papers have expressed caution about the effect of anoxia on colourants (2), biodeterioration (77, 78), and auto-catalytic degradation due to encapsulation (32-34).

1.3.2 Anoxia and the Paper Substrate

It has long been established that paper benefits from anoxia by the limitation of oxidation and yellowing due to photodegradation of lignin and (hemi)-cellulose (44, 46, 48, 79, 80),

With regard to oxidation, if one considers the Bolland-Gee scheme, see Schematic 3, then the means of anoxia limiting the degradation of paper is obvious. By eliminating available molecular oxygen, production of reactive oxygen species is limited and the autocatalytic loop broken. This is supported by accelerated degradation studies, which have shown that, unless it is initially acidic, paper retains a greater degree of its fold endurance, yellows less, carboxyl production is limited, and there is a decrease in chemiluminescence intensity under anoxic conditions (81). Early studies by Farquhar *et al* found that when raw cotton cellulose was heated in air and nitrogen to 75-220 °C, there was a decrease in the viscosity of the dissolved samples as well as an increase in carboxyl content, hydroxyl content and weight loss at any given temperature and

time for samples heated in air than in nitrogen (12, 82), Major found similar results with cotton linters in an anhydrous environment (12). In a series of papers, Arney found that the rate of yellowing and strength loss for both cotton rag papers and newsprint varied linearly with oxygen concentration, but did not go to zero in the total absence of oxygen; he concluded that there were competing oxygen-dependent and independent reactions, and that the rates of these reactions were increased by higher moisture content and elevated temperatures independent of pH within a range of pH 4-9 (13-15). The observation by Arney has been further developed by researchers who have proposed the application of mixed-control kinetics to account for the complexity of paper degradation (32, 35, 83), a concept which helps to describe the interconnection between oxidative and hydrolytic reactions in the degradation of paper. This is especially appropriate when considering the degradation of objects within enclosures.

For a work of art on paper, an enclosure can be as simple as using a glazed and backed frame for display, encapsulation, or Solander boxes for storage (84, 85). It is well documented that sealed storage and display systems create a microenvironment and protect objects from exogenous pollution; what must be remembered, especially for hermetically sealed systems, such as a passive anoxic frame, is that the enclosure can also negatively affect the object by trapping endogenous pollutants including volatile organic compounds (VOCs) (9, 86-91), as outlined in Schematic 1. Unless they are scavenged, VOCs can react with all components of the system, directly participating in the degradation of the paper, *e.g.* organic acids (87, 92), acting as photo-initiators *e.g.* carbonyls (16, 49, 50), or participating in a host of other gas and surface reactions resulting in a complex degradation system. Analysis of the atmospheres surrounding samples subjected to accelerated degradation under an inert atmosphere reveals the presence of VOCs. The reaction pathway that led to their production cannot be elucidated, but their presence is indicative of degradation (91). A point that must be remembered is that oxidation is the loss of localised electron density and does not require the presence of molecular oxygen. Under anoxia oxidation can continue via Norrish type mechanisms and/or through rearrangement reactions such as the Nef-Isbell mechanism for alkaline degradation of D-glucose, Schematic 7 (27).

(i) keto-enol tautomerism

(ii) enediol deprotonation

(iii) β-hydroxycarbonyl elimination

(iv) keto-enol tautomerism

(v) benzillic acid rearrangement
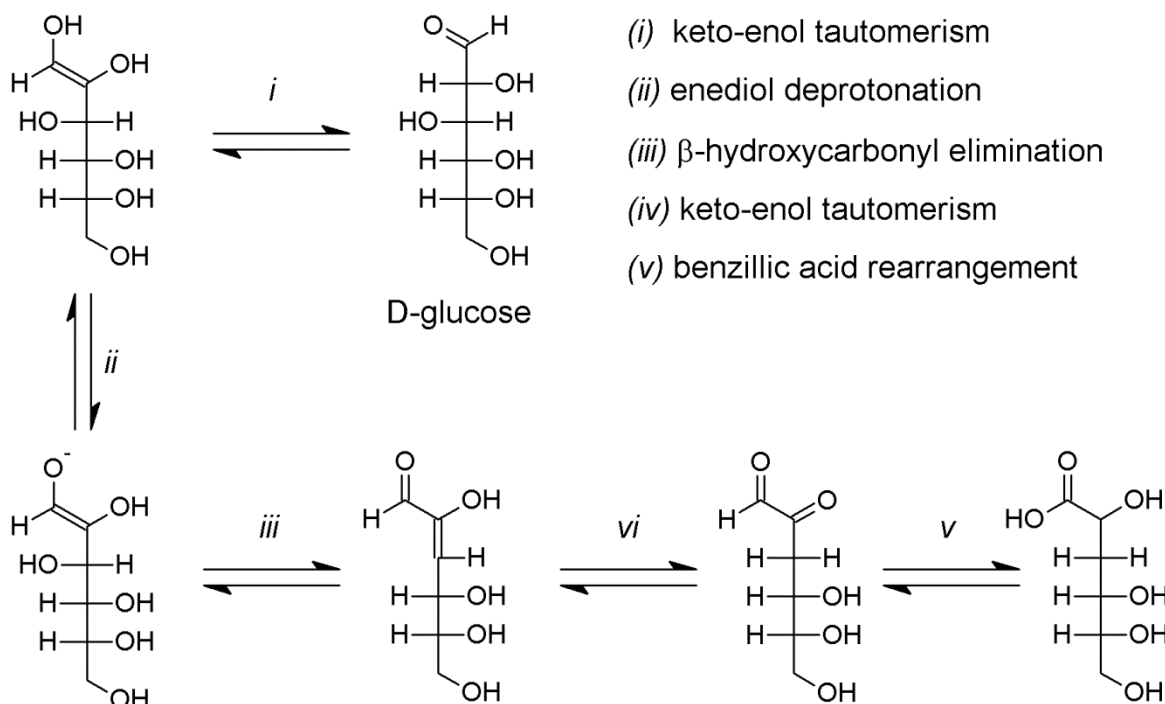
Schematic 7 Nef-Isbell mechanism for the alkaline degradation of D-glucose and alkaline peeling reactions of 1-3 and 1-4 linked polysaccharides. This reaction results in oxidized functionalities and is independent of atmospheric oxygen.

With respect to biodegradation, anoxia has been applied as a de-infestation method for cellulosic materials, and for obligate aerobic organisms it has been shown to be effective (70). However, anaerobic, both obligate and facultative, organisms must be considered with respect to anoxic storage and display. Leschine has reviewed anaerobic degradation of cellulose (93), and Pinzari *et al.* studied the effects of anoxic storage on moulds found on books and paper (77, 78). Of the 14 species studied only 4 are obligate aerobes, the remainder were facultative anaerobes or facultative aerobes with reduced or increased diametric growth respectively under anaerobic conditions. More significant is a priming effect that anaerobic conditions had for fungal colonies when re-introduced to aerobic conditions; this resulted in a change of pigmentation, exudation, sporulation, and increased colony size (78). These results are of particular interest if one considers the occasional opening of an anoxic environment or catastrophic failure of the encasement, and is a good argument for lowering water activity within an anoxic frame to reduce anaerobic growth, and for careful environmental control when opening anoxic frames.

Additionally the method of establishing anoxia must be considered. Kobiakova and Dobrusina found increased degradation of paper after accelerated aging in a high humidity environment under CO_2 when compared to similar conditions in air. The increased degradation can be attributed to acid hydrolysis by carbonic acid formed when the CO_2 is solvated by the water present in the system (94). For this reason, whilst it is inexpensive, CO_2 is not the best choice for anoxia by gas displacement.

1.3.3 Anoxia and Binding Media

There is very little published literature on the effects of anoxia on binding media for paint. However much can be inferred from the behaviour of analogous materials. Presumably binding media will benefit from anoxia as polysaccharides, olefins, resins, fatty acids, proteins, and most synthetic polymers are known to undergo oxidative degradation via a Bolland-Gee-like pathway, Schematic 3. Support for this assumption can be drawn from the common inclusion of antioxidants in contemporary paint formulations, and their positive effect on the permanence of the material (95).

1.3.3.1 Gums

Gum-based media are non-crystalline polysaccharides. They should behave very similarly to hemicelluloses and simpler saccharides, and thus be highly susceptible to oxidation. It can be safely assumed that they will benefit from anoxia. For new watercolours, one point should be considered. As a watercolour ages the gum medium forms cross-links. The absence of cross-links in newer watercolours accounts for their tendency to washout during aqueous treatments. Cross-linking is an oxidative process, and anoxia should limit it. It is not clear whether this should be considered beneficial or not.

1.3.3.2 Proteinaceous Materials

Animal glues and gelatine are derived from collagen in hides, hooves, horns, and bones. Collagen, as well as other proteins, is susceptible to oxidation (96-98), and it has been shown that these materials benefit from storage and display in anoxia (56, 99). Since gelatine and glue are essentially denatured collagen with other associated compounds including lipids, then they should benefit from anoxia (100). This applies for both animal glue as a binding medium and for gelatine as a sizing agent.

1.3.3.3 Oleoresinous Media and Varnishes

Oleoresinous materials both dry and degrade through oxidative pathways. As they dry they interact with oxygen to form a three-dimensional polymer network of cross-linked units, stabilised by metal cations, such as Pb^{2+}, (101). The rate of drying and relative rates of oxidation and hydrolysis during subsequent degradation are highly dependent on the driers, extenders, additives and pigments that are present, which raises concern about putting any given painting with an unknown but certainly complex and locally varied history of degradation into anoxia. The question is how to determine when a painting has completed the drying process but not yet begun to degrade. This is the point where anoxic storage could first be considered, and would be least difficult to assess in chemical terms. Film thickness tends to dominate over other factors that influence the time for drying (102), but oil films on paper tend to be relatively thin, and should dry quickly in comparison to oil-based paint on other supports, which can be quite thick and take decades to dry, fully. It has been proposed in recent decades that an oxygen barrier varnish should be developed to prevent further oxidation of the binding medium. Thomson discussed intentional oxygen starvation in oil paint films and proposed using a polymer as an oxygen barrier to prevent the degradation of

binding media (103); and Volz *et al.* reported on the photodegradation of coatings (104).While the benefits of limiting the detrimental oxidation of oil paint films are tangible, the dangers of retarding the drying process by anoxic storage as well as the trapping of off-gassed materials (including solvents from varnishes) must also be considered.

1.3.3.4 Non-Traditional Paint Binding Media

Though they are known to be susceptible to photo- and autoxidation, there is no literature about the effect of anoxia on modern paints. The Bolland-Gee autoxidation scheme, Schematic 3, should be applicable; therefore oxidative degradation should be limited by anoxia. This is supported by a body of evidence that shows that oxidation reactions are prevented in nitrogen atmosphere for a number of polymers (105, 106). Furthermore, the benefit for anoxia can be inferred from the inclusion of antioxidants as common additives to commercial paints (95).

1.3.4 Anoxia and Colourants

There have been numerous studies on the photo stability and fading of colourants under room atmosphere (107-115), while others have studied the effect of atmospheric pollutants on the fading of colourants (116-121). With regard to anoxia, by vacuum, gas displacement, or oxygen scavenging, there have been fewer studies (4, 52, 54, 59, 60, 73, 122-126). For convenience the results of the above-mentioned studies, many discussed previously in general terms (2), are listed in Table 1 at the end of this Chapter. Particular results will be discussed in further detail below.

1.3.4.1 Inorganics

Prussian blue is a mixed valence coordination compound with a complex chemistry. Ware's book on cyanotypes is the best authority on the chemistry of Prussian blue in art objects (127). To summarise, Prussian blues form a family of pigments with differing properties dependent on their particular crystal structures, inclusions, occlusions, associated waters, and substitutions. The presence of extenders affects their light fastness (6). Early literature reports that Prussian blue fades under strong light, but regains its colour after a period in the dark, a property called phototropy (5). Recent published research using oxygen scavengers and/or gas purging confirms that Prussian blue changes or loses colour in anoxia (4, 6, 7, 127). Prussian blue can undergo several reactions yielding different coloured products, but photochemical reduction of Prussian blue is of particular interest, as it is reversible in the presence of oxygen, while under anoxic conditions reversion does not take place (4, 6, 7, 11, 127). It has also been found that soluble Prussian blue fades more rapidly than the insoluble form, and within the soluble form, light sensitivity depends upon what alkali species is included and what other metals have been taken up into the crystal lattice (6, 127-131).

Red lead and yellow lead oxide have both been cited as undergoing colour change in anoxia in the presence of moisture (62, 73, 122, 124, 132). Kenjo has also found that a yellow-brown sienna, as an unbound

pigment, darkens in anoxia (73). Interestingly, Kenjo found that read lead, litharge and sienna exhibited the same fading behaviour at 4.5-5.5% oxygen as at normal atmospheric oxygen concentrations. It was concluded that when modified atmospheres are used for pigmented objects they should contain an appropriate amount of oxygen (73). That the same oxygen concentration was found to be appropriate for three oxide pigments with different chemistries suggests that the required oxygen concentration is not dependent on the chemistry of a particular pigment, but rather on an oxygen adsorption isotherm for the surface which can be modelled from an ideal surface (133). If this is the case, then it helps to explain the observed variance in behaviour between bound and unbound pigments, between different binding media for the same pigment, and different humidity levels, any of which would change the surface properties and thus the isotherm.

1.3.4.2 Organics

The behaviour of organic colourants is complex due to the sheer multitude of colourants used, their complex chemistry, the multitude of binders extenders, etc. used, frequent changes in formulation for synthetic colourants, and the lack of characterisation of historic colourants. It is possible that a case-by-case analysis and evaluation must be made for each object. However, some generalisations can be made. The photochemistry of an organic colourant can be classified into one of three reaction types: direct photodecomposition; excitation and reaction; and reaction with an excited species (including photo-catalytic decomposition) see Schematic 8.

$$(1) \quad Q \xrightarrow{\ h\nu\ } Q*$$
$$Q* \longrightarrow \text{decomposition products}$$
$$(2) \quad Q \xrightarrow{\ h\nu\ } Q*$$
$$Q* + A \longrightarrow \text{reaction products}$$
$$(3) \quad A \xrightarrow{\ h\nu\ } A*$$
$$Q + A* \longrightarrow \text{reaction products}$$
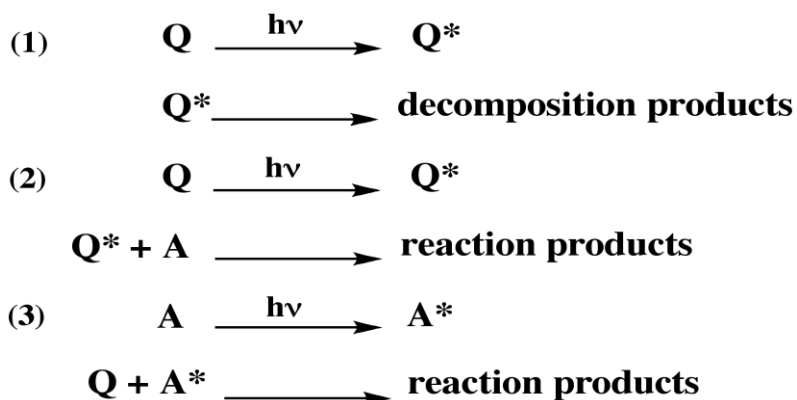
Schematic 8 Photo-reactivity of organic colourants. Q = colourant, A = colourless reactant also present in the system, * = excited state. Reaction 1 is direct photodecomposition of a colourant. Reaction 2 is photo-excitation of a colourant followed by reaction with a colourless species to form reaction products. Reaction 3 is the photo-excitation of a colourless species and its subsequent reaction with a colourant.

An organic colourant molecule is typically made up of the main structure, the chromophore, and substituent groups, auxochromes. The chromophore determines the average light fastness of a family of colourants and the auxochromes determine the specific reactivity within a group (134). With regard to natural colourants, flavonoids are highly fugitive in air and anthraquinones and indigoids are generally more lightfast in air. Within these groups symmetrical molecules are generally more light fast than asymmetric molecules, and with regard to anthraquinones, light fastness decreases with increased hydroxyl substitution (113, 134-137).

In addition to the molecular structure, the local environment, whether cellulosic, proteinaceous, or oleoresinous (109, 137, 138), the mordant and preparation method (113, 136, 139), and the particle size and distribution affect the light fastness of an organic colourant.

In Schematic 8, the reaction scheme (1) is not typically seen in natural colourants in the absence of UV light, but schemes (2) and (3) are typically encountered (140). Schemes (2) and (3) depend upon the presence of a reactive species. In the absence of these species, the reactions cannot take place. If a particular colourant is susceptible to oxidation the exclusion of oxygen might lead to increased light fastness (59, 141, 142). On the other hand, light fastness of dyes that are susceptible to reduction might decrease with the exclusion of oxygen; since reduction is limited by oxygen preferentially oxidising the proton donor that would otherwise reduce the colourant. Care must be taken with organic colourants and the entire system should be considered: the colourant, the substrate, the binding media, and any VOCs that might be present in the atmosphere (143, 144). Any of these might function as the reducing or oxidising agent. There are several good reviews of the photoreactivity of organic colourants, which provide good indications of which classes of colourants might benefit and which might be harmed by anoxia (59, 108, 110, 111, 113, 142, 145).

1.3.5 Graphic Media

1.3.5.1 Traditional Drawing Media

The majority of traditional drawing media such as metal point, graphite pencil, charcoal, and natural chalks should be stable under anoxia, but they will not receive any particular benefit either. The permanence of pastels, wax crayons, and coloured pencils has not been researched with regard to anoxia. However, it can be assumed that their behaviour will relate to that of the constituent pigments and binding media, with their intrinsic extenders and white pigments influencing the light fastness of some pigments. The binding media used in these materials should benefit from anoxia by limiting degradation that could lead to flaking, and changes in optical properties. Additionally anoxia will benefit the substrate and it has been shown that papers used as the substrate for graphic media have hugely variable permanence, and generally are among the least stable of the constituent materials in the object (146, 147).

1.3.5.2 Inks

Plant-based inks and washes generally should benefit from anoxia, though it should be noted that these are highly variable in composition, and it will be difficult to identify the specific colourants. Carbon-based inks are stable under anoxia though they receive no benefit. With regard to iron-gall inks and anoxia, further research is required. Anoxic display has been implemented for several documents containing iron-gall ink, including the American Charters of Freedom (57, 148), but concerns about VOCs production and trapping have been raised (149).

In general, non-traditional polymer-based media should benefit from anoxia, as well as inks from ballpoint, fibre-tipped, and marker pens and other materials not intended for long-term permanence (59, 150-153). These are all likely to have complex formulations with several dyes, and the overall benefit will be determined by the most fugitive constituent. On the other hand some porous tipped pens and "erasable ink" pens are less stable in anoxia (150, 152, 153). With regard to all of the above-mentioned materials anoxic enclosures would provide protection from atmospheric pollutants, to which the inks of porous pens are very susceptible (150, 153).

1.3.6 Literature Review Conclusions

Despite research dating to the 19th century, there are limited publications directly relating to the effect of anoxia on artists' materials. Published research is typically uncorrelated to previous work, the experimental conditions are typically poorly defined and/or controlled, and the materials studied can be quite variable. These factors lend a certain ambiguity to the results and cause difficulties in the evaluation of the application of anoxia to a particular object. However several general conclusions can be drawn.

Generally speaking, polymeric materials follow the Bolland-Gee reaction scheme, Schematic 3, during autoxidation, therefore substrates and binding media, assuming an appropriate drying/curing time is allowed for, will benefit from anoxia. With respect to colourants, more research is needed. Most traditional colourants, the vast majority in the published research, exhibit reduced colour change in the absence of oxygen. Some colourants, notably Prussian blue, some siennas, red lead, litharge and some organic dyes exhibit increased colour change in the absence of oxygen, and differing fading behaviours dependent on substrate and/or binding media. Synthetic organic colourants, in their sheer variety, represent the greatest challenge to heritage science research. Their reactivity can be categorised by the chromophore structure, but auxochrome substitution can drastically change the photochemistry of the colourant. In the absence of direct research into their reactivity in anoxia, research into the effect of antioxidants on the colourant or, if known, their reduction potential are the best indications of the potential benefit of anoxia.

Kenjo's observation that ca. 5% oxygen served as a "break point" in the colour change behaviour of several pigments known to be adversely affected by anoxia and her conclusion that appropriate levels of oxygen are needed to maintain a surface equilibrium for pigmented objects are significant, and indicate that the system can be modelled with an adsorption isotherm. The implication is that for colourants in a binding medium, their reactions with oxygen are defined by the surface properties of the system. If so, then a reduced oxygen level can be maintained at which the colourants undergo "normal" colour change behaviour as if in room atmosphere, while the paper substrate, and presumably binding media, undergo reduced oxidative degradation.

Beyond colour change, the production and accumulation of VOCs in a hermetically sealed anoxic frame needs to be considered. The role of these endogenous pollutants in the degradation of the system is poorly

understood and undefined, but VOCs can participate in reactions with all constituents resulting in potential autocatalytic degradation of the substrate and binding media, as well as causing colour change of all components of the object. Research into VOCs emitted from heritage objects and the use of VOC analysis as a diagnostic tool for monitoring single objects and entire collections is in its preliminary stages, but several research groups are focusing on this area (32, 89-91, 154, 155).

With regard to current and historical research, it is often difficult to compare results between studies due to unreported, unmeasured, or uncontrolled parameters. To facilitate dissemination and application of research into anoxia, minimum reporting standards should be agreed upon by the active research groups so that inter-laboratory comparisons of results can be made and end-users can be more confident in their applications.

1.4 Case Study Objects and Their Reconstruction

While anoxic storage and display can be applied to many classes of heritage objects, the scope of this research has been limited to works of art on paper (WOP), with an emphasis on watercolour drawings, sketches, etc., by J.M.W. Turner (1775-1851). This decision was based on several factors.

- Tate holds the Turner Bequest which includes more than 40,000 WOP by the artist, archival materials and a collection of artists' materials from his studio.
- Turner's methods and materials have been well characterised by several researchers and there is a long history of Turner research at Tate (156-162).
- During Turner's active period (1790-1850), there were many new artists' materials and colourants produced. Turner experimented with many of these new materials as they became available (161, 162). The result is that his palette is much broader than many of his contemporaries, and as such his works can be seen as representative of the class of WOP from the period.
- While Turner was very experimental in his use of colourants, he was quite conservative in his choice of papers. During Turner's active period there were many changes in the technology of paper production (158, 159, 163, 164), and there were many new types of papers from different processes and fibre sources with which he could have experimented (158, 159, 163, 164). In fact, he is documented in using hundreds of types of paper (158, 159), but the differences between papers are related to the finish and working properties rather than the fibre furnish and chemical properties. Nearly all of his papers fall within the broad category of hand-made, gelatine-sized paper from rag sources. This category of paper is generally quite stable and lacks many of the additives and fillers that typify modern papers (19th century onwards) and that can complicate the elucidation of the degradation process.

Having narrowed the focus of the research and identified the heritage objects of interest, it was necessary to design experiments to test the hypothesis that anoxic storage and display can safely be applied to WOP by J.M.W. Turner, and by generalisation to WOP in traditional media on unsized and gelatine-sized papers from rag fibre sources.

Based on the literature review, it was possible to identify specific objects in Tate's collections that could safely serve as representative samples for experimental application of anoxic storage and display. However, after consultation with stakeholders at Tate it became clear that it would not be possible to use objects from the Tate collection as 'experimental subjects'; rather it would be necessary to generate model materials for testing and demonstration purposes. This was accomplished by selecting case study objects in the collection, and then by using Art Technological Source Research (ATSR) to recreate the materials and even the objects of interest. These were then used by the AFP for all of its lines of research between 2006 and 2009.

1.4.1 Art Technological Source Research

Art technological source research (ATSR) is an interdisciplinary research method that can be applied to heritage science research to prepare historically informed reconstructions. ATSR was conceived by Ad Stijnman in 2002 (165), and it is accorded working group status within ICOM-CC. The goal of ATSR is to reconstruct artist materials and techniques. This is accomplished by consultation of available documentary and material sources to inform the production of model materials that can then be tested. The processes can be repeated and refined to produce historically accurate and representative sacrificial samples for destructive testing and full reproductions of objects for display.

ATSR was a central theme of the Anoxic Frames Project at Tate; it was used to de/reconstruct Turner's painting materials and techniques and to prepare the experimental samples and object reconstructions (166, 167).[7] The applied process will be briefly outlined below.

1. Several watercolour drawings by J.M.W. Turner were selected and examined, in most cases there was sufficient information about the colourants present, but when lacking, XRF spectra were taken to supplement the records and verify the presence of Prussian blue. The selected objects, Table 1, served as both the initial and final material references for the preparation of material reconstructions and object reproductions.
2. The Winsor and Newton Archive and Roberson Archive were consulted to find recipes for watercolour paints contemporary to Turner's active period. The archive research identified much variation in the paint recipes. In addition to differences between colourmen[8], there were also changes to a recipe with time and differences between pigments. However, this variability pertained mostly to wetting agents and other additives. Thus the recipes could be refined to a base recipe that was usable for all pigments and made for a simple sample matrix.
3. Samples of historic pigments and watercolours were collected from several sites throughout the UK and Netherlands. These samples were characterised by SEM-EDX and ATR-FTIR, and they will serve as a reference collection for further research.
4. Samples of J.M.W. Turner's studio pigments, held by Tate as part of the Turner Bequest, samples taken from the Cornelissen Pigment collection held by the Tate Conservation Archive and samples, from the historic pigments mentioned above were used to prepare watercolour paints based on the

---

[7]The reconstruction of Turner's watercolour paints, production of sample paint-outs and reproduction of drawings were conducted by Charlotte Caspers during her internship at Tate under the supervision of Dr. Joyce Townsend; a detailed description of the process can be found in her Thesis.

[8] Colourmen are suppliers of artists pigments, prepared paints and other supplies.

refined recipe mentioned above. These were supplemented as necessary by well characterised 19th century watercolour paints sets purchased for the project.

5. A reproduction paper, modelled on a gelatine-sized wove paper watermarked 1794/ J. WHATMAN favoured by J.M.W. Turner, was designed and commissioned by the author, and produced by Ruscombe Paper Mill, Chapter 4.

6. The prepared paints and paper were used to generate the samples used in this research as well as copies of several watercolour drawings[9].

Title	Tate registration number	Thumbnail of original watercolour drawing
The Red Rigi: Sample Study	D36123	
The Blue Rigi: Sample Study	D36188	
Newcastle-on-Tyne	D18144	
The Scarlet Sunset	D24666	

Table 1 Watercolour drawings by J.M.W. Turner that were studied as part of the Anoxic Frames Project at Tate. All images © Tate 2011.

Through the use of ATSR the resulting samples and reconstructions are historically informed in composition and faithful to the painting style of J.M.W. Turner. Despite the fact that the samples are modern in production, short of sacrificing a WOP by J.M.W. Turner, they can be considered both accurate and representative of WOP by J.M.W. Turner, and thus they can be used to test the application of modified atmosphere display and storage on WOP.

---

[9] The materials used in this research will be discussed in detail in the relevant materials section below.

1.5 Experimental Approach

Consider the experimental question behind this Thesis, 'how will modified atmosphere affect watercolour drawings'; a simple question that is difficult to answer. It can easily be argued that each drawing is unique, and will behave differently from every other drawing. Empirical evidence seems to support this. Each object is visibly different, exhibiting a range of colours and hues, and some objects have visibly degraded while others have not.

Neither the artistic uniqueness nor the differences in degrees of visible damage in related objects can be denied, but the former is a property imbued into the object by the artist, not one that is inherent to the materials from which the object is made, and the latter is a point observation based on uncontrolled and unknown variables. In fact, if works by a particular artist are grouped by date and location of execution, such as what has been done for the *Turner Colour and Line* exhibition at Tate Britain (2007 – 2012) (168), then one finds that an artist, like Turner, who might have used a huge range of colorants over his active period, can be remarkably constrained in the use of colorants for a given series of objects (168). So, while the subject and execution might be unique, the object itself can be reduced to a relatively short list of materials.

Next, if one groups the same objects by known display history (even the early the display history of the objects in the Turner Bequest is remarkably detailed (169, 170)), then one finds that objects subjected to similar display practices show similar visible degradation. That is the same colorants are observed to change in every object (170). Therefore, at least for the watercolour drawings from Turner's 1801 Scottish tour featured in the First Loan Collection (169, 170), visible degradation is a function of material properties and display practice, and is influenced by the 'uniqueness' of the object only insofar as the artist's choice and application of the colorants.

If we assume that the above observation holds true for other WOP and the model samples, then the research question: how will modified atmosphere affect watercolour drawings, can be answered in terms of classes of objects rather than individual objects, but this does not make the question any simpler to answer.

If one next considers the materials: watercolour paints (prepared from hand-ground, historic pigments) applied with a brush (similar to that used by Turner) onto handmade, gelatine-sized paper. Even if a reduced sample set of pigments is studied and the potential for inter-colorant interaction is ignored, the problem of sample variability necessitates a huge sample set (at least triplet samples per degradation time per atmosphere per colorant type) to answer the question with any confidence. If GC-MS analysis used, and the standard practice of hypothesis-driven, peak-by-peak evaluation of each mass chromatogram is applied then the task becomes unmanageable both in terms of processing time, but also with respect to spotting patterns by eye in a hugely variable data set.

To make more efficient use of time, one can focus on the major peaks or target analytes in the mass chromatograms, however, these peaks might not be the most informative. Perhaps the near base-line peaks or ratios of different components, that would otherwise be overlooked, would be more informative, but how to identify meaningful peaks and patterns in the data? This problem is not unlike that which is encountered in areas such as molecular biology and biochemistry, and to solve it they use what has been termed the –omics approach, which uses chemometric analyses to explore the data matrices: identifying patterns in the data, significant features in the data and sample outliers and from those analyses new hypotheses can be built and tested by further analyses.

I have transferred the data-driven methods of metabolomics to heritage science and termed it heritage degradomics. Heritage degradomics was developed during the execution of this research, initially in parallel with and then in collaboration with the PaperVOC project (2007-2009) (171). The idea at its core, that WOP can be considered pseudo-organisms/complex systems, served as the guiding principle when preparing sample sets and selecting analytical methods for their study. The initial speculations on the method were presented at Conservation Science 2007 in Milan (172). The finished concept was presented at the 2009 MASC meeting in London (173, 174), and it was later published in *Analytical Chemistry* (9).

At the start of my research only the barest outline of the idea of heritage degradomics existed in my mind, and only recently have the envisioned data handling methods become readily achievable for independent researchers outside of metabolomics research groups.[10] As a result, several unfortunate decisions were made in the data generation stage of the experimental process resulting in changes to the quality of the data.[11] However, the data is useable, and through a non-targeted degradic footprinting approach, it is possible to begin to answer the research question of this Thesis: what is the effect of modified atmospheres on watercolour drawings.

---

[10] Metabolomics research institutes have begun to give free access to independent researchers to software pipelines, like XCMS (175) and Metaboanalyst (176, 177) run on their servers. This server time is invaluable, while metabolomics software packages can be run locally on a PC, they are incredibly resource intensive, and simple data handling, like TIC alignment, can take hours or days to execute on even a modest sample set.

[11] The headspace autosampling and the GC-MS and parameters were refined over the course of data collection to improve the extraction efficiency, optimise sample throughput and improve base-line separation of components in the TICs. It is ironical that these changes, which improved the data quality interms of classical analysis of the mass chromatograms, degenerated the quality of the data (by impeding the operation of retention time correction algorithms) for statistics-based degradomics analysis of the same mass chromatograms.

Table 2 The reported behaviour of colourants in anoxia relative to normal oxygen levels.

Publication	Anoxia reduces the rate of colour change	Anoxia does not affect the rate of colour change	Anoxia increases the rate of colour change
(2008) (4)	Alizarin crimson,[a] Orpiment[a]	Chrome deep,[a] Realgar[a]	Prussian blue,[a] Antwerp blue[a]
(2008) (122)	Madder/potash,[b] Yellow lake,[b] Powdered kermes,[b] Madder lake,[b] Carmine,[b] Eosine,[b] Dragon's blood,[b] Cochineal,[b] Lac/alum,[b] Bitumen,[b] Brazilwood,[b] Gummigut,[b] Lac/lake,[b] Quercitron lake,[b] Gamboge,[b] Saffron,[b] Brazilwood/potash,[b] Alizarin Crimson,[b] Lac/potash,[b] Indian lake,[b] Magenta,[b] Purple madder,[b] Brazilwood/lake,[b] Realgar powder,[b] Lac/no mordant,[b] Naples yellow,[b] Lithol red,[b] Mauve,[b] Sepia,[b] Orpiment,[b] Madder/no mordant,[b] Madder/alum,[b] Brazilwood/alum,[b] Brazilwood/no mordant[b]	Prussian blue,[b] Rhodamine,[b] Cinnabar,[b] Indian yellow,[b] Emerald green,[b] Indigo[b]	Red lead,[b] Verdigris,[b] Rose madder[b]
(2003) (126)	several different indigo preparations		
(2001) (141)	Blue wool 2,[c] Xenon reference fabric,[e] Fustic,[c] Turmeric[c]	Blue wool 6,[c] Indigo,[c] Fluorescent yellow[d]	Fluorescent pink[d]
(1998) (124)		Malachite,[b,k] Azurite,[b,k] Vermilion,[b,k] Iron oxide red,[b,k] Yellow ochre,[b,k] Hematite,[b,k] White lead,[b,k] Indigo[b,k]	Red lead,[b,k*] Massicot,[b,k*]
(1980) (62, 73)		Malachite,[b] Cinnabar,[b]	Red lead,[b] Sienna,[b] Litharge[b]
(1979) (59)	Carmine,[†] Green felt pen (acidic triphenylmethane),[g] Geranium lake,[f] Alizarin,[a] Gamboge,[d] Blue Wool 2,[c] Blue Wool 1,[c] Yellow felt pen (acidic triphenyl		Vermillion azo,[†] Prussian blue[f]

	methane),[g] Gamboge,[a] Mauve,[a] Red felt pen (acidic triphenylmethane),[g] Carmine,[a] Purpurine,[d] Carmine,[d] Alizarin[f]		
(1967) (60)	Magenta (rosaniline, fuchsine),[a] Brazilwood,[a] Saffron,[a] Yellow Persian Berries,[a] Green Persian Berries[a]		
(1959) (63)	C.I. Basic Blue 3 (oxazine),[h] C.I. Basic Orange 22 (methin),[h] C.I. basic Blue 18 (triphenylmethane),[h] C.I. Basic Blue 12 (oxazine),[h] Astra Violet FN Extra (methin),[h] C.I. Basic Blue 26 (triphenylmethane)[h]		Diazacyanine blue,[h*] Diazacyanine yellow[h*]
(1888) (52)	Carmine,[a] Crimson lake,[a] Scarlet lake,[a] Rose madder,[a] Madder lake,[a] Brown madder,[a] Gamboge,[a] Aureolin,[a] Cadmium yellow,[a] Yellow ochre,[a] Naples yellow,[a] Indian yellow,[a] Emerald green,[a] Olive green,[a] Indigo blue,[a] Leitch's blue (cyanin),[a] Permanent blue,[a] Paynes grey,[a] Vandyke brown,[a] Burnt umber,[a] Brown pink,[a]	Vermillion,[a] Indian red,[a] Venetian red,[a] Burnt sienna,[a] Chrome yellow,[a] Lemon yellow,[a] Raw sienna,[a] Terre verte,[a] Chrome oxide,[a] Cobalt blue,[a] French blue,[a] Ultramarine ash,[a] Violet carmine,[a] purple carmine,[a] purple madder,[a] sepia[a]	Prussian blue,[a*] Aureolin,[a*] Cadmium yellow,[a*] Naples yellow,[a*] Indian yellow,[a*] Emerald green,[a*] Olive green,[a*] Antwerp blue,[a*] Leitchs blue (cyanin),[a*] Brown pink,[a*]
(1837) (54)	Turmeric,[i] Annatto[i]		Prussian blue[i]

a) pigment in gum Arabic	g) pen on paper	j) dye on cotton
b) pigment without binding media		
c) dye on wool	h) dye on cotton, viscose rayon, cellulose acetate, silk, wool, and orlon	k) pigment in glue
d) dye on cellulose		
e) dye on polyester		* indicates that colour change is increased in anoxia in the presence of moisture
f) oil paint with flake white extender	i) dye on cotton, silk and wool	

Chapter 2 Heritage Degradomics: An Introduction

2.1 Introduction

The aroma of an old book is familiar to every user of a traditional library. A combination of grassy notes with a tang of acids and a hint of vanilla over an underlying mustiness, this unmistakable smell is as much part of the book as its contents. It is a result of the several hundred identified volatile and semi-volatile organic compounds (VOCs) off-gassing from paper and the object in general (89, 178). The particular blend of compounds is a result of a network of degradation pathways and is dependent on the original composition of the object including paper substrate, applied media and binding as well as the sum of its 'biography'. The biography of an object can be very complex, and it includes its complete storage and treatment history: any radical events (fire, flood, microbiological infestation, burial etc, applied conservation interventions, usage history, its past and present local environment and even what sort of objects have been in its vicinity. Recently, there has been an increased interest in the 'smell of old books' and in VOCs emitted from historic paper in general (89, 155, 179, 180). The food and pharmaceuticals packaging industries have studied the transfer of taint and odour from paper and cardboard packaging during shipping and storage, extensively (181, 182). Other studies have developed VOC screening methods to identify the fraction of recycled pulp in board stock (183, 184), and identification of volatiles is now an almost routine analytical challenge. Heritage institutions (libraries, archives, and museums) are interested in quantitative VOC analysis as a rapid diagnostic tool for the degradation and condition of their collections as well as evaluation of conservation treatments and materials analysis (185). Can degraded books be identified by their smell or even extract information about why the books degraded? This question is especially interesting as heritage objects present particular problems for analysis either due to their uniqueness or due to diverging histories. Another factor is that it is often impossible to sample. This necessitates non-destructive/non-invasive methods, and headspace sampling coupled to GC-MS is especially appropriate.

The uniqueness and complexity, as well as limitations of destructive sampling, have limited much of heritage research to single object technical/material studies or to the degradation of constituent materials and/or simple surrogate objects. Yet models based on simple systems fall short of describing the complexity of heritage objects, and single object studies do not answer larger questions about classes of objects. The complexity of heritage objects is to an extent comparable to the complexity of living organisms. '-Omics' type methodologies have been developed for the study of living organisms (186, 187), could these methodologies be transferred to the study of heritage objects?

In this regard, the concepts of metabolomics (187-190) are most applicable to the purposes of heritage science. Metabolism, as a process in living organisms that have the power to adapt and renew, could be seen in parallel with degradation if one treats material objects as pseudo-organisms. Immediate parallels

can be drawn between the degradome (the sum of the products of various degradation processes) and the metabolome of an organism. Through similarities with metabolomics (191), a new field of heritage degradomics (and related terms, Table1) can be proposed.

2.2 Analogy to Metabolomics

Metabolism is a process in living organisms that have the power to adapt to changes in their environment, and metabolomics is defined as the analysis, both qualitative and quantitative, of the arrays of metabolites produced in biological samples, their dynamics, composition, interactions, and responses to changes in environmental conditions (187, 192, 193). While not living, a heritage object is by no means static; rather it presents a complex and dynamic system of degradation reactions that parallels that of metabolism, such that with little stretch of the imagination it is possible to think of the object/display system as a pseudo-organism, and the application of metabolomics techniques, particularly those targeted at the study of plants and micro-organisms seems appropriate (186, 194-198).

Further parallels can be sought between the genotype of an organism and historic recipes/procedures used to make a historic material/object (186, 199). The phenotype of an organism, which results from expression of its genes and environmental factors, can be seen as analogous to the measurable or observable properties of a historic object. In this way, quasi-genotype-phenotype mapping experiments could be performed for heritage objects, either through systematically altering recipes (suppression, over-expression, knockout, etc.) and/or through experiments with altered environmental sequences to determine how these change the appearance and/or permanence of historically informed replicas.

Table 1 Heritage degradomics and related terms

metabolomics	The analysis, both qualitative and quantitative, of the arrays of metabolites produced in biological samples, their dynamics, composition, interactions, and responses to changes in environmental conditions (193).
metabolome	The complete set of metabolites in an organism (193).
metabolomic profiling	Quantitative analysis of a set of metabolites in a selected biochemical pathway or a specific class of compounds. This includes target analysis (193).
metabolic fingerprinting	Unbiased, global screening to classify samples based on metabolite patterns or 'fingerprints' that change in response to disease, environmental or genetic perturbations with the ultimate goal to identify discriminating metabolites (193).
metabolic footprinting	Fingerprinting analysis of extra-cellular metabolites in cell culture medium as a reflection of metabolite excretion or uptake by cells (188, 193).
heritage degradomics	The analysis, both quantitative and qualitative, of the degradation products produced by a heritage object, their dynamics, composition, interactions, and

	variations due to different microenvironments.
degradome	The sum of the products of the various degradation reactions and their interactions to which an object is subject.
degradic profiling	Quantitative analysis of a set of degradation products in a selected degradation pathway or a specific class of compounds for a particular object.
degradic fingerprinting	Unbiased, global screening to classify samples based on patterns of degradation product production or 'fingerprints' that change in response to storage conditions or conservation treatments.
degradic footprinting	Fingerprinting analysis of degradation products in the microenvironment surrounding the object.

2.2.1 -Omics Approach

Metabolomic techniques have been devised to understand the system-wide, complex and variable mixtures of small molecules produced as the end products of genetic expression in an organism. The suffix '-omics' designates a particular methodology for experimental design, data generation, and data handling. Because little is known about the system initially, a hypothesis-driven, reductionist cycle of knowledge is better substituted with a holistic and inductive approach to experimentation (188). Typically very large sample sets of hundreds to thousands of replicated samples are used to generate a statistically significant sample space and distinguish interesting sample variability from obscuring variability by application of various data processing methods, descriptive statistics and visualization, and supervised and unsupervised multivariate techniques (187, 189, 192, 193, 200, 201). Hypotheses are then generated and tested *in silico*, and the cycle repeats.
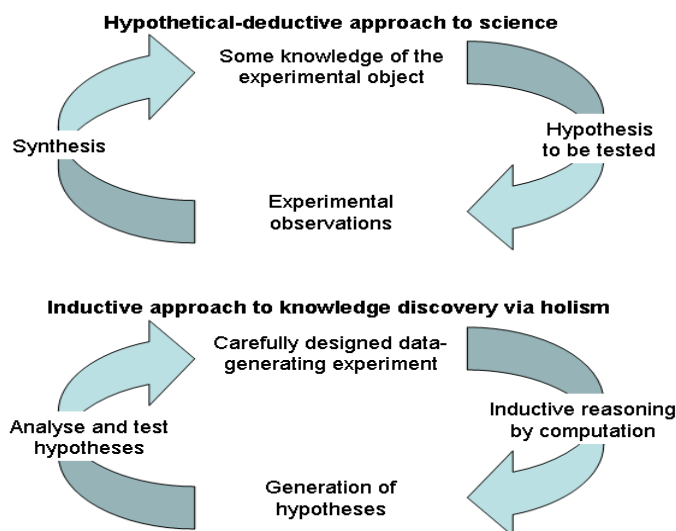
Figure 1 The cycle of knowledge and holism [13].

For both metabolomics and heritage degradomics, the method of data acquisition depends on the sample type and experimental question. In metabolomics, the main tools are NMR, GC/MS, LC/MS, CE/MS, hyphenations and derivatives thereof, and to a lesser extent, spectroscopic methods (187, 189). For heritage degradomics similar methods can be employed, but with a greater emphasis on non-invasive methods. In this light, SPME coupled to a separation technique (CE, GC, or LC), headspace analysis, and various spectroscopic methods (NIR, FTIR, RAMAN) will likely prove fruitful.

Three metabolomic techniques are of interest for heritage science: fingerprinting, footprinting and profiling. Fingerprinting and footprinting methods are used in metabolomics to identify a unique signature of marker compounds for a particular environment/genotype/disease. Fingerprinting involves sampling the subject of study for analysis, while footprinting is concerned with the metabolites released into the environment and is therefore non-invasive for the subject. In heritage science there is an emphasis on non-sampling/non-invasive analytical techniques, thus footprinting techniques to analyze VOCs off-gassed by an object into its autonomous atmosphere is particularly attractive. For some objects there are sampling opportunities, either due to the disintegration of the object or because sampling is considered to be acceptable damage, and then fingerprinting experiments to identify the materials comprising an object and their degradation products can be extremely powerful (202, 203). Once the marker compounds have been identified profiling experiments can be performed to quantify the markers, explore the reaction system and to evaluate the effect of various exogenous and endogenous parameters on the concentrations of targeted analytes (194). In heritage science this would translate to quantification of target analytes and their correlation to properties of an object (9, 184, 204-206) and to evaluate conservation treatments (207) and object micro-environments (84, 85, 208-214).

2.3 Transfer to Heritage Science

The -omics approach, i.e., the data-driven holistic and inductive approach to experimentation replacing the hypothesis-driven, reductionist cycle of knowledge, has not been explored in relation to material characterization yet. The need for large sample sets (e.g. ASTM E1655-05 (215)) to generate a statistically significant sample space is undoubtedly a drawback of this approach. Heritage degradomics differs from other -omics-type research in that it is not possible to clone an object or grow new ones in a controlled environment. In relation to historic objects, it is often possible to collect expendable ones, and if the research question is related to variations in composition, it is possible to combinatorially prepare historically informed samples to study how small variations in composition affect the degradome.

While desirable, the luxury of large sample sets is often not available if one is working with unique heritage objects; as such it is necessary to construct replica objects or historically informed reconstructions to provide a large, consumable sample population for experimentation. The preparation of the samples must be conducted with care to ensure that applicable data is generated for hypothesis building and generation

of models of the degradic systems. Once the hypotheses and models have been generated, they can be tested on a small sample set taken from a heritage object.

If it proves possible to generate the needed sample matrix, this experimental methodology is well suited to dealing with the complexities of heritage objects whose degradomes are the product of a system of chemical reactions that are influenced by the original composition of the object, the sum of its biography. The constituents of an object's degradome can be sub-classified according to their volatility and/or solubility: volatile, extractable, and insoluble degradomes (VD, ED, and ISD respectively). Analysis of each class of degradome yields different information about the stability and degradation of a particular object, and, if a large enough sample set is used, about a class of objects.

2.3.1 Volatile Degradome

The VD is the population of volatile and semi-volatile organic compounds (VOC) in the autonomous atmosphere of an object. These VOCs are the products of the degradation of all of the component materials in a heritage object as well as the object's display system. When compared to the ED and ISD, analysis of the VD has many advantages –particularly, the VD is not integral to the object and therefore it is accessible for sampling.

Once sampled, the VOCs can readily be analyzed with little to no pre-treatment by a variety of techniques depending on the goal of the study. Rapid analysis of the VD *in toto* is possible with a total-VOC (TVOC) sensor or dosimeter to yield simple data and generate alerts for threshold exceeding events. More information-rich TVOC data can be gathered with gas phase FTIR,[12] ion mobility spectrometry (IMS)[13] or mass spectrometry (MS) based detectors; data from these devices should be enough, when combined with chemometrics, to generate a model of the 'normal' VD environment and then to create alarm events when the VD deviates from the norm. This method is used for fire detection and air quality/flue-gas monitoring in various industries. If a pre-separation technique, such as gas chromatography (GC), is implemented before the detector, such as in GC-MS, then more detailed data can be collected. Through pre-separation the individual analytes in the VD can be identified as in footprinting experiments and quantified in profiling experiments. This information can be used to diagnose an object and collections of objects (e.g. library or archive storage spaces), identify microbiological contamination (206, 218, 219) and evaluate conservation and display methods (220).

The sampling of VOCs for later analysis can be integrated into standard preservation practice through the inclusion of VOC sorbents in the display/storage environment. For instance, carbon cloth with a known surface area can be included in an anoxic frame. At the time of sealing of the frame, a sample of the same cloth can be retained in cold storage to serve as a blank sample. When the frame is opened the carbon cloth

---

[12] An example of a sensitive, online, photo acoustic FTIR spectrometer for gas analysis can be found at (216).
[13] An example of a field asymmetric ion mobility spectrometer for online gas analysis can be found at (217).

can be sampled and analyzed by thermal desorption GC-MS to provide information about the elapsed VD in the display case.

Because of the ease of sampling, pre-concentration, integration of the above into standard preservation practice and potential for online/automated sampling, the VD is an especially appealing and information-rich subject of study.

2.3.2 Extractable Degradome

The ED is the population of small, non-volatile molecules that can be extracted from a material without destruction of the object. Typically the ED is less accessible than the VD as solvent extraction typically requires sampling of the object. Once the ED is extracted it can be concentrated and analyzed *in toto* by vibrational spectroscopy (hyphenated FTIR, RAMAN, etc.) (221) or by MS. As with the VD, these techniques are rapid and provide a 'fingerprint' of the degradome; however the lack of pre-separation makes interpretation difficult. Better would be to use a suitable separation method (TLC, LC or CE) prior to analysis to identify individual components in the ED (90).

An instance when the ED of a work of art on paper (WOP) is accessible is following a conservation washing treatment (207). The collected wash solution would contain a mixture of the degradation products from all of the components of the WOP, and it can be used to determine the condition of the object as well as evaluate the effectiveness of the conservation treatment. However, it must be remembered that the quality of the data will reflect the extraction efficiency of the wash rather than the real ED population, and if the wash was conducted as a conservation treatment rather than a sample collection method, then it is likely that a less than complete and non-reproducible extraction was performed.

The ED is potentially information-rich; however its usability is limited by the accessibility of materials for sampling. If conservation treatments are relied upon for sample collection, caution must be exercised when comparing sample sets with the data normalized for both surface area of the object and volume of solvent used for extraction.

2.3.3 Insoluble Degradome

The ISD is that which remains after extraction of the ED and VD; it can be roughly approximated by physical properties of the material. Analysis of the ISD is almost always destructive, and it is therefore the least accessible of the three degradomes.

Considering paper, the insoluble degradome can be equated to several parameters: the DP, carbonyl/carboxyl content, ash content, etc. The DP of cellulose can be measured by viscometry (20, 222) or SEC (21, 223, 224), various spectroscopic techniques (225, 226) or evaluated by mechanical tests such as the double fold, tensile, and tear tests (227, 228). All of the above are destructive methods, and with the

exception of some SEC methods (22), require large samples, as such they are not applicable to a work of art on paper.

An alternative to destructive sampling is NIR/chemometrics (23) which must be trained on a set of sacrificial samples and correlated to the above techniques to construct a model that can then be used to estimate the degree of polymerization (DP), and many other properties, of paper. A NIR/chemometrics tool has been developed for library and archive materials in the SurveNIR project (23, 24, 26, 229).[14]

2.3.4 A Case Study: Degradic Footprinting of J.M.W. Turner Watercolours

As noted in Chapter 1, heritage institutions are beginning to adopt new methods for the storage and display of heritage objects (micro-climate control and anoxic frames as opposed to gallery wide HVAC systems) and are shifting more and more from single-object interventive treatments to collection-oriented preventive treatments. With these changes comes an intense interest in the role of endogenous pollutants (VOCs generated by the degradation of an object itself) on the stability and condition of an object (185). The above changes lead to new questions, rather than 'what can be done for *this* object?' heritage scientists are asked, 'what can be done for *this class* of objects?' The significance of the change in question is subtle, and it is more than a matter of volume. By shifting focus from the object as an individual to an object as an element of a collective, a paradigm shift from the hypothetical-deductive approach to science to an inductive approach to knowledge discovery via holism is needed, Figure 1.

In an effort to define the field of heritage degradomics; degradic footprinting experiments were designed to test the effect of microclimate, anoxic and 5% oxygen atmosphere display and storage methods on watercolours by J.M.W. Turner. These conditions were selected based on display methods employed and proposed by Tate.

Following extensive research into historic watercolour recipes, historically informed samples of watercolours were prepared using pigments taken from the Tate Turner Bequest, (Chapter 3). These samples were painted out to similar colour saturation on gelatine-sized watercolour paper produced for the study (Chapter 4). Depending on the experiment, the samples were then cut to size and sealed in reactors, typically 20 ml headspace tubes, under room atmosphere or argon. Care was taken to ensure that the atmospheres in each reactor were at 50% RH. The sealed reactors were then light or thermal aged for various times. The aged samples were then analysed by the above methods and the data processed by multivariate data analysis methods.

The VD was selected as the primary target degradome because of its accessibility with respect to actual objects and because it was possible to automate much of the purge-and-trap-headspace-GC-MS (P&T-HS-GC-MS) analyses (Chapter 7).

---

[14] Please see the SurveNIR project's webpage for more details, (230).

The knowledge gained from these experiments has been used to evaluate the application of anoxia for the storage and display of 19th century watercolours (Chapter 9) as well as to define new methods to monitor and evaluate the environment within sealed anoxic cases (Chapter 8).

Chapter 3 Materials and Methods

3.1 Materials

3.1.1 Reconstruction of Turner's Painting Materials

Ideally a selection of well characterised historic materials with known provenance, preferably from the works of J.M.W. Turner, would have been used for this research. However it was not possible to sample the objects, nor was it deemed prudent to "experiment" on intact paintings from the Tate collection.

The option of collecting 18th and 19th century watercolour drawings for use in the study was explored, but the number of unknowns (provenance, composition, and biography) associated with the sample objects was deemed to be too great. Therefore, it was necessary to reconstruct the materials used by J.M.W. Turner.

Modern artist materials significantly differ from historic materials in preparation and composition, and these differences can significantly affect the accuracy, and therefore, applicability, of any studies that attempt to employ modern materials to recreate historic objects for study. To overcome these difficulties, ATSR methods were used to research recipes and in the reproduction of the materials used to create the samples used in this study. For experimental simplicity the materials were limited to the paper substrate and applied media, and these were prepared with as simple a composition as possible while still retaining the historical accuracy of the reconstructions.

3.1.1.1 Applied Media

It is known that J.M.W. Turner used both prepared watercolour cakes, as purchased from a colourman, and prepared his own watercolour paints in his studio (162). Some of the watercolour palette associated with Turner as well as his studio pigments have been analysed by several researchers (161, 162, 166, 231-233). The recipe used to prepare the paints used for this study was informed by the above mentioned analyses as well as source research at the archives of colourmen, Winsor and Newton and Roberson. While the addition of wetting agents (ox gall), softening agents (honey, sugar and/or glycerol), and/or extenders was a possibility, medium analysis limited to his palettes has identified gum mixtures and the addition of sugar (234). The simplest recipe of colourant, gum and water was selected as it provided a homogenous paint and simplified the sample matrix.

3.1.1.1.1 Gum Arabic

Gum Arabic solution 2:1 (w:w) water to gum Arabic was prepared from nodules of the raw gum (purchased from Kremer Pigmente GmbH) and dissolving them in deionised water with gentle heat. The resulting solution was stored in a refrigerator until use and re-prepared if a precipitate formed or if it became infested with micro-organisms (167).

3.1.1.1.2 Pigments and Paint Preparation

Samples of known provenance and characterised pigments were taken from J.M.W. Turner's studio pigments held by Tate as part of the Turner Bequest (designated TTBx here and Q04074 in the Tate conservation archive) otherwise from the early- to mid-20th century Cornelissen pigments held by the Tate Conservation Archive (here designated TCAx), see Table 1. The pigment samples were weighed and ground by hand on a glass slab with a muller with deionised water and gum Arabic solution[15]. The resulting slurry was transferred to Petri dishes and allowed to dry by evaporation at room temperature. For a detailed description of the production of the paint please see Charlotte Caspers' masters Thesis (167).

Sample	Description of the dry pigment	Colourant type	Other information
TCA1	Medium blue powder	Antwerp blue	From Cornelissen pigments, contains Zn and Ba based extenders
TCA7	Dark blue powder	Chinese Blue	From Cornelissen pigments, very pure Prussian blue
TCA13	Orange powder	Orange Madder	From Cornelissen pigments, unclear if synthetic or derived from madder
TTB1	Brownish-red powder	Madder lake	*R. tinctorum* L.
TTB2	Bluish-red powder	Madder lake	*R. tinctorum* L.
TTB3	Brownish fragments	Gamboge	*G. gummi-gutta*
TTB5	Dark brown powder	Madder lake	*R. tinctorum* L.
TTB6	Dark blue powder	Prussian Blue	Synthetic precursors possibly from animal sources
TTB8	Bluer red powder	Madder lake	*R. tinctorum* L.
TTB11	Bluish-red powder	Madder lake	*R. tinctorum* L.
TTB13	Dull yellow fragments	Madder lake	*R. cordifolia* L.
TTB14	Bluish-red powder	Madder lake	*R. tinctorum* L.
TTB15	Dark brown powder	Madder lake	*R. tinctorum* L.
TTB16	Dark brown powder	Madder lake	*R. tinctorum* L.

Table 1 Pigments used in this research.

3.1.1.2 Paper Substrate

Samples of historic papers were collected, but they were not available in sufficient quantity to perform the research detailed within this Thesis as well as the parallel light fastness research conducted by Andrew Lerwill presented in his PhD Thesis and research into J.M.W. Turner's painting techniques as presented in Charlotte Casper's MA Thesis (11, 167). Therefore a reproduction paper was needed.

---

[15] Note that the samples used for this research were prepared in collaboration with Charlotte Caspers.

A white, wove drawing paper watermark: 1794/ J WHATMAN, made by William Balston and the Hollingsworth brothers at Turkey Mill, Maidstone, Kent was used as a basis for the reconstruction paper. This paper was used by J.M.W. Turner throughout much of his active period, both cut down and bound into sketchbooks and in a variety of full sheet sizes (159). Ruscombe Paper Mill was commissioned to produce the reproduction paper. When commissioning the paper several parameters were considered in its design.

- The resulting paper needed to accept watercolours in the same way as we imagine Turner's papers did.
- It needed to have a composition similar to historic rag papers.
- It needed to have similar optical properties to historic papers.
- Ideally, it should age in the same way as historic papers.

Please see Chapter 4 for more details about the design of the reconstruction paper.

Six papers with identical furnish, three different finishes and two sizing treatments were prepared for the Anoxic Frames Project. This was accomplished by dividing the freshly prepared sheets from a single post into three populations and applying different drying, surfacing and sizing treatments.

- One population was dried as single spurs.
    - Sheets of this paper experienced the most shrinkage and have the roughest surface finish.
    - They are designated as rough (R).
- A second population was exchanged and pressed at 40 tons overnight before being dried as spurs of 5 sheets.
    - Sheets of this population have a pebbly, intermediate roughness finish.
    - They are designated as cold pressed (CP).
- The third population was cold pressed and dried in spurs of five sheets as above, but once dry they were remoistened and restraint dried before being glazed between stainless steel sheets with a roll load of 200 bar.
    - Sheets of this population are thinner, and they have a very smooth finish.
    - They are designated as glazed (G).

The three populations were then halved to form six populations. Half were left as is, and they were then designated as waterleaf (WL), unsized paper thus generating the populations: WLR, WLCP and WLG. While the second half was gelatine sized to generate the populations: GSR, GSCP and GSG.

The preparation of six papers allowed for the same paper substrate to be used for each of the separate subprojects in the Anoxic Frames Project and for the effect of finish and size to be studied while still limiting the sample matrix by holding all other preparation variables, such as furnish, constant.

In addition to the Turner reproduction papers, several other papers including lignocellulosic news print, aquapel sized watercolour paper, lining paper, an alkyl-ketyl dimer sized printing paper and a gelatine sized watercolour paper were used in the experimental development stage of the research. The results from these studies were used to optimise the degradation and headspace analysis parameters for the Turner papers.

3.1.1.3 Paint-Outs

Paint-outs for experimentation were prepared by taking a small flake of the dried paint and dissolving it in a minimum of deionised water[16]. The paint solution was then applied to pre-wetted and stretched paper with a squirrel hair 'mop' brush similar to that used by J.M.W. Turner. As part of experimental design, different papers were used to prepare paint-outs for different experiments.

- GSR and WLR were used for headspace studies because the finish was proposed to be a non-contributing variable to this line of research, and therefore the smoother papers could be retained for other studies.
- GSG and WLG were used for chemiluminometric studies because they had the most homogenous and smooth surfaces, and previous studies indicated that surface roughness is a contributing variable (235).
- GSCP, WLCP, GSG and WLG were used for creation of object reproductions. The choice of paper was dependent upon the finish of the original that was being copied (167).
- Various papers were used for micro-fadeometry studies to explore the effect of finish and sizing agent on the fading of colourants (11).

Figure 1 presents a generalised schematic of the sample structure, in this case a two-colourant system on gelatine sized paper. Because the gelatine-sized paper was pre-wetted prior to application of the paint layer, the gelatine was softened and the pigment particles are fully incorporated into the paper/gelatine matrix.

---

[16] The amount of water needed varied with each paint and was judged by eye.
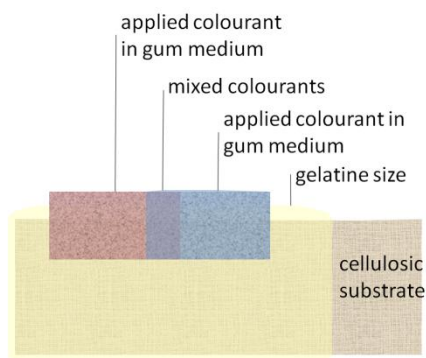
Figure 1 The cellulosic substrate, containing the crystalline, amorphous and pre-oxidised cellulose fractions as well as any hemicelluloses, lignin, and additives (such as alkali earth metal carbonates added for an alkali reserve) that might be present, is impregnated with gelatine size. While there is a perceptible layer of gelatine on the surface of the sheet, it is distributed throughout the fibre matrix such that cellulose fibres and fibre groupings are coated. The paint layer consisting of a colourant in gum medium and water is applied to either a dry or a pre-wetted paper surface. The degree of pre-wetting and post application working influences the degree to which the colourant particles are carried into the gelatine layer and even the fibre matrix itself.

3.1.2 Laboratory Ware and Supplies

3.1.2.1 Water

Deionised water was used for all aqueous preparations.

3.1.2.2 Laboratory Gasses

Zero grade argon, zero grade helium and 5% oxygen/95% nitrogen gas blend were used as supplied by BOC.

3.1.2.3 Headspace Vials

20-ml headspace vials with PTFE lined silicone septa and either crimp caps or screw caps were used as supplied by Chromacol.

3.1.2.4 Headspace Traps

A purge/trap K, Supelco Vocarb 3000, was used in the Tekmar HT3 purge and trap system.3.1.2.5 Chromatography Columns

A Varian CP-57 gas chromatographic column 30 m x 0.32 mm was used early in the experimental process, but was soon rejected due to difficulties with integrating the HT3, gas flow, and optimising the chromatographic method. The CP-57 was replaced with a Supelco VOCOL gas chromatographic column 60 m x 0.25 mm x 1.50 µm which allowed for stable gas flow during headspace analysis and provided good chromatographic separation of both polar and non-polar analytes.

Both columns were used in a Varian CP 3800 GC with a Varian Saturn 2200 quadrupole ion trap mass analyzer as a detector.

3.2 Methods

3.2.1 Accelerated Degradation

WOPs degrade due to chemical reactions. The rates of these reactions at ambient conditions are often low and therefore the products would be unobservable within a typical experimental timeframe. However, the rates of degradation reactions are influenced by many factors: concentration, temperature, surface area, pressure, intensity of electromagnetic radiation, etc. By changing a parameter, *e.g.* increasing the temperature, light intensity or reactant concentration, the rates of the reactions can be increased and degradation products can be observable within an experimental time frame on the order of days to months rather than years to decades. Accelerated degradation experiments are the core of standard tests and are applied throughout the world as a means to test materials' stabilities under various conditions (236).

In heritage science, accelerated degradation is a contentious topic with expert opinions both for and against the applicability of such experiments to evaluate the permanence of WOP (236-241). The main arguments against accelerated degradation focus either on the harsh conditions employed to elicit observable changes or that the observable degradation of naturally aged materials differs from that of objects that have been subjected to accelerated degradation regimes. This discontent with existing standards has led to a proliferation of non-standard degradation conditions that in turn leads to difficulty in inter-experimental comparisons of data (242, 243). If a generalisation can be made, it is that for heritage science type research, less extreme conditions are favoured. A new ASTM standard (ASTM D6819 - 02(2007)) for the evaluation of the relative stability of printing and writing paper by sealed tube degradation was introduced (238, 244) and served as the starting point for the design of the accelerated degradation experiments employed in this study.

While still contentious, it is generally felt that sealed tube degradation better simulates the environment inside of a book (89, 179, 245-248) and that of a well-sealed display/storage system (33, 34, 68, 249, 250) as is typical for WOP as it allows for the accumulation and interaction of volatile organic compounds (VOCs) with the samples. Of interest for this study is that sealed vial degradation allows for the establishment of modified atmospheres within the vial (thereby simulating an anoxic frame) and monitoring of the generated VOCs by headspace sampling. To meet analytical method parameters, ASTM D6819-02 was modified to include the use of 20-ml headspace vials sealed with Teflon-lined silicone septa and crimp caps as the degradation vessels (high throughput headspace analysis by GC-MS was used to follow the evolution of VOCs and thereby the degradation of the samples).

3.2.1.1 Sealing the Vials

In all cases the samples were desiccated over Dririte for a period of at least 48 h followed by conditioning at 25 °C and 50% RH in an environmental chamber for at least 48 h. The conditioned samples were placed in vials and sealed under an atmosphere at room temperature and 50% ±5% RH. Standard atmosphere

samples were sealed in vials when ambient conditions in the laboratory were at 50% ±5% RH. If a reduced-oxygen atmosphere was required, the sample-filled vials were placed in a glove box and purged with the desired gas for at least 2 h prior to sealing. Zero grade argon and 5% oxygen in nitrogen were humidified prior to induction to the glove box by splitting the gas stream, bubbling one half through degassed deionised water and mixing the 'dry' and 'wet' streams to achieve the desired RH. During manipulations the glove box was maintained at a slight overpressure to limit oxygen ingress. Oxygen concentration in the glove box was checked by GSS oxygen sensor prior to initiating manipulations. RH was monitored in the mixing chamber as well as the glove box.

3.2.1.2 Photodegradation

Photodegradation in sealed vials was conducted under banks of UV filtered Phillips TLD/865 Super 80 fluorescent lamps at 15,000 lux, 25 °C and 50 ± 5% RH in a Sanyo M351H environmental chamber. Phillips TLD/865 Super 80 bulbs have a 'cool white' colour temperature equivalent to what is used in the gallery space at Tate, however they have a different spectral distribution, Figure 2, than sources employed in light-fastness testing standards, *i.e.* xenon or mercury arc lamps.
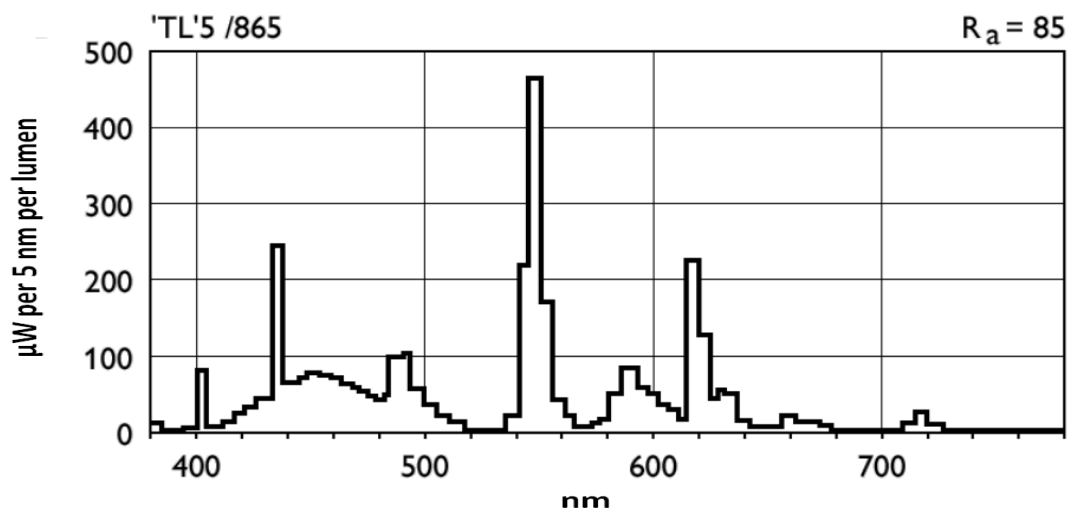
Figure 2 Spectral distribution of Phillips TLD/865 Super 80 cool white daylight fluorescent bulb. Data from Phillips TL-D Aperture lamps guide.

For chemiluminescence studies and some viscometry studies, a Suntest CPS+ fitted with a xenon arc lamp. In these studies, samples were either aged in a sealed reactor, under a watch glass or in the open sample compartment. In all cases the Suntest was operated at 765 W and was fitted with both the supplied UV filter and with an additional filter prepared from UV filtering Perspex to remove all wavelengths shorter than 400 nm. For chemiluminometric experiments degradation duration was from 15 to 600 s, and for viscometry a period of 20 h was used.

3.2.1.3 Thermal degradation

Derivation of degradation rates at elevated temperatures and extrapolation back to room temperature by an Arrhenius-type experiment was not a goal of this research as the emphasis was on the effect of light degradation under simulated display conditions. However, thermal-degradation was conducted as it was thought to produce more VOCs at detectable levels, and thus allow for easier identification of target analytes to be searched for in the GC-MS data from photodegradation experiments.

The samples were prepared as above with at 50 ± 5% RH at the time of sealing. Two temperature regimes were selected, 95 °C and 160 °C.

The 95 °C regime was used for all sample types. It was selected because it is a commonly used regime for thermal oxidation studies (243). Furthermore, while it is below the boiling point of water, it was sufficiently high to allow for rapid sample turnover, degradation experiments were 1 – 25 days in duration.

The 160 °C regime was used as a second regime for papers without colourants. Coloured samples were not included for reasons of economy. Thermal-degradation at this temperature has been used for studies of papers used in electrical transformers with evaluation of produced VOCs by GC-MS analysis (251, 252). Additionally, this regime was postulated to produce more thermal decomposition and Maillard reaction products than the lower temperature regime and photodegradation experiments (27). Degradation duration for this regime was 1 – 48 h.

3.2.2 Analytical Methods

Despite the fact that this research was conducted on expendable materials, and sampling or even complete homogenisation were possible, the VD was targeted. This choice was made because the VD was thought to be the most information rich of the three degradomes, and the VD of a WOP is accessible while, as noted above, the ED and ISD typically are not. Thus by targeting the VD, data from actual WOP could be added to the model generated from this research to better close the experimental knowledge to collection care practice loop.

What follow are a brief outline of the analytical methods applied in this research, a synopsis of how the data can be used and a description of other possible methods that could have been employed.

3.2.2.1 Fibre Microscopy

The fibre furnishes of the papers used in this study as well as the case study historical paper for the reconstructions were confirmed by visible light microscopy. In the case of the case study paper, a section of a sheet of paper bearing the watermark 1794/ J WHATMAN was available at a fibre identification course. Several small samples of fibres were collected from the surface of the sheet with a needle. The fibres were transferred to a microscope slide with water as the medium. This initial study confirmed that the paper was mostly flax, but the fibres were highly disrupted and there seemed to be some non-flax fibres. At a later

date it was possible to attain a more significant sample of the paper, and 1 mm^2 of the paper was dispersed in 0.5 ml deionised water. Aliquots of the fibre suspension were transferred by pipette to a microscope slide and a cover slip added. The fibres were observed in both bright field and dark field; then a drop of neocarmine dye solution was pulled under the cover slip by capillary action. After five minutes the excess dye was rinsed with deionised water in a similar manner. Neocarmine is a dye commonly used by textile conservators to differentiate different fibres allowing easy identification of cellulosic fibres (253).

3.2.2.2 X-Ray Fluorescence

Elemental analysis of the paper, pigments, paintouts and WOP was conducted with several different instruments. For WOP a Bruker Tracer handheld XRF was used to screen an object and confirm the presence of Prussian blue and other inorganic pigments. Pigment samples were analysed by SEM-EDX. Paper and paintout samples were analysed with either a Bruker ARTAX or a Thermo Electron ARL Quant'X ED-XRF. While different instruments were used throughout the research project, a single instrument and operating parameters were used for each sample within an experiment thus allowing for comparison of the results.

3.2.2.3 pH Determination

The pH of a paper is a good indicator of the overall stability of the material. I proposed that anoxia would reduce the acidification of paper by limiting oxygen uptake, and thereby carboxyl production, during display. Additionally it was noted that encapsulation of acidic paper would lead to accumulation of volatile acids and autocatalytic hydrolysis of the paper (33, 92, 254).

As such, the measurement of the pH of a WOP prior to anoxic framing was proposed as being necessary. As noted above sampling of a WOP is not permissible, so standard methods employing sampling and homogenisation, while more accurate, are not permissible (255); instead, a surface probe was used to measure the pH of the samples (256). The inaccuracies of this method, particularly for gelatine-sized paper, as well as the potential for disfiguring a WOP by generation of tide marks were noted (221, 257-260). However, as this is a commonly applied and accepted technique in paper conservation it seemed most amenable to museum use.

With respect to this research, a Thermo Orion 5-star plus multi-parameter meter with an Orion ROSS Ultra pH surface electrode was used. The probe was selected as optimum for use with gelatine sized paper. Three-point calibration was applied at the start of each measurement session. Between measurements the probe was rinsed with deionised water and blotted dry. The deionised water used in the measurements was degassed by bubbling nitrogen through the vessel. For a measurement, 0.5 ml of deionised water were applied by a graduated pipette. The drop was allowed to stand for 60 s to allow for the gelatine to soften prior to the application of the probe. pH was recorded when the measurement stabilised or after 5 min if it proved to be unstable. Five measurements per sample were taken and the average recorded.

3.2.2.4 Colorimetry

Colour change is a particularly important parameter for WOP. For this study colour measurements were made with several instruments including hand-held colorimeters, a HunterLAB ColourQuest XE instrument and micro-fadeometers of varying designs. There is much variation in measurement quality and accuracy between these instruments and for a particular experiment only a single method was applied. However, in all cases colour coordinates were calculated in terms of illuminant D65 and a 10 degree observer.

3.2.2.5 Viscometry

Viscometry is a standard method to determine the DP of a cellulosic sample, but it is a destructive method requiring a significantly large sample and is thus not applicable to WOP. However it was applied to the samples as it would provide hard data about the degradation of the paper substrate for correlation to by other experimental methods.

For this research DP of cellulose in paper was determined by the standard viscometric method (ISO 5351/1:1981) (19). DP was calculated from intrinsic viscosity using the Mark-Houwink-Sakurada equation, Equation 1 (20).

$$DP^{0.85} = 1.1[\eta]$$

Equation 1

3.2.2.6 Chemiluminometry

Many oxidation reactions of organic materials, including polymers such as paper, are accompanied by weak photoemission, chemiluminescence (CL). CL is defined as the generation of visible light in the process of a chemical reaction. The energy required to generate an excited state, ΔE^*, is related to the enthalpy of reaction, ΔH_r, and the activation energy, $\Delta H^{\neq}$, Equation 2 (261).

$$\Delta E^* \leq -\Delta H_r + \Delta H^{\neq}$$

Equation 2

Since the visible spectrum extends from 400 to 700 nm, a reaction must produce a molecule with an excited state 171– 301 kJ mol^{-1} above the ground state to be able to generate a visible photon (262). CL-generating reactions have been classified into three groups: direct, indirect, and activated (261). Generalised reaction schemes are given in Schematics 1 – 3, respectively.

$$R \longrightarrow P^* \longrightarrow P + h\nu$$

$$R \longrightarrow P^* \xrightarrow{F} P + F^* \longrightarrow F + h\nu$$

$$R + A \longrightarrow R\cdots A \longrightarrow P + A^* \longrightarrow A + h\nu$$
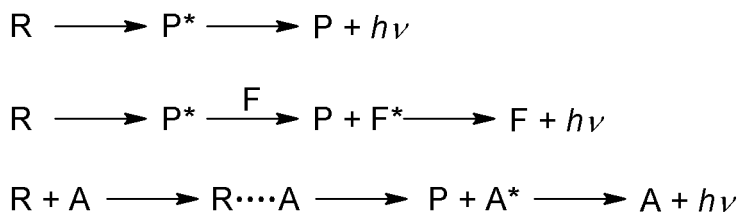
Schematic 1-3 General schematics for direct CL (3), indirect CL (4), and activated CL (5).

In the above schematics "P*" is an excited-state product of a chemical reagent "R" that can relax to the ground state "P" by emitting a photon through direct CL, Schematic 1. "P*" can also transfer energy to a fluorescer "F" to form the excited state "F*", which can then relax to the ground state by emitting a photon through indirect CL, Schematic 2. Alternatively, a bimolecular reaction between "R" and a catalyst activator "A" can occur to form an encounter complex. In this complex "A" donates an electron to R forming a radical cation of "A" and a radical anion of "R". The radical anion of "R" then rearranges to form a radical anion of "P" and undergoes charge recombination with the radical cation of "A" to produce the product "P" and an excited state of the activator "A*" that can then relax to the ground state through emission of a photon via activated CL, Schematic 3 (262).

The intensity of CL can provide information on the kinetics of oxidation reactions at early stages of a material's degradation process (during the so called 'induction period'). Chemiluminometry is therefore an extremely sensitive technique that has been used to study the effect of preparation/processing methods, additives (both pro- and anti-oxidative), and postproduction environments on the oxidative stability of numerous polymer systems (263); its application to paper has been reviewed elsewhere (28). 3.2.2.6.1 Chemiluminometry of Paper

Chemiluminescence from paper degradation can arise from several processes, and dynamic chemiluminometric experiments in nitrogen atmosphere are informative, as different luminescing species decompose at different temperatures in the absence of oxygen thus indicating different thermal stability.

While the exact mechanisms of CL emission are not known, previous studies have related chemiluminescent activity during oxidative degradation to three phenomena (264): in the sub-100 °C region, decomposition of a charge transfer complex between atmospheric oxygen and some appropriate structure in the polysaccharide (activated CL) (18, 245, 264-266); 100 – 160 °C decomposition of hydroperoxides and/or peroxy radical termination (direct CL) (245, 264, 267-271), and >160 °C to transglycosidation of cellulose (direct CL) (270).

The effect of many parameters on CL from paper, including: degree of crystallinity, sample morphology and size (272), water content (273, 274), light exposure (18, 264, 266, 275, 276), atmosphere, super oxide (273), lignin content (245, 266), transition metal cations (277, 278), have been studied.

3.2.2.6.1.1 Works of Art on Paper

However, much of the recent focus has been on the autoxidation of printed and written media, such as library and archive collections, with comparatively little research on the oxidative degradation of works of art on paper, which present a challenge due to their complexity.

A well-studied example of a material that is used for the preparation of both documents and art, is iron gall ink where localised hydrolytic and transition metal catalysed oxidative degradation destroys the paper substrate creating a 'stencil-like' effect (279), however, in this case the degradation has been allowed to progress beyond a point that it is noticeable by eye to when radical interventions are needed. Chemiluminometry on the other hand, has proven to be a useful tool in evaluating the effect of different iron gall ink formulations on the early stages of paper degradation (280).

A watercolour drawing on gelatine-sized paper is a more complex system than an ink drawing on paper as a variety of pigments were typically used. It consists of intercalated components: cellulosic substrate, gelatine size and applied paint, forming a composite material, Figure 1. The paint layers are discretely applied with some areas of over painting, such that neighbouring regions could have different chemistries dependent upon the composition of the applied paint. The hypothesis that chemiluminometry could be used to study the effect of individual colourants on the localised degradation of watercolours and evaluate the effect of anoxia in limiting this degradation was tested in this Thesis.

3.2.2.6.2 Chemiluminometric Instrumentation

Figure 3 is a generalised diagram of a typical top down geometry chemiluminometer. The samples are placed in an aluminium pan within a light-tight sample chamber. Temperature programming and gas flow/composition are controlled by a computer interface. In the diagram, and in the experiments performed on a Lumipol 2 as part of this study, a cooled photo multiplier tube (PMT) was used as a photon-counting detector.
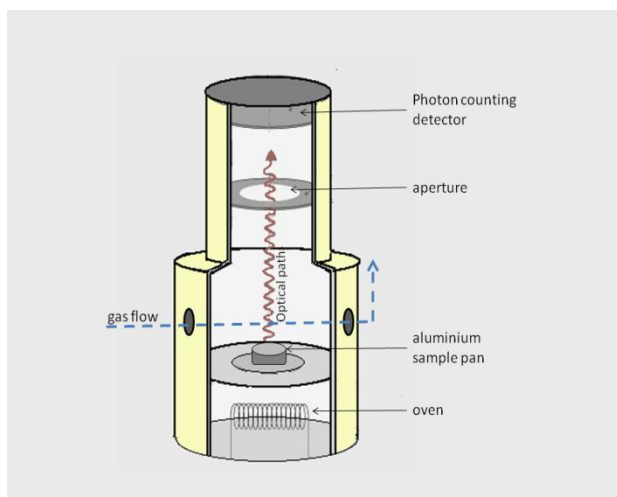
Figure 3 A generalised diagram of a typical chemiluminometer.

Highly sensitive PMTs are a limiting factor in the instrument design as they integrate the signal from the total area per unit time/temperature, and thus there is no spatial separation in the data. It is possible to place filters in the optical path to gain information about the spectral distribution of the CL photons, but due to the extremely low intensity of the phenomenon this method is uncommon. Due to recent advances in charge-coupled device (CCD) design, imaging chemiluminometers, where the PMT is replaced by a CCD, are now being produced. With CL imaging, it is possible to gain information about the spatial distribution of CL within a sample (262). Alternatively the CCD can be configured as a spectrometer for spectral information (262).

3.2.2.7 Headspace Analysis

The VD is the population of volatile compounds in the headspace of an object. A point to remember when considering the VD is that it is comprised of VOCs from the entire object/display/storage system. This fact can be used to evaluate how a new conservation or preservation method (such as modified atmosphere display) affects the degradation of an object, but it can also mean that a highly off-gassing material, such as a laminated wood product or a polymer gasket in the system can overwhelm the signal from the object. Therefore care must be taken in choosing degradation vessels and reactors for these experiments.

When compared to the ISD and ED, analysis of the VD has many advantages: particularly, the VD is not integral to the WOP and therefore it can be sampled. Several sampling methods are available, and they are typically rapid, non-invasive and can be done *in situ.* The collected VOCs can be readily analysed with little to no pre-treatment.

The VD can be analysed *in toto* yielding information about the total VOC (TVOC) content either with a TVOC sensor or a dosimeter or by a more information-rich detector, such as a mass spectrometer (MS). However the data quality is improved through the use of a pre-separation method such as gas chromatography (GC) to create a hyphenated technique, *i.e.* GC-MS. GC-MS is perhaps the most widely applied hyphenated

66

chromatography method, and it is the basis of flavour and aroma analysis (281, 282) and residual solvent analysis (283-287) in the food and pharmaceutical industries as well as several applications in the field of metabolomics (187, 189, 190, 196, 201, 288-292). Through column selection and optimisation of chromatography parameters it is possible to achieve acceptable separation of components prior to detection thereby simplifying the comparison of samples and allowing for the identification of individual components in the degradome.

In addition to denoting detection methods, hyphenation can also refer to the sample introduction methods, for example headspace-GC-MS. Headspace-gas chromatography-mass spectrometry (HS-GC-MS) is a useful tool for monitoring the gas phase within microenvironments. This is being effectively employed within the food packaging industry with regard to taint, odour, and contamination control (183, 219, 293, 294). The techniques used by the food packaging industry can easily be adapted to the microenvironments within museum display cases and frames in general and in anoxic frames in particular.

HS-GC-MS can be accomplished by a variety of means with technical division by differing methods of sample introduction and possible derivatisation techniques. Most HS-GC-MS techniques have the advantage that the methods can be designed to be solventless, non-contact, non-sampling (of the solid phase), and non-destructive (with respect to the object). Data acquisition is relatively straightforward, qualitative results can easily be gained, but matrix effects and method limitations make reliable, direct quantification difficult. This is especially true for complex composite systems such as WOP.

The goal of HS-GC-MS analysis is the qualitative and semi-quantitative analysis of the volatile components in the atmosphere above a sample. HS-GC-MS analysis can be categorised into three main types, static, dynamic, and solid phase extraction (SPE) HS analysis, based on the sampling method (295, 296). All headspace analysis methods rely upon the partition of the analytes between the condensed and vapour phases, and as such the efficiency of the analysis is affected by matrix affects. Readers are directed to Kold and Ettre, *Static Headspace-Gas Chromatography* for a thorough treatment of the theory and practice of HS analysis (295).

3.2.2.7.1 Static Headspace

Static Headspace (SHS) is perhaps the simplest and most mature of the headspace techniques. SHS theory requires that the analytes of interest be at equilibrium between the sample phase and the gas phase above it (295, 297, 298). The samples are typically thermostatted at an experimentally determined temperature for an experimentally determined time prior to sampling. The temperature/time relation is such that the time spent thermostatting is minimised by selecting an elevated temperature level to increase desorption rates from the sample (295, 297).

Upon equilibrium an aliquot of the gas phase is removed from the sample space and introduced into the carrier gas stream in the GC. This can be accomplished with something as simple as a gas-tight syringe or

with automated sampling instruments. These automated sampling instruments provide improved sample throughput and greater reproducibility relative to human operated syringes. Regardless of the means of sample introduction, GC/MS analysis is conducted in the usual manner (295).

Matrix effects, which reduce the concentration of the analyte in the vapour phase, are particularly problematic for static headspace applications that depend upon a reproducibly establishable equilibrium between the condensed and vapour phases of the analytes (295). Several methods have been developed to reduce matrix effects, but they typically involve sample disruption and/or addition of an appropriate solvent or electrolyte to modify the activity coefficient of the system with a goal to shift the equilibrium towards the vapour phase (295, 299). Any method that relies upon sample disruption cannot be termed non-destructive and is therefore not applicable to WOP.

3.2.2.7.2 Dynamic Headspace

An alternative to SHS is dynamic headspace analysis, which is not reliant upon the establishment of an equilibrium. This is principally a method for continuous gas extraction. There are several variants, but in this case purge and trap (P&T) technique is of interest. The idea behind P&T is to achieve 100% extraction of the volatile analytes from the sample matrix (295, 296, 300, 301). This is an exponential process and can take some time. In dynamic headspace analysis the underlying tenet is that the change of mass of a volatile analyte in the sample matrix with time can be expressed in terms of the volumetric flow of the purge gas, thus matrix effects are minimised, and if given long enough purge time, effectively eliminated.

During the process the analytes are diluted in the purge gas and must be concentrated prior to introduction to the carrier gas stream to allow for chromatographic separation. This can be accomplished by various means, but in most recent methods a cooled trap with multi-sorbent packing is employed. The analytes are trapped on the adsorbents and after a complete purge cycle the trap is rapidly heated and back-flushed with the carrier gas. Again upon introduction the GC/MS analysis is conducted in the usual manner.

3.2.2.7.3 Solid Phase Extraction

There are many variations of solid phase extraction (SPE), but they are all based on trapping of volatile constituents on a adsorbing substrate followed by thermal desorption either directly onto the GC injector port, as in solid phase micro extraction (SPME) (302), or into a heated auxiliary chamber/transfer line as in a number of different thermal desorption techniques (284, 296). Following desorption, GC/MS analysis is again conducted in the usual manner. In a sense this is not all that different from purge and trap dynamic headspace analysis, except that each analysis has its own 'trap' that can be tailored to the targeted analytes.

SPE and SPME have been successfully applied in the analysis of heritage objects (89, 179, 303) and in paper degradation studies (304-307). A key advantage of SPME is that the fibre can be used to extract VOCs from the headspace of the sample, or it can be placed on the object, as in contact SPME, to extract semi-VOCs as well as VOCs (89, 204). Through selection of sampling sites, contact-SPME could be used to map VOC

emission relative to the cross section of an object, for instance a book, or with respect to applied materials and conservation treatments (204, 308).

3.2.2.7.4 Selected HS-GC-MS Method

For this research a Tekmar HT3 was used to implement a high throughput method of dynamic P&T-HS-GC-MS. P&T-HS-GC-MS was selected over other HS techniques including static HS and solid-phase micro extraction (SPME) because it greatly simplified experimental design, minimised matrix effects, significantly increased the repeatability of measurements, and facilitated unattended, high throughput analysis of more than a thousand samples with very good reproducibility of the extraction and injection parameters. Another advantage of the technique is that it allowed for 20 ml headspace vials to be used as sealed vial degradation vessels. This last point is significant because it greatly reduced sample preparation time and thereby increased the total number of samples that could be degraded and analysed.

Figure 4 A 20-ml, crimp-cap headspace vial with a sample of watercolour on paper. After degradation in the sealed vial, the sample is loaded into the HT3 and analysed by P&T-HS-GC-MS.

As can be seen in Figure 4, a sample of paper with watercolour is inserted into the head space vial. The vial can then be sealed under a specific atmosphere, and the sample/vial system subjected to accelerated degradation. Batches of samples were thus treated and loaded onto the HT3 sample carousel.

During analysis, a vial is moved to the sample oven, equilibrated at an elevated temperature and hot helium is purged over the sample surface. VOCs are stripped from the sample and flushed from the headspace in the vial onto a cooled trap. After purging is complete the trap is back-flushed and then rapidly heated to desorb the VOCs and transfer them onto the column head. In this set up the column head was not cryogenically cooled, while this option would have increased the resolution of the chromatogram it was not available. Once loaded onto the column the GC operates as per usual according to the temperature programme. The eluted analytes are then ionised by electron impact and detected by the ion trap mass analyser operated in total ion mode to generate a total ion chromatograph (TIC). The TICs were then collected into sample sets and prepared for chemometric analysis to extract information about the degradation of the samples based on their VD.

3.2.2.8 X-ray Absorption Spectroscopy (XAS)

XAS is a widely-used analytical technique for determining the local geometric and/or electronic structure (including oxidation state) of materials, and it typically requires an intense and tunable x-ray source, *i.e.* synchrotron radiation.

Each element on the periodic table has a set of unique x-ray absorption edges corresponding to different binding energies of its electrons. XAS spectra are obtained by tuning the incident photon energy from the synchrotron beam line with monochromator to a range where core electrons can be excited to a higher

energy level. When the incident x-ray energy matches the binding energy of a core electron of an atom within the sample, the x-ray absorption drastically increases, resulting in a drop in the transmitted x-ray intensity, and thus the feature known as an absorption edge. The 'name' of the edge depends upon the core electron which is excited: the principle quantum numbers, n=1, 2, and 3, correspond respectively to the K-, L-, and M-edges (309).

3.2.2.8.1 XAS Spectral Regions

A full XAS spectrum contains both x-ray absorption near-edge structure (XANES) and extended x-ray absorption fine structure (EXAFS) regions. The XANES region begins several eV before the absorption edge and can be considered to extend up to 150 eV beyond the absorption edge. The EXAFS region extends from the absorption edge (309).

XANES K-edge spectra arise from excitation of a 1s electron to orbitals at higher energy levels, and beyond the edge, to continuum. XANES spectra can be divided into 3 data regions: the pre-edge, the rising edge, and the near edge, see Figure 5.
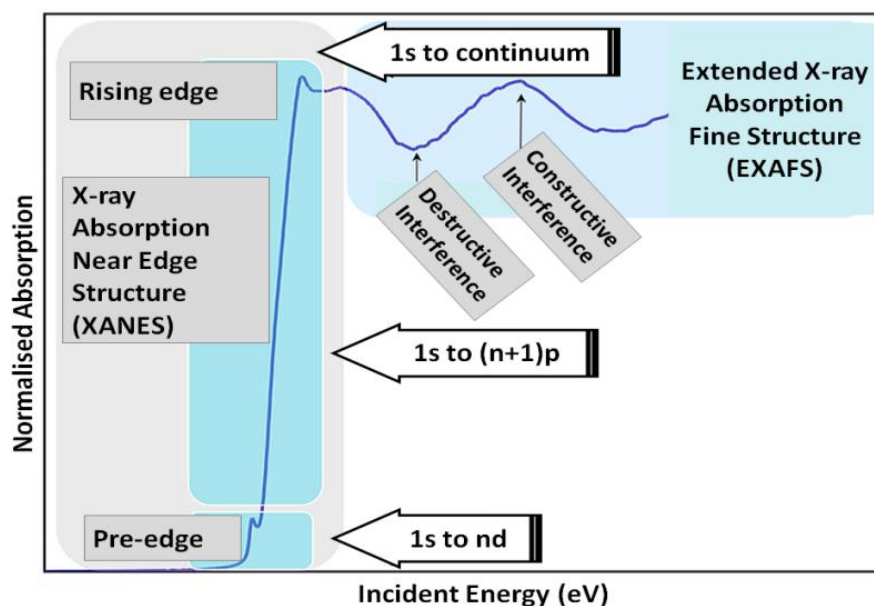
Figure 5 Regions in XANES spectra.

The pre-edge region contains information about the metal oxidation state and metal-ligand field. The K-edge of an open shell transition metal ion displays a weak pre-edge 1s to valence metal d transition. Higher oxidation of the metal leads to greater stabilization of the 1s orbital with respect to the metal d orbitals, thus, leading to higher energy of the pre-edge. Bonding interactions with ligands also change the charge on the metal leading to changes in the energy of the pre-edge (310). Furthermore, the intensity under the pre-edge transition depends on the geometry around the absorbing metal and can be correlated to the structural symmetry in the molecule (311).

The rising-edge follows the pre-edge region and may consist of several overlapping transitions that are difficult to resolve. The energy position of the rising-edge contains information about the oxidation state of the metal, with higher eV corresponding to higher oxidation states.

The near-edge region is difficult to quantitatively analyze. This region is analogous to the EXAFS region and contains structural information about the sample that can be calculated from the radial distribution functions derived from the EXAFS spectra. If the ejected photoelectron is considered to have a wave-like nature, and the surrounding atoms are described as point scatterers, one can imagine the backscattered electron waves interfering with the forward-propagating waves resulting in an interference pattern. This is visible in the spectra as an oscillation in the EXAFS spectra due to a modulation of the measured absorption coefficient. The phase and amplitude of the backscattered wave are dependent on the type of atom responsible for the backscattering and the distance of the backscattering atom from the photon-absorbing atom. The dependence of the scattering on atomic species makes it possible to obtain information pertaining to the chemical coordination environment of the original absorbing atom (309).

3.2.2.8.2 XANES and EXAFS Interpretation

The interpretation of XANES and EXAFS spectra has progressed much in recent years with the application of computational methods to fit the experimentally observed spectra with theoretical spectra and/or combinations of spectra from model compounds (312). This method has been found to work well for mixtures of compounds with known stoichiometries and geometries (311, 313, 314), such as the evaluation of metal oxide mixtures. Though, if the stoichiometry of the sample is unknown, it is a complex mixture of several compounds, or there are contaminants in the material, or the geometry is variable and/or otherwise pure samples of model compounds are not available, these methods are not generally applicable. Unfortunately, in the case of historic Prussian blue pigments all of the above are true for a single sample, and this is complicated further by the huge variability between samples. However, even without a computation-based approach, much can be learned from XANES data of unknown samples if a matrix of relatively well-characterised reference samples can be measured and used in the interpretation of the unknown sample.

3.2.2.9 Alternative Analytical Methods

The list of methods applied to the study of heritage materials in general and WOP in particular is ever growing, and the lag time between the development of a new analytical method and its application to a heritage object is near zero. In addition to the above listed analytical methods several additional techniques could have been applied to answer the question, whether anoxic display is safer than standard display. The following methods could also have been used: size exclusion chromatography (SEC) (20-22, 223, 315, 316), atmospheric pressure ionisation mass spectrometry (API-MS) and spectroscopic methods such as UV-Vis (317-319), NIR (23-26, 229, 320), FTIR and Raman spectroscopy (32, 321, 322). However, the selection of applied analytical methods had to be made based both on the research problematic and upon what

instrumentation and expertise was available at Tate. When considered in this light, GC-MS, and particularly

HS-GC-MS was the obvious choice.

Chapter 4 Turner's Papers and Their Reconstruction

4.1 Turner's Papers

J.M.W. Turner, 1787-1851, was active during an exciting period in the development of paper: the transition from a craft-based to an industrialised system in conjunction with the development of new materials and production technologies (163, 164, 323, 324). Yet examination of the papers he used reveals that, with the exception of some experimentation and use of 'materials at hand', his paper selection, while extremely diverse, is at the same time quite refined and conservative (158, 159).

Some generalisations can be made about the papers used by Turner:

- Turner almost exclusively used handmade papers.
- The fibres in the paper were typically from rag stock with a high flax content.
- The pulp was beaten in a Hollander beater.
- Both wove and laid papers were used throughout his active period.
- The papers were often sized with gelatine.
- The papers have high surface and internal strengths and relatively smooth finishes.
- Examples of papers from non-rag fibre sources, machine made papers, or rosin sized papers are rare to non-existent in Turner's oeuvre (158, 159).

In his early period Turner primarily used writing, wrapping and cartridge papers for his watercolour and pencil drawings, while in his later years he used specialty drawing papers as they became available in addition to his stocks of the above papers (156-160, 164, 323). These new papers refined the traits that made the earlier writing and wrapping papers ideal for use as artist's materials (163, 164, 323), however they did not totally supplant the re-appropriation of other papers for artists' work. Peter Bower has catalogued Turner's use of papers, and the results of his work can be found in his two excellent books and several articles on the subject (156-160). Readers unfamiliar with the craft of hand papermaking are advised to consult *Papermaking* by Dard Hunter(163) and/or the monograph by Timothy Barrett (324) for a thorough review of the subject.

4.2 Contemporary Handmade Watercolour Papers

As noted in Chapter 3 it was not possible to sample the papers in the Tate collection, nor was it possible to collect significant quantities of matched historic paper for the Anoxic Frames Project's (AFP) research. Therefore it was necessary to either identify or commission a modern paper that reproduces the properties of the papers used by Turner.

The tradition of high quality handmade artists papers has not been completely lost, and several papermakers market 'Turner' watercolour papers and/or papers prepared from 'linen' rags (325)[17]. Samples of several of these papers were acquired, examined and compared to papers in the Turner collection at Tate. However, all of the papers examined significantly differed from those used by Turner (326). Generally, the contemporary handmade watercolour papers:

- Are thicker and stiffer with a much higher grammage than the papers used by Turner.
- They tend to have high cotton linter content, which, due to the short length of the fibres, leads to lower surface and internal strengths.
- Papers prepared from 'linen' rag stock contain a multitude of non-flax fibres, including a not insignificant amount of manmade fibres as identified by light microscopy (326).
- Furthermore some papers marketed as gelatine-sized were actually made from pulp stocks treated with a synthetic internal size and later sized with a gelatine solution; this double sizing would give both different working properties and different degradation products.

In addition to the identifiable inadequacies in the 'off the shelf' papers, there was the spectre of the unknown. It was decided that there were too many unknown and uncontrollable variables when buying paper from a stationer, and it was decided that a bespoke paper, designed to reconstruct a type of paper used by Turner, should be produced. This paper would have a controlled composition, furnish (processed fibre content), size (a treatment to increase the hydrophobicity of the paper surface), grammage (gm^{-2}) and finish (surface treatment). Furthermore, a post from a single vat could be purchased thus ensuring homogeneity of the sample materials for all experiments conducted within the AFP.

4.3 Selection of a Case Study Paper

A white, wove drawing paper bearing the watermark: 1794/ J WHATMAN, made by William Balston and the Hollingsworth brothers at Turkey Mill, Maidstone, Kent was used as a basis for the reconstruction paper. Works attributed to both Turner's early period and his later years can be found on this paper. It was used both 'cut down' and bound into sketchbooks and in a variety of full sheet sizes (159). It can be reasonably concluded that this was a 'favourite' of his and that he had a large stock of the paper for his use. Furthermore, papers bearing the same watermark were available in a private collection for sampling and fibre analysis.

When taken in hand, the paper is relatively thin with a nice tooth and no fibres are loosened after dragging a fingernail, this indicates that it has a good surface strength and is in good condition. It has pleasant rattle indicating high internal strength. Visual observation of the papers reveals that the surface is relatively smooth with no heavy marking from the felts. The paper would be described as having a NOT finish. That is

---

[17] Falkiners in London stocks a selection of fine handmade papers from various paper mills.

that it was 'not glazed', but probably exchanged pressed before drying (to remove felt marks) and pack pressed after sizing.

In reflected light microscopy it is readily observable that the bulk of the fibres are white to off white, and based on common practice of the time, they are presumably from rag sources (157, 160, 163). In addition to the white fibres, there are darker coarser fibres, probably from ropes or coarse textiles as well as some coloured fibres, primarily red and blue, these were probably added during beating as a colour corrector (157, 163). White particles are observable in the paper; this is likely calcium carbonate, perhaps chalk, that would have been added as a bulking agent/filler but also as a whitener and an alkali reserve and stabiliser.

Fibre analysis, by transmitted light microscopy, was conducted on samples of fibres lifted from papers bearing the same watermark/counter mark that are held in private collections[18]. This analysis reveals that the bulk of the white fibres are flax with measurable cotton content; the visual observation of fibre morphology was supported by addition of neocarmine W which is used to distinguish different cellulose fibres, staining cotton bluish and flax reddish, Figure 1. The coarser fibres observed in the paper are likely hemp, and the coloured fibres are predominantly wool.

Figure 1 A fibre sample stained with neocarmine, dark field, and 40 x. The fibres are quite disrupted and identification by structural features alone is difficult, but by adding neocarmine W it is possible to note that most of the fibres are flax, reddish, with a few cotton fibres, blue, also present. The fibre ratio was variable between slides, but ca. 50:1 flax/cotton is typical. Also visible in the upper right is a wool fibre that is stained yellow by the neocarmine W.

That the paper is gelatine-sized is supported by positive results for hydroxyproline by Erhlich's reagent, and a red colour appears upon the addition of Aluminon reagent, thus indicating that alum was likely added to the gelatine solution. The results of these observations and analyses served as the starting point for designing the reconstruction paper.

---

[18] A sheet of this paper was available for analysis at the paper fibre identification workshop conducted by Peter Bower in July 2007, additional samples of the same paper were later collected by the author as part of his reference paper collection.

4.4 Turner White Reconstruction Paper

The design of a reconstruction paper is an involved process. It is not simply a task of analysing the materials and properties of the case study paper, and then using the same materials to make a new batch of the old paper. The availability of materials and the technologies of their processing have changed significantly with time. To account for these changes, and select appropriate substitute materials, the final purpose of the paper must be considered when selecting new materials for its production (325, 326).

In the case of the AFP, there were three threads of related research – reconstructing Turner's materials and techniques, developing tools to predict the display-associated colour change of WOP and developing and evaluating modified atmosphere display technologies – that required an accurate reconstruction paper. These three end-uses exhibited different pressures on the refinement of the design, and a balance between the three had to be struck. Three parameters were considered during design optimisation:

- The paper needed to have a composition similar to historic rag papers.
- The paper needed to have similar optical properties to historic papers.
- The resulting paper needed to have similar working properties and accept watercolour paints in the way as we imagine that the papers used by Turner did.

Master papermaker Chris Bingham of Ruscombe Mill was commissioned to make a white Turner reconstruction paper according to my specifications, and the resulting recipe derives from the above described analyses and observations and his and the author's experience as papermakers.[19] The process was complicated by the fact that the author was not able to travel to his mill, but test samples were exchanged by post and discussed over the phone.

4.4.1 Reconstruction Paper Recipe

4.4.1.1 Fibre Furnish

- 60% flax 40% cotton
  - 6.6 kg Total Chlorine Free (TCF) bleached, LINCELL B supplied by Celesa, Tortosa, Spain
  - 4.4 kg TCF bleached, security grade cotton linters (DS11) supplied by Celsur, Fonelas, Spain

---

[19] The author studied papermaking under Timothy Barrett at the University of Iowa Centre for the Book from 1997 to 2001. His experience as a hand papermaker has greatly informed this research as it gives me an insight into the materials, technology, properties and applications of the papers used by Turner and those available on the market today.

4.4.1.2 Beating

- The pulp was beaten in 300 l of tap water for 3.5 h in a Hollander beater with the roll lowered and brushed for 1 h with the roll raised.
- An unrecorded amount of precipitated $CaCO_3$ was added during beating to ensure an alkaline reserve in the paper.

4.4.1.3 Sheet Forming

- Sheets were formed to approximately 200 gm^{-2} on a Imperial (56 x 76 cm) wove mould and couched onto Voith woollen wove HN marking felts[20],
- The post was then pressed, exchanged and pressed again.

4.4.1.4 Drying

- 40 sheets were separated from the post and loft dried in single spurs to produce a rough finish.
- The remaining 80 sheets were exchanged a second time and pressed to 40 ton overnight, and they were then loft dried in spurs of 5 sheets, to produce a NOT finish.
- After loft drying 8 spurs of 5 sheets were parted, and the 40 sheets rewetted and restraint dried before glazing.

4.4.1.5 Sizing

- 20 sheets of each of the drying regimes were tub sized at 35 – 40 °C with 3% (w/w) edible hide gelatine, type 200 single bloom supplied by Trobas, Dongen, Netherlands to which a solution of 5% $KAl(SO_4)_2$ (w/w) was added.
- The sized sheets were gently pressed to remove excess gelatine.
- The sized sheets were loft dried in single spurs for 3 weeks to produce sized paper.
- The remaining papers were left unsized (waterleaf).

4.4.1.6 Finishing

- The 40 sheets that had been restraint dried were trimmed to 52 cm wide and glazed in a single pass between stainless steel sheets at a roll load of 200 bar to produce a glazed finish.
- The resulting 120 sheets, 20 sheets of six types of paper, were then pack pressed to render them flat prior to shipping.
- Upon delivery the paper was allowed to rest for at least two weeks before being used. Ideally this period would have been closer to six months, but time constraints did not allow for this.

---

[20] Note that due to abnormally cold temperatures and a broken vat heater, the water temperature was 20 °C instead of the typical 28 – 29 °C.

Furnish	Size	Finish	Acronym
60/40, linen/cotton	gelatine	rough	GSR
60/40, linen/cotton	waterleaf	rough	WLR
60/40, linen/cotton	gelatine	NOT/cold pressed	GSCP
60/40, linen/cotton	waterleaf	NOT/cold pressed	WLCP
60/40, linen/cotton	gelatine	glazed	GSG
60/40, linen/cotton	waterleaf	glazed	WLG

Table 1 A summary of the six papers produced by Ruscombe Mill for the AFP.

The result was a set of 6 papers with identical fibre furnish, three different finishes: rough, NOT/cold pressed and glazed, and two size treatments: waterleaf and geatine-sized, see Table 1. These papers were used in the preparation of samples for the bulk of research described in this Thesis as well as in the other research conducted by the AFP. For samples of the papers please see the tip-ins included in Appendix A in the printed version of this Thesis. Please contact Tate Conservation Science with regards to obtaining samples of this paper.

4.4.2 Comparison with the Historic Papers

There are some significant differences between the reconstruction and case study papers, and there are points for improvement that would bring the reconstruction papers closer to the case study paper, however, generally the reconstruction papers compare favourably to the case study paper, and they were adequate for the AFP, and they can be considered representative of papers used by Turner.

4.4.2.1 Composition

When compared to modern papers with their host of additives and coatings, the compositions of the papers used by Turner are relatively simple. Turner's papers can be reduced to a system of two major components: fibre and size.

4.4.2.1.1 Fibre Source

The case study paper's fibre furnish is predominantly flax with some cotton fibres, ca 50:1 or more. These fibres undoubtedly came from rag sources. It is still possible to purchase rags for papermaking, and several companies market rag papers. However, rags today differ significantly from those of the late 18th to mid 19th centuries. The key difference is in rag source; it used to be that paper mill was the final destination of a textile after years of use when it could no longer be repurposed to any other application – thus, post-consumer rags (324, 326). Today rags for papermaking are often the off-cuts, scraps and other refuse of the garment industry – thus, post-industry rags (326-328). The difference in origin results in two very different pulp stocks. Years of use and the practice of washing clothes by boiling them with a lye soap, scrubbing/beating, then rinsing and drying in the sun leads to increased degradation and oxidation of the fibres as well as to a more off-white to grey hue to the material (163, 324, 326-331), while the rags of today have never been worn, and they have often been pre-treated with various chemicals, including optical

brighteners, to render them bright white and suitable for the modern consumer. Another consideration when approaching modern 'linen textiles' is that term linen broadly refers to a textile weave, and not to a fibre source. A 'linen textile' typically includes predominantly flax fibres; however it can have significant portions of cotton, hemp and even manmade fibres. Microscopic examination of modern 'linen rag' papers certainly bears this out, as cotton, manmade and other non-flax fibres are readily distinguishable (326).

Considering the differences between rags of today and those of yesteryear, it was decided that paper with a known composition was of greater importance than one with a literal match in fibre source. This left three options for sourcing the fibres:

1. Acquisition and pulping of historic textiles with known composition,
2. The use of raw fibres,
3. The use of commercially prepared pulp stocks.

It was not possible to acquire enough historic linen textiles to prepare a large enough batch of paper for this research, and so this option was discarded.

Raw flax as a fibre source was also explored, but raw flax requires long retting periods, and a paper prepared from raw flax has significant lignin content due to the remaining shive on the flax bast fibres. Thus the paper would be chemically different from the case study paper. Furthermore, paper prepared from raw flax would have been buff or drab in colour rather than the white of the case study paper.

The final option, using commercially prepared pulp stocks, was chosen because it had several merits that could not be ignored:

1. Commercial pulp stocks are available in effectively limitless quantities.
2. They have known composition and pre-treatment; thus allowing for greater confidence in the final product and its degradation behaviour.
3. They are commonly used by hand paper mills; therefore the experience of the papermaker can be directly applied and little experimentation during beating is needed.
4. Different batches of pulp stock are quite homogenous allowing for the papermaker to reproduce the same paper from a recipe.
5. It is possible to choose pulp stock with a specific pre-treatment; thereby the pre-oxidised nature of pulp made from historic rags can be simulated.

Through evaluation of the properties of available pulp stocks and consultation with Chris Bingham, TCF bleached LINCELL B supplied by Celsa, Tortosa, Spain and TCF bleached DS11 security grade cotton linters supplied by Celsur, Fonelas, Spain were selected.

The case study paper is mostly flax, ca. 50:1 flax/cotton ratio, however a 3:2 flax/cotton ratio was agreed upon for the reconstruction paper. This ratio was chosen to adjust for differences between modern pulp

stock and historic rag pulp: LINCELL B has long fibres and produces very strong but stiff papers, and security grade cotton linters, while pure cellulose, are very short, and they give the paper more suppleness. If a paper would be made with a 50:1 ratio of LINCELL B and security grade cotton linter it would have more in common with a cigarette rolling paper than an artists' paper. The stiffness of the LINCELL B is due the fact that flax fibres initially have a high degree of crystallinity; extended use, repeated launderings and as well as chemical and microbial degradation lead to a reduction in the degree of crystallinity and an increase in supplenesss of flax fibres from rag sources. As a virgin fibre, LINCELL B has not been significantly degraded and retains a high degree of crystallinity. By adjusting the flax/cotton ratio it is possible to account for the differences in pulp properties, and thus the paper can be tuned to a specific application.

4.4.2.1.2 Fibre Pre-Treatment

The state of pre-degradation of the pulp stock was considered when selecting a fibre source. Ideally the fibres used in the reconstruction paper would have a similar pre-degraded state as the historic rag fibres. As such, the pre-treatments, such as delignification and bleaching, of the reconstruction papers' pulp stock were carefully considered.

With respect to the case study paper, upon arrival at a paper mill, the (already well worn and degraded) rags were sorted by quality. After sorting the rags were often washed in a hot caustic solution and sometimes bleached with chlorine gas (157, 163, 331). These treatments would render the rags softer and whiter, but also more degraded and oxidised (163, 164, 323, 331). The exact pre-treatment of the pulp stock used to prepare the case study paper is unknown, but XRF analysis of watercolours by J.M.W. Turner did not detect chlorine which would be indicative of chlorinated residues, and thus chlorine bleaching (331-334). Therefore it is unlikely that chlorine bleached rags were used in the preparation of the case study paper; this is supported by the general good condition of the case study paper (331). It is impossible to verify whether or not the rags were washed in a hot caustic solution, but as that was the common practice of the time (157, 163, 324), it can be assumed.

From the above it can be assumed that the pulp stock of the case study paper was:

- Pre-oxidised and degraded through extended use, microbial attack, abrasion and laundering in hot alkaline solutions (36, 335-337),
- It is also likely that these rags were boiled in a caustic solution after they were sorted at the paper mill. This treatment would have led to mercerisation of the fibres and conversion from type 1 to type 2 cellulose (338, 339),
- It is unlikely that a chlorine bleaching agent was used on the rags (334).

Based on these three points total chlorine free (TCF) bleached pulp stocks that had been delignified by oxygen/alkaline treatment were selected. TCF bleached pulp was selected over elemental chlorine free (ECF) bleached pulp because TCF bleaching excludes all chlorinated compounds and thus the production of

chlorinated residues that remain in the pulp stock (340). Furthermore through the use of oxidising agents such as H_2O_2, oxygen and enzymes, as well as hot alkaline stages, oxidised functionalities and morphological changes analogous to that of historic rags are introduced onto the cellulose macromolecules (27, 333, 341-347).

Because we were attempting to make very accurate reconstructions of watercolours by J.M.W. Turner, the issue of forgeries and their identification was discussed. Security grade cotton linters were selected as the cotton fibre; linters are the shortest fibres adhering to the cotton boll after removal of the textile fibres. Due to their short length and distinct morphology they are easily distinguishable from textiles fibres during microscopic examination. Additionally cotton linters were not used in industrial papermaking until the 1940s (328); therefore they can be used to firmly establish an earliest possible date for an object. Thus any painting prepared on the reconstruction paper would clearly be distinguishable late 20th – early 21st century, and not a Turner, after only the most precursory fibre microscopic examination.

Through these fibres it is possible to not only recreate the properties of the case study paper using known modern materials, but also to embed a 'tracer fibre' in the paper for easy identification of forgeries.

4.4.2.2 Optical Properties

The optical properties of the reconstruction paper were assessed by eye and with a colorimeter, with both the surface texture and colour evaluated. The surface texture (finish) of the reconstruction paper and whiteness were a concern for the micro-fadeometry and chemiluminometry experiments where the finish and homogeneity as well as colour of the substrate are hypothesized to be significantly contributing variables. These parameters can affect the scatter and absorption of light (both incident upon and emitted from the surface) as well as the perception of colour. Furthermore the same factors greatly affect the application of watercolour paint and the appearance of the final work.

4.4.2.2.1 Surface Finish

After evaluating the papers it was determined that while not perfectly matching the case study paper, they were useable for the project's purposes. It was found that the WLR and GSR papers were too rough in finish to be used neither for micro-fadeometry samples nor for reconstructions of the originals. The WLCP and GSCP were also too rough when compared to a writing paper, but comparable to some more textured papers that Turner used. The WLG and GSG papers were found to be almost too smooth, but they accepted paint very well.

The WLR and GSR were used to prepare samples for headspace analysis where surface finish was thought to be a non-contributing variable with respect to the degradation of the the samples. The WLCP, GSCP, WLG and GSG were used to make reconstructions of Turner's watercolour drawings. WLG and GSG were used to prepare samples for micro-fadeometry as well as for chemiluminometry experiments where a smooth and homogenous finish is desirable.

A recommendation for a second batch of the paper would be to eliminate all of the rough finish papers and produce only WLCP, GSCP, WLG and GSG. The finish of cold pressed papers, WLCP and GSCP, could be rendered smoother by adopting the restraint drying practice used to prepare the glazed papers. The glazed papers, WLG and GSG, should be glazed at a lighter roll load. The load pressure must be determined by experimentation. There are significant quantities of the WLCP and GSCP remaining such that they can be used to undertake the proposals mentioned above.

4.4.2.2.2 Colour

The waterleaf papers are significantly whiter than the historic papers. The gelatine-sized papers are slightly less white than their waterleaf counterparts; they are still whiter than the case study papers. This fact is not surprising as there is more than 200 years difference in age and a significant difference in fibre sources. Additionally, the goal of the reconstruction paper was not to make a new paper that looked old, but rather to make a new paper that behaved like the papers that Turner used when they were new.

With respect to micro-fadeometry and chemiluminometry, the increased whiteness is a desirable feature as it should reduce the interference of the substrate through absorption of both the incident and emitted photons. For the preparation of reconstructions, the difference in colour was not considered to be a detriment as Turner was known to tint his papers on occasion, particularly the new white drawing papers used in his later works, to match the warmer drabs and browns of the papers from his earlier period (156, 158, 159). If a less white paper is needed for a reconstruction, an experienced watercolourist is capable of doing the same.

4.4.2.3 Working Properties

Turner was very innovative in his watercolour technique, employing atypical tools and methods to achieve his desired effect (162). Using modern watercolour papers, several artists have attempted to recreate Turner's techniques (348, 349). Their attempts have led to greater or lesser success in recreating the effect, but arguably they have not recreated the technique because they were using a different type of paper from what Turner was using. The working properties of paper substrate in part defines what techniques can be used in watercolour drawing, and unlike any other medium, in watercolour, the substrate is as important as the applied paint in achieving a desired effect.

The working properties of a paper stem from many variables, from the fibre furnish to every factor in the process of making the sheet. A small change in beating time, vat temperature, pressing pressure, temperature/humidity in the drying loft will change the properties of a sheet. It takes years of experience to understand the subtle interplay of variables and how to correct for changes, and even then there can be significant differences between batches of the same paper.

The case study paper was not available for use in the preparation of watercolour drawings and thus a direct comparison of the working properties was not possible. But by comparing the results of object reconstructions to the originals the comparison can be inferred.

4.4.2.3.1 Thickness

When comparing the reconstruction paper to the case study paper it is immediately apparent that the reconstruction paper is much thicker than the case study paper and as a result much stiffer. However, the difference is not too gross and it should not affect most watercolour techniques. An exception to this would be any technique that relies upon the translucence of the substrate to impart luminosity to the object either in bulk, as with a thin sheet of paper, or by localised thinning of the reverse to create highlights.

In a subsequent batch of this paper, it is recommended that instead of pulling sheets to achieve 200 gm^{-2}, sheets with a grammage of 140 – 160 gm^{-2} be produced. In addition to reducing the grammage, pressing the post at a higher pressure with more exchanges would also produce a thinner and more homogenous sheet with enhanced internal and surface strengths. Though care must be taken to not render the paper too crisp.

A reduction in grammage will reduce the thickness and stiffness of the sheet, but the internal and surface strengths, which are dependent upon other factors, should remain the same.

4.4.2.3.2 Wet Working Properties

The reconstruction papers have high internal and surface strengths, comparable to historic handmade papers. These properties were assessed by a trained conservator, Charlotte Caspers, who is specialised in the reconstruction of painting techniques as well as by a master papermaker, Chris Bingham, who has previously reconstructed historic papers. The internal and surface strengths of a sheet are perhaps the two most important properties with regard to watercolour drawing. They define what techniques are possible on a paper and directly lead, along with the size, to the wet working properties. These properties derive from several factors including pulp stock selection and preparation as well as the paper production process (324).

In addition to the above the type and hardness of the sizing agent plays an important role. When compared to modern watercolour papers, even those sized with gelatine, the reconstruction papers are extremely hard sized. This feature can be disconcerting for contemporary watercolour artists accustomed to neutral synthetic internal sizes, and it requires different methods of preparation and a different working style. Because of the gelatine size the sheet must be thoroughly wetted and stretched before use. This helps to prevent cockling and also help to even the surface of the NOT finished papers. Once stretched and dried, the paper can be used as is or re-wetted for wet working.

The high strength of the reconstruction papers allows for more aggressive brush work and alternative tools, *e.g.* etching tools, brush ends, bread crusts, to be used even when working on a fully wetted sheet. Turner is

noted to have used such tools when preparing his paintings. Papers with a low strength will tear and pill with rough treatment.

A hard size also inhibits the adsorption of the pigment particles into the fibre matrix, such that the colours float on the surface of the sheet. This allows for colours to be moved about the surface, blended, as well as to be lifted off with a dry brush. The 'lifting off' of paint to form an image is a technique that modern artists have gone to great measures, *e.g.* painting a resist onto the paper surface (348, 349), to duplicate on modern papers, but the reconstruction paper is sized sufficiently hard degree that a resist is not needed and the artist can work closer to Turner's free technique. If a more hydrophilic region is desired, the sheet can be wetted and the size removed (either generally or locally) with mild abrasion. In the de-sized areas the colours will enter deeper into the fibre matrix and 'bleed' slightly.

In addition to improving the wet working properties of the watercolour paper, a heavy gelatine size has been correlated to increased permanence and durability of papers (316, 350-354).

4.5 Conclusions

There are several differences between the reconstruction papers and the case study paper, predominantly relating to weight and texture, but also whiteness. It is probable that with 200 years of natural ageing the reconstruction papers will undergo some whiteness reversion and mellow to the off-white that is visible in the target. Despite the noted differences, the reconstruction papers prepared for the AFP are adequate for the purposes of the research.

With respect to the ageing of the reconstruction papers, during their preparation every care was taken to ensure that they are free from modern and synthetic fibres and sizing agents. Fibre microscopy has confirmed the lack synthetic fibres in the fibre furnish. This care, while not a guarantee, is enough to give confidence in the results of the analyses of the headspace above aged samples.

With regard to workability, the fact that many of the effects observed in Turner's paintings can be produced on this paper using the techniques and tools that Turner is reported to have used is a good indication that the reconstruction paper is representative of the target paper.

Chapter 5 A Chemiluminometric Study of Watercolour Paints on Paper

5.1 Introduction

The photodegradation of watercolour drawings prepared with madder lake and Prussian blue (PB) pigments was studied by chemiluminometry, viscometry, and colorimetry. A method of *recto* irradiation and *verso* measurement was developed to overcome absorption of the chemiluminescent photons by the paint layer.

A complex relationship between paper substrate, applied chromophores and associated transition metals was observed with strong correlations between the presence of transition metals associated with the madder lakes and the degradation of the paper substrate and the applied paint layer as well as evidence of prooxidative activity by the chromophores in the applied paint layers. The prooxidant behaviour appears to be dependent on the type of transition metal present. This is the first in depth research into the photodegradation of madder lake-based watercolours where the chemistry of the processes is attempted to be understood. The presence of Prussian blue (PB) pigments also has a complex effect on the oxidation of the paper substrate: heavy applications seem to have a protective, filtering effect; photoactive pigments, such as ZnO, added as extenders (a common practice with PB), results in increased peroxide production; and there is evidence that the peroxides produced during the photo-oxidation of paper can participate in the re-oxidation of photoreduced PB. The PB samples used in this study are all of the soluble type, with a formula of $M^+Fe^{(III)}[Fe^{(II)}(CN)_6]^- \cdot 1\text{-}5\ H_2O$ where $M^+ = Na^+, K^+, Rb^+, Cs^+, Tl^+, NH_4^+$, see Chapter 6 for a description of the structure and reactivity of Prussian blue.

Paper is the most prevalent information vehicle in human history, and the preservation of paper-based materials has been the focus of numerous recent research projects (355). However, much of the recent focus has been on printed and written media, such as library and archive collections, with comparatively little research on the preservation of works of art on paper, e.g. watercolours.

In the case of works of art on paper, emphasis is on the visual impact of the object and less on its mechanical stability. Photo-induced degradation, which can result in colour change of the paper support and/or the applied colourant, is of prime interest. It can be divided into two broad groups of reaction pathways, direct photolysis and photosensitised degradation (18). Typically, in a museum, lighting is filtered to cut out ultraviolet wavelengths below 400 nm, and direct photolysis of cellulose does not occur. On the other hand, various chromophores, e.g. applied colourants, reactive groups (carbonyls) attached to the cellulose backbone or additives, fillers and sizing agents, which do absorb in the visible region, can participate in direct photolysis and photo-initiated reactions to produce reactive species (18) and thereby photosensitised degradation.

In works of art, organic colourants have been noted to have a beneficial light-filtering effect at high colour densities (356). However, photodegradation of textiles in the presence of applied dyes is also a known problem (357-359). Additionally, transition metal containing salts are often used in the preparation of lake pigments from organic dyes, and transition metals in paper have been shown to promote oxidative degradation of cellulose through the formation of hydroxyl radicals via Fenton-like decomposition of peroxides(37, 360). To further complicate the situation; most organic colourants have a polyphenolic structure that can have potent antioxidant activity through multiple mechanisms (361-365), and in some cases, in the presence of transition metal cations, pro-oxidant activity via a modified photo-Fenton-like process (366-371).

Alizarin	R1=R2=OH, R3=R4=H
Purpurin	R1=R2=R4=OH, R3=H
Pseudopurpurin	R1=R2=R4=OH, R3=COOH
Rubiadin	R1=R3=OH, R2=CH3, R4=H
Munjistin	R1=R3=OH, R2=COOH, R4=H
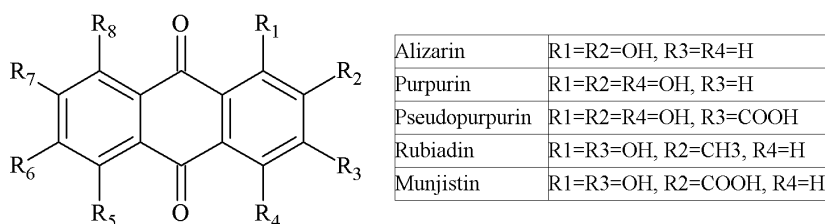
Figure 1 Structures of primary chromophores found in madder lake.

Madder lake pigments are a good example of such an organic colourant system that has the potential for anti/pro oxidant activity. They are prepared from an acid hydrolysed dye solution extracted from the roots of the madder plant, typically *Rubia tinctorum* L., but also *Rubia cordifolia* L. The dye is laked to a pigment by adding hot $KAl(SO_4)_2$ solution, and precipitating pigment with soda or borax. Additionally, metal salts, kaolin, and/or alumina might be added prior to precipitation to provide a support for or to change the hue of the resulting lake pigment (372, 373). In the early years of manufacture of these pigments, a wide range of such additives can be found in surviving examples. In madder lake pigments, the primary chromophores are alizarin and purpurin, but also pseudopurpurin, munjistin, rubiadin, and the glycosidic forms of each chromophore can also be present depending on the preparation conditions and species of *Rubia* used (319, 373). All of the chromophores share the base 9,10-anthraquinone (AQ) structure but with different functional groups at carbons 1-4, Figure 1.

Chemiluminometry (CL) has been used as a means to assess the oxidative stability of numerous polymer systems (374), and its application to paper has been reviewed elsewhere (28). Chemiluminescence from paper can arise from several processes, and dynamic chemiluminometric experiments in nitrogen atmosphere are especially informative, as different luminescing species decompose at different temperatures in the absence of oxygen thus indicating different thermal stability. Previous studies have related chemiluminescent activity during dynamic experiments under nitrogen to three basic phenomena: in the sub 100 °C region, decomposition of a charge transfer complex between atmospheric oxygen and some appropriate structure in the polysaccharide (16, 18); 100 – 160 °C decomposition of peroxides, and >160 °C to transglycosidation of cellulose (375).

86

Based on the success of previous chemiluminometric studies on paper-based systems, we investigated whether chemiluminometry could be an effective tool to study the effect of colourants on works of art on paper. However, as the photomultiplier tube used as a detector has a peak sensitivity between 300-600 nm, there is potential for competition for photons with any chromophores present in the sample that absorb light in the same interval. In this study, a method was developed to minimise the absorption of CL photons by monofacially-applied colourants, and evaluate the effect of applied colourants on the oxidative stability of a paper object.

5.2 Materials

5.2.1 Paper

A reconstruction, hand-made paper based on an 18th century white wove writing paper (watermarked J WHATMAN countermarked 1794) was prepared by Ruscombe Mill, Margaux, France, using 60% total chlorine free bleached LINCELL B supplied by Celesa, Tortosa, Spain, and 40% security grade cotton linters (DS11 HS) supplied by Celsur, Fonelas, Spain. The average grammage of the resulting paper is 200 gm^{-2}.

Half of the resulting glazed waterleaf was then sized with a 3% solution of type 200 single bloom hide gelatine supplied by Trobas, Dongen, Netherlands, at 35 – 40 °C to which was added 5% w/w $KAl(SO_4)_2$. Hereafter the gelatine sized glazed paper is referred to as GSG and the unsized waterleaf glazed paper is WLG.

The pH of the papers was measured with a surface probe and found to be 7.4 and 6.2 for WLG and GSG respectively. The average DP of WLG and GSG prior to application of paint and irradiation are 2260 and 2170 respectively.

Please see Chapters 3 and 4 for a detailed protocol for the preparation of the reconstruction paper and an evaluation of the paper.

5.2.2 Paint[21]

Madder lake pigments were popular amongst artists in the 19th century, and the British artist J.M.W. Turner (1775-1851) made extensive use of them in both his oil and watercolour paintings (233). The colour range of

---

[21] NB: *chromophore* refers to conjugated organic compounds that are constituents of organic colourants, *pigment* refers to a solid colourant without added binding media, *dye* refers to a liquid organic colourant (solution), *lake pigment* refers to a solid organic colourant prepared from a dye by precipitation/sorption of the chromophores, *paint* refers to a prepared liquid, pigment/binding media system capable of forming a dry film and *colourant* is a generic term to refer to all of the above.

his madder palette is very broad with hues ranging from pink and red to yellow to brown. Watercolour paints were prepared from J.M.W. Turner's dry studio pigments held in the Tate Conservation Archive (233). The pigments were ground by hand with deionised water and gum Arabic solution to make the paints. They were allowed to evaporate at room temperature and were then stored in sealed Petri dishes for later use. Flakes of the prepared paints were reconstituted in deionised water, painted onto wetted and stretched GSG or WLG, and allowed to dry restrained. After drying, the colour of each sample was measured in CIE 1976 L*a*b* colourspace to evaluate the density of the paint layer. See Table 1 for a description of the pigment samples used in this study. Readers are directed to Chapter 3 for a detailed description of the paints used in this study as well as to Charlotte Casper's Thesis, *Reconstructing British 19th-century Watercolour Paint* (167).

Table 1 A description of the pigments used in this study.

Sample	Description of the dry pigment	Madder species	Chromophores as determined by TLC [25]
TTB1	brownish-red powder	*R. tinctorum* L.	purpurin, pseudopurpurin, alizarin, other unidentified high hR_f component
TTB2	bluish-red powder	*R. tinctorum* L.	purpurin, pseudopurpurin, alizarin, other unidentified high hR_f component
TTB5	dark brown powder	*R. tinctorum* L.	purpurin, pseudopurpurin, alizarin, other unidentified high hR_f component
TTB8	bluer red powder	*R. tinctorum* L.	purpurin, pseudopurpurin, alizarin, other unidentified high hR_f component
TTB11	bluish-red powder	*R. tinctorum* L.	purpurin, pseudopurpurin, alizarin, other unidentified high hR_f component
TTB13	dull yellow fragments	*R. cordifolia* L.	munjistin, rubiadin, alizarin, other unidentified high hRf component
TTB14	bluish-red powder	*R. tinctorum* L.	purpurin, pseudopurpurin, alizarin
TTB15	dark brown powder	*R. tinctorum* L.	purpurin, pseudopurpurin, alizarin, other unidentified high hR_f component
TTB16	dark brown powder	*R. tinctorum* L.	purpurin, pseudopurpurin, alizarin, other unidentified high hR_f component
Sample	**Description of the dry pigment**	**Source**	**Other comments**
TCA1	medium blue powder	Cornelissen Antwerp blue	soluble PB with ZnO and $BaSO_4$ added as extenders, analysed by SEM-EDX and light microscopy
TCA7	dark blue powder	Cornelissen Chinese blue	pure, soluble PB no detectable extenders, analysed by SEM-EDX and light microscopy
TTB6	Dark blue solid	Turner's Prussian blue	soluble PB, significant amount of Al detectable by SEM-EDX, but no extenders are visible via light microscopy indicating that the Al is incorporated into the PB lattice

5.2.3 Sample Preparation

For colorimetric and viscometric studies, 2.5 by 5 cm samples were excised. For chemiluminometric studies, 9 mm diameter samples were excised with a disk cutter and flattened between 2 sheets of Whatman filter paper.

5.3 Methods

5.3.1 Photodegradation and Thermal Degradation

The samples were irradiated in air in a Suntest CPS+ operated at 765 W and fitted with an air cooled Xenon arc lamp and a glass filter as well as a custom made filter from UV filtering Perspex to effectively limit transmitted light to 400 – 800 nm. The unit was operated with constant cooling, and the black body thermometer registered 35 – 40 °C during the experiments for varying lengths of time (0 – 20 h) for colorimetric and viscometric studies, and (0 – 300 s) for chemiluminometric studies.

Samples to be irradiated in room atmosphere (RA) were placed in their pans on a glass dish and covered with a watch glass within the Suntest chamber. Samples to be irradiated under a modified atmosphere, such as anoxia by argon displacement, were placed in their pans in a glass flow cell. The cell was purged with a gas for a minimum of 1 hour prior to being sealed and placed into the Suntest chamber. All samples were irradiated on the *recto* (painted) surface. After irradiation the samples were removed, from the ageing apparatus and reversed so that the *verso* surface is upwards and immediately placed within the Lumipol 2 instrument's sample chamber.

Samples for viscometric studies were light aged in sealed head space vials under oxygen or argon. The headspace vials were then placed in Schott glass bottles, and the bottles were then filled with oxygen or argon and sealed with a Viton rubber lined screw cap. All of the vial filling and sealing took place in a glove box actively purged with either oxygen or argon. Samples to be photo degraded were placed in the Suntest chamber (fitted with the filters described above) and were subjected to 1-8 h irradiation at 765 W. Samples to be thermally degraded were placed in a laboratory oven, preheated to 160 °C and were subjected to 1-6 h thermal-degradation.

5.3.2 Chemiluminometry

Chemiluminometric (CL) experiments were performed using a Lumipol 2 chemiluminometer, manufactured at the Polymer Institute of the Slovak Academy of Sciences, Bratislava, Slovakia. Non-isothermal experimental conditions under a 3 L h^{-1} flow of zero grade nitrogen gas were used in all experiments. The samples were first annealed at 40 °C for 10 min; then the temperature was ramped from 40 °C to 220 °C at a rate of 4 °C min^{-1}.

In order to exclude photon emission from non-sample sources, 'blank runs' on empty aluminium pans were conducted. In each case the aluminium pan was baked out at 200 °C for 1 hour under a flow of 3 L h^{-1} of zero grade nitrogen. It was then allowed to cool to 40 °C before being ramped to 220 °C at a rate of 2.5 °C min^{-1} followed by a 120 min thermostat. The resulting CL signals from the blank aluminium pans were on the order of 10 to 15 counts per second at 220 °C, and thus distinguishable from the CL signals resulting from the samples. The CL intensity for all measurements was recorded in counts per second [s^{-1}].

5.3.4 Colorimetry

A Gretag Macbeth Spectrolino spectrophotometer was used with a 6 mm mask to record the reflectance spectrum of the *recto* (painted) surfaces of the samples between 380 – 730 nm at 10 nm resolution. A 2° observer and a D65 filter were used to calculate the CIE 1976 (L*, a*, b*) values at the time of measurement. Colour measurements were recorded at 5-h intervals during the photodegradation experiments. The total colour change value (CIE ΔE*) after a given interval was calculated according to CIE 1976 (L*, a*, b*) colour change formula. For the PCA model, the initial CIE L*, a*, b* colour space values for the *recto* surfaces were used to estimate pigment density in the paint layer; while the CIE ΔE* following 10 h irradiation was used to evaluate the degradation of the chromophores in the paint layer.

5.3.5 Viscometry

Following irradiation, ca. 20 mg samples were prepared for viscometric analysis as per the standard procedure (ISO 5351/1) by defibration and dissolution in cupriethylenediamine (19). According to the literature (20), DP was calculated from the intrinsic viscosity measurements using the equation: $DP^{0.85}$ = 1.1[η].

5.3.6 ED-XRF

A Thermo Electron ARL Qunat'X ED-XRF was used for elemental analysis by energy dispersive x-ray fluorescence. Four instrument configurations were used to analyse the metal content of the paper. All measurements were conducted under air with an acquisition time of 100 s (live time) and the current was set to auto control. For high Z elements a 40 kV excitation voltage with a thin Cu filter was used, for mid Z elements both a 16 kV excitation voltage with a thin Pd filter and a 20 kV excitation voltage with a medium Pd filter were used. For low Z elements a 12 kV excitation voltage with an Al filter was used. The Thermo Electron ARL Quant'X control and data analysis software was used for semi-quantification of transition metals by background subtraction and integration of peak area. The differences in current between each measurement were corrected for by dividing the counts per second by the beam current, such that all measurements are expressed relatively, in cps/mA.

5.3.7 Data Analysis

Origin 8 Pro, OriginLab, was used to deconvolute the CL data by base line fitting and subtraction followed by iterative fitting of three Gaussian curves, hereafter referred to as peak 1, peak 2 and peak 3. For ease of comparison between samples, the maximum of peak 1 was fixed at 95 °C. The averages of the fitted areas of each peak for all irradiation intervals for each sample were calculated. The average peak areas were then used to calculate the ratio (TTBx:GSG) of the fitted area under peak 1 and peak 2 (RFAP1 and RFAP2 respectively). RFAP1 and RFAP2 were then inputted into the PCA model. It should be noted that the variable were not autoscaled before application of PCA. Autoscaling is useful when different types of variables or

variables of different orders of magnitude are used within the same PCA model as it makes all variables have equal importance (376).

XLSTAT Pro, Addinsoft, was used within Microsoft Excel 2007 for multivariate analyses. In PCA analysis all correlations are reported with a confidence of 90% unless otherwise stated.

5.4 Results and Discussion

5.4.1 Recto vs. Verso

With the goal to develop a method to understand the effects of the paint layer on paper during photodegradation, samples of paper, WLG and GSG (hence no paint applied), were irradiated and their oxidation was followed by chemiluminometry. Prior to this study, it was not clear if chemiluminometry could be applied to materials with a thin monofacial layer of a colourant, e.g. watercolours.

The CL signal of the irradiated (*recto*) surface was compared to that of the non- irradiated (*verso*) surface. That the signals in peak 1 region are essentially identical for both the *recto* and *verso* surfaces of GSG and WLG, Figure 2, is a good indication that the effect of light on the production of CL species is uniform throughout the material. This is in good accordance with a study that found that incident light had a degradative effect on stacked newsprint almost to the fifth sheet (245). The results of the *recto-verso* comparison for WLG and GSG indicate that *recto* irradiation followed by *verso* observation is valid and could therefore be applied to other (painted) samples.
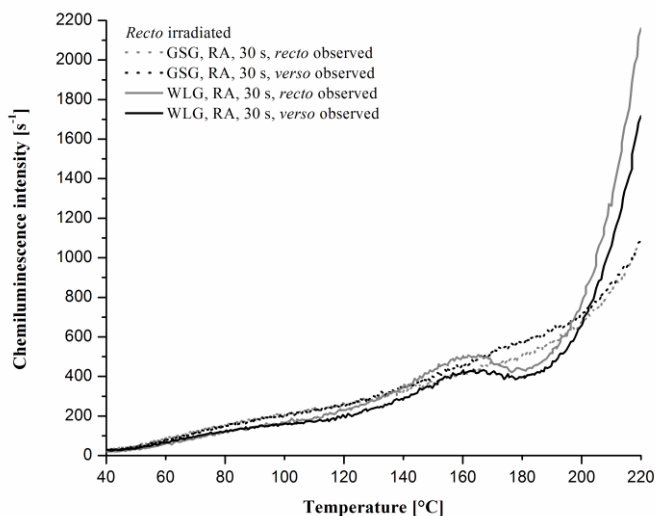
Figure 2 Plot of CL intensity during dynamic experiments in N$_2$ atmosphere following 30 s irradiation under air, a comparison of recto-irradiated and differently observed WLG and GSG samples.
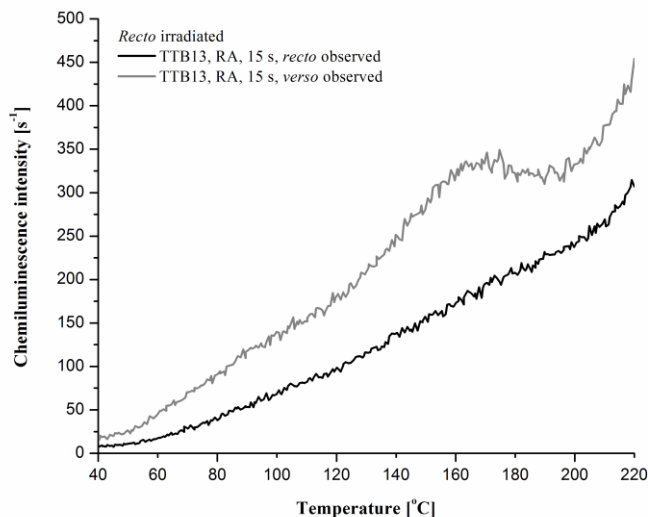
Figure 3 Plot of CL intensity during dynamic experiments in N$_2$ atmosphere following 15 s irradiation under air, a comparison of recto-irradiated and differently observed surfaces for TTB13.

In Figure 3, the signal from the *recto* (painted and irradiated) surface of TTB13 is very low, the peaks only indicated, while the signal from the *verso* (un-painted and non-irradiated) surface is higher, and the peaks are better defined and can be deconvoluted Figure 4. The poorly defined peaks and attenuation in signal for the TTB13 *recto* sample indicate that there is significant self absorption of emitted CL photons by the applied paint, while the fact that well defined peaks are observed for the TTB13 *verso* sample, when compared to both the TTB13 *recto* sample and to GSG *verso*, is a demonstration that *recto* irradiation and *verso* observation is a viable method for chemiluminometric studies of mono-facially coloured materials such as watercolour drawings.
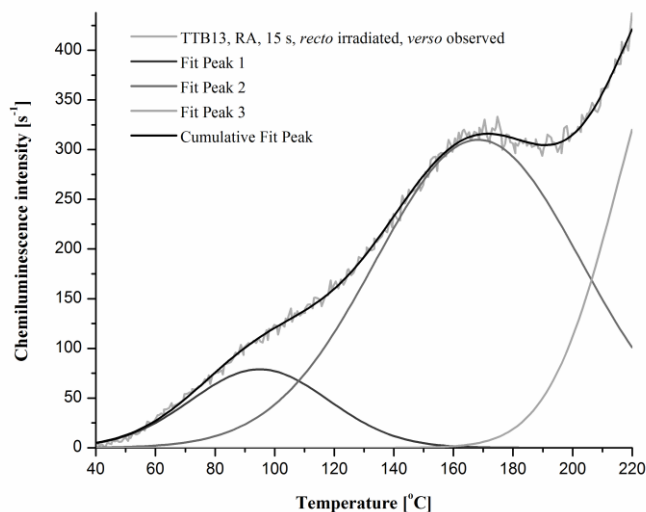
Figure 4 An example of the deconvolution of a CL intensity plot into 3 composite peaks by base line fitting and subtraction followed by iterative fitting of three Gaussian curves. For ease of comparison between samples, the maximum of peak 1 was fixed at 95 °C. This example, TTB13, RA, 15s, *recto* irradiated, *verso* observed, is typical of the goodness of fit for all *recto* irradiated and *verso* observed samples.

5.4.2 Chemiluminometric Peaks

Irradiation of paper with a UV-filtered xenon lamp leads to formation of species that can be easily observed using chemiluminometry. In the absence of oxygen, different luminescing species decompose at different temperatures indicating different stabilities and different origins, as discussed in the Introduction.

For all samples, regardless of the presence of paint or whether the *recto* or *verso* surface was measured, the area of peak 1 increased with increased duration of irradiation, Figure 5. However, in the majority of cases, a thin layer of the paint reduces the content of luminescing species leading to peak 1, which indicates an inhibitive effect in terms of formation of this species.
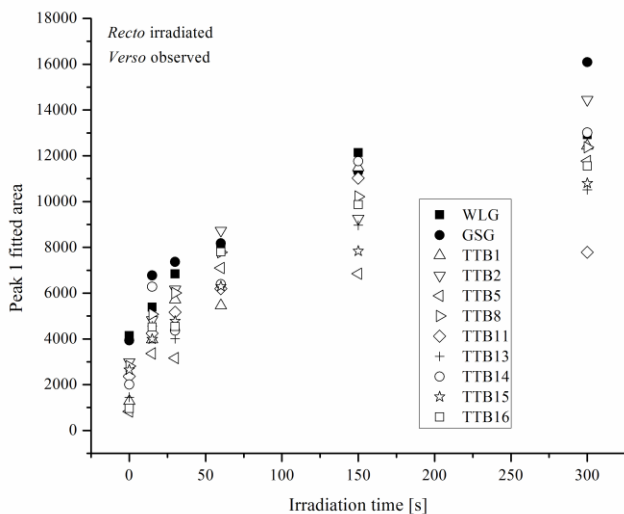
Figure 5 Plots of peak 1 area of the verso surfaces vs. irradiation time for each of the samples. Experimental conditions: dynamic CL N2 atmosphere following 0 - 300 s irradiation under air.

Peak 100 °C < T < 160 °C (peak 2) is of particular interest for this study, as the peak has been linked to the decomposition of peroxides in both thermal and photo degraded cellulose (16, 18, 269, 270, 274, 375, 377, 378) and in collagen derived materials (276, 303, 379-382).

Cellulose photodegradation in the presence of oxygen is thought to occur according to a photo-initiated chain reaction mechanism; this mechanism has been compared to the Bolland-Gee mechanism, and has an estimated photooxidation kinetic chain of about 40 cycles (18, 276). The deconvoluted peak is centred at 160 – 180 °C, which is at a higher temperature than for either cellulose or collagen derived material alone. A temperature shift during chemiluminometric experiments can be due to many factors, and irregularities in heating due to sample morphology are of particular significance (377). Due to the composite and artisanal nature of the materials studied, inhomogeneities certainly introduce errors, but it is also likely that several unresolved CL processes associated with paper and gelatine occur simultaneously, thus a temperature shift is not entirely unexpected.

The region T > 160 °C (peak 3) is typical of the monotonous rise in chemiluminometric intensity due to transglycosidation of cellulose under inert atmosphere (375).

5.4.3 Interactions

The picture that begins to emerge is that the discolouration of pigments and the degradation of works of art on paper is a much more complex process than initially conceived, with interactions between transition metals, chromophores, and the paper substrate.

Principal component analysis is a useful and widely applied tool for data exploration, and with it, it is possible to begin to untangle the interactions and to generate data-driven hypotheses about the behaviour of the paint/paper degradation system. The experimental results (relative transition metal content, ratios of the average fitted areas of CL peaks, DP, CIE ΔE*, relative chromophore concentrations, and initial CIE L*, a*, b* coordinates of the paint layer) were inputted to generate the PCA model. The resulting model requires 7 factors to describe 99% of the variability in the data; however, a satisfactory 81% is explained by the first 3 principal components.
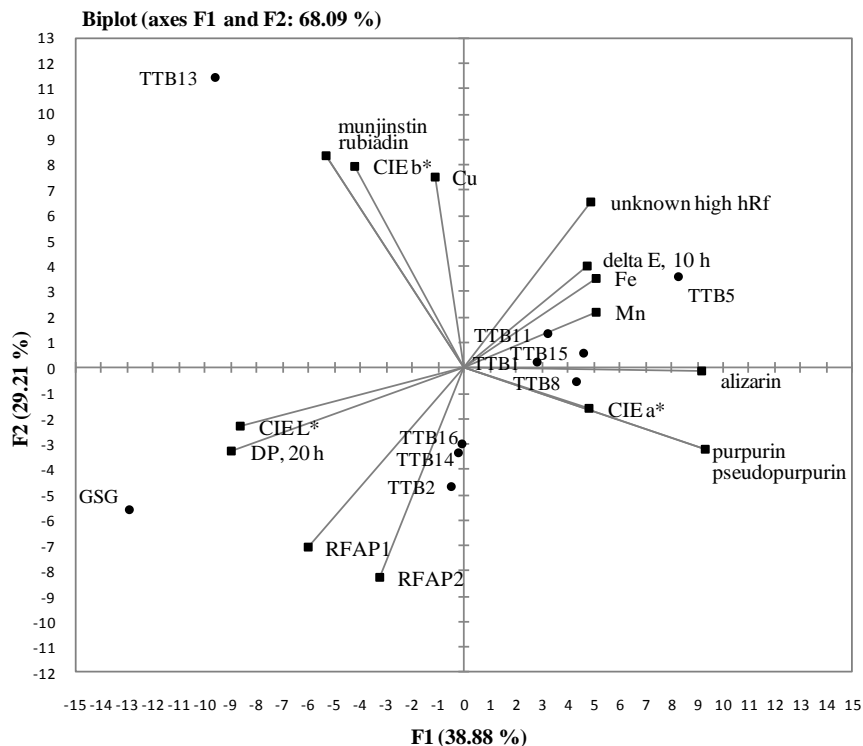
Figure 6 A biplot of the PCA model based on TTBx and GSG data. The active variables used to generate the PCA model are squares and the observations are circles.

Figure 6 is a biplot of the PCA model. Five clusters of samples are easily discernable: TTB13 with high transition metal content and primarily *meta*-substituted AQs; TTB5 with very high iron content and *ortho*-substituted AQs; TTB1, 8, 11 and 15 with moderate to high transition metal content and *ortho*-substituted AQs; TTB2, 14 and 16 with low transition metal content and *ortho*-substituted AQs; and GSG with low metal content and no AQs.

5.4.3.1 Filtering Effect

It has been noted in the literature that paint films containing alizarin lake can have a protective effect by limiting the depth of penetration of light (356). If the paint films have a protective filtering effect then it is reasonable to assume a correlation between peak 1 area and at least one of the CIE colour space parameters of the paint application.

PCA analysis reveals a positive correlation between RFAP1 and the CIE L* colour coordinate, meaning that samples with larger positive CIE L* tend to have higher peak 1 fitted areas than those with lower CIE L* values. The CIE L* colour coordinate can be associated with the density of the paint application; in watercolour drawings, pigment particles are highly dispersed in a transparent medium such that the paper substrate is visible through the paint application. The lighter the application (lower pigment density), the more exposed paper, and thus (in the case of white paper) a higher CIE L* value, and such samples, particularly TTB16, tend to have peak 1 areas similar to those for GSG at a given irradiation exposure interval. This indicates that, at least with respect to the formation of the charge transfer complex, inferred by peak 1 area, there is an inhibitory effect that is likely due to a general attenuation of the light incident on the cellulose by either absorption or reflection by the applied paints.

That there is no correlation to either CIE a* or b* values indicates that there is no colour dependent, band filtering effect for the applied paints.

5.4.3.2 Gelatine

Examination of the CL curves from WLG and GSG at each irradiation interval reveals distinct differences in the shapes of the curves in the peak 2 region. After iterative Gaussian fitting it is apparent that the full width half maximum (FWHM) for peak 1 is nearly identical for WLG and GSG, but for peak 2, GSG has a FWHM that is nearly 50% larger than that of WLG, Figure 2. Other than the presence of gelatine, the papers are identical in furnish, finish, and biography, and thus gelatine might be playing a role in the production of CL species during irradiation. Analysis of covariance (ANCOVA) can be used to test this hypothesis.

ANCOVA is a merger of analysis of variance (ANOVA) with linear regression, and it generates a general linear model where the outcome variable(s), in this case the fitted areas of peak 1 and peak 2, are continuous variables, and at least one of the predictor variables is continuous (irradiation time) and at least one is categorical (presence of gelatine). ANCOVA tests whether a categorical predictor variable has an effect on the outcome variable after removing the variance attributable to the quantitative predictor variable (383).

An ANCOVA model using duration of irradiation and the presence of gelatine as predictor variables was constructed to explore the observed differences in the plots of CL intensities. The constructed model can explain 90% of the variance in peak 1 fitted area and 61% of the variance in peak 2 fitted area for the WLG and GSG samples; addition of other variables, such as transition metals, did not improve the model and were thus excluded, see Figures 7 and 8.
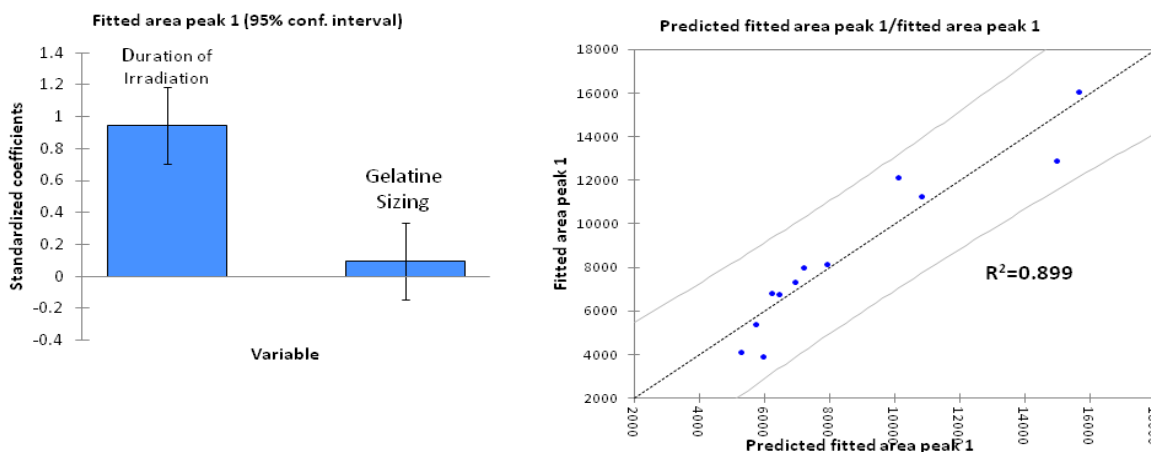
Type I Sum of Squares analysis (Variable Fitted area peak 1):

Source	Degrees of Freedom	Sum of squares	Mean squares	F	Pr > F
Duration of irradiation	1	138010489.556	138010489.556	79.657	< 0.0001
gelatine	1	1446427.565	1446427.565	0.835	0.385

Tukey analysis of the differences between the categories with a confidence interval of 95%:

Contrast	Difference	Standardized difference	Critical value	Pr > Diff	Significant
GSG vs. WLG	694.365	0.914	2.262	0.385	No
Tukey's d critical value:			3.199		

Figure 7 A summary of the ANCOVA results for the fitted areas of peak 1 with respect to duration of irradiation and the presence of gelatine.
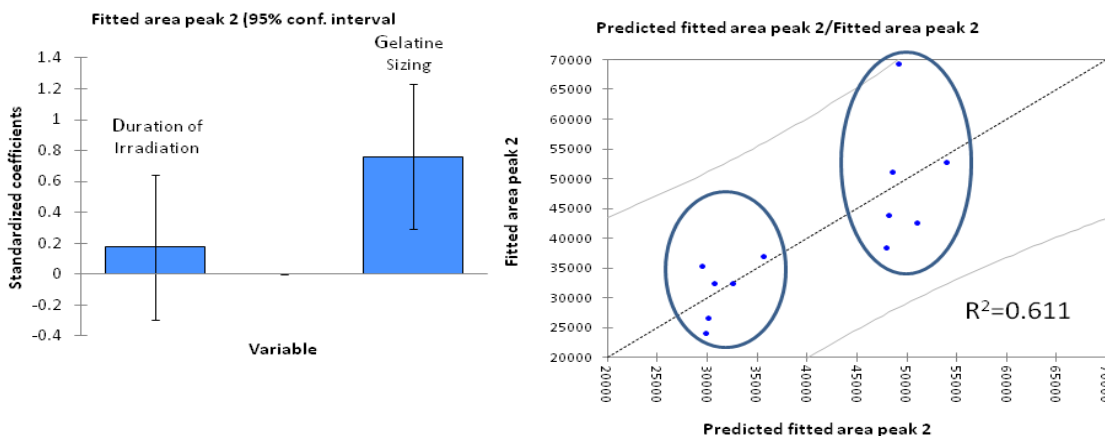
Type I Sum of Squares analysis (Variable fitted area peak 2):

Source	Degrees of Freedom	Sum of squares	Mean squares	F	Pr > F
Duration of irradiation	1	53856325.503	53856325.503	0.714	0.420
Gelatine sizing	1	1014774056.938	1014774056.938	13.448	0.005

Tukey analysis of the differences between the categories with a confidence interval of 95%:

Contrast	Difference	Standardized difference	Critical value	Pr > Diff	Significant
GSG vs. WLG	18391.792	3.667	2.262	0.005	Yes
Tukey's d critical value:			3.199		

Figure 8 A summary of the ANCOVA results for the fitted areas of peak 2 with respect to duration of irradiation and the presence of gelatine.

Examining Figure 7, we can see from the sum of squares analysis from the ANCOVA model that the fitted area of peak 1 correlates to duration of irradiation with good statistical confidence (PR>F is <0.0001) and the presence of gelatine was found to not be a significant contributor to the variance by Tukey analysis which gave a single group assignment. This is to be expected because peak 1 has been attributed to a photo-imitated charge transfer complex between oxygen and cellulose.

On the other hand, examining Figure 8, according to the sum of squares analysis we can see that the fitted area of peak 2 does not correlate to irradiation time but according to the Tukey analysis (which assigned two groups with a Pr > Diff significance of 0.005) the presence of gelatine is a significant generator of observed variance.

The fact that the WLG and GSG samples belong to a single population with respect to variance in peak 1 fitted area indicates that the difference in variance of peak 2 fitted area does not arise from differences in the samples' morphology. If differences in sample morphology, due to the application of gelatine size, were a contributing factor, then it is reasonable to assume that they would equally affect the CL signal for both peak 1 and peak 2 and thus there would be two sample populations for both peak 1 and peak 2. As this is not observed, then another explanation must be found.

Chemiluminometric studies of gelatine and parchment run under experimental conditions similar to those used in this study indicate that CL intensity is dependent on the quality, the moisture content/glass transition temperature, the degree of pre-oxidation of the gelatine and the emission of volatile organic compounds (VOCs).

Figure 9 presents the mechanism for the oxidation of gelatine via the formation of peroxyl radicals and subsequent CL photon emission. This process should generate a CL signal in the peak 2 region and thus help to explain the observed broadening and temperature shift in the peak 2 signal.
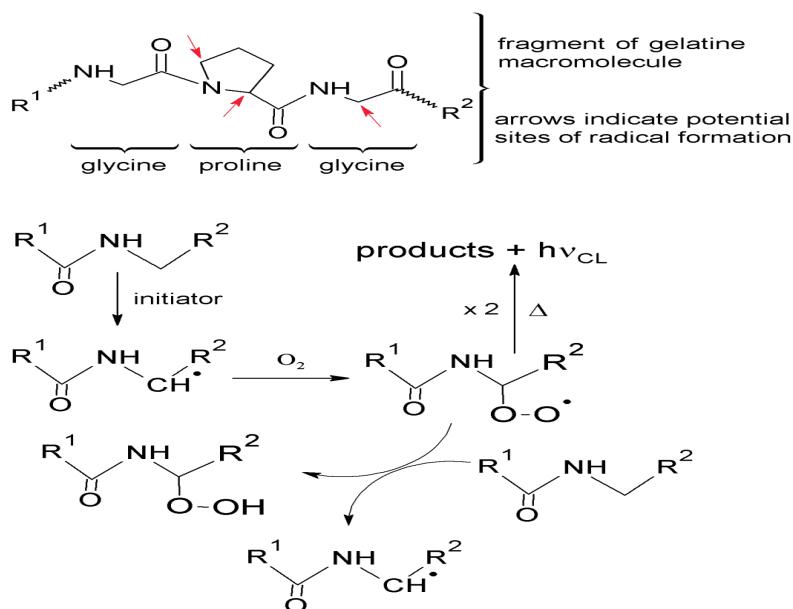
Figure 9 Mechanism for the oxidation and CL photon emission of gelatine (380).

Alternatively VOC emission is another possible explanation. Strlič *et al*. report an increase in CL intensity in the peak 2 region for parchment with higher VOC emissions (303). The broadening and higher temperature shift in the peak 2 area of the CL spectrums for the same samples, however, were not discussed in detail (303). Headspace-GC-MS studies of the samples taken from the same papers indicate that photodegraded gelatine sized papers emit many more VOCs at higher concentrations than unsized papers, see Chapter 7.

It is likely that a combination of the two factors contributes to the observed phenomena, and further experimentation is needed to better understand this degradation phenomenon.

5.4.3.3 Chromophores

The concentrations of the chromophores on the samples have not been quantitatively measured, but the relative content of each chromophore in each colourant has been analysed by TLC (233) and the relative pigment density evaluated from the CIE L* values.

According to the literature AQs can act as both Type 1 and Type 2 photosensitisers (144, 367, 368, 384) generating reactive oxygen species (ROS). These ROS can then directly react to degrade organic materials or they can interconvert in the presence of water to form peroxides among other ROS (28, 385). Furthermore AQs have been found to be potent co-catalysts for both Fenton and visible light induced photo-Fenton processes leading to the accelerated degradation of organic materials (371) by both photo-initiated charge transfer and through the quinone/hydroquinone cycle, Figure8, (370, 371). On the other hand, it has also been reported that AQs are antioxidants with both chain-breaking and metal-chelating effects (362, 364, 365). With respect to metal chelating all published studies show that *ortho*-di hydroxyl substitution of AQs, and polyphenols in general, increases their ability to bind iron (361, 364, 365, 386). It is quite probable, that

all of the above are occurring simultaneously, and correlations and the lack thereof in the PCA model can be explained by accounting for the presence of the chromophores in addition to transition metals in the applied paints.

RFAP2 is usually attributed to peroxide content, and a reduction in peak 2 fitted area for paper alone is observed with the addition of transition metals (37, 360). Indeed, in the PCA an anti-correlation was observed to copper content, but not specifically to iron content. Additionally there is positive correlation to RFAP1 indicating that the photo-initiated charge transfer species inferred from peak 1 probably leads to peroxide formation. The positive correlation to CIE L* can be simply interpreted in light of transition metal content (there is a strong correlation between CIE L* and total transition metal content), but it is also possible that the chromophores in the applied paints are acting as co-catalysts in a photo-Fenton process rapidly recycling reduced transition metal cations as described by (370, 371).

5.4.3.4 Transition Metals

The metal content of the raw, madder lake pigments from the Turner Bequest has previously been analysed by SEM-EDX (233), but the relative concentrations of the associated transition metals after the pigments have been processed and applied to paper in watercolour medium are of interest here. We propose that the associated transition metals present in the madder lake pigments are able to act as Fenton-like catalysts, possibly with the chromophores in the applied paints as co-catalysts in visible light induced photo-Fenton processes (366, 370, 371) leading to the oxidative degradation of paper.

The catalytic effect of transition metals on the oxidative degradation of paper is a well known phenomenon (28, 37, 360), and the effect of transition metals on chemiluminescence of paper has been studied by Šelih *et al*. who found that that the presence of transition metals generally reduces the peroxide associated peak during CL experiments conducted on mildly alkaline paper samples in the absence of light. When compared to iron, manganese, and other transition metals, copper had by far a greater catalytic effect (360). However, research groups focusing on Fenton and photo-Fenton degradation of dyes in acidic solution have found that iron is more reactive than copper in solution phase Fenton-like processes (366, 387).

The lack of a specific anti-correlation between RFAP2 and iron indicates that iron is somehow not available to participate in a Fenton-like process, or that the effect of copper overshadows that of iron. Transition metal compounds are added to madder root extracts in the laking process and to dye preparations as mordants (372), thus it is probable that there are chromophore-metal complexes and that these complexes have different stabilities for each metal/chromophore(s) combination.

Based on the RFAP2 data it is reasonable to propose that iron is sequestered by the chromophores such that it is less available for Fenton processes while copper is in a more available form to decompose peroxides generated in the paper substrate (364, 366, 388). An analogous behaviour is observed for knipholone anthrone and derivatives, where antioxidant effect, as defined by a reduction in the Fenton decomposition

of peroxides, occurs through iron chelation (363), but a prooxidant effect was observed for the same compounds in the presence of copper (369).

5.4.4 Degradation of the Paint and of Paper

The degradation of paper was measured in terms of DP decrease,and the degradation of the paint layer was measured in terms of CIE ΔE*. These two values are anti-correlated, meaning that a bigger total colour change will lead to a lower DP after 20 h of irradiation. Also, the correlation between CIE L* prior to the photodegradation experiment and DP afterwards, indicates that a lighter application (higher CIE L*) leads to less degradation of the paper support.

Interestingly, following 20 h of irradiation, the DP of coloured samples is, in all cases lower than that of GSG or WLG. This finding is significant, however, it is difficult to point to the underlying chemical mechanism leading to it, as the content of transition metals is positively correlated with the content of the chromophores. It is possible that the chromophores act as photosensitisers through ROS generation (144, 367, 368, 384) in the degradation of the paper substrate (389, 390). Ignoring possible interactions due to the chromophores, there is a significant anti-correlation between iron and manganese content and the DP of the sample.
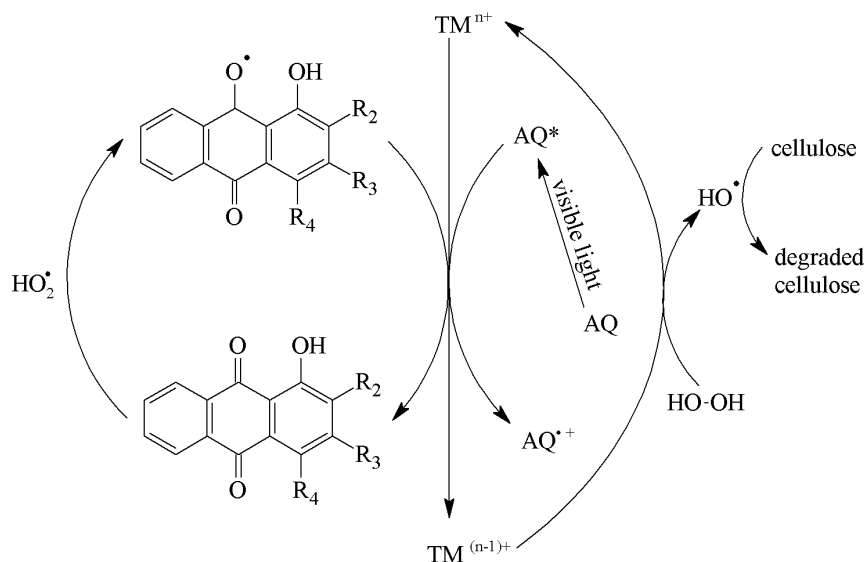
Figure 10 A general mechanism of Fenton-like degradation of paper in the presence of madder lake pigments under visible irradiation. Adapted from (371).

With respect to colour change, the relationship to metal content is less clear. Anthraquinones have been shown to be co-catalysts in photo-Fenton processes that can lead to accelerated degradation of organic compounds under visible irradiation (370, 371), Figure 10. If this is the case, then an increased content of transition metals associated with the madder lakes, which should lead to a faster decomposition of

peroxides (and thus lower peak 2 and thus higher extent of degradation in terms of DP) should also lead to a faster rate of discolouration due to degradation of the dye as a sacrificial co-catalyst (371).

Review of the literature reveals that particle size is considered to be the primary factor in the rate of fading for a given colourant under a given condition (135, 137, 236), and TTB8 which has the greatest CIE ΔE* value was noted by Townsend to have finer pigment grains when compared to other pigments in the Turner Bequest (233).

5.4.4.1 Anoxia

The absence of oxygen, anoxia, has been noted by several researchers to have a beneficial effect on the permanence and durability of paper (12-15) as well as in preventing the fading and colour change of applied colourants (4, 11, 59, 122, 124, 141). In these studies focus has been upon quantifying the secondary effects of oxidation (colour change, loss of DP and mechanical properties, production of oxidised functionalities, decrease in pH etc (4, 12-15, 59, 122, 141) rather than a direct measure of the effect of simulated anoxic display on the production of oxidising species. Here chemiluminometry has been used to directly measure the effect of anoxia on limiting the production of photo-initiated reaction products.
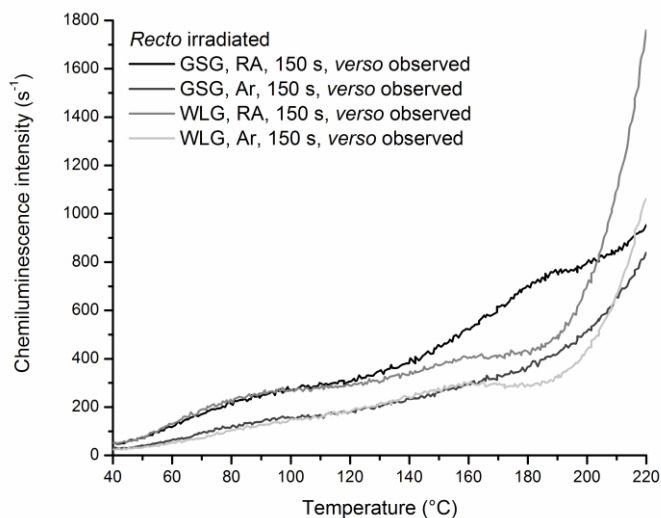
Figure 11 Effect of anoxia by argon displacement. Plot of CL intensity during dynamic experiments in N_2 atmosphere following 150 s irradiation in air or argon.

Samples were prepared and irradiated as described above. Figure 11 compares the CL intensity from GSG and WLG samples after 150 seconds irradiation in both room atmosphere (RA) and argon (Ar) environments. As above the CL curves can be deconvoluted into three temperature regions. Under anoxic conditions there is a significant reduction in the fitted areas for both peak 1 and peak 2 for both GSG and WLG samples. This reduction in peak area is indicative of a reduction of the formation of CL species leading to both peak 1 and peak 2 when oxygen is excluded during irradiation.

That the peaks are reduced but not to zero is not entirely surprising. Considering peak 1, there are threepossibilities: not all of the oxygen is removed during purging, there are long-lived charge transfer complexes already present in the samples, or that atmospheric oxygen is able to react with photo-excited species in the samples to form both the charge transfer complex associated with peak 1 (16, 18) during the short time when the samples are exposed to air during their transfer to the Lumipol 2. The third optionr is not likely as Hon found that exposure of cellulose irradiated under nitrogen to molecular oxygen that had not been photo-excited did not lead to significant production of peroxides or ROS (391). Rather it is likely that there is residual oxygen included and/or chemi/physi sorbed onto the sample matrix. This oxygen is then able to react with the cellulose to form the charge transfer complex associated with peak 1. This conclusion is supported by the reduction of the peak 1 fitted area when the purge time is increased from 10 minutes to 24 hours. With regard to peak 2 fitted area, the residual oxygen that is in the paper is able to react with the cellulose and gelatine to form peroxides as described above. Furthermore, considering the fibre source, TCF bleached pulps, it is very likely that there are long lived peroxide species within the paper, and that these peroxides then are decomposed during the CL experiment.

5.4.4.2 Prussian Blues

In this study three different PB-containing pigments were studied: TCA1, TCA7 and TTB6. TTB6, dating from the mid 19th century, is the PB used by the artist J.M.W. Turner. By the presence of potassium, but also aluminium, SEM-EDX analysis confirms that it is a soluble form of PB. The aluminium is likely incorporated into the PB crystal lattice because by optical microscopy, alumina was not found as a pigment extender. Other than the presence of aluminium, TTB6 is a remarkably pure PB. TCA7 is Cornelissen Chinese Blue dating from the early 20th century; it is an extremely pure soluble PB, with only potassium and iron detectable by SEM-EDX and only PB particles present by optical microscopy. TCA1 is Cornelissen Antwerp blue (a PB with white pigments added as extenders) dating from the early 20th century. In addition to iron, SEM-EDX analysis has identified the presence of potassium (indicating that this mixed pigment was prepared with soluble Prussian blue), zinc, barium and sulphur (that these elements constitute the white pigment extenders, ZnO and BaSO$_4$, has been confirmed by optical microscopy). The presence of ZnO is very interesting because it is a photoactive compound that can act as a Type 1 photosensitiser by producing superoxide anions. These can react with water to form hydroperoxyl radicals which can then diproportionate to form singlet oxygen and hydroperoxide (28). As a pigment, zinc oxide has been found to lead to photocatalytic oxidative degradation of paper and textiles (42, 392, 393), and recently ZnO has been used to produce photocatalytic paper to decompose volatile organic compounds (VOCs) (394). Samples containing these pigments were prepared on WLG paper to avoid the additional complications of the presence of gelatine.

5.4.4.2.1 Chemiluminometry of PB Containing Watercolour Drawings

Figure 12 presents plots of *verso*-observed CL intensities for WLG, TCA1, TCA7 and TTB6 samples following *recto* irradiation in air for 0-300 s. Starting in the upper left we see that with no irradiation the WLG sample has a comparatively large population of long-lived peroxides, as evidenced by the maximum intensity of about 560 counts s^{-1} in the peroxide-related, peak 2 region centred at 160 °C (indicated by an arrow in the plot). For the WLG samples this peak decays with increasing irradiation due to photodecomposition of peroxides, and reaches an intensity of about 300 counts s^{-1} after 150 s of irradiation. The PB samples however exhibit different behaviours. All of the PB samples have a low, pre-irradiation, peroxide-related peak, maximum of about 300 counts s^{-1} indicating a lower peroxide population. For the TCA7 and TTB6 samples this peak does not significantly change with irradiation, but for the TCA1 sample this peak increases with further irradiation, thus indicating the formation of additional peroxides.
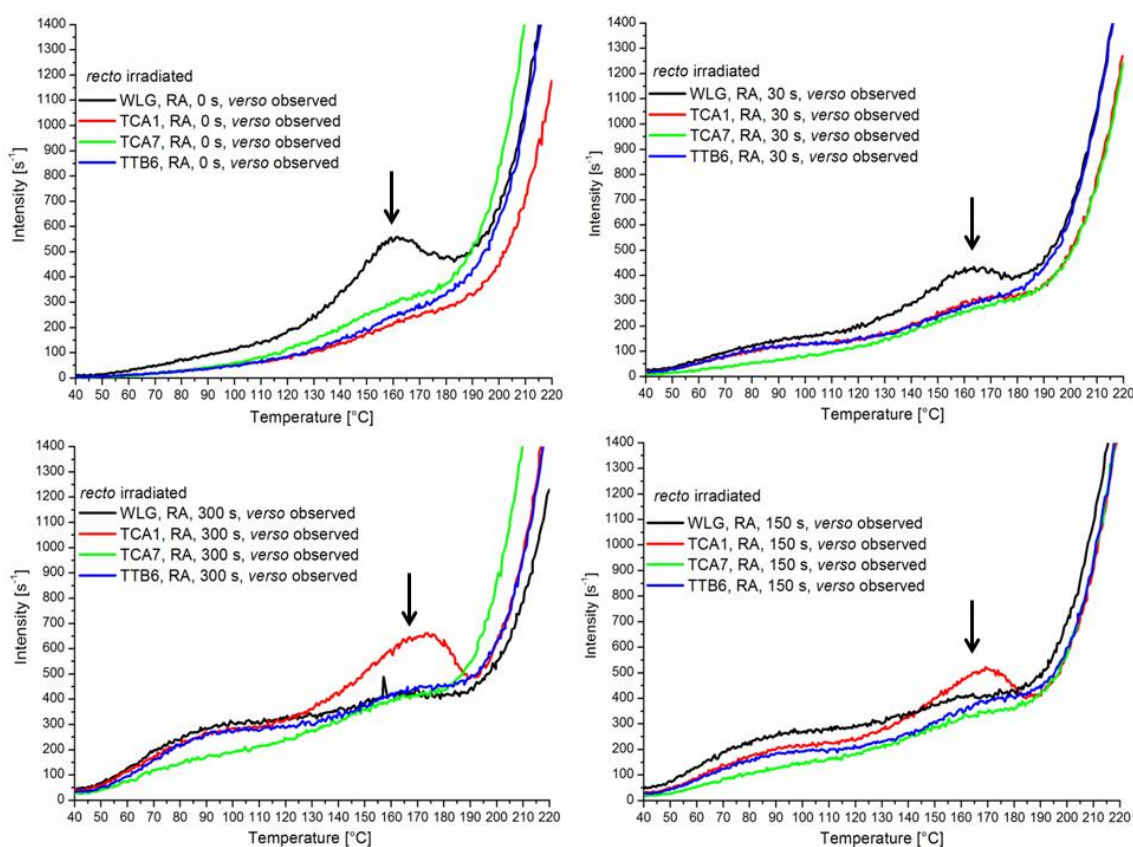
Figure 12 Plot of CL intensity during dynamic experiments in N$_2$ atmosphere following (clockwise from the upper left) 0 s, 30 s, 150 s and 300 s *recto* irradiation under air with *verso* observation. The arrows indicate the peroxide-related, peak 2 region in the CL intensity plots.

5.4.4.2.1.1 Filtering effect

The first hypothesis for the low peroxide peak for the PB samples is that the PB has a protective filtering effect on the paper. This can be tested by examining the peak 1 region which has been associated with a photo-initiated charge-transfer complex between molecular oxygen and cellulose. The TCA7 sample has a lower intensity and less well-formed peak in peak 1 region, for all irradiation times indicating reduced

formation of the charge transfer complex and thus a protective filtering effect, Figure 12. However, the TCA1 and TTB6 samples have no significant differences from the WLG samples in the peak 1 region indicating no protective filtering effect. TCA7 and TTB6 are both soluble PB so the difference in behaviour is not likely to be chemically related, but rather due to the presence of more pigment in the TCA7 samples which are visibly darker than the TTB6 andTCA1 samples. The formation of the charge transfer complex between atmospheric oxygen and the glycosidic bond in cellulose has been proposed as an initiating step in the photo-oxidation of paper (16, 18), which proceeds through a radical chain reaction, and in the above PCA model, Figure 6, there is a strong correlation between the charge transfer complex related peak (peak 1) and the peroxide-related peak (peak 2). Therefore it is reasonable to expect a reduced peroxide peak for TCA7 samples relative to the TTB6 samples, but if the plots of CL intensity following 30 s – 300 s of irradiation are examined, no such reduction (TCA7 relative to TTB6) is observed, Figure 12. This indicates that the limitation of the formation of the charge transfer complex through light filtering granted by a heavier application of paint does not necessarily translate into a protective effect as could be concluded from a correlated reduction in the peroxide-related peak.

5.4.4.2.1.2 Peroxide Decomposition

The next hypothesis is that there is a distribution of more and less mobile (even volatile) peroxides in the paper, and that a fraction of these peroxides are in contact with PB or are mobile enough to enter into the PB lattice where they are decomposed by Fe^{2+} centres in the PB in a Fenton-like process. Because this peroxide decomposition is occurring in conjunction with irradiation, the nitrogen-coordinated Fe^{2+} centres generated by the photoreduction of PB to Berlin white ($Fe^{2+}[Fe^{2+}(CN)_6]^{2-}$) are likely the reactive sites because the carbon coordinated, low-spin ferrocyanide coordination complex is relatively unreactive. The photoreduction of PB is rapid, thus the Fe^{2+} Fenton catalyst is easily regenerated (127), but because the PB is immobilised as a paint film, only peroxides in contact with the pigment or those sufficiently mobile to come into contact with the pigment are able to react, thus we can imagine a situation where during irradiation the Fenton catalyst is always available to decompose the mobile peroxide fraction resulting in a near constant peak 2 intensity, as observed in the samples. Once irradiation has ceased, the produced Berlin white can be re-oxidised to PB by air and water, but this process is slow (127), and thus any remaining mobile peroxides are scavenged resulting in a lower peroxide population as observed in the samples.

5.4.4.2.1.3 Effect of ZnO

The TCA1 samples on the other hand exhibit an increasing peak 2 intensity with irradiation longer than 150 s. This is the opposite of the trend observed for WLG and GSG samples as well as most samples with organic colourants. An increase in peak 2 is due to increased peroxide formation. As noted above ZnO is a type 1 photoinitiator producing superoxide anions which can react with water to form hydroperoxyl radicals which can then disproportionate to form hydrogen peroxide and singlet oxygen, according to the reaction mechanism in Figure 13.

$$ZnO + O_2 \xrightarrow{h\nu} (ZnO)^+ + O_2^{\cdot -}$$

$$O_2^{\cdot -} + H_2O \longrightarrow HO^- + HO_2^{\cdot}$$

$$2\,HO_2^{\cdot} \longrightarrow H_2O_2 + O_2^{*}$$
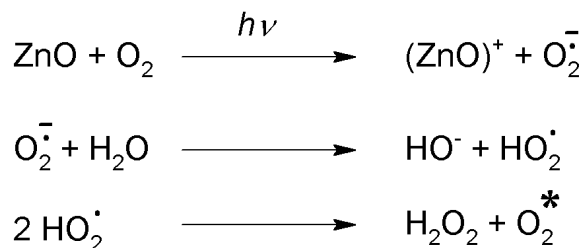
Figure 13 Photo-initiated superoxide anion formation by ZnO and its conversion to hydrogen peroxide by reaction with water via a hydroperoxyl radical intermediate (395) .

Hydrogen peroxide formed in this way would account for the observed increase in peak 2 intensity. However, with a band gap of 3.37 eV, ZnO has a peak absorbance in the near UV spectrum at 360-380 nm (395), and unless the ZnO has been sufficiently n-doped (by oxygen vacancies in the crystal structure or inclusion of metals) superoxide anion formation should not occur under the experimental conditions. However, from Figure 10, it is evident that peroxides are being produced. The ZnO in TCA1 was prepared for use as a pigment, and it is unlikely that it received any intentional n-doping, and at this time, it is not possible to estimate the native n-doping present in the material (396). However, there is another factor that could lead to visible light activation of the ZnO; the PB has broad absorption bands at 400 and 700 nm corresponding to electron transfer from low-spin Fe(II) to high-spin Fe(III) and the formation of a reactive excited state of PB, see Chapter 6 Section 6.2.2.1. It is possible that this excited PB can then transfer sufficient energy to ZnO to promote an electron across the band gap (396). Organic dyes are used in this way to sensitise TiO_2, ZnO and other photocatalytic semiconductors to visible light (396) and zinc oxide and PB analogue hybrid film electrodes have been prepared for electro-catalysis studies (397).

5.4.4.2.2 Effect of Anoxia: viscometry data

As with the organic colourants above, when the samples are irradiated under N_2 or Ar atmosphere, both peak 1 and peak 2 are suppressed which is indicative of the absence of the formation of both the photo-initiated charge-transfer complex and peroxides. This can be interpreted as evidence of the benefit of anoxia for paper, and was further explored using viscometry. Figure 14 presents the viscometric results following thermal-degradation at 160 °C for 1 – 6 h. Thermal-degradation at 160 °C was selected because it would provide a sufficiently rapid proof of the degree of paper degradation at a low enough temperature that it is comparable with the temperatures used in CL experiments.

Here we can see that the samples of blank WLG and WLG painted with TCA7 degrade at a similar rate, the slopes of the fitted lines for both sample types are quite similar for each atmosphere, indicating that PB does not affect the autoxidation rate of paper at these conditions. We can also see that anoxia gives nearly equal protection to both sample types with the ratios of the slopes of the fitted lines oxygen:argon being 1.3 for WLG and 1.8 for WLG with TCA7 respectively. In terms of paper degradation, this indicates that these

samples would receive equal benefit from anoxic storage.
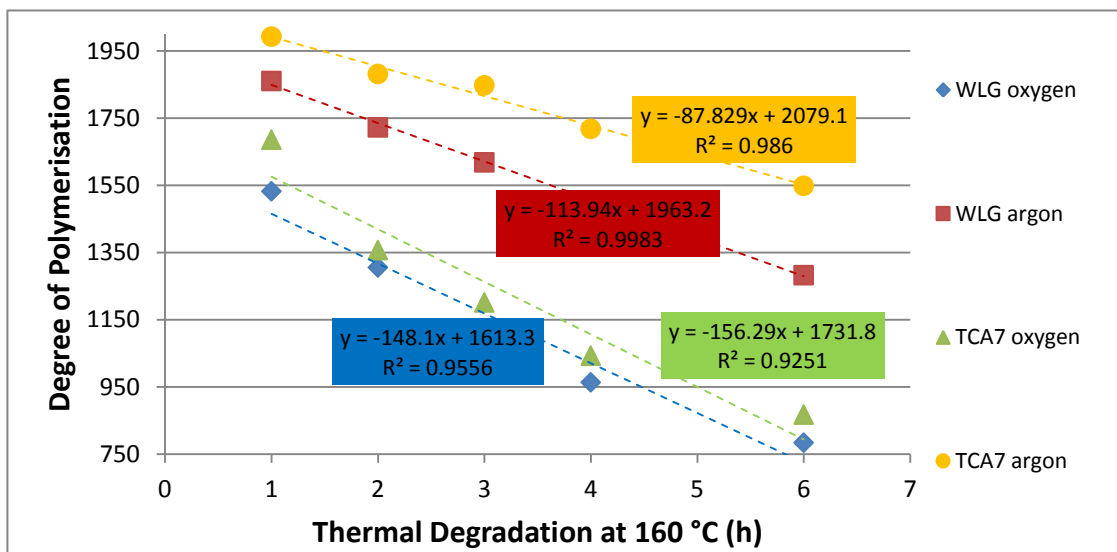
Figure 14 Samples of WLG and WLG with TCA7 thermally degraded at 160 °C for 1 – 6 h under oxygen or argon.

Figure 15 presents the viscometric results following 1 − 8 h of photodegradation with recto irradiation in a Suntest chamber operated at 765 W. From the slopes of the fitted lines we can see that during photodegradation something different is happening. Anoxia still gives benefit to both sample types, with ratios of the slopes of the fitted lines oxygen:argon being 6 for WLG and 1.7 for WLG with TCA7 respectively. But there is an obvious interaction between PB and light that results in a more 6-fold increase in the slope when WLG degraded in anoxia is compared to WLG with TCA7 degraded under the same conditions.
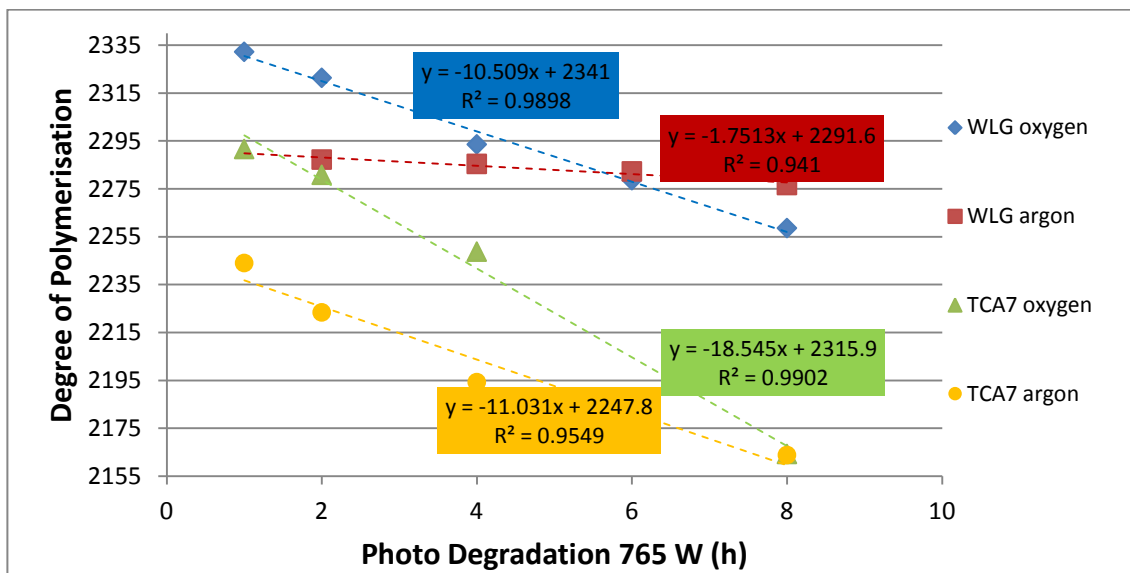
Figure 15 Samples of WLG and WLG with TCA7 photo-degraded in a Suntest chamber at 765 W, for 1 – 8 h under oxygen or argon.

That this increased degradation is photo-initiated, and not related to acidic residues in the PB or some other chemical process, is confirmed by the fact that thermal treatment at 160 °C had an equal effect on samples

with and without PB, Figure 12. We can also conclude that much of the photodegradation observed in the samples with PB is independent of oxygen concentration because the rates of reaction did not increase to the same extent for the WLG and WLG with TCA7 samples when photo degraded under oxygen. Therefore the loss of DP of the paper substrate is due to a species in the paper or the gum Arabic binding media, probably the reducing ends of the polysaccharides, which is acting as a reducing agent (and being photo oxidised in turn) during the photo reductive fading of PB. Therefore it can be concluded that paper without applied PB will experience a beneficial effect of anoxic display, but paper with PB will only experience a minor positive effect from anoxic display.

5.5 Conclusions

Concerning the oxidative stability of watercolours, there is a complex relationship between transition metals and chromophores. To the author's knowledge, this is the first in depth research into the photodegradation of watercolours where the chemistry of the processes, rather than phenomenological observations, is attempted to be understood. Prior to this study it was not clear if chemiluminometry could be applied to watercolours to understand the oxidative processes better as absorption of the emitted photons could represent a problem. Contrary to expectations, in the case of light watercolour washes on paper, *recto* irradiation followed by chemiluminometry of the *verso* surface is a viable tool to assess the oxidative stability of the material.

Using this technique in conjunction with measurements of DP of the paper support and colorimetry of the pigment layer, it was found that:

- Light acts evenly throughout the bulk of paper. Therefore, *recto* irradiation and *verso* observation is an effective method to study monofacially coloured materials.
- The presence of gelatine results in an increased fitted area and FWHM for peak 2, this indicates that there are additional CL processes in gelatine sized paper: oxidation of amino acids, physical changes in the gelatine and VOC emission.
- The absence of oxygen during irradiation leads to a reduction in peak 1 and peak 2 fitted areas and can be interpreted as direct evidence of the benefit of anoxia for works of art on paper.
- The presence of AQ-based madder lake pigments reduced the fitted area under peak 1 indicating an inhibition in the formation of the oxygen-cellulose charge transfer complex; this effect increased with higher pigment density.
- The presence of AQ-based madder lake pigments, regardless of transition metal content, increased the degradation of the paper under the paint layer indicating an effect on photodegradation, possibly through ROS generation; this effect is enhanced by the presence of iron.

- The fitted area of the peak attributed to peroxide content (peak 2) is reduced by the presence of transition metals, particularly copper, indicating Fenton-like decomposition of peroxides in the proximity of the paint layer.
- The anti-correlations between the peroxide associated peak *meta*-substituted AQs and correlations to *ortho*-substituted AQs supports a structural dependence on metal chelation and reactivity, and it is possible evidence of antioxidant activity of *ortho*-substituted AQs.
- The presence of PB pigments increases the rate of degradation of the paper substrate during photodegradation.
  - This process is photo-initiated and largely independent of oxygen concentration and is likely related to species in the paper being oxidised during the photoreduction of PB.
  - Irradiation of samples with PB under oxygen results in an additional increase in the rate of degradation of the paper substrate indicating a photo-oxidative degradation pathway is also possible. This pathway might be related to Fenton-like decomposition of peroxides by the photo-reduced iron centres in Berlin white.
- The presence of photo catalytic white pigments, such as ZnO, as extenders increases the formation of peroxides and the rate of degradation of the paper substrate.

The results of this study can be used to interpret the oxidative degradation potential of watercolours under conditions of photodegradation. The presence of AQs, especially in the presence of transition metals, and PB with or without photo catalytic pigment extenders in watercolours enhances the oxidative degradation of the underlying paper thus endangering the long-term visual impact of the objects, *e.g.* watercolour drawings by J.M.W. Turner in Tate's collection. Application of protective antioxidant treatments that might change the visual impact of an object is typically not an option for such objects; however, a suitable method to limit the localised oxidative degradation of the watercolour drawing would be to use oxygen-free storage and display (2, 3) which was demonstrated to give a measurable reduction in the rate of peroxide formation and in the loss of DP of the paper substrate.

Chapter 6 X-Ray Absorption Spectroscopy Studies of Prussian Blue

6.1 Background

Oxygen-free (anoxic) and low-oxygen storage and display of paper-based artworks could minimise the effects of photo-deterioration, particularly during long-term display, and thus they are an attractive preventive conservation strategy (2, 3, 122, 124, 141, 398-402). However, before anoxic and/or hypoxic display can be widely accepted in the heritage community and applied to important artworks, its effect upon artists' materials must be assessed, and the risk of applying anoxic treatment to an object analysed. Research to this end has been ongoing for more than a century (52, 54, 55), and 'anoxic' frames have been applied to a limited extent in the intervening years. A survey of the conservation literature identifies several historic pigments or dyes that may be unstable in anoxia, because reduction reactions that are normally inhibited or reversed by O_2 can proceed in its absence (2, 73, 140), see Chapter 1 for a review of these sources. Of these colourants, Prussian blue (PB) and related pigments have attracted the greatest attention partly because of their apparent stability in ambient atmosphere, and their striking, total, though temporary, loss of colour after extended light exposure in the absence of oxygen, but also because of the popularity of the pigment and its wide use in a variety of media.

That both exposure to high levels of visible light and near UV radiation induce fading and colour change in PB pigments have been known for some time (5, 6), but they are known to be lightfast at gallery lighting conditions (50 lux) and ambient atmosphere (127, 403). At lower to moderate light levels, the rate of fading is less than the rate of reversion, thus while photo-initiated fading is occurring, there is no net observable change in the colour of the pigment. Light exposure in the absence of oxygen, or in a sealed case with depleted oxygen has been shown to lead to a gradual fading to white for PB pigments in watercolour medium, on textiles and in cyanotypes (4-7, 52, 54, 127, 403, 404). Lerwill *et al.* and Ware found that most faded samples, upon return to ambient atmosphere and reduction of light levels, reverted to within experimental error of the original colour coordinates (127, 404). On the other hand, Rowe found that textiles dyed with PB did not revert completely after indoor daylight exposure in anoxic conditions (7), and Korenberg notes that Winsor and Newton PB and Antwerp blue watercolour paints do not fully recover after fading under anoxic conditions (4).

The discrepancies between different studies can be attributed to many factors (differences in particle size, substrate, paint/pigment composition etc.), but it suggests that perhaps the fading of PB and moreover the interaction of PB with a substrate is more complex than commonly assessed. Thus understanding the fading of PB under anoxic conditions became a research priority for the Anoxic Project at Tate. Questions that the Anoxic Frames Project at Tate (AFP) felt needed to be addressed are:

1. What is the range of fading behaviours of PB pigments?

2. Is an atmosphere of 21% oxygen required to 'maintain' the colour of PB?

   o If not, what is the lower critical oxygen concentration at which the rate of reversion of PB is faster than the rate of fading?

3. Does PB fade differently in anoxia than in standard atmosphere?

   o That is, can fading in a predominantly nitrogen atmosphere cause irreversible changes to the crystal structure resulting in a less than full reversion?

   o Is an argon atmosphere safer, as it cannot interact with the iron centres?

4. Can different PB pigments, particularly those which have been substituted or ion exchanged with transition metal cations be distinguished by x-ray absorbance spectroscopy?

5. Do PB pigments interact with the substrate to promote the oxidative degradation of cellulose?

As a means to understand the fading behaviour of PB and related pigments, and answering the above questions, a considerable library of samples of pigments and watercolour paints containing PB were collected by members of the AFP and, when sufficient quantities were present, prepared into a library of watercolour paint outs. The collection of the samples and preparation of watercolour paints from the samples, as well as preparation of paint outs was primarily undertaken by Charlotte Caspers; an account of this work can be found in her Master's Thesis of 2008 (167).

The prepared paint samples and raw pigments were used for a number of analyses. Notably: micro-fadeometry, x-ray absorption spectroscopy (XAS) including x-ray near-edge absorption structure (XANES) and extended x-ray absorption fine structure (EXAFS), chemiluminometry, headspace analysis by GC-MS and viscometry. The results of this research led to the writing of a patent (405), and a successful application for a second round of public sector research exploitation (PSRE) funding. Micro-fadeometry was used to address the first and second questions, and was the focus of the PhD Thesis of Andrew Lerwill (11), partly published by Lerwill *et al. (404, 406).* The final question was addressed by chemiluminometry, headspace GC-MS and viscometry. The chemiluminometry and viscometry research is presented in Chapter 5, Section 5.4.4.2 of this Thesis. The GC-MS research is presented in Chapter 7 of this Thesis. XAS was used in an attempt to answer questions 3 and 4.

6.1.1 Collaboration for XAS Studies of PB

Through collaboration with Dr. Sven Schroeder of the University of Manchester it was possible to secure beam times at Daresbury Synchrotron Radiation Source (SRS) (now decommissioned) and the Diamond Light Source at the Rutherford-Appleton Laboratory, Oxfordshire. The underlying purpose of these SR studies was

to test different configurations of a new automated *in situ* XAS setup for 96-well plates, which was being developed as part of Dr. Schroeder's EPSRC project in collaboration with DIAMOND, the SRS and The University of Southampton. A new type of automated high throughput cell that allows for simultaneous measurement of *in situ* XAS under a controlled atmosphere with or without visible light photo-excitation, by transmission, fluorescence yield and total electron yield (TEY), was designed and constructed for these SR studies. The cell design arose from a 'brain storming' session between Dr. Schroeder and me. The first cell was constructed at Manchester University for Dr. Schroeder's group, and a new version, incorporating collimating optics for simultaneous photodegradation and *operando* UV-Vis spectrometry and XAS was designed and machined by myself at Tate, Figure 8A and 8B below.

Additional collaboration with the Pigmentum Project, Oxford University, provided access to a library of PB pigment samples (407). This library has been the subject of extensive research by Dr. Nicholas Eastaugh and colleagues at the Pigmentum Project and the samples have been characterised by numerous analytical techniques including Raman, FTIR, XRF and in some cases XRD. The new high throughput cell designed for the studies was needed not only to survey the large sample library (more than 100 pigments) but also because many of the samples were both minute and not expendable. Similarly, as we wished to study the fading of pigments *in* situ as applied in a watercolour wash, transmission in polyethylene (PE) was not possible. As such the standard practice of pressing a pellet from the mixture of the sample ground in PE could not be applied in all cases.

The experimental goals of the work were to first characterize the pigment library with XAS to see if the different pigments, could be differentiated by their XANES and/or EXAFS spectra, and second to study the photodegradation of PB *in situ* under various atmospheres to determine if fading under anoxic conditions results in the formation of a chemically or structurally different species than fading under ambient air. However, as the high throughput setups were at best untested in the beam lines at SRS and Diamond or in the case of the TEY cell, a rough prototype completed on site, much of beam time allocations were spent in configuration and characterisation of the setups and measurement methods. Furthermore, due to technical difficulties at Daresbury SRS, much of our allotted time was not usable, and the time allotted at Diamond Light Source occurred during the evaluation period of the beam line before it had been fully commissioned.

Presented below are initial interpretations of extracts from data sets produced at the two beam times. The first beam time, autumn 2007, at Daresbury Synchrotron Radiation Source, provided an opportunity to survey a large collection of pigments samples with XAS. At the second beam time, spring 2008, at Diamond Light Source, the fading of the PB pigment used by J.M.W. Turner, prepared as a watercolour, was studied. Initial attempts at spectral deconvolution and fitting of the EXAFS regions from PBs using $K_4[Fe(CN)_6]$ and $K_3[Fe(CN)_6]$ as model materials did not prove successful, and therefore the interpretations are comparative and rely heavily upon the XANES region, identifying regions of greatest difference and similarity between samples; when possible samples are grouped based on spectral features and the oxidation state of the

transition metals postulated. A computational approach based on that used by Wilke et al. for the interpretation of pre-edge features might be applicable to garner more information from the data and serve as a basis for future beam time applications (313, 408).

6.2 A Brief Review of Prussian Blue

Before discussing the results from the XAS studies of PB it is useful to briefly review the chemistry of PB so that the results can be better interpreted.

6.2.1 PB, Its Composition and Preparation

PB, iron hexacyanoferrate, is the model compound for a class of mixed-valence transition-metal hexacyanometalates. These compounds are receiving increasing attention due to their unique photo switchable electronic and magnetic properties (409-411), chromic behaviour (129), as well as their potential for gas and metal sorption (131, 412-414) as well as catalytic potential.

PBs, including all metal hexacyanometalates, are a complex family of pigments, all of which have complex stoichiometries, and have even been described by many researchers as 'non-stoichiometric' (415). Different types of PB can be formed from the same reagents depending on the ratio of reactants as well as the reaction conditions.

Mike Ware in his excellent book *Cyanotype. The history, science and art of photographic printing in Prussian blue*, gives perhaps the most complete review of both the chemistry and application of PB in the preparation of works of art (127).[22]

6.2.1.1 Structure

In its ideal form PB has an open, cyanide-bridged, face-centred cubic lattice, see Figure 1 (127). The lattice structure is that of a mesoporous 3-D polymer with zeolitic properties. Interstitial voids and lattice vacancies are capable of accommodating significant quantities of water as well as ionic and molecular impurities, which can be ion-exchanged with relative ease. Furthermore, the open structure of the crystal lattice allows for ion conductivity, which is a requirement for both fading and reversion of PB.

---

[22] Mike Ware's insights are particularly valuable as he has lectured and researched structural and inorganic chemistry at Manchester University with a focus on mixed valence coordination complexes, acted as a consultant for the conservation of early photographs and he is a practising photographic artist specialising in early photographic processes, including cyanotype.
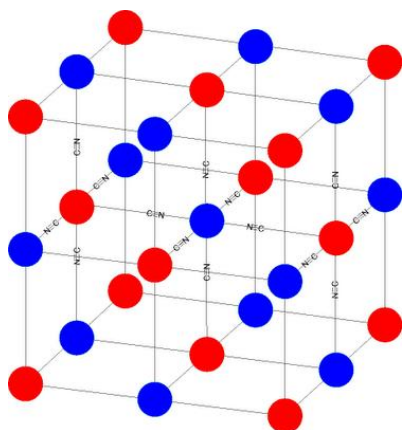
Figure 1 Ideal cubic crystal lattice of PB. The red circles represent Fe^{2+} and the blue circles represent Fe^{3+}.

However, one of the difficulties in working with PB is that it does not have a well-defined stoichiometry, and its composition varies with the method of preparation. Perhaps Itaya *et al.* best summarised:

> "In fact, the chemical designation of Prussian blue should be regarded as essentially a generic term for complex materials which may contain co-precipitated or occluded ions, indefinite amounts of water, possibly hydrolysed ferrocyanide, variable stoichiometry, and structural disorder." (415)

6.2.1.2 Preparation

Three common methods of preparation are summarised below in Schematic 1 to yield PB and related compounds, see Table 1 (127).

(1)　$Fe^{(III)}_{(aq)} + [Fe^{(II)}(CN)_6]^{4-} \longrightarrow Fe^{(III)}_4[Fe^{(II)}(CN)_6]_3 \cdot 14\text{-}16H_2O$

(2)　$Fe^{(II)}_{(aq)} + [Fe^{(III)}(CN)_6]^{3-} \longrightarrow Fe^{(III)}_3[Fe^{(II)}(CN)_6]_2^+ X^- \cdot nH_2O$

(3)　$Fe^{(II)}_{(aq)} + [Fe^{(II)}(CN)_6]^{4-} \longrightarrow M^+_2Fe^{(II)}[Fe^{(II)}(CN)_6] \xrightarrow{O_2} M^+Fe^{(III)}[Fe^{(II)}(CN)_6]^- \cdot H_2O$
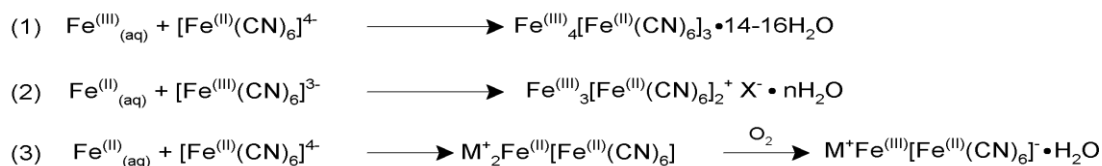
Schematic 1 Reactions to prepare PBs.

Typically PB is defined as being 'soluble' and 'insoluble'. This designation is a misnomer, as all types of PB are insoluble, but the 'soluble' form is a colloidal suspension in water. The type of PB prepared from reaction 1 in Schematic 1 depends upon the relative proportions of the reactants as well as upon reaction conditions (127). During preparation, a 1:1 stoichiometric ratio of transition metal cation to hexacyanometalate anion and the presence of an alkali metal cation tend to favour the formation of 'soluble' PB. However, if the metal cation is in great stoichiometric excess, the insoluble variety is favoured. A third pigment, Turnbull's blue, can be formed by reaction 2 in Schematic 1, and reaction 3 is the industrial process used to produce soluble PB through the oxidation of Berlin white, Schematic 1.

Under conditions where rapid flocculation, such as by reductive electro-deposition in a Fe^{3+} and [Fe(CN)$_6$]$^{3-}$ solution or by rapid co-precipitation (416), the kinetically-favoured insoluble variety is favoured even in the

presence of K^+ (127). This product can be ripened by K^+ ion exchange and redox cycling to form the thermodynamically favoured soluble variety.

To further complicate the matter, PBs intermediate between 'soluble' and 'insoluble' can be formed via reaction 1, as well as other PBs that incorporate some Fe^{3+} [$Fe^{3+}(CN)_6$] (Berlin green) or some iron aquapentacyano ferrate to give a greenish hue, and other PBs can be formed by substituting other transition metal salts for the Fe3+ and Fe2+ in reactions 1 and 2 above, Schematic 1 (417).

Table 1 Varieties of PB and related compounds

Substance	Formula
Soluble PB	$M^+Fe^{(III)}[Fe^{(II)}(CN)_6]^- \cdot$ 1-5 H_2O where M^+ = Na^+, K^+, Rb^+, Cs^+, Tl^+, NH_4^+
Insoluble PB	$Fe^{(III)}_4[Fe^{(II)}(CN)_6]_3 \cdot 14-16$ H_2O
Turnbull's blue	$Fe^{(III)}[Fe^{(II)}(CN)_6]_2^+X^- \cdot nH_2O$ where X^- = is typically a halide anion, but other monovalent species can also substitute into the structure.
Everitt's salt	$K_2Fe^{(II)}[Fe^{(II)}(CN)_6]$
Berlin white	$(NH_4)_2$ $Fe^{(II)}[Fe^{(II)}(CN)_6]$
Berlin green	$\{Fe^{(III)}[Fe^{(III)}(CN)_6]\}_{1/2}$ $\{Fe^{(III)}[Fe^{(II)}(CN)_6]_{1/2}\}^-$
Prussian yellow	$Fe^{(III)}[Fe^{(III)}(CN)_6]$
Iron aquapentacyanoferrate	$Fe^{(III)}[Fe^{(II)}(CN)_5H_2O]$

6.2.1.2.1 Soluble PB

If reaction 1, in Schematic 1, is carried out in 1:1 molar ratio of Fe^{3+} to $[Fe^{2+}(CN)_6]^{4-}$, or when the $[Fe^{2+}(CN)_6]^{4-}$ is in excess, the soluble form of PB, $M^+Fe^{(III)}[Fe^{(II)}(CN)_6]^- \cdot$ 1-5 H_2O (where M^+ is typically an alkali metal or ammonium cation) is formed rather than the insoluble form as shown in the reaction 1 schematic. Reaction 3, In Schematic 1, first yields Everitt's salt (or Berlin white) which is oxidised by air or another oxidant to form soluble PB.

While single crystals of soluble PB have not been grown, based on powder diffraction XRD, it is believed that it comes closest to the 'ideal' face-centred cubic lattice (127). The octahedral $[Fe^{2+}(CN)_6]^{4-}$ units are centred on the lattice sites, and the nitrogen-surrounded octahedral holes are occupied by Fe^{3+}. The low-spin Fe^{2+} centres are surrounded by six carbon ligands with a Fe^{2+}-carbon distance of 1.92 Å, and the high-spin Fe^{3+} centres are surrounded by six nitrogen ligands with a Fe^{3+}-nitrogen distance of 2.03 Å (127). The tetrahedral holes are alternately occupied by water and a monovalent cation, typically K^+, to maintain charge balance. The lattice parameter is a=1016 pm, and the number of formula units per unit cell are Z=4 (127).

Other monovalent cations, NH_4^+ and Na^+, can be used to prepare soluble PB; it has been noted that these PBs have different light fastnesses than K^+-containing soluble PB (6), and research has indicated that the cation species plays a significant role in the charge transfer process (131, 418). Furthermore, other cations

with an ionic radius less than 182 pm (127), notably Rb^+, Cs^+, Cu^+, Cu^{2+}, $Fe^{3+}$and Ni^{2+}, but also heavier elements can be ion exchanged for some of the K^+ in the crystal lattice (127). A PB containing copper has recently been found in a water-based paint used in the early 1870s by J.A.M. Whistler, and Pb^{2+} and Tl^+ can be ion exchanged into PB to alter the colour, as in the toning of cyanotypes (127). Additionally, there is some evidence that H_3O^+ can be accommodated into the lattice structure during preparation of PB under acidic conditions or during purification of the pigment by washing in HCl (127). It should be noted that incorporation of different cations into the crystal lattice not only results in changes to the optical properties of the pigment, but also can generate irregularities due to lattice contractions/expansions, bond angle/length changes etc, and these changes can be observed in the PB analogues and should be observable in the EXAFS spectra of metal substituted PB (419).

6.2.1.2.2 Insoluble PB

If reaction 1, in Schematic 1, is conducted with a molar ratio of 4:1 (or greater) of Fe^{3+} to $[Fe^{2+}(CN)_6]^{4-}$ and the solution does not contain stoichiometric quantities of K^+, then the insoluble form, $Fe^{(III)}_4[Fe^{(II)}(CN)_6]_3 \cdot 14 - 16\ H_2O$, is largely the product. This can be favoured by co-precipitating the PB on a substrate, such as $Al(OH)_3$ that can be later removed by washing with an acidic solution.

Insoluble PB can be considered the defect version of the 'ideal' face-centred cubic lattice in Figure 1. One fourth of the $[Fe(CN)_6]^{-4}$ subunits in the lattice are vacant and filled with water that coordinate with Fe^{3+}; thus yielding Fe^{3+}which is octahedrally coordinated to 4.5 nitrogen atoms and 1.5 oxygen atoms, and thus a $Fe^{3+} : Fe^{2+}$ ratio of 4:3. An additional 8 water molecules, either as isolated molecules or hydrogen bonded to the coordinated water, are present in the channels of the unit cell (420). Despite the defects from the ideal lattice structure, single crystal x-ray diffraction studies have found a lattice parameter of a=1017 pm indicating some ordering to the lattice vacancies (127, 421). If so, then one fourth of the Fe(III) sites will have a regular octahedral $[Fe(NC-)]^{3+}$ coordination sphere, while the remaining three fourths of the Fe(III) sites will be of distorted octahedral geometry of $trans$-$[Fe(NC-)_4(OH_2)_2]^{3+}$ (127). Furthermore, depending on the preparation conditions, hydrolysis by proton loss, which is favoured by alkaline conditions, can occur at the hydrated Fe^{3+} sites to yield $[Fe(OH)(NC-)_4(OH_2)]^{2+}$ and $[Fe(OH)_2(NC-)_4]^+$ (127). This hydrolysis of the Fe(III) centres is thought to be responsible for the broadening and splitting of the cyanide band in the infrared spectrum (127) and should also affect the crystal structure such that it might be distinguishable in the EXAFS spectrum as well as in XRD data (127). Like soluble PB, insoluble PB can readily undergo ion exchange, and it appears that the lattice vacancies result is a higher uptake of metal ions, an effect that is exploited in the use of insoluble PB as an antidote for heavy metal poisoning (422).

6.2.1.2.3 Turnbull's Blue

Reaction 2, In Schematic 1, yields Turnbull's blue; it is the least studied of the iron blue pigments. Once thought to be $Fe^{(II)}_3[Fe^{(III)}(CN)_6]_2$, it has been found that it undergoes a self-redox reaction to form the iron(III) hexacyanoferrate(II) (127). While being an iron(III) hexacyanoferrate(II) like PB, Turnbull's blue

exhibits some significant differences from soluble and insoluble PB: one third of the $[Fe(CN)_6]^{-4}$ sites are vacant, giving an Fe^{3+}: Fe^{2+} ratio of 1:2, and resulting in more lattice disorder. Turnbull's blue has an even less well defined stoichiometry than insoluble PB, but an average formula of $Fe^{(III)}[Fe^{(II)}(CN)_6]_2^+X^-\cdot nH_2O$ has been proposed, with X^- representing a singly charged anion accommodated into the lattice to maintain charge neutrality.

6.2.2 PB Reactivity

While the fading behaviour of PB as a historic pigment and in cyanotypes is well documented, pure, insoluble PB has been found to be lightfast, and the pigment is given an excellent light fastness rating (423). However at higher light levels or lower oxygen concentrations PB can be seen to change colour.

Much of the reactivity of PB is dependent of the presence of contaminants in the crystal lattice or that can diffuse into the lattice and that can act either as electron donors in the redox reaction or to balance any changes in charge. Outside of electrochemical experiments, the reactivity of PB is photoinitiated but limited by the rate of mass transfer of reactants into the crystal lattice.

6.2.2.1 Interaction with Light

PB has broad absorption bands at ca. 700 nm and 400 nm; both are associated with electronic transfer. The absorption band at 700 nm is stronger and corresponds to electron transfer from low-spin $Fe^{(II)}$ to high-spin $Fe^{(III)}$:

$$\{Fe^{III}(t_{2g}{}^3e_g{}^2)Fe^{II}(t_{2g}{}^6)\} \rightarrow \{Fe^{II}(t_{2g}{}^4e_g{}^2)Fe^{III}(t_{2g}{}^5)\}*$$
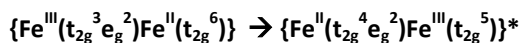
where the star indicates an excited state. This transition is spin-allowed because the electron is transferred from one t_{2g} orbital to another with no change to the net spin of the molecule (127).

The absorption band at 400 nm is weaker, while it is still low to high, it is forbidden because it is from a t_{2g} orbital to an e_g orbital (127):

$$\{Fe^{III}(t_{2g}{}^3e_g{}^2)Fe^{II}(t_{2g}{}^6)\} \rightarrow \{Fe^{II}(t_{2g}{}^3e_g{}^3)Fe^{III}(t_{2g}{}^5)\}*.$$
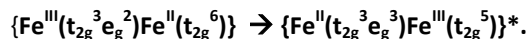
6.2.2.2 Photoreduction

It has been proposed that the underlying cause of the photo fading of PB pigments is the photo induced reduction of $Fe^{(III)}$ to $Fe^{(II)}$, yielding pigments similar to Berlin white (Everitt's salt) and a loss of the intervalence charge transfer that is responsible for the broad absorption band at ca. 700 nm thereby resulting the loss of the blue colour of the material. The excited state of PB is a much better oxidiser than PB in its ground state (127)., however, to proceed, the photo-reductive fading of PB to Berlin white requires:

- Light (wavelengths ca. 400 nm and/or 700 nm),

- A reducing agent/electron donor in the immediate chemical environment of the PB, either as an impurity in the crystal lattice or adsorbed onto the surface,
- Cations that can migrate into the lattice to maintain charge neutrality.

$$2\,OH^- \qquad \frac{1}{2}\,O_2 + H_2O$$

$$h\nu + Fe^{III}[Fe^{II}(CN)_6]^- \;\longleftrightarrow\; \{Fe^{II}[Fe^{III}(CN)_6]\}^\star$$

$$\{Fe^{II}[Fe^{III}(CN)_6]\}^\star + \tfrac{1}{2}C_2O_4^{2-} \;\longrightarrow\; Fe^{II}[Fe^{II}(CN)_6]^{2-} + CO_2$$
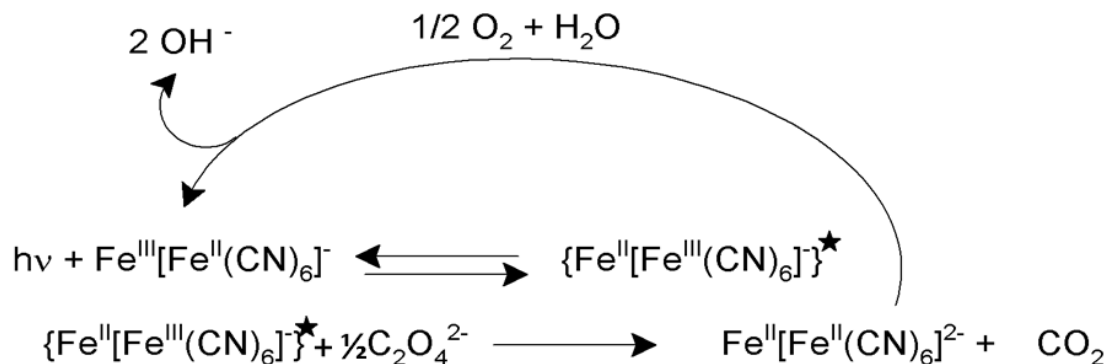
Schematic 2 Photoreduction of PB in the presence of oxalate. The star indicates an excited state (127).

The absorption of light at 700 nm or 400 nm and electron transfer results in an excited state that can be approximated as Fe(II) hexacyanoferrate(III). This photo activated compound is a much stronger oxidising agent and in the presence of a suitable electron donor, it can be reduced to Berlin white (this is the basis of some cyanotype processes) (127). The presence of white pigments, TiO_2 and ZnO, as extenders increases the rate of fading. This is likely due to the fact that these pigments are photo catalysts generating electron-hole pairs thus promoting the reduction of PB (4, 6, 127, 424, 425).

The reaction likely takes place in the solid phase, but requires not only a suitable electron donor (*e.g.* oxalate, citrate, lignin residues, monosaccharides, ferrocyanide, etc.) to be in the chemical environment of the photo-excited centre, but also cations that can diffuse into the crystal lattice to maintain charge balance, as well as water in order to facilitate the diffusion of both the donor and the cations. If either a suitable reducing agent or cations capable of diffusing into the crystal matrix are not available, the photo-excited PB can decay back to the ground state.

Following reduction, the resulting Berlin white (redox potential +0.46 V) can then be readily oxidised by air and water to reform PB as well as hydroxide anions. Electrochemical studies have proven that this process is fully reversible provided there are enough cations present to act as a charge balance (417). However, if the hydroxide anions are not scavenged by protons in the crystal lattice, a localised alkaline environment can result in the irreversible hydrolysis of PB.

6.2.2.3 Alkali Hydrolysis

PB is not stable in an alkaline environment. Exposure to pH 8 to pH 10 can result in the destruction of PB by the following reaction (127).

$$Fe^{(III)}[Fe^{(II)}(CN)_6]^- + 3OH^- \longrightarrow Fe^{(III)}OH_3 + [Fe^{(II)}(CN)_6]^{4-}$$
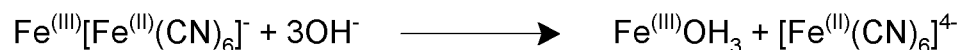
Schematic 3 Alkaline hydrolysis of PB.

Alkali sources can include deacidification treatments, ammonia-based cleaners, pigment extenders such as lead white that are added during paint preparation (127, 426) or, as noted above, the hydroxide anions generated during the reversion of Berlin white to PB (127). Thus, cycled fading and reversion can consume the chemically available protons and result in the loss of colour density of PB and a irreversible colour change.

6.2.2.4 Formation of Aquapentacyanoferrate

In addition to reductive fading, exposure of PB to high levels of light with some UV component can lead to the oxidation of some of the cyanide ligands to irreversibly form the iron aquapentacyano complex, $\{Fe^{(III)}[(Fe^{(III)}(CN)_5(OH_2)]\}^-$, and cyanogen gas via the following reaction.

$$h\nu + 2Fe^{(III)}[Fe^{(II)}(CN)_6]^- + 2H_2O \longrightarrow 2Fe^{(II)}[Fe^{(II)}(CN)_5](OH_2)]^- + (CN)_2$$

Schematic 4 Photodegradation of PB to the aquapentacyano complex.

This compound behaves similarly to PB, and results in little contraction of the crystal lattice (127), however, it has a bathochromic shift of the 700 nm band to approximately 780 nm; this results in a greenish hue to the pigment, and might be responsible for the residual colour change reported by some researchers following the reversion of PB (5, 6, 127).

6.2.2.5 Oxidation of PB to Berlin Green and Prussian Yellow

Berlin green is a true mixed valence compound exhibiting self-electron exchange (417). Once thought to have the formula $Fe^{(III)}[Fe^{(III)}(CN)_6]$, Berlin green is now known to be a meta stable intermediate with the formula $\{Fe^{(III)}[Fe^{(III)}(CN)_6]\}_{1/2} \{Fe^{(III)}[Fe^{(II)}(CN)_6]_{1/2}\}^-$.

Berlin green can be formed by the oxidation of PB in the presence of strong oxidants or in an electrochemical redox cell. Further oxidation of Berlin green leads to Prussian yellow or brown, $Fe^{(III)}[Fe^{(III)}(CN)_6]$. Pure Prussian yellow can be prepared via cyclic voltametry in an irreversible process (127, 417).

Berlin green can also be formed, along with Cl_2, by reaction of 1:1 molar ratio $FeCl_3$ with $K_3[Fe(CN)_6]$. The same reaction when conducted with excess $FeCl_3$ will produce PB upon contact with an oxidisable substrate such as cellulose (127). It is likely that historic preparations of PB contain a certain amount of Berlin green due to impurities in the starting materials or the preparation process (127).

6.3 Experimental Section

6.3.1Introduction

Predicting the influence of environmental conditions on PB pigments is considerably complicated by the known existence of different forms of historic PB. Substitution at iron sites and/or ion exchange by heavier elements such as copper, antimony, cobalt, chromium is feasible, and a copper exchanged pigment may have been found recently in a water-based paint used in the early 1870s by J.A.M. Whistler.[23] Micro-fadeometry work has found that there is a range of fading rates for PB in both room atmosphere and anoxia (11), but the response of these different types of PB to anoxia has yet to be fully quantified, and has not been investigated previously due to the experimental difficulties associated with characterising PB pigments used in historic artworks. It is known that soluble PB as well as PB with pigment extenders are less lightfast than insoluble PB (6, 11).

Within the conservation field, studies on the lightfastness of PB under non-ambient atmospheres have made use of N_2 or N_2-dominant atmospheres (4, 7, 122, 427, 428). While the results of the various studies are somewhat contradictory, a general conclusion that fading of PB in anoxia results in a residual, irreversible colour change when compared to fading of PB in ambient atmosphere has been drawn (4, 7). However, no fundamental structural investigations have been undertaken to actually determine the underlying changes in crystal and/or molecular structures that accompany the observed pigment deterioration.

The possibility exists that N_2 may indeed act as a reactant, recalling in this context the elemental composition of the N_2-activating component in the Haber-Bosch NH_3 synthesis catalyst: potassium-doped $Fe^{(II)}/Fe^{(III)}$ oxide. Furthermore, recent work indicates that substituted PB analogues can interact with atmospheric N_2: its sorption by Co-, Ni-, and Mn-substituted PBs results in a partial or complete framework collapse of the material (414). Such framework collapse could be the cause of the observed irreversible colour change of PB under nitrogen .. Furthermore, the difference in degree of framework collapse in substituted PBs is related to the substituting species as well as to alkali metal cation in 'soluble' analogues (131, 414, 429). If extended to PB pigments, this argument could explain the disagreement in observations by various studies on the fading PB under non-ambient atmospheres.

XANES characterisation of these PB pigment libraries at the Fe K-edge was used to determine whether the reported irreversible colour change of PB occurs due to chemical degradation of the pigment or the adsorption-induced collapse of crystal structures. In this respect XANES is a better method than XRD for detecting such structural decay phenomena at room temperatures, because they tend to not result in crystalline structures, and powder XRD analysis can thus miss the formation of new non-crystalline phases

---

[23] Personal communication with J. H. Townsend.

even if they are present in significant proportions. The variability and environmental stability of PB pigments was assessed through a high-throughput screening approach. Libraries containing:

1. well-defined synthetic PB reference structures (variation of the substituting species and their concentration), as well as,
2. a wide range of modern and historic PB pigments (including samples of PB used by J.M.W.Turner)

were collected. Many of these samples had been analysed by qualitative x-ray fluorescence and diffraction analysis by Tate or the Pigmentum Project thus providing needed information for data interpretation.

Measurements were carried out on raw pigment samples as well as *in* situ on watercolour paint outs. Detection was by transmission in a PE pellet or by combined detection of the transmission (probing the bulk), TEY (probing the near-surface) and, where necessary, the fluorescence yield (to probe substituting species present in low concentrations) in a newly designed sample cell, see Figure 8 below[24]. The design of a new sample cell allowed for non-expendable samples, as well as watercolour paint outs, to be measured and recovered. Furthermore the addition of TEY measurements, which probe approximately the top 500 Å of the samples at the Fe K-edge, gives the potential of additional mechanistic insight and possible detection of near-surface degradation of the pigment particles before they have become macroscopically visible through a bulk manifestation of any fading, as the process likely occurs at the surface of the material and progresses inwards.

6.3.2 Materials

6.3.2.1 Pigments

A library of over 100 samples of PB and related pigments was assembled between the collection of the Pigmentum Project and Tate (for a summary of the pigment library, see Table 4 at the end of this chapter). Roughly 1/3 of the samples in the library were historic, that is taken from pigment collections and or watercolour paint sets that were at least 50 years old. Several samples were prepared from the PB pigment used by J.M.W. Turner, the focus of the AFP. The remaining samples were modern preparations of PB according to historic recipes or those prepared in a quasi-combinatorial fashion to study the effect of metal substitution in the crystal lattice. Most of the samples in the library were in minute quantities and were considered to be non-expendable. As such, great care was taken to prevent sample loss and or cross contamination.

---

[24] This reaction cell, as well as the second prototype with an integrated Ocean optics 74-UV collimating fibre end for simultaneous photodegradation, UV-Vis spectroscopy, and XAS studies are the products of a collaboration between Dr. Sven Schroeder, University of Manchester, and myself. They form part of a new automated *in situ* XAS setup for 96-well plates, which was being developed as part of Dr. Schroeder's EPSRC project in collaboration with DIAMOND, the SRS and the University of Southampton. To our knowledge this is the first reaction cell to combine all three detection methods as well as high throughput micro positioning system into a single instrument. A description of this cell and its application will be the subject of a forthcoming publication.

6.3.2.2 Paper and Paint Outs

The paper used in the XAFS studies was produced by Two Rivers Paper mill. This 200 gm^{-2} paper is prepared from 100% cotton linters and has a hard gelatine size, with a medium rough finish. Chemically it is analogous to GSR described in Chapter 4. Pigments were prepared into paints by grinding them in a gum Arabic solutions with deionised water as per the protocol in Charlotte Caspers' Master's Thesis (167). The paints were then applied in an even, medium-dark wash to the paper and allowed to dry restrained.

6.3.3 Methods

6.3.3.1 Sample Preparation

Most pigments and paintouts were used as is, and were placed on a sample stub in sample tray of the high throughput (HTP) TEY cell. The cell was then positioned in the beam line for experimentation. Paint outs were adhered to the sample stubs with carbon tape.

If sufficient quantities of an otherwise expendable sample were available a 7-mm pellet was prepared by grinding sufficient sample to contain 1.5 mg of iron according to the stoichiometry of the compound (ca. 4.5 mg of PB) in PE and pressing the mixture into an aluminium 96 well plate at 5 tons pressure. The well plate was then sealed on both sides with Kaptan tape.

The RH was not controlled in these experiments and was the ambient level in the beam line.

6.3.3.2 HTP Transmission in PE Pellet Using Scanning XAFS

The 96 well plate and positioning system were placed in the beam line and aligned to maximize the signal. When necessary aluminium attenuators were used to prevent saturation of the detector.

The samples were characterized at the relevant transition metal K-edges (Fe for all samples and Co, Ni, Cu, Cr where suitable). Both XANES and EXAFS spectra were collected via transmission through the sample. The specification of the X-Ray beam line 9.3 at Daresbury SRS can be found at the SRS website (430).

6.3.3.3 Simultaneous HTP Transmission and TEY of Raw Pigments Using Scanning XAFS

The TEY-sample holder and positioning system containing up to 9 sample stubs with samples were placed in the beam line. The sample holder and the upper section of the cell were machined from PEEK plastic while the sample stubs were machined from aluminium. Samples of pigments were placed on the stubs without adhesive, and paint outs were adhered to the sample stubs with carbon tape, Figure 8A below.

To perform a measurement the sample holder was positioned such that the sample of interest was centred under the upper section of the cell. The sample holder was then raised to meet the upper section so that the TEY probe was optimally positioned relative to the sample and the beam just grazed the sample stub while passing thought a pigment sample.

The samples were characterized at the relevant transition metal K-edges (Fe for all samples and Co, Ni, Cu, Cr where suitable). Both XANES and EXAFS spectra were collected via transmission through the sample. The specification of the X-Ray beam line 9.3 at Daresbury SRS can be found at the SRS website (430)

6.3.3.4 XANES of Watercolour Drawings

The sample stubs described above were redesigned such that the upper portion on which the sample was placed was machined from high purity PEEK plastic to eliminate signal from iron contamination in the aluminium stub. Additionally the upper portion of the cell was redesigned and machined from aluminium so that it functioned as the TEY probe as well as to allow the samples to be illuminated with high intensity collimated visible light from an Ocean Optics HPX-2000 Xenon light source via a 200-µm optical fibre and an Ocean Optics 74-UV collimating lens adapter. A Viton o-ring was fitted to the upper section such that a gas-tight seal was achievable, Figure 8B below.

As above, the paint outs were attached to the stub with carbon tape and the Fe K-edge was characterized by XANES via fluorescence-yield orthogonal to the beam line. When necessary, aluminium attenuators were used to prevent saturation of the detectors. Periodic characterization was conducted before and after fading as well as during fading and reversion under specific atmospheres such that chemical, electronic and structural changes during fading and reversion could be followed. The X-Ray micro-focused beam line I18 Diamond light source specifications can be found at the Diamonds light source website (431)

6.3.4 Results and Discussion

6.3.4.1 Soluble Vs. Insoluble

Initial work focused on distinguishing between samples from the Pigmentum Project's collection that were known to be soluble (p946) or insoluble (p950) PB, Figure 2 below. $K_4[Fe(CN)_6]$ and $K_3[Fe(CN)_6]$ were included as reference compounds to determine the position of the Fe K-edge when either Fe^2 or Fe^{3+} are octahedrally coordinated to 6 cyanide ligands. The samples were prepared by grinding ca. 4.5 mg of pigment in PE and pressing the mixture into a pellet. The XAFS spectra were collected in transmission mode, and the resulting spectra were normalised by subtracting the function of a line fitted to the region before 7100 eV from the entire spectrum and scaling to the EXAFS region.

After normalising and scaling the data, subtle differences between the insoluble and soluble PB were apparent in the XANES spectra as well as significant differences with the reference compounds, Figure 2.

The first observable difference is the shift and broadening of the Fe K-edge relative to the reference compounds. $K_3[Fe(CN)_6]$ and the two PBs have a main absorption K-edge intensity at 7130.33 eV while $K_4[Fe(CN)_6]$ is at 7129.60 eV. A shift to higher energy is indicative of greater ferric ion content (313). The broadening of the main edge feature for PBs relative to those of the reference compounds is due to contribution from both ferric and ferrous species. This feature will prove to be useful to distinguish between

metal substituted-PBs (metal-iron) and metal exchanged (iron-iron + metal) PBs as XRF data will only identify the presence of another transition metal. However, main edge shift is not a precise measure of metal oxidation state, as factors including metal site geometry and lattice vacancies can influence both shift and peak broadening (313).
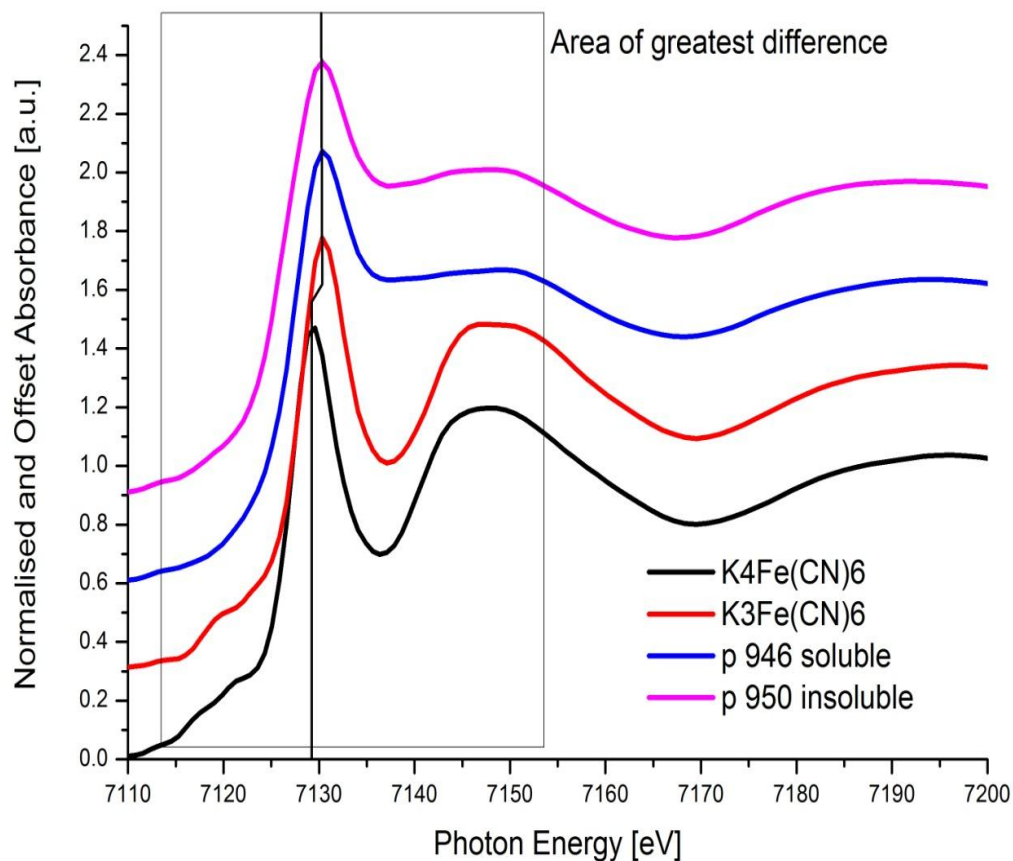
Figure 2 Fe K-edge XAFS spectra of soluble and insoluble PB. K4[Fe(CN)6] and K3[Fe(CN)6] are included as reference compounds. The spectra were collected by transmission through PE pellets that contained ca. 1.5 mg of iron (ca. 4.5 mg of PB samples). The vertical line designates the photon energy for the 1s to continuum electronic transition. The break in the line indicates the shift in the main edge for transitions from Fe^{2+} and Fe^{3+}.

To overcome this imprecision Wilke *et al.* have focused on pre-edge features, as these are due purely to electronic transitions and are un-influenced by site geometry, to determine the iron oxidation state in iron gall inks on paper using a calibration developed by Wilke for glass, melt and mineral analysis (313). Iron gall ink and PB can be considered similar systems in many ways, and this method should prove useful in analysing the data from these samples, however to be applied, further analyses of oxidation state distribution of the iron centres by Mössbauer electron spectroscopy or a related method and quantification of trace elements and occluded materials would be required. At the time of writing these analyses have not been conducted and thus Wilke's quanitative method has not been applied (313).

Regardless, close examination of the pre-edge region, Figure 3B, reveals pre-edge features between 7112 and 7124 eV where the rising edge region begins. In the PB samples the observed pre-edge features are not distinct due to overlapping contributions from both Fe(II) and Fe(III) centres. However, using the reference compounds they can be partly attributed. It is known that the pre-edge features are shifted to higher energy levels with increased oxidation state due to stabilisation of the core electrons. Examination of the reference compounds reveals 3 distinct pre-edge features at ca. 7113.8, 7117.6 and 7121.3 eV for $K_4[Fe(CN)_6]$; these features are shifted to ca. 7114.5, 7119.8 and 7123.6 eV for $K_3[Fe(CN)_6]$. It is reasonable to propose that the indistinct nature of the pre-edge features of PB samples is due to the overlap of these features arising from a mixture of two iron oxidation states, and that an increase in the Fe(III) to Fe(II) ratio as is the case for 'insoluble' PB should result in an observable change to the pre-edge features.

If the spectra from p946, known to be of the 'soluble' variety of PB, and therefore to have a Fe(III) to Fe(II) ratio of approximately 1:1, and p950 known to be 'insoluble' PB, and therefore to have a Fe(III) to Fe(II) ratio of approximately 4:3, are compared, the pre-edge features of the p946 are flatter between 7112.5 and 7119.0 eV indicating less contribution of the Fe (III) features observed in $K_3[Fe(CN)_6]$, Figure 3B.

To test this, insoluble PB was prepared according to Reaction 1 in Schematic 1, in the presence of $KAl(SO_4)_2$[25]. In this preparation $FeCl_3$ was in great excess and the pigment was rapidly co-precipitated on $Al(OH)_3$ with residual $FeCl_3$ present in the sample. The resulting pigment has a greenish tinge, which was reduced by washing in deionised water to remove some of the residual ferric chloride. A sample of the washed and dried pigment was characterised as above and the XAFS spectrum compared to those of soluble and insoluble PB, Figure 3. Examination of the pre-edge region shows similar features to that of the insoluble PB, as was expected.

---

[25] The $KAl(SO_4)_2$ was used so that there would be a significant aluminium content in the pigment to render it more similar to the PB used by J.M.W. Turner (TTB6). Known through SEM-EDX to have significant aluminium content. This aluminium is not observable by optical microscopy as a white extender, thus it is likely a co-precipitated or occluded ion in the PB lattice.
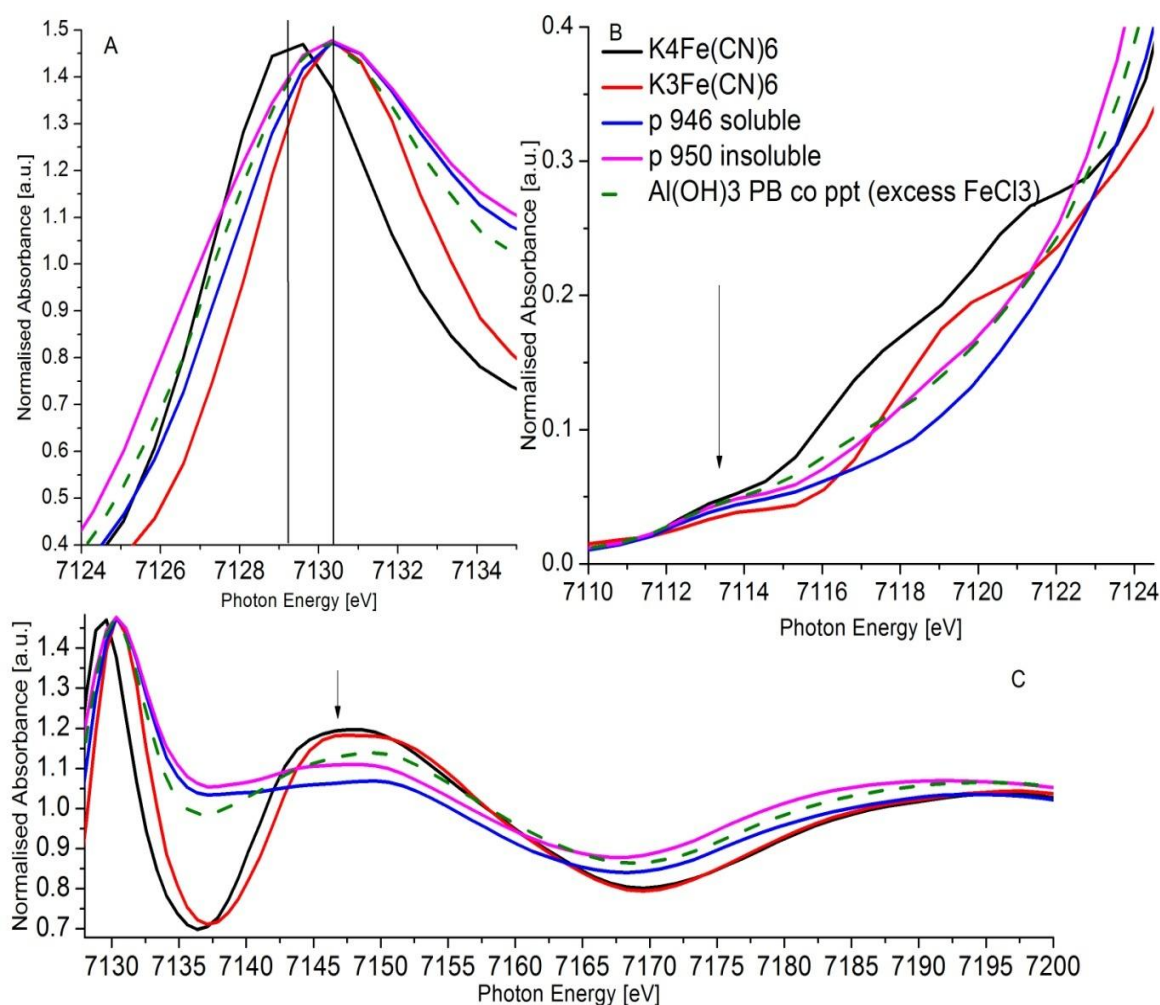
Figure 3 Main edge (A), pre-edge (B) and EXAFS (C) regions of soluble and insoluble PB. K$_4$[Fe(CN)$_6$] and K$_3$[Fe(CN)$_6$] are included as reference compounds. The spectra were collected by transmission through PE pellets that contained ca. 1.5 mg of Fe (ca. 4.5 mg of PB samples). The vertical lines in 3A are the photon energies for the continuum electronic transitions. The arrows in 3B and 3C indicate the areas of interest in the pre-edge and EXAFS regions that are discussed in the text.

The EXAFS region of the PB samples shows significant differences between the preparations, Figure 3C. The EXAFS region, however, is difficult to quantitatively interpret for historic samples as the region is due to electron scattering and any variation in the structural or chemical environment will significantly affect this region, and good model materials for historic PBs do not exist. Be that as it may, a visual inspection of the absorption bands in the EXAFS region between 7135 and 7155 eV allows for soluble and insoluble types to be distinguished with the former having a flattened response in this region, and the latter a more distinct peak shape, Figure 3C. The sample prepared with great excess FeCl$_3$ has an even more distinct shape and a shifting of the oscillation to a higher energy level possibly indicating the presence of occluded Fe(III). This possibility was examined by comparing the XAFS spectra of PBs prepared with different Fe(III) to [Fe(CN)$_6$]$^{4-}$ ratios.

6.3.4.2 Effect of Fe^{3+} to $[Fe(CN)_6]^{4-}$ Ratio During Preparation

The effect of different ratios of Fe^{3+} to $[Fe(CN)_6]^{4-}$ during PB preparation was explored by preparing PB with a 0.1:1, 1:1 and 1.3:1, as well as ca. 10:1, Fe^{3+} to $[Fe(CN)_6]^{4-}$ ratios. A preparation with roughly 1:1 should result in a soluble PB, while if Fe^{3+} is in large molar excess, insoluble PB should result. The result of a sub 1:1 ratio is not described in the literature, but has a blue colour, thus confirming the formation of PB, but its XAFS spectra are significantly different than that of other PBs.
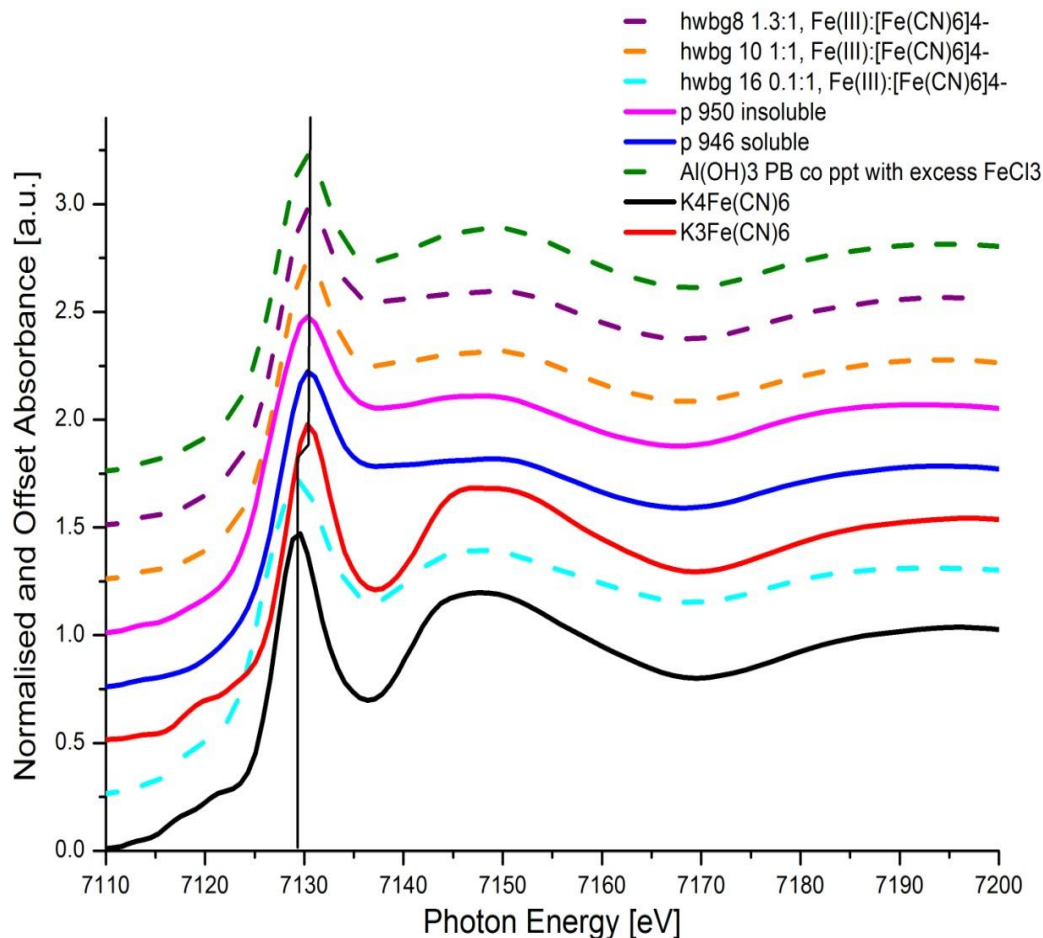
Figure 4 Fe K-edge XAFS spectra of PB prepared with different Fe(III): $[Fe(CN)_6]^{4-}$ ratios. $K_4[Fe(CN)_6]$ and $K_3[Fe(CN)_6]$ are included as reference compounds. The spectra were collected by transmission through PE pellets that contained ca. 1.5 mg of iron (ca. 4.5 mg of PB samples). The vertical line designates the photon energy for the 1s to continuum electronic transition. The break in the line indicates the difference between the required energies for transitions from Fe^{2+} and Fe^{3+}. Changes in the continuum electronic transition energy are indicative of changes in the Fe^{3+} to $[Fe(CN)_6]^{4-}$ ratio.

The samples were prepared by grinding ca. 4.5 mg of pigment in PE and pressing the mixture into a pellet. The XAFS spectra were collected in transmission mode, and the resulting spectra were normalised by subtracting the function of a line fitted to the region before 7100 eV from the entire spectrum and scaling to the EXAFS region. The normalised and offset spectra are presented in Figure 4, and the regions of interest identified above for soluble and insoluble PB are enlarged in Figure 5 A-C.

127
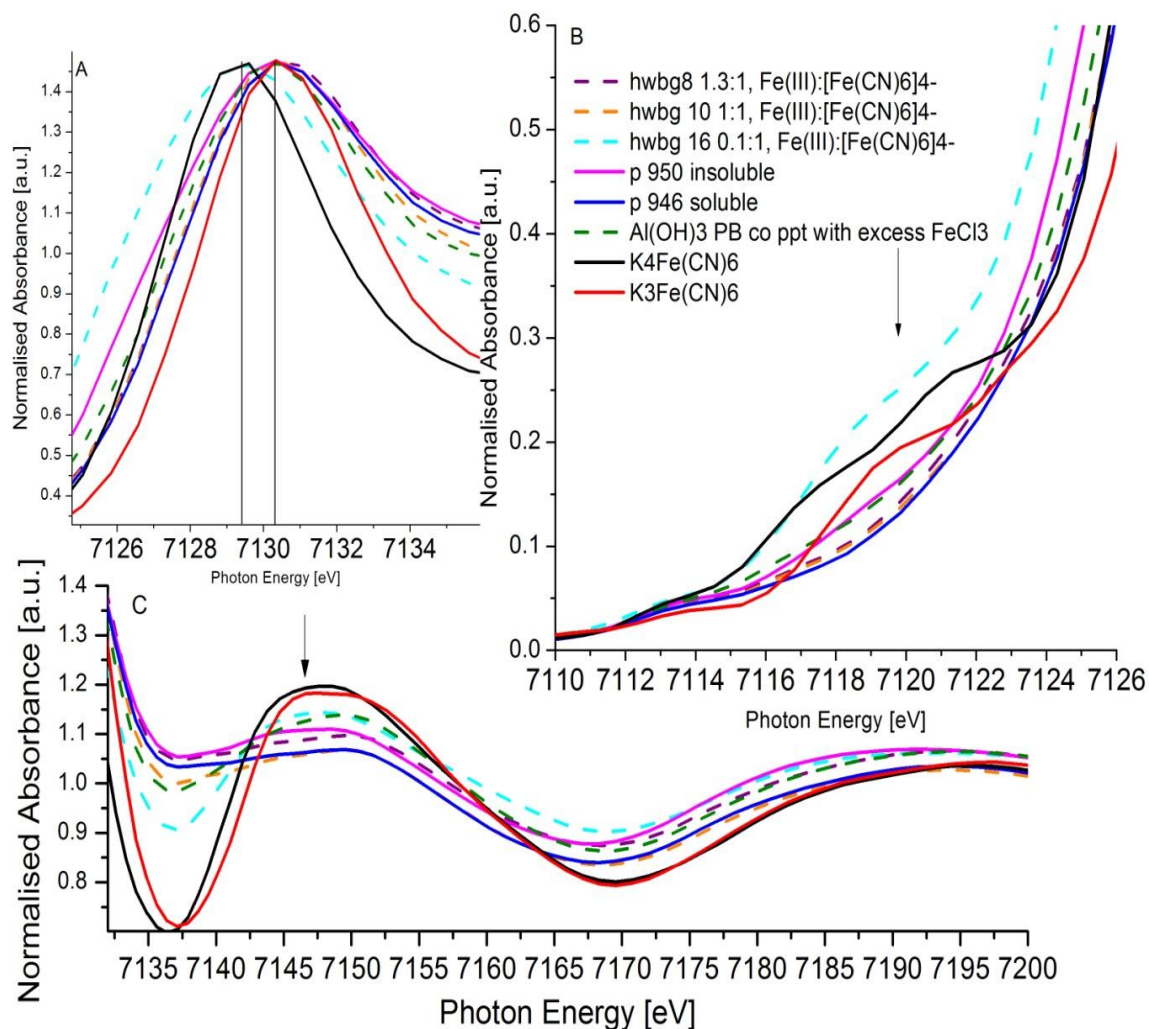
Figure 5 Main edge (A), pre-edge (B) and EXAFS (C) regions of PB prepared with different Fe(III): [Fe(CN)$_6$]$^{4-}$ ratios. K$_4$[Fe(CN)$_6$] and K$_3$[Fe(CN)$_6$] are included as reference compounds. The spectra were collected by transmission through PE pellets that contained ca. 1.5 mg of iron (ca. 4.5 mg of PB samples). The vertical lines in 5A are the photon energies for the continuum electronic transitions. The arrows in 5B and 5C indicate the areas of interest in the pre-edge and EXAFS regions that are discussed in the text.

Figures 4 and 5 present the Fe K-edge and the pre-edge and EXAFS regions of the Fe K-edge for a selection of PB prepared with a range of Fe^{3+} to [Fe(CN)$_6$]$^{4-}$ ratios. Samples p950 and p946, insoluble and soluble PB respectively, as well as K$_3$[Fe(CN)$_6$] and K$_4$[Fe(CN)$_6$] were included for reference. In this sample set, there are several interesting observations.

1. The shift in the main Fe K-edge from ca. 7129.60 eV for Fe^{2+} to ca. 7130.33 eV for Fe^{3+} is not observable for the sample with a 0.1:1 Fe^{3+} to [Fe(CN)$_6$]$^{4-}$ ratio, Figure 5A.

   a. The main edge for this sample is still significantly broader than the reference K$_4$[Fe(CN)$_6$], thus indicating contribution from both Fe(II) and Fe(III) and thereby the formation of PB. This is supported by the blue colour of the sample. However, as the shift is still more typical of Fe(II), it

128

can be postulated that there is residual $[Fe(CN)_6]^{4-}$ incorporated into the sample, and that this is overlaid on the PB signal, Figure 5A, resulting in a more Fe(II)-character of the main edge region.

b. Examination of the pre-edge region also reveals significant differences for the 0.1:1 sample, with a much more distinct shoulder between 7117 and 7122 eV, again likely arising from signal from residual $K_4[Fe(CN)_6]$ in the sample being overlaid with that from the PB formed during reaction, Figure 5B.

c. The EXAFS region for this sample has a more distinct sinusoidal shape in the first deconstructive and constructive interference regions and less flattening than either the soluble or insoluble samples indicating some order to the postulated contamination of the PB with residual starting material, $K_4[Fe(CN)_6]$, Figure 5 C. Indeed, the PB lattice is sufficiently spacious to accommodate either $[Fe(CN)_6]^{3-}$ and $[Fe(CN)_6]^{4-}$ in its channels (127).

2. For PB with roughly 1:1 Fe^{3+} to $[Fe(CN)_6]^{4-}$ ratio (thus the soluble type), the main Fe K-edge peak absorbance with a shift to ca. 7130.33 eV, Figure 5A.

a. In these samples, this feature is broader than that of both reference compounds, $K_3[Fe(CN)_6]$ and $K_4[Fe(CN)_6]$, indicating contribution from both Fe(II) as well as Fe (III) sites. However, the degree of broadening is not significantly affected by the changes to the Fe^{3+} to $[Fe(CN)_6]^{4-}$ ratio from 1:1 to 1.3:1 for samples prepared under the same or similar conditions, Figure 5A.

b. If the molar ratio between Fe^{3+} to $[Fe(CN)_6]^{4-}$ is roughly 1:1 the resulting pigment has pre-edge characteristics similar to those of the soluble PB, Figure 5B. The region between 7115 eV and 7122 eV seems to be important in distinguishing soluble like PBs.

c. The EXAFS region between 7137 eV and 7155 eV, Figure 5C, is also important for distinguishing 'soluble PB'-like characteristics, as a flattening in this region seems to indicate soluble PB.

d. There seems to be a progression in peak height at ca. 7148 eV in the samples hwbg 10, p946, hwbg 8, p950 (corresponding to Fe^{3+} to $[Fe(CN)_6]^{4-}$ ratios 1:1, unknown but soluble PB, 1.3:1 and unknown but insoluble PB).

Other than the sample of insoluble PB (p950), these samples all have a similar peak shape, and a progression in peak height (and shape) towards that of the insoluble PB could be interpreted as a progression of intermediates between soluble and insoluble PB, Figure 5C.

3. According to Ware, if PB is formed with $FeCl_3$ in great molar excess then insoluble PB is formed (127). Indeed this seems to be the case in the sample of $Al(OH)_3$ and PB co-precipitate in which $FeCl_3$ in great excess.

   a. For this sample, the main edge is shifted to 7130.33 eV, and greater broadening than the soluble samples is apparent, though to a lesser extent than that of the insoluble reference sample, Figure 5A. This indicates that perhaps the degree of broadening of the main edge could be used to evaluate the soluble vs. insoluble character of a PB sample, but it is less reliable than the pre-edge region as it arises from electronic promotion to the continuum and it is affected by iron site local environment, which will vary from preparation to preparation (313).

   b. The pre-edge features of this sample are indistinguishable from that of the insoluble type PB, Figure 5B. Features in this region arise solely from finite electron transitions and are only affected by the oxidation state of the metal site, and as such they are much more reliable in interpreting the Fe(III) to Fe(II) ratio in PB.

   c. The EXAFS region between 7130 eV and 7160 eV, Figure 5C, is difficult to interpret. Insoluble PB has less flattening than soluble PB, as noted above. The co-precipitated sample has more distinct features in this region than that of the insoluble type, and this might be due to residual Fe^{3+} regularly included or occluded in the lattice, however, this cannot be verified at this time, Figure 5C.

6.3.4.3 Metal Substitution/ Metal Exchange[26]

Transition metals can be introduced into PB by several methods. On the one hand, PB analogues can be prepared from several transition metals, Cu, Co, Cr, Mn, etc. In these mixed valence compounds, the transition metal typically substitutes at the Fe^{3+} sites, and they have a generic formula of

---

[26] Metal substituted PBs have transition metal substituted for Fe^{3+} in the formula $Fe^{(III)}_4[Fe^{(II)}(CN)_6]_3 \cdot 14 - 16$ H_2O. Metal exchanged PBs have metal cations (as well as anions for charge balance) ion exchanged into the meso-porous PB lattice in a manner similiar to ion exchange of zeolites.

$(M^{n+})_x([Fe^{(II)}(CN)6])_y$. On the other hand, metals can be ion exchanged into a prepared PB, as in the metal exchange of zeolites, this effect is taken advantage of in the toning of cyanotypes (127).

Based on the interpretation of the above sample matrices, it was proposed that the edge shift as well as pre-edge and EXAFS features could be used to fingerprint PBs and categorise them as being metal-substituted, that is a PB analogue, or metal-exchanged, that is PB with either included or occluded transition metals by either co-precipitation or by ion exchange into the zeolitic PB structure. To test this, a library of PBs known to contain transition metals was assembled. Some of the samples in these libraries were prepared by a researcher at the Pigmentum Project (407), and were thus known to be metal-substituted PB analogues, while others were from historic samples and thus it was not known whether they were substituted or exchanged.
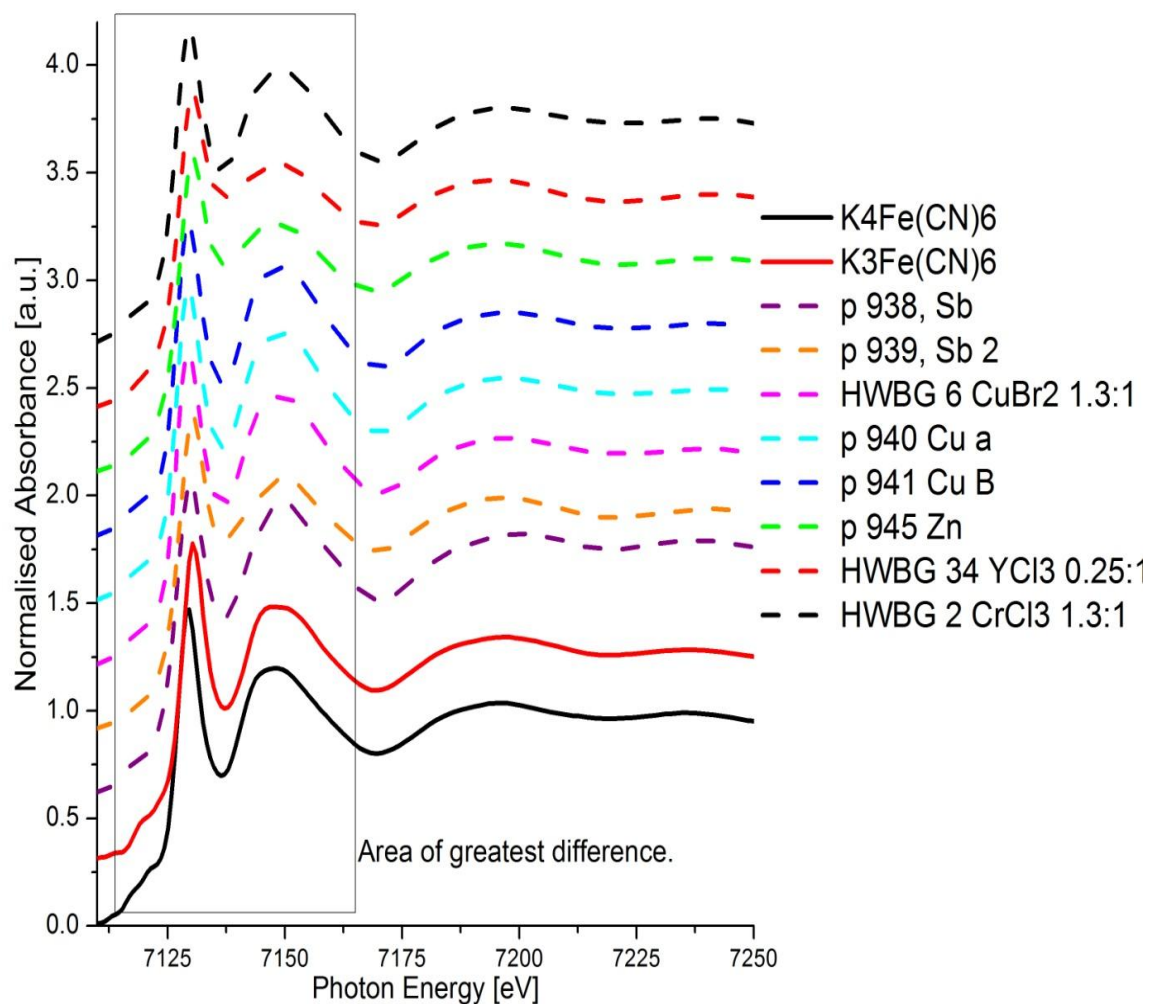
Figure 6 Normalized and offset XAFS spectra of metal substituted PBs. The area of greatest difference is indicated. The spectra were collected by transmission through PE pellets that contained ca. 4.5 mg of PB samples.

The samples were prepared by grinding ca. 4.5 mg of pigment in PE and pressing the mixture into a pellet. The XAFS spectra were collected in transmission mode, and the resulting spectra were normalised by subtracting the function of a line fitted to the region before 7100 eV from the entire spectrum and scaling to

the EXAFS region. The normalised and offset XAFS spectra in Figure 6, $K_3[Fe(CN)_6]$ and $K_4[Fe(CN)_6]$ were included for reference. Approximately 4.5 mg of each sample of PB was prepared by grinding in PE and pressing into the 96 well plate. The spectra were collected in transmission mode and normalised, scaled and offset to the Fe main edge feature. The spectra from the antimony containing samples were significantly different from the other samples.

Examination of the main edge shift indicates three classes of PBs, those with a main edge at 7129.6 eV, 7130.3 eV and the sample p938 with a shift at 7129.9 eV, Figure 7A.
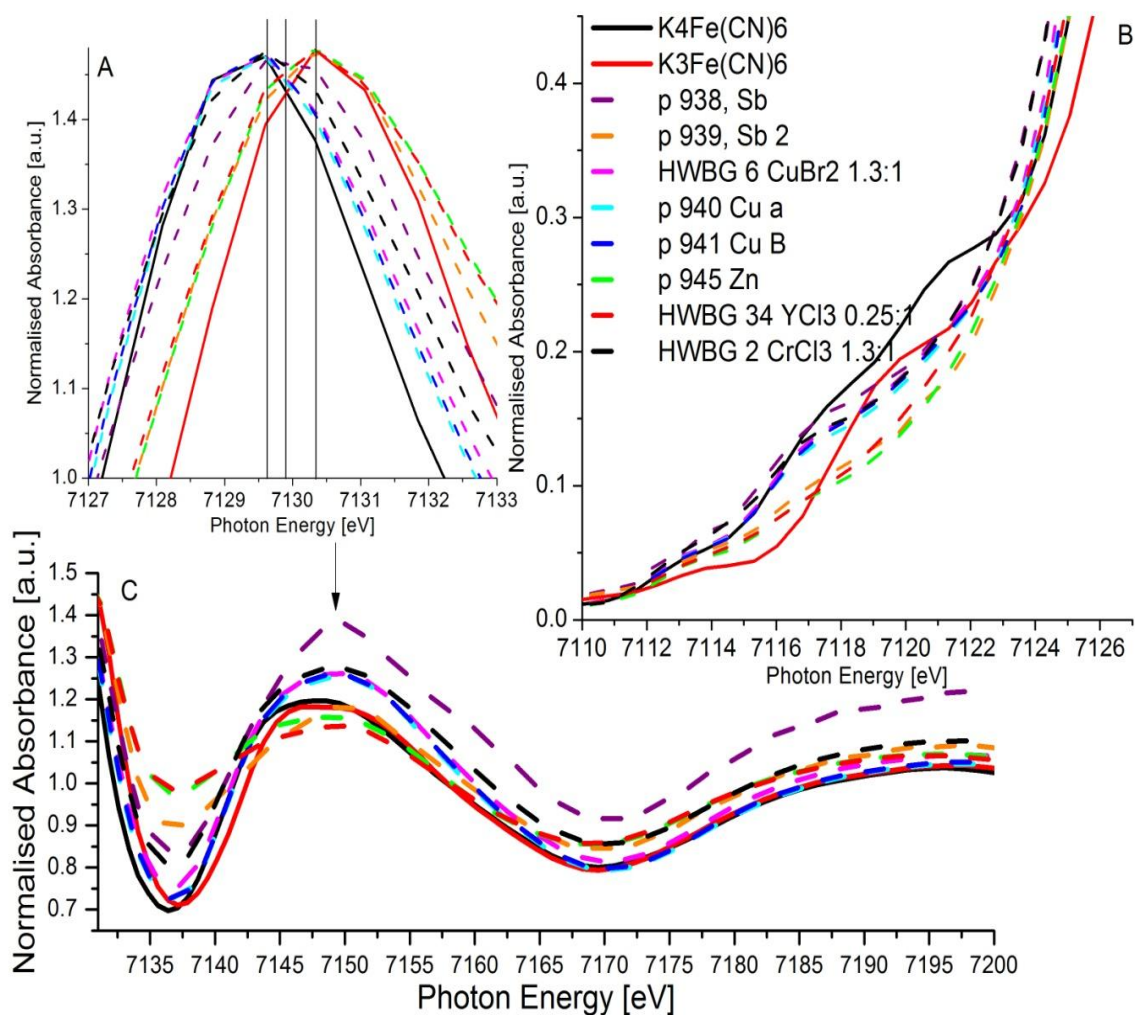
Figure 7 Main edge (A), pre-edge (B) and EXAFS (C) regions metal substituted and exchanged PBs. $K_4[Fe(CN)_6]$ and $K_3[Fe(CN)_6]$ are included as reference compounds. The spectra were collected by transmission through PE pellets that contained ca. 4.5 mg of sample. The vertical lines in 7A are the photon energies for the continuum electronic transitions. The arrow in 7C indicate the areas of interest in the EXAFS region that is discussed in the text.

Based on the shift of the main Fe K-edge to 7129.6 eV, the first class of samples, HWBG 6 (Cu containing), p940 6 (Cu containing), p941 6 (Cu containing) and HWBG 2(Cr containing), can be considered to have mostly Fe(II) present in the form $[Fe(CN)_6]^{4-}$, Figure 7A. The main edge features are quite similar indicating a

132

similar octahedral environment for the Fe centres in all of the samples, Figure 7A. This is to be expected for samples HWBG 6 (Cu containing) and HWBG 2 (Cr containing) which are known to have been prepared with $K_4[Fe(CN)_6]$. Again the main edge is broader than that of the reference spectrum of $K_4[Fe(CN)_6]$, though less than in Fe(III)-Fe(II) PBs, thus peak broadening can be interpreted as being characteristic of the charge transfer process typical of PBs, Figure 7A. The pre-edge region of this group of samples is nearly identical and is closer to that of the reference $K_4[Fe(CN)_6]$ spectrum, thus supporting the postulation that most, if not all, of the iron in the samples is in the Fe(II) state, Figure 7 B. The Cu K-edge XANES spectra for samples p940, p941 and HWBG 6 indicate that the Cu in all of the samples is in the same oxidation state. The EXAFS spectra for these samples is much more ordered, possibly indicating the presence of only a single iron oxidation state participating in electron scattering, Figure 7 C. From the knowledge that we have about the Cu(II) and Cr(III) containing samples we can propose the following formulae for these samples, see Table 2 below.

Table 2 Proposed Formulae for samples with Fe main K-edge shift 7129.6 eV based on XAS spectra interpretation.

Pigment Reference	Metal	Metal oxidation state	Iron oxidation state	Proposed formula
HWBG 6	Cu	Cu(II)	Fe(II)	$K_2Cu[Fe(CN)_6]$
HWBG 2	Cr	Cr(III)	Fe(II)	$KCr[Fe(CN)_6]$
p940	Cu	Unk, but likely Cu(II)	Fe(II)	$K_2Cu[Fe(CN)_6]$
p941	Cu	Unk, but likely Cu(II)	Fe(II)	$K_2Cu[Fe(CN)_6]$

Moving on to the next group of samples with a main edge shifted to 7130.3 eV: p939, HWBG 34 and p945. A shift to 7130.33 eV indicates that at least 50% of the iron in the samples is in the Fe(III) oxidation state; remember that all iron containing PBs with a ratio of Fe(III) to Fe(II) exhibited a similar shift . Furthermore, there is significant broadening of the main edge feature relative to the reference compounds, thus indicating the charge transfer process typical of PBs as postulated above, and the similar shape to the rising edge indicates that the iron sites are all octahedrally coordinated. The pre-edge region for these samples reveals a shoulder in the 7115 to 7120 eV region that could be attributed to a contribution from the shoulder observed at 7119 eV in the spectrum of the reference compound $K_3[Fe(CN)_6]$, however the connection is not as clear as above, thus it is possible that there is a mixture of iron oxidation states in these samples, and some differences in the pre-edge region could be attributed to the presence of different iron ratios between the samples Figure 7B (313). Of these samples, only HWBG 34, Figures 11 and 12, has a known preparation, and was prepared from Y^{3+} and $[Fe(CN)_6]^{4-}$. That the main edge is shifted to 7130.3 eV for HWBG 34 indicates that the iron in the sample is in the Fe(III) state and that a redox reaction occurred where Y(III) was reduced to Y(II) and a corresponding fraction of the Fe(II) was oxidised to Fe(III). It is possible that this redox process was not complete and that some Fe(II) remains in the sample. Samples p945 and p939 are known by SEM-EDX analysis to contain significant amounts of Zn and Sb respectively, however, their preparations are unknown, though that at least 50% of the iron is in the Fe(III) form can be concluded

from the main edge shift. The EXAFS region of these samples is significantly different between samples, as can be expected since they contain different metals, but it is not interpretable by eye; perhaps a computational method could shed more light on this region, Figure 7C.

Examination of the third sample group, sample p938 (Sb containing), also containing antimony, is helpful in interpreting the spectra from p939 (Sb containing) and p945 (Zn containing), Figures 11 and 12. Sample p938 has a very broad, main edge shifted to an intermediate value of 7129.9 eV, Figure 7A, and pre-edge features that combine aspects of both reference compounds, Figure 7B, as well as a significantly different EXAFS region. Based on these features it is proposed that pigment p938 is actually a Sb-exchanged PB. This is feasible, because with ionic radii of 90 and 76 pm respectively, both Sb(III) and Sb(V) could easily be accommodated into the PB lattice.

Based on the conclusion for sample p938, we can reinterpret sample p939, which has a much narrower Fe edge centred at 7130.3 eV, we can propose that all of the iron in p939 is in the Fe^{3+} state, and that it is a possibly a Sb^{3+} substituted PB, Table 3.

Sample p945 is odd in that the main Fe K-edge shift is in a position that suggests the presence of Fe(III), and the broadening of the rising edge features indicates the postulated charge transfer process typical of PB, however for charge transfer to occur the Zn would need to be in the reduced Zn(I) state which is not electrochemically common. Therefore this compound is likely a Zn-substituted iron PB. See Table 3 below for the proposed chemical formulae.

Table 3 Proposed formulae based on XAS spectra interpretation.

Pigment Reference	Metal	Metal oxidation state	Iron oxidation state	Proposed formula
p945	Zn	Unknown, but likely Zn(II)	mixture Fe(III) and Fe(II)	Zn exchanged PB
HWBG 34	Y	Y(II)	Fe(III)	$Y_3[Fe(CN)_6]_2$
p939	Sb	Unknown, but likely Sb(III)	Fe(III)	$Sb[Fe(CN)_6]$
p938	Sb	Unknown	mixture Fe(III) and Fe(II)	Sb exchanged PB

6.3.4.4 Historic Pigment Survey

The next step was to survey a library of historic and modern PBs and to apply the above interpretations to the spectra. For PBs where sufficient sample was available and considered expendable, measurements were made in the transmission mode as above. For samples that were not expendable the prepared TEY cell was used. See Figure 8A for a diagram of the TEY cell.
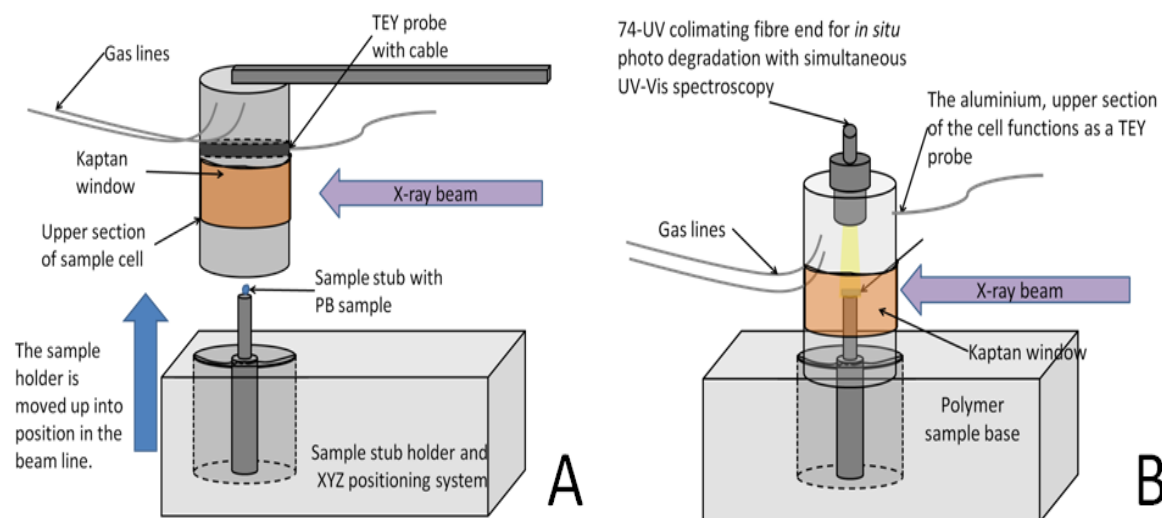
Figure 8 A diagram of the prototype sample cell used for the historic PBs survey at SRS. Spectra can be collected in transmission, fluorescent yield or TEY. Figure 8B a diagram of the prototype cell used for studying the fading and reversion of PB at Diamond Light Source. This cell allows for photodegradation, UV-Vis spectrometry and XAS to be conducted simultaneously under controlled atmosphere.

6.3.4.4.1 Transmission Results

Samples of 14 PBs including both historic and modern pigments were prepared by grinding ca. 4.5 mg of sample in PE and pressing them into a pellet within the 96 well plate. The resulting spectra were normalised by subtracting the function of a line fitted to the region before 7100 eV from the entire spectrum and scaling to the EXAFS region. The XAFS spectra are presented in Figure 9.
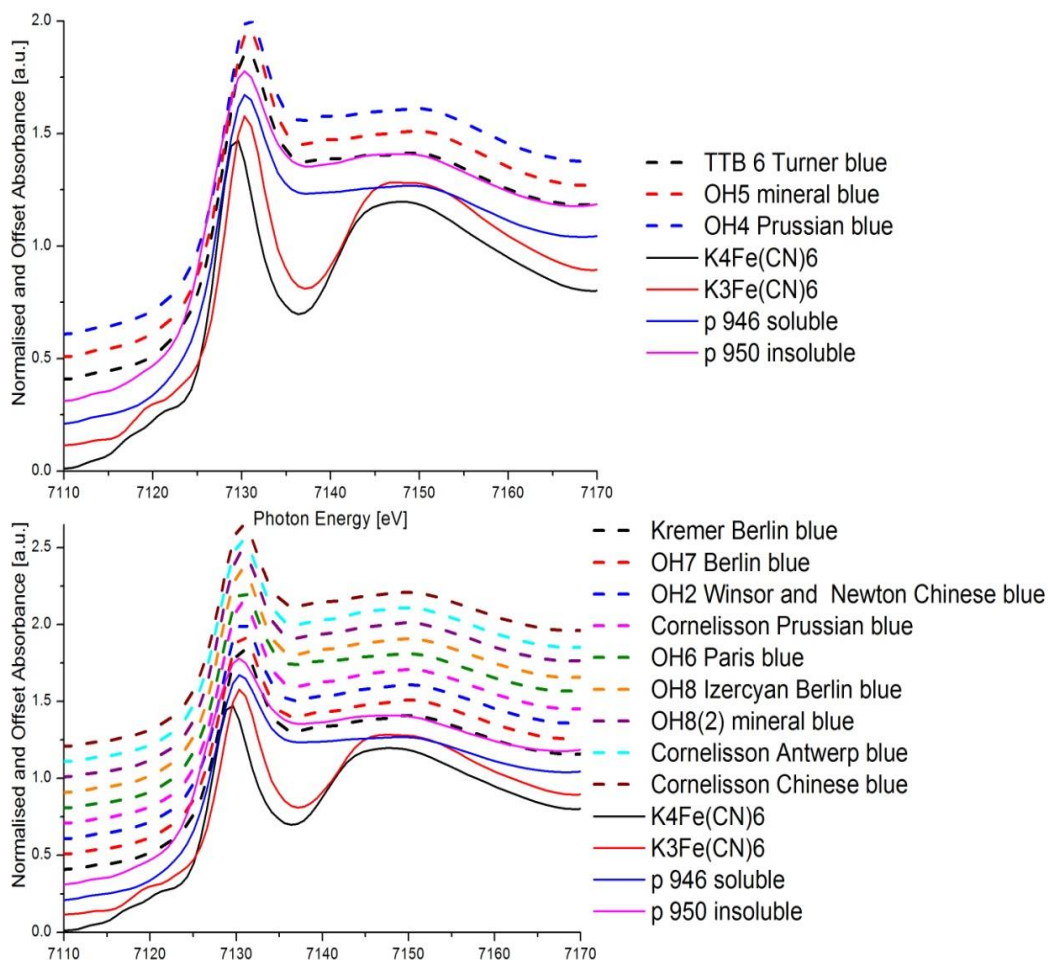
Figure 9 PBs survey, spectra collected in transmission, with ca. 4.5 mg of PB in a PE pellet. The upper graph presents pigment samples found to be similar to TTB6, and the lower graph presents samples that are similar to a modern industrial preparation of soluble PB, Kremer Berlin blue.

Examination of the region of greatest difference identified in the previous samples revealed great

similarities between samples, Figure 9. All of the samples had a broad main Fe K-edge shift of 7130.3 eV

indicating both the presence of both Fe(III) and Fe(II) and the charge transfer complex, as proposed above.

The pre-edge regions were all remarkably similar and were more or less like soluble PB in character. This is

supported by the SEM-EDX spectra of the pigments, all of which were found to contain significant quantities

of potassium and/or sodium thus indicating a soluble PB. Examination of the pre-edge and edge regions of

the XANES spectra revealed more differences that could be used to fingerprint the samples into families,

with OH5 and OH4 being found to be quite similar to TTB6, that is the PB used by J.M.W. Turner, Figure 10.

The other pigments were found to be quite similar to a sample of Kremer Berlin blue that is known to be a

soluble PB, though, the sample OH6, that is Paris blue, is significantly different at about 7135 eV from the

other samples, see Figure 10.
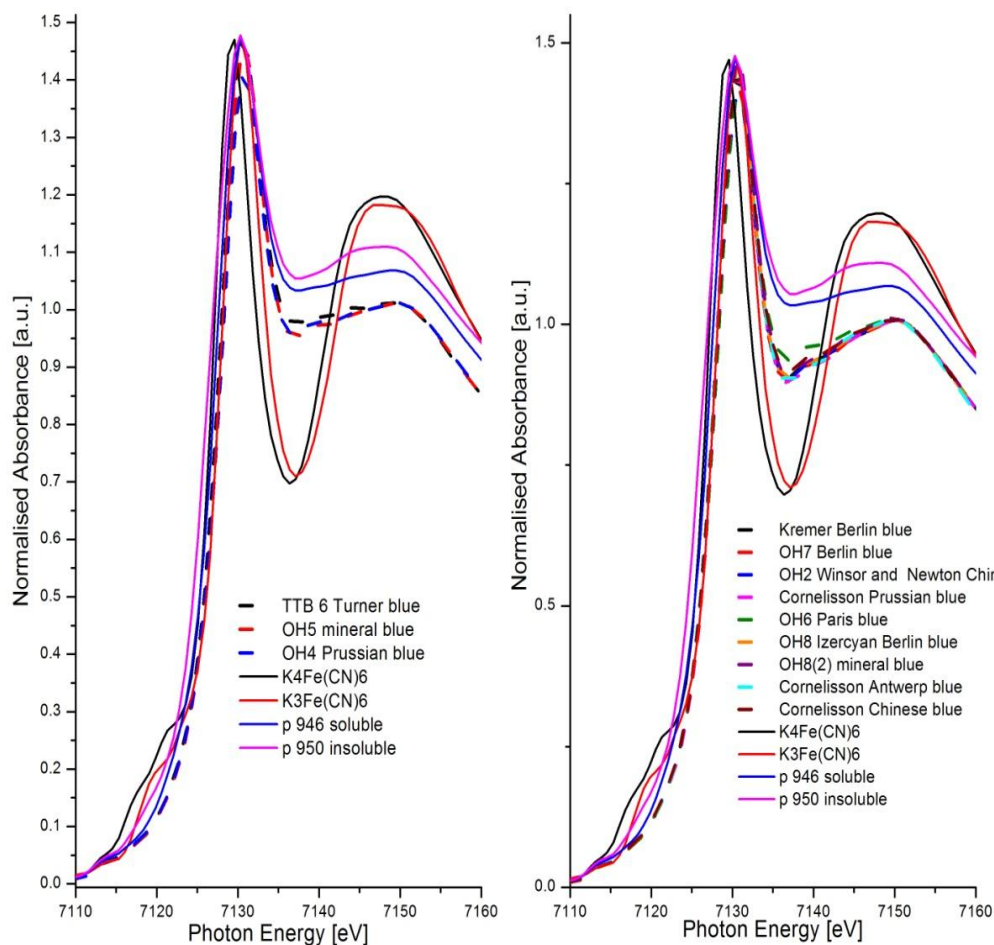
Figure 10 PB samples are divided into samples similar to TTB6 and those similar to modern Kremer Berlin blue known to be of the soluble variety. The pre-edge XANES region (7110 – 7125 eV) and the EXAFS feature at 7135 eV can be used to fingerprint the samples.

It was surprising to find such similarities between samples when, aside from the general presence of potassium in all of the samples, the pigments had very different elemental compositions when analysed by SEM-EDX or XRF. An explanation for this could be that the TTB6, OH5 and OH4 are older and were made by a similar process, while the remaining pigments, many of which are modern samples, are made by a different process. In the former case the contaminants seem to be included or occluded in the samples, while in the latter, the PB is relatively pure, and the detectable differences in the elemental composition are due to extenders and other pigments added to the PB. These additives would not participate in electron scattering events, and therefore would not affect the XAS spectra. This is supported by the similarities between the samples of Cornelissen Chinese blue, Cornelissen PB and Cornelissen Antwerp blue. These three pigments samples are from the same source, and are thought to be from the same PB preparation with increasing amounts of pigment extenders such as ZnO and $BaSO_4$.

6.3.4.4.2 TEY Survey

The sample cell pictured in Figure 8A was successfully used to collect XAFS spectra from non-expendable PB samples. Much of the Daresbury SRS beam time was spent in method development to determine experimental parameters and how to collect transmission, fluorescent yield and TEY spectra from the same samples. The success of the TEY application came as a great surprise, as the technique is known to be fraught with difficulties, and is therefore little used. The spectra from the TEY survey were normalised by subtracting from each spectrum a line fitted to the pre-edge region up to 7000 eV and then by scaling all of the spectra to coincide in the EXAFS region. Figure 11 presents the normalised TEY XAFS spectra of a selection of PBs.
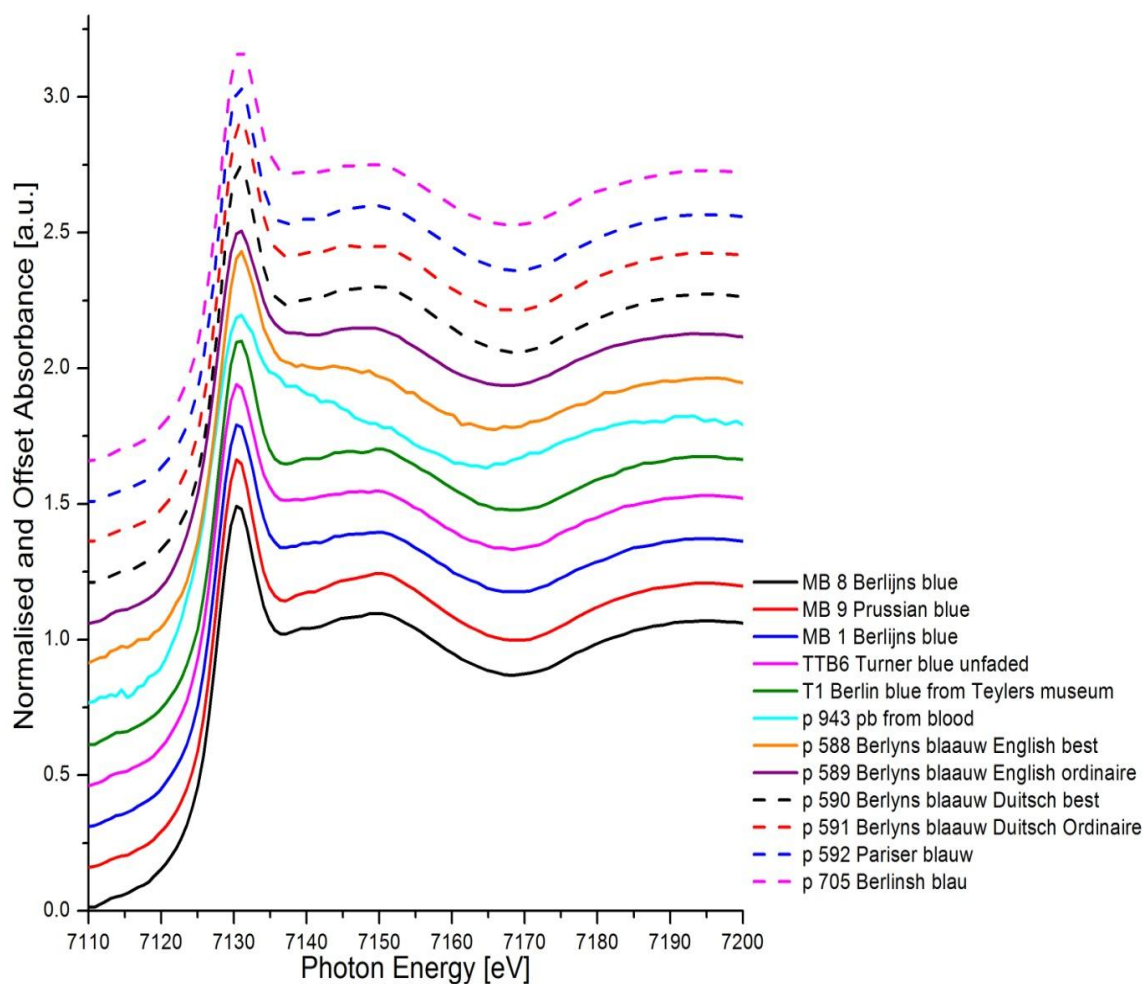
Figure 11 XAS spectra of PBs collected by TEY in ambient atmosphere.

Examination of the TEY spectra reveals immediate differences between samples. The most striking is p 943, a modern preparation of PB from ox blood, that seems to be nearly non-ordered based on the EXAFS spectra, Figure 11. Other spectral features (small undulations) in the EXAFS region between 7130 and 7150 eV, that are not present in the transmission spectra, are also visible for many samples; possibly indicating a difference between the surface and bulk environments. However, there are several points that must be

remembered before these spectra are interpreted. First, the spectra present the initial testing of a first, and by no means optimized, prototype sample cell. Second, the amount of iron in the samples was in no way controlled. Third, the experimental conditions were optimized to protect the samples: samples were not adhered to the sample stub; the presented surface geometry was not controlled. Spectral collection was rapid to minimize x-ray induced changes to the samples. All of the above make for variable spectra that can be over interpreted. Rather than drawing conclusions about differences between the surface and bulk PB from this spectral set, it is better to simply recognize that XAS of historic pigments with no sample preparation is possible by TEY, and that this technique has great potential for exploring material composition and degradation as an *in situ* technique for future beam time applications in which the sample cell and spectral collection conditions can be better optimized.

6.3.4.5 Fading of PB Studied by XAS

The studies on the visible light induced fading of J.M.W. Turner's PB, TTB6, as prepared in a watercolour wash were conducted at Diamond Light Source, x-ray micro-focus Beam Line I18. The Fe K-line was characterised with an emphasis on the XANES region. Due to the low iron content in the watercolour washes, detection was by fluorescence yield. Due to technical difficulties with the control software and monchromators, the EXAFS region between 7148 and 7151 eV was not collected. This region falls within the area of greatest difference between the samples and as such interpretation of the EXAFS data is not reliable for evaluating fading induced changes to the crystal structure of the samples. However, much can be learned from examining the XANES region and the near edge portion of the EXAFS region. The spectra from the TEY survey were normalised by subtracting from each spectrum a line fitted to the pre-edge region up to 7000 eV and then by scaling all of the spectra to coincide in the EXAFS region.

6.3.4.5.1 X-Ray Induced Changes

While the photon flux was much greater at Diamond Light Source than at Daresbury SRS, the low iron content of the samples required spectrum collection times of slightly less than 15 min. This is significantly longer than those required for the raw pigment samples at Daresbury, and though no changes to the pigment samples were detected during the Daresbury SRS beam time, it is well known that intense x-ray exposure can lead to the reduction of Fe(III) to Fe(II) and that it can also lead to lattice responses in PB analogues (313, 432). Since this process also is the result of visible light induced photoreduction of PB, the first concern was to identify x-ray induced changes to the samples so that they can be differentiated from visible light induced changes. The near edge features proved to be most useful in determining the difference between x-ray induced changes and those as a result of visible light exposure, Figure 12.
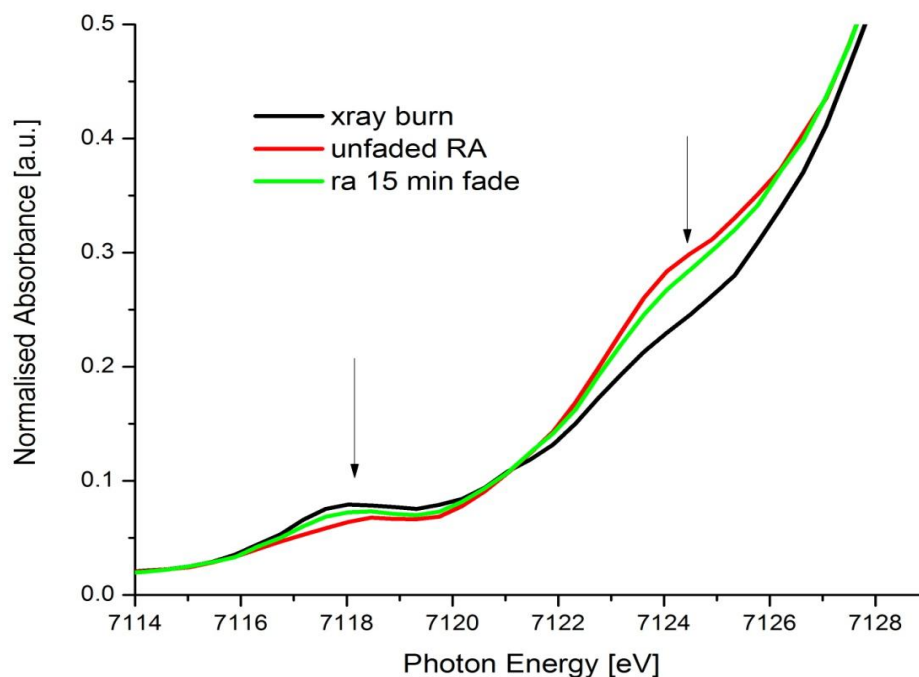
Figure 12 The effect of x-ray exposure on PB samples as prepared in a watercolour wash. The samples were either untreated, exposed to 15 minutes UV-Vis irradiation or exposed to 2.5 h of x-rays before the XAS spectra were collected. The arrows indicate the positions of pre-edge features showing the greatest change during fading and x-ray exposure.

All samples were prepared as described above in room atmosphere, and spectrum collection time was ca. 15 min. The light faded samples were exposed to intense visible radiation for 5, 15 and 30 min, respectively, before the x-ray shutter was opened and the spectra collected. The x-ray burn sample was exposed to x-rays for 2.5 h before the spectrum was collected. Examination of the spectra confirms that extended x-ray exposure results in the same changes to the pre-edge spectral features (a reduction in shoulder at 7124.3 eV and a shift to a lower energy and growth of the shoulder at 7118 eV) as does visible light fading. However, the changes due to visible light exposure for as little as 15 min in room atmosphere are distinguishable from the x-ray induced changes after 2.5 h of exposure, and therefore a spectrum collection time of 15 min is applicable.

6.3.4.5.2 Fading Behaviour in Different Atmospheres

The differences in fading behaviour between PB in ambient, N_2, and He atmospheres was next explored. Figure 13 presents the normalised and offset XANES region of the spectra; and Figure 14 presents the pre-edge region which exhibits the greatest change with increased light exposure.

The same unfaded spectrum was used as a reference for all samples. If a non-ambient atmosphere is specified, the spectrum was collected after purging the sample chamber for at least 15 min at a flow rate of 80 ml/min with the specified gas. Purging at this flow rate was continued during spectrum collection and between individual runs as it was possible to re-position the sample in the x-ray beam without interrupting the gas flow.
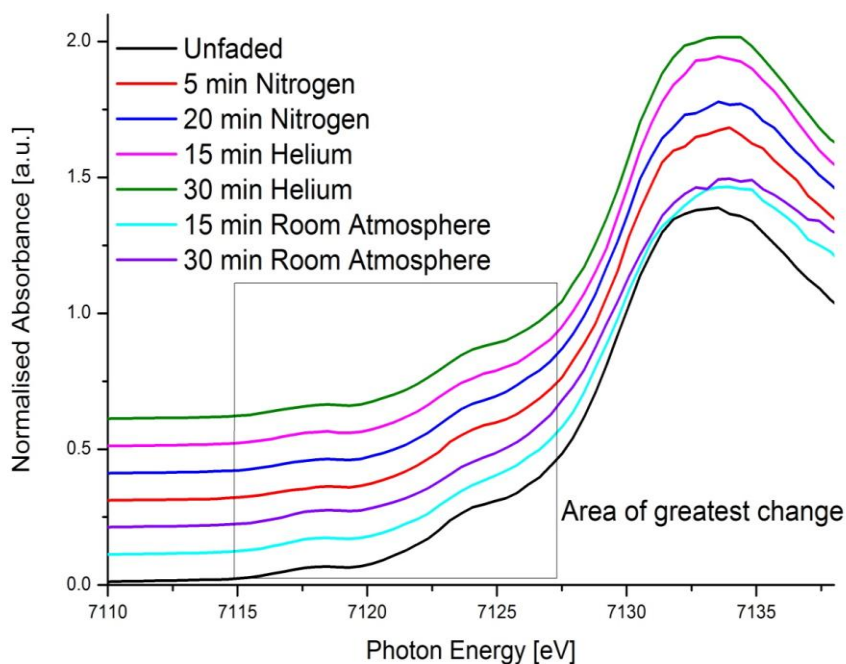
Figure 13 Normalised and offset XANES spectra of the visible light induced fading of TTB6 PB prepared as a watercolour.
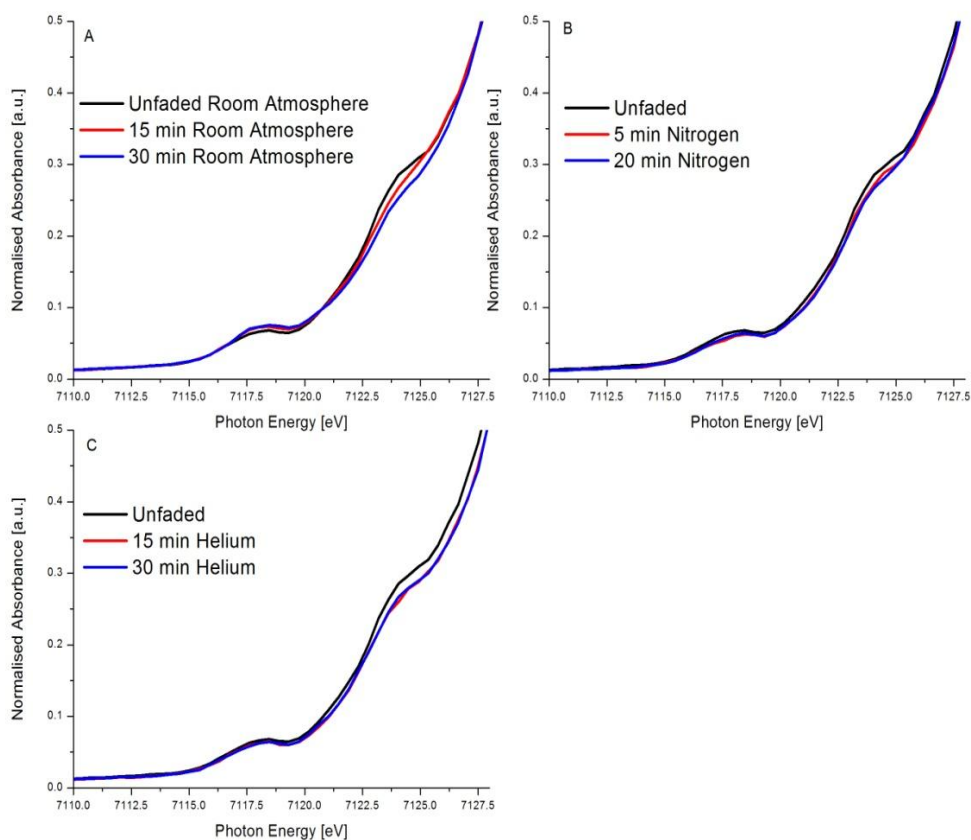
Figure 14 Pre-edge region of TTB6 prepared as a watercolour and faded in room atmosphere (A), nitrogen (B) and helium (C).

The fading spot from the visible light was significantly larger than the spot from the x-ray beam, therefore it was possible to reposition the sample after each measurement so as to avoid cumulative x-ray damage as noted above in Figure 12. This practice worked well at Daresbury SRS which has a much larger spot size, however at the micro-focus beam line I18 at Diamond Light Source this led to some problems due to the heterogeneous nature of the samples. Not only are the pigment particles inhomogeneous, as can be observed in SEM-EDX spectra, but the brush-applied paint layer itself is also inhomogeneous.

Because the sample composition and preparation was not alterable, the variability in the spectra was minimised by first evaluating the effect of sample presentation on the XANES spectra. Sample rotation was found to affect the data, and it was proposed that this was due to the x-ray beam passing through more or less paint. If one imagines a brush stroke is composed of peaks and troughs where more or less paint is deposited onto the surface due to the position of the individual brush fibres, then one can imagine three boundary scenarios of beam orientation. One where the focused beam passes down a trough in the paint layer and very little signal results, the second where the beam passes down a peak of paint and maximum

signal results, and a third where the brush strokes are perpendicular to the beam and an intense but intermediate signal results. The third scenario has the added advantage in that the sample can be re-positioned in the x-axis between samples and theoretically the same amount of paint will be characterised in each spectrum, and this presentation was applied to all samples.

As noted above, exposure to intense visible light results in a reduction of the shoulder at 7124.3 eV on the rising edge. A shoulder in this position has been proposed to correspond with an electronic transition from a Fe(III) site. Thus, changes to this shoulder's intensity and shape indicates a reduction of the Fe(III) sites to Fe(II) sites generating Berlin white from PB according to the reaction in Schematic 2, however, these changes did not manifest in a measurable shift in the Fe edge feature. The room atmosphere samples show a clear progression in the spectra, while the samples that were faded in N_2 and He the reduction in the shoulder is present, but the progression is less clear, Figure 14.

The experimental set up was replicated in the sample preparation lab, and by microscopic examination, it was found that the room atmosphere samples were completely faded to white after 30 min light exposure, while the He and N_2 faded samples were completely faded in less than 15 min. This is due to the fact that the generated Berlin white in the room atmosphere samples was able to re-oxidise to PB, while this was not possible in the anoxic samples. Thus, with spectrum collection interval of 15 min, it was not possible to have time resolution in the fading of anoxic samples. As no means were available either to attenuate the light source nor to measure its incident power, this problem was partly overcome by fading a sample under N_2 for 5 min, then shuttering the light off before spectrum collection; and small differences in the spectra are visible. However, due to beam time constraints it was not possible to explore this further. Regardless of the lack of time resolution of the fading process in anoxia, the final position of the shoulder in the fully faded samples, regardless of atmosphere, is nearly the same, Figure 14, and thus it can be concluded that the electronic mechanism of fading is the same in all cases.

The near edge portion of the EXAFS spectrum in Figure 13 is tantalising in that room atmosphere faded samples seem to have a different slope between 7135 and 7138 eV than the anoxically faded samples and the samples faded under ambient atmosphere. This could be due to the presence of a mixture of both Berlin white and PB, due to the slower fading rate of PB in ambient atmosphere relative to those in anoxic atmospheres. However without a complete EXAFS spectrum this is impossible to evaluate.

6.3.5 Conclusions

From the XAS experiments several conclusions can be drawn:

1. The XAS high throughput methodology and sample cells developed for these experiments have shown to be useful in the characterisation of PB samples, as raw pigment in PE pellets, recoverable raw pigment samples and watercolour drawings. Using the automated

sample positioning and spectrum collection software, it was possible to characterise a large library of samples over the course of the beam times.

2. While the differences between the transmission and TEY spectra were not evaluated herein, the TEY probe is a surprisingly easy to use surface analysis technique that generates high quality spectra of the surface of samples. With a further refined sample cell, this technique should be extremely useful for many applications in heritage science and beyond.

3. Evaluation of the pre-edge and main edge regions of XANES and near edge regions EXAFS regions of the transmission spectra allowed for the definition of spectral characteristics of soluble-like and insoluble-like PBs. These were then applied to a collection of pigments with known semi-quantitative elemental composition and either known or unknown preparation. It was possible to classify the pigments into soluble and insoluble types, and to identify families of historic and modern pigments, possibly indicative of different preparation methods.

4. Examination of the same spectral regions also allowed for the tentative assignment of PBs known to contain transition metals other than iron into classes: metal-substituted or metal-exchanged PBs as well as to propose chemical formulae for the compounds.

5. Based on the pre-edge features it was found that the electronic mechanism of the fading of PB in a watercolour medium is the same regardless of atmosphere. If this is the case, residual colour changes in PBs faded in anoxia as reported by some researchers (4, 7) remains to explained. The residual colour change reported by Rowe can be partly explained by examining her light ageing method (7). Since she used indoor daylight to age her samples by placing them in a window; they were exposed to near-UV light. Near-UV light is known to cause the oxidation of cyanide ligands to form iron aquapentacyano ferrate as in the reaction in Schematic 4 (5, 127). The residual colour change reported by Korenburg is not explainable in the same way (4), but one possible explanation is that photodegradation in anoxia resulted in a nearly complete reduction of the PB to Berlin white and that there were not enough hydronium cations present in the PB lattice to scavenge the hydroxide anions produced during the oxidation of Berlin white back to PB, as per the reaction in Schematic 2, and that these hydroxide anions were then able to hydrolyse the PB as per the reaction in Schematic 3. Because the PB samples light aged in anoxia faded to a greater extent than those aged in ambient atmosphere, there were more hydroxide anions produced upon reversion possibly resulting in localised alkaline regions and the hydrolytic degradation of the PB.

6. Thus, it is not the reductive fading of PB in anoxia that causes the non-reversible colour change but rather the oxidative regeneration of faded PB once re-exposed to ambient

atmosphere. It is probable that similar residual colour change would be observed if samples in ambient atmosphere were faded to the same degree as those in anoxic atmospheres before being allowed to revert to PB. It might also be found that if the same samples are cycled several times, the colour of the anoxically faded PBs will have stabilised with no further accumulated residual colour change, while the ambient aged samples accumulate more residual change. This would be akin to the 'burning out' process described by Ware, where cyanotypes are light cycled to remove impurities that lead to colour change (127).

7. Therefore, if the mechanism of fading of PB is the same in anoxia as in ambient atmosphere, then anoxic storage and display poses no greater long-term risk to the object. If fading of PB is suspected the object should be de-cased before the fading becomes extreme, and the faded PB can then revert producing only moderate amounts of hydroxide anions at a given time (which should be neutralised by organic acids present in the binding media) thereby reducing the risk of alkaline hydrolysis of the PB.

Table4 Sample library characterised at Daresbury SRS

SAMPLE LIBRARY USED AT DARESBURY SYNCHROTRON RADIATION SOURCE								
ID	Institution	Sample	Sample Description		ID	Institution	Sample	Sample Description
1	PP	P588	H XI 20 Berlyns blaauw engelsch best		28	PP	P954	PB copper a I
2	PP	P589	H XI 21 Berlyns blaauw engelsch ordinair		29	PP	P955	PB copper a I
3	PP	P590	H XI 22 Berlyns blaauw duitsch best		30	PP	P956	PB copper b I
4	PP	P591	H XI 23 Berlyns blaauw duitsch ordinair		31	PP	P957	PB copper b I
5	PP	P592	H XI 20 Pariser blaauw		32	PP	P958	PB sodium soluble I
6	PP	P705	H XIX #5 Berlynsolblau		33	PP	P959	PB carpet soluble
7	PP	P933	PB insoluble NH_3		34	PP	P965	PB
8	PP	P934	PB soluble NH_4		35	PP	HWBG 1	CrCl3 LIQUID/1.3:1:0/N
9	PP	P935	PB ammonia III		36	PP	HWBG 2	CrCl3/1.3:1:0/Y
10	PP	P936	PB insoluble sodium		37	PP	HWBG 3	CoCl2/1.3:1:0/N
11	PP	P937	PB soluble sodium		38	PP	HWBG 3a	CoCl2 ON FILTER PAPER/1.3:1:0/N
12	PP	P938	PB antimony I		39	PP	HWBG 4	CoCl2/1.3:1:0/Y
13	PP	P939	PB antimony II		40	PP	HWBG 5	CuBr2/1.3:1:0/N
14	PP	P940	PB copper a		41	PP	HWBG 6	CuBr2/1.3:1:0/Y
15	PP	P941	PB copper b		42	PP	HWBG 7	FeCl3/1.3:1:0/N
16	PP	P942	PB copper d		43	PP	HWBG 8	FeCl3/1.3:1:0/Y
17	PP	P943	PB from blood		44	PP	HWBG 9	FeCl3/1.0:1.0:0/N
18	PP	P944	PB zinc I		45	PP	HWBG 10	FeCl3/1.0:1.0:0/Y
19	PP	P945	PB zinc I		46	PP	HWBG 11	FeCl3/0.5:1:0/N
20	PP	P946	PB soluble I		47	PP	HWBG 12	FeCl3/0.5:1:0/Y
21	PP	P947	PB soluble I		48	PP	HWBG 13	FeCl3/0.25:1:0/N
22	PP	P948	PB soluble II		49	PP	HWBG 14	FeCl3/0.25:1:0/Y

ID	Institution	Sample	Sample Description		ID	Institution	Sample	Sample Description
23	PP	P949	PB insoluble I		50	PP	HWBG 15	FeCl3 ON FILTER PAPER/0.1:1:0/N
24	PP	P950	PB insoluble I		51	PP	HWBG 16	FeCl3/0.1:1:0/Y
25	PP	P951	PB insoluble II		52	PP	HWBG 17	TaF5/1.3:1:0/N
26	PP	P952	PB ammonia II		53	PP	HWBG 18	TaF5/1.3:1:0/Y
27	PP	P953	PB ammonia II		54	PP	HWBG 19	TaF5/1.0:1.0:0/N
55	PP	HWBG 20	TaF5/1.0:1.0:0/Y		82	TATE	[---]	Berlijns Blauw
56	PP	HWBG 21	TaF5/0.5:1:0/N		83	TATE	[---]	Kremer Berlin Blue
57	PP	HWBG 22	TaF5/0.5:1:0/Y		84	TATE	[---]	Cornelissen PB
58	PP	HWBG 23	TaF5/0.25:1:0/N		85	TATE	TCA11	Cornelissen Antwerp Blue
59	PP	HWBG 24	TaF5/0.25:1:0/Y		86	TATE	TCA7	Cornelissen Chinese Blue
60	PP	HWBG 25	TaF5/0.1:1:0/N		87	TATE	TTB6	Turner PB
61	PP	HWBG 26	TaF5/0.1:1:0/Y		88	TATE	[---]	Turner PB on paper, faded
62	PP	HWBG 27	YCl3/1.3:1:0/N		89	TATE	[---]	Turner PB on paper, unfaded
63	PP	HWBG 28	YCl3/1.3:1:0/Y		90	TATE	[---]	Turner PB on paper, faded
64	PP	HWBG 29	YCl3/1.0:1.0:0/N		91	TATE	[---]	Turner PB in medium on paper, unfaded
65	PP	HWBG 30	YCl3/1.0:1.0:0/Y		92	TATE	[---]	Turner PB in medium on paper, faded
66	PP	HWBG 31	YCl3/0.5:1:0/N		93	TATE	[---]	Potassium hexacyanoferrate(II)
67	PP	HWBG 32	YCl3/0.5:1:0/Y		94	TATE	[---]	Potassium hexacyanoferrate(III)
68	PP	HWBG 33	YCl3/0.25:1:0/Y		95	TATE	[---]	Castle Amerongen Prussian green
69	PP	HWBG 34	YCl3/0.25:1:0/N		96	TATE	[---]	Castle Amerongen PB
70	PP	HWBG 35	YCl3/0.1:1:0/Y		97	TATE	[---]	Ackermann PB
71	PP	HWBG 36	YCl3/0.1:1:0/N		98	TATE	[---]	Ackermann Antwerp blue
72	TATE	1 MB	Berlijns Blauw		99	TATE	[---]	Ackermann Prussian green

ID	Institution	Sample	Sample Description		ID	Institution	Sample	Sample Description
73	TATE	8 MB	Berlijns Blauw		100	TATE	[---]	Bourgeois Aine PB
74	TATE	2 MB	Dark smalt		101	TATE	[---]	Bourgeois Aine Prussian green
75	TATE	OH 4	Bleu de Prusse		102	TATE	[---]	Rowney Cake nr 3
76	TATE	OH 7	Vetterwinkel Berlijns Blauw		103	TATE	[---]	Rowney Cake nr 4
77	TATE	OH 5	Scheveningen Mineraal Blauw ijzer…		104	TATE	[---]	Rowney Cake nr 6
78	TATE	OH 6	Scheveningen Parijs Blauw		105	TATE	[---]	Winsor & Newton Prussian green
79	TATE	OH 8a	Scheveningen Ijzercyaan Berlijns Blauw		106	PP/TATE	[---]	Aluminium hydroxide-PB co-precipitate
80	TATE	OH 8b	Scheveningen Mineraalblauw					
81	TATE	OH 2	Winsor & Newton Chinese blue		In the above table, PP= Pigmentum Project OH=samples taken from the Oulde Holland collection, HWBG= a preparation by Helen Wilson, MB= samples taken from the collection of Martin Bilk, pXXX= a sample from the PP's collection, TTBX= a sample taken from the Tate Turner Bequest collection, TCAX= a sample taken from the Tate Conservation Archive.			

Chapter 7 Non-Targeted Degradic Footprinting Analysis of VOCs from Watercolour Drawings

7.1 Introduction

The degradation of a WOP can be defined as changes to its visual impact, and from this research tends to focus on changes to applied colourants (2, 3). However, the visual impact of a WOP is dependent upon more than the applied media. In addition to the rate of change of applied colourants, heritage institutions should also be concerned about the condition of the paper substrate, and how its useable lifetime might be extended. Through the limitation of oxidation pathways, anoxic display and storage should also extend the useable lifetime of paper.

Arney *et al.* (13-15) and Major (12) have studied the thermal degradation of paper in nitrogen and in air to determine the role of oxygen dependent and independent processes in paper degradation. Using sealed glass tubes, Arney found that yellowing of paper was due primarily to oxygen-dependent processes while the loss of tensile strength (related to the degree of polymerisation (DP) of the cellulose fibres) is primarily due to oxygen-independent processes(13-15). Major found that carboxyl and hydroxyl content and weight loss were greater in raw cotton fibres heated in a flow of air than those heated in a flow of nitrogen, and they found that samples heated in a flow of air had a lower viscosity (an indicator of loss of DP) than those heated in nitrogen (12, 82). Arney's (13-15) and Major's (12) results can be further summarised:

- as cellulose degrades, regardless of atmosphere, volatile organic compounds (VOCs) are produced, (thus explaining the observed weight loss) (12-15), and
- if cellulose is degraded in a sealed environment, then these VOCs accumulate, and some of the VOCs can react with the cellulose in oxygen-independent processes to reduce the DP of the sample (12-15).

Additionally, Major observed that samples of cellulose heated in air lost more weight than those heated in nitrogen (12). Major did not evaluate the headspace around his samples, but a difference in weight loss between samples degraded in nitrogen and samples degraded in air can be interpreted as a difference in VOC production and emission (the major pathway that could lead the observed weight loss). That less weight was lost for samples aged in nitrogen is curious, and it can be interpreted that either the processes leading to VOC formation are slower in nitrogen than in air (thus supporting the claim that anoxia is beneficial for paper), or that different VOCs are produced under nitrogen atmosphere than under air (also possibly supporting the anoxic claim). In either case, Major's observations provide a foundation for further research comparing the degradation of WOP in anoxia and in air, and they hint that VOC profiling could prove to be fruitful in this process.

The volatile degradome of paper can be incredibly information rich with hundreds of identifiable compounds. VOCs emitted by degrading paper have been the subject of much research in recent years (89, 90, 220, 246, 433-437), and research has progressed from purely qualitative identification of VOCs emitted by paper (89, 179), to estimation of the kinetics of VOC emission (435), to semi-quantitative research correlating the concentration of a particular VOC to the pH (155) and DP (205) of paper. Subsequent successful research has led to correlations of the concentration of particular VOCs to fingerprinting different types of paper (9), identification of microbial degradation in recycled paper (183, 184), and general degradative processes (225). It has also been proposed that the VOC profile of a paper-based (as well as other organic polymer-based) heritage objects can be diagnostic of both the properties of the material and the active degradation processes (9, 183, 184, 220, 294, 436).

From the above I propose:

- identical samples aged in different atmospheres will follow different degradation pathways, this is supported by the chemiluminometric and viscometric data presented in Chapter 5;
- the differences in degradation pathways will affect the volatile degradomes;
- purge and trap-headspace-gas chromatography-mass spectrometry (P&T-HS-GC-MS) is a suitable method to follow the changes in the volatile degradome;
- chemometric methods can be used to explore the volatile degradomes and build models to discriminate between sample classes and generate hypotheses as to the reason for the observed differences in the volatile degradomes.

7.2 Materials

7.2.1 Paper

GSR and WLR papers were used in this research. Please see the Materials and Methods section of Chapter 5 for a description of the papers used and please see Chapters 3 and 4 for a detailed protocol for the preparation of the reconstruction paper and an evaluation of the papers.

7.2.2 Gum Arabic

A gum Arabic binding medium was prepared by dissolving lumps of raw gum in deionised water with heating and stirring, with a ratio of 2:3 gum to water to prepare a stock solution. The prepared gum solution was used for grinding pigments and preparing paints, see Chapter 3 for a detailed description of the preparation of the gum solution used in this study as well as Charlotte Casper's Thesis (167).

7.2.3 Paint

Pigments for this research were selected from both the Tate Conservation Archive collection (designated as TCA) and from the Tate Turner Bequest collection (designated TTB). This research focused on Prussian blue pigments and madder lake pigments because they had been identified in the literature as being less lightfast in reduced oxygen conditions. The exact choice of colourants was based on their availability in the Tate archives and the potential for answering other experimental questions concerning the effect of photo-initiating extenders, the role of transition metals and evaluating the technique's discriminating power between related and un-related organic colourants.

A set of 3 Prussian blue pigments were selected to determine if the presence of extenders affect the VOC profile and if a historic Prussian blue can be distinguished from a modern Prussian blue. The pigments are as follows: a historic Prussian blue used by J.M.W. Turner (TTB6), a modern soluble Prussian blue with no extenders (Cornelissen's Chinese blue, TCA7), and a modern Prussian blue with copious extenders (Cornelissen's Antwerp blue, TCA 11). See Chapter 6 for a discussion of Prussian blues.

The madder lake pigments were primarily taken from the TTB pigment archive and include a selection of madder lakes from *R. tinctorum* L. including rose madder, scarlet madder, purple, and brown madders (TTB1, TTB2, TTB5, TTB8, TTB11 and TTB14), as well as a madder lake from *R. cordifolia* L. (TTB13). In addition to the historic pigments, Cornelissen's orange madder (TCA13), which may be the synthetic, *β*-nitro-alizarin on an alumina substrate was included in the madder sample set. Gamboge (TTB3) was included in the sample set. These pigments were selected because, with the exception of TTB13, TTB3 and TCA13, they are known to have essentially the same chromophores but different amounts of associated transition metals, see Chapter 5 for a discussion of the role of transition metals in madder lakes and the oxidative degradation of watercolours, and it was proposed that the presence of different quantities of transition metals would affect the VOC profile. The inclusion of TTB3 tests the discrimination power of HS-GC-MS for unrelated organic colourants, and the inclusion of TCA13 and TTB13 tests the discriminatory power for related organic colourants.

Table 1 is a description of the pigment samples used in this study. Readers are directed to Chapter 3 for a detailed description of the paints used in this study as well as to Charlotte Casper's Thesis, (167).

Sample	Description of the dry pigment	Madder species	Chromophores/colourants as determined by thin layer chromatography or x-ray fluorescence
TTB1	brownish-red powder	*R. tinctorum* L.	purpurin, pseudopurpurin, alizarin, other unidentified high R_f component
TTB2	bluish-red powder	*R. tinctorum* L.	purpurin, pseudopurpurin, alizarin, other unidentified high R_f component
TTB5	dark brown powder	*R. tinctorum* L.	purpurin, pseudopurpurin, alizarin, other unidentified high R_f component
TTB8	bluer red powder	*R. tinctorum* L.	purpurin, pseudopurpurin, alizarin, other unidentified high R_f component
TTB11	bluish-red powder	*R. tinctorum* L.	purpurin, pseudopurpurin, alizarin, other unidentified high R_f component
TTB13	dull yellow fragments	*R. cordifolia* L.	munjistin, rubiadin, alizarin, other unidentified high R_f component
TTB14	bluish-red powder	*R. tinctorum* L.	purpurin, pseudopurpurin, alizarin
TCA13	orange powder	Unknown/possibly synthetic	Cornelissen Orange Madder, possibly β-nitro-alizarin
TTB3	yellow powder	N/A, ground gamboge gum	gambogic acid
TTB6	dark blue lumps	N/A, Prussian blue	soluble Prussian blue with aluminium
TCA1	light blue powder	N/A, Antwerp blue	soluble Prussian blue with zinc oxide and barium sulphide present as extenders
TCA7	dark blue powder	N/A, Chinese blue	soluble Prussian blue with no extenders

Table 1 A description of the pigments used in this study. Thin layer chromatography (TLC) was used to separate the chromophores in the madder lake samples based on their retardation factor (Rf). If known compounds are run together with the unknown mixtures then the unknown chromophores can be matched to the known chromophores by their Rf.

The pigments were ground by hand in a solution of gum in water made by mixing a part of the stock gum solution with 3 parts water. The resulting paints were collected in Petri dishes and the water was allowed to evaporate at room temperature so that the paints could be stored for later use. Flakes of the dry paints were reconstituted in deionised water, painted onto wetted GSR with a squirrel hair brush, and allowed to dry unrestrained. The paint was applied in a heavy, opaque wash, and care was taken to yield an even paint layer within a sample preparation and similar wash strength between samples.

However, it must be noted that this application method does increase the heterogeneity of the samples. This was evaluated by colour measurement with a Minolta spectrometer; after drying, colour measurement of a random selection of samples within each pigment type was performed to evaluate the density of the paint layer. The mean values and standard deviations of the CIE L*a*b* parameters were calculated for each pigment. The colour of a second set of samples was then measured and evaluated for outliers, defined as having at least one CIE L*a*b* value greater than two standard deviations from the mean value of the parameter for a pigment type. Outliers were pruned from the sample set.

7.2.4 Headspace Vials, Caps, and Septa

Vials, caps, and septa were used as supplied by Chromacol. New vials, caps and septa were used for each sample. Before use the septa, caps and vials were baked overnight at 180 °C to desorb any VOCs. Crimp cap were used for most samples with the exception of TCA1, TCA7, TTB6, TTB3, TTB13, and TCA13.

7.2.5 Gases

Standard room air as found in the Anoxia laboratory at Tate Britain was used for the ambient atmosphere samples (designated RA). The RH in the laboratory was monitored, and care was taken to seal the vials when the RH in the laboratory was at 50 ±5%.

Zero grade argon supplied by BOC was used for the anoxic samples (designated AR). The gas was humidified to 50 ±5% RH by splitting the gas stream and bubbling one stream through deionised water. The streams were combined in a mixing chamber and the flow rates adjusted to achieve the desired RH level as monitored by a Tiny Tag View (Gemini Data loggers, UK).

Zero grade helium supplied by BOC was used for headspace sampling and GC-MS analyses.

7.3 Methods

7.3.1 Experimental Process

HS-GC-MS analysis can generate an incredibly information-rich data set, but this information richness, coupled with the lack of standards for evaluation of the headspace around WOP can make interpretation of the data set difficult. A combined non-targeted approach using chemometric methods to evaluate the GC-MS data can be a powerful tool for discrimination between sample groups (187, 200, 289, 438-441). To be effectively employed these methods require significant data (pre-) treatment to identify and align common features between samples and then filter the data set to identify features and reduce meaningless sample variation before application of the chemometric methods (175, 189, 192, 193, 201). Several software 'pipelines' have been produced that automate much of the above processes (175-177, 189, 192, 200, 201, 442). XCMS (175) and MetaboAnalyst (176, 177) were used to respectively process and analyze the data. These two pipelines are publicly available and can be run locally on a PC, and versions with reduced functionality running on servers at the Scripps Institute of Metabolomics (443) and the University of Alberta (444) have recently been made freely available.

The experimental process used in this research can be divided into two distinct phases, data generation and data handling (including data processing and data analysis). Figure 1 presents the experimental process from data generation to data analysis.
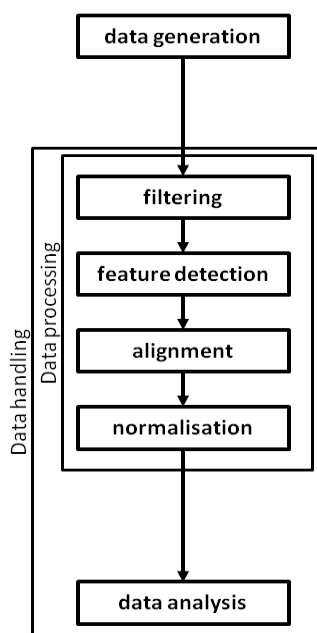
Figure 1 Experimental process used in degradic footprinting of watercolour drawings.

7.3.1.1 Data Generation

At the start of this research, a high throughput experiment (to generate a statistically significant data set and overcome sample variability) was designed and implemented. The goals of the experimental design were to:

1. Minimise within-class sample heterogeneity,

2. Minimise sample handling,

3. Increase sample throughput and minimise operating costs,

4. Build instrumental methods that could be universally applied to all of the sample types,

5. Generate high quality data sets that were suitable for automated analysis.

Sample handling was reduced to a minimum through the use of 20 ml headspace vials with Teflon-lined silicone septa as both the degradation vessels and as a means to trap VOCs for high throughput P&T-HS-GC-MS analysis. The headspace, chromatographic, and mass spectrometric methods were optimised in parallel to maximise throughput, reduce helium consumption, maintain base-line separation of chromatographic peaks and retain mass spectral resolution with rapid scan intervals. The instrument parameters are summarised in the methods section below.

After generation the generated total ion chromatograms (TICs) were analysed visually as an initial judge of quality, before being organised into paired sample groups for downstream data handling. Any odd looking TICs were noted and the sample vial retrieved for confirmation. If the sample was substantially identified as an outlier, it was pruned, and either the data generation stage repeated or not depending on the availability of additional material for samples, duration of accelerated degradation and whether or not sufficient multiples already existed in the sample set.

154

7.3.1.1.1 Sample Preparation

Sample sets were prepared by painting 3 cm wide stripes of paint or gum solution onto sheets of GSR and WLR, which were then cut into 2.5 cm by 5 cm rectangles each with a 3 cm wide stripe across the centre of the sample.

The samples were then labelled with the paper type, pigment type, number in the series and atmosphere, for example, GSR, TTB2, 47 for the 47th sample of pigment TTB2 painted onto GSR paper.

The labelled samples were then loaded into headspace vials, the sample data was recorded onto the vials with the addition of information about the atmosphere and degradation time.

The labelled but unsealed headspace vials were placed in desiccators and the samples dried over Drierite (Fluka) for a minimum of 1 week before being transferred to a climate chamber maintained at 25 °C and 50% RH for acclimatisation for an additional week. Once acclimatised to 50% RH, the vials intended for anoxic degradation were transferred to a glove box purged with argon humidified to 50 ±5 % RH. The samples were purged in the box for at least 2 h before sealing. At sealing, each vial was filled with argon from a gas line in the glove box prior to capping with either a crimp cap or a screw cap fitted with a Teflon-lined silicone septum. The samples of GSR, WLR, and the madder lakes were sealed with crimp caps while the samples containing TCA1, TCA7, TTB6, TTB3, TCA13 and TTB13 for light degradation were sealed in screw-capped vials.

7.3.1.1.2 Accelerated Degradation

A Sanyo MLR 351H fitted with Phillips TLD/865 Super 80 cool white daylight fluorescent bulbs. See Chapter 3 for more information about the light source used in the degradation of samples.

All accelerated degradation experiments were conducted in sealed headspace vials. Light degradation was conducted at 15,000 lux at 25 °C for 10 to 100 days.

After a light degradation regime samples were kept in the dark at ambient conditions for typically 1 week before being processed on the headspace autosampler. The vials were inspected and the seal tested by attempting to twist the cap. Vials that passed the 'twist test' were loaded into the headspace autosampler, and a more stringent pressurisation test was conducted on every vial. All vials that failed one of these tests were discarded and new samples prepared provided that additional samples were available.

7.3.1.1.3 Headspace Sampling

A Tekmar HT3 autosampler operated in dynamic, purge and trap, mode was used for headspace sampling. Sealed headspace vials containing the aged samples were randomly loaded onto the sample carousel. Empty

headspace vials as well as 'no vial blanks'[27] alternately inserted at every tenth position, were used to check for column bleed and trap carryover.

For analysis, a vial is lowered into the HT3 sample oven and preheated to 75 °C for 30 min. After preheating, the vial is raised onto the needle and pressurised with helium to perform a leak check. If pressure can be maintained for 1 min, the vial is swept with 100 ml/min helium for 10 min onto a Supelco Type K, VOCARB 3000 trap[28], held at 35 °C. A dry purge step is not used because significant quantities of water are not found in the headspace. Once loaded, the trap is rapidly heated to 245 °C and flushed with 100 ml/min helium for 5 min to desorb the VOCs onto the injection port of a Varian CP3800 GC via a transfer line held at 255 °C.

After desorbing, the trap is reconditioned by heating to 260 °C for 8 min while being back flushed with 200 ml/min helium.

7.3.1.1.4 GC-MS Method

A Supelco VOCOL column (60 m x 0.25 mm x 1.5 µm) was used for analyses. This column has a medium polarity, bonded methyl phenyl cyanopropyl polysiloxane stationary phase, and it is intended for analyses of complex mixtures of VOCs encountered during environmental sampling. It gives good retention and separation of highly volatile compounds and it is designed for coupling to purge and trap headspace analysis systems. The chromatographic method is summarised in Table 2. At 39 min, the chromatogram is relatively short to maximise sample throughput and minimise helium consumption. Longer chromatograms were evaluated during method design, but they did not yield significantly better base line separation for most components eluting before 30 min.

---

[27] A "no vial blank" is an empty slot left in the sample carousel. The autosampler would go follow the normal sampling procedure, but without a vial. No vial blanks were used to evaluate carry-over, due to poisoning or overloading of the trap, between runs.

[28] This multi-sorbent trap is particularly good for VOC analysis from headspace and environmental sampling. It has the highest retention values for the broadest range of VOCs. Furthermore, its high thermal stability allows for high temperature desorption and reconditioning to reduce the risk of carry over and cross contamination between injections.

Gas chromatographic method			
Injection port temperature		200 °C	
Split injection ratio		20	
Column flow rate		1.7 ml/min	
Column oven temperature programming			
Temperature (°C)	Rate (°C/min)	Hold (min)	Total (min)
60	---	5.00	5.00
110	10.00	0.00	10.00
180	4.00	10.00	37.50
210	20.00	0.00	39.00

Table 2 Gas chromatographic method.

A Varian Saturn 2000 iontrap mass spectrometer was used as a detector. The transfer line between the GC and the MS was kept at 225 °C to prevent cold spots. The MS was operated in total ion chromatogram (TIC) mode with electron impact (EI) ionisation and detection between 27 m/z to 600 m/z. The mass spectrometer method settings are summarised in Table 3.

Mass spectrometer method	
Ionisation mode	EI auto
Low mass (m/z)	27
High mass (m/z)	600
Scan time (sec/scan)	0.49
Multiplier offset (V)	0
Emission current (µA)	10
Count threshold (counts)	1
Target TIC (counts)	20,000
Max ionisation time (µsec)	25,000
Pre-scan ionisation time (µsec)	100
Background mass (m/z)	39
RF dump value (m/z)	650

Table 3 Mass Spectrometric Method.

7.3.1.2 Data Handling

Data handling includes both data processing and data analysis. Two software packages, XCMS Online (443) and MetaboAnalyst (444)were used to create a data handling pipeline.

7.3.1.2.1 Data Processing

Data processing began with uploading paired datasets (ambient vs. anoxic for a given sample type) onto the XCMS Online server at the Scripps Center for Metabolomics (175, 443). The TICs were filtered to remove baseline level noise and identify features that could be used for alignment.

Correct TIC alignment is necessary to generate meaningful information about the sample sets and avoid 'false discoveries' in the data (175, 441, 445, 446), as such it is one of the most important and function critical features of an automated data analysis pipeline. With XCMS, retention time (RT) correction is optional, users can select between: no RT correction, peak group RT correction by non-linear fitting using 'well-behaved' groups of features retained between samples and RT correction through the application of the Obi-Warp algorithm (175, 446, 447). During method development, examination of the overlaid TICs and the plots of retention time deviation vs. retention time revealed that in most cases the deviations in retention time were small and generally easily corrected for with non-linear warping using 'well behaved' peak groups as anchors present in each sample (175, 446). After data processing, XCMS Online provides data visualisation tools that can be used for initial evaluation of the aligned TICs before the data is passed on into the next element in the data handling pipeline.

Readers interested in using XCMS are highly encouraged to read Smith *et al*. for a thorough description of XCMS theory and functionality (175), as well as Boccard *et al.* (201) and Katajamaa *et al.* (192) for a more general review of mass spectrometry-based metabolomics data handling and knowledge discovery.

7.3.1.2.1.1 XCMS Method

The applied XCMS method parameters are given in Tables 4-7 below. The values used in the table are those recommended by the Scripps Center for Metabolomics for use with single quad GC-MS (443). Aside from adjusting the p-value thresholds to return more significant features, changes were made.

Feature Detection	
full width half maximum (FWHM)	3
Step	0.3
signal/noise (S/N) ratio cut-off	10
max # chromatographic peaks per EIC	100
min difference in m/z for peaks with overlapping retention times	0.5

Table 4 Settings for feature detection using XCMS Online.

Alignment	
width of overlapping m/z slices (mzwid)	0.25
min fraction of samples necessary in at least one of the sample groups for it to be a valid group (minfrac)	0.5
band width (BW) in seconds	3
max number of groups to identify in a single slice	100
min number of samples necessary in at least one of the sample groups for it to be a valid group (minsamp)	1

Table 5 Settings for TIC alignment using XCMS Online.

Retention Time Correction (RTC)	
Peak Groups RTC	
number of extra peaks to allow in RTC groups	1
number of mission samples to allow in RTC groups	1
ignore sample class?	TRUE
initial grouping: band width	5
initial grouping: mzwid	0.25
initial grouping: minfrac	1
initial grouping: minsamp	1
Alignment	non-linear (loess)
degree of smoothing for local polynomial regression fitting	2

Table 6 Settings for retention time correction using XCMS Online.

Statistics	
p-value threshold for highly significant features	0.05
p-value threshold for significant features	0.1

Table 7 Table 7 Settings for statistical analysis of significant features using XCMS Online.

7.3.1.2.2 Data Analysis

The XCMS-generated peak lists, with m/z intensities ordered by retention time, were converted into peak intensity tables and imported into MetaboAnalyst (176, 177, 444) for further processing and analysis. With respect to its statistical components, MetaboAnalyst is a metabolomics-specific implementation of the R statistical software package with a graphic user interface overlay.

In MetaboAnalyst the data was first quality checked for zero, missing and negative values, which can have a negative impact on data analysis. Any feature that was missing from more than 50% of the samples (the recommended default value) was excluded as well as late-eluting, high-molecular weight features which were identified as being due to column bleed. Other zero and missing values were replaced with a low value equal to one half of the lowest observed value for that feature in the data sets (176, 192, 193, 201).

After quality and integrity check, interquantile range (IQR) filtering was applied to reduce the number of features in the data set by 5%. IQR is a robust method that identifies features that are near constant between samples, and therefore unlikely to contribute to any classification models that might be built using the data set. No phenotype (sample class) data is used during the filtering step so the reduced set can be used in all downstream analyses (176, 192, 201).

Because of the large dynamic range of many features, column-wise normalisation, which aims to make each feature, within a sample, more comparable in magnitude, is highly recommended for –omics data sets. High-abundance features, which might not lead to meaningful information can dominate some multivariate analyses, and conversely the ratios of low abundance features might lead to better discriminatory models. Several column-wise normalisation methods are available in MetaboAnalyst, and each affects the data in different ways (376) For the data sets, log 2 transformation, Pareto scaling or auto-scaling were applied.

The filtered and normalised data then passed into the MetaboAnalyst statistical analysis pipeline which implements: fold change analysis, *t*-tests, volcano plots, principal component analysis (PCA), partial least squares-discriminant analysis (PLS-DA), hierarchical clustering analysis (HCA) with dendrogram and heat map plots, K-means clustering, self-organising maps (SOM), and random forest decision trees (RF). An overview of these statistical methods is given below at their first application in the WLR results and discussion section 7.4.1.3.

A typical work flow begins with univariate methods which are easy to understand. While providing a starting point for analysis, the student t-test and fold change analysis have limited applicability to high dimensional data sets. After the univariate analyses, unsupervised multivariate methods such as PCA and HCA are good methods to reduce data dimensionality and begin to identify underlying patterns and groups in the data. PLS-DA is commonly used next. The PLS-DA generated models can be very compelling, but care must be taken to evaluate the models using both cross-validation and permutation tests to avoid false discoveries (448). K-means nearest neighbour and self-organising maps are useful to identify groupings in the data, however, care must be taken when initializing these methods. RF and SVM are both good at identifying significant features and classifying samples into groups even in the presence of noisy data, missing samples, and outliers. RF analysis has the added benefit of identifying outliers in the sample set. After completion of the analyses MetaboAnalyst generates a detailed report with tabular and graphical information as well as descriptions of the statistical methods which can be an aid in post-analysis interpretation (176, 177).

7.3.1.3 Post-Analysis Interpretation

The first step in post-analysis interpretation is to attempt to explain the observed models and begin to assign chemical meaning to the significant features. To do this the raw data is returned to and 'hot spots', those which contain the most commonly identified significant features can then be deconvoluted and evaluated qualitatively by application of AMDIS and NIST database searching. Once the chemical identity of the significant features have been tentatively identified, their up or down regulation (determined by fold change analysis) can be used to assign chemical meaning and explain the differences in degradation behaviour.

7.4 Results and Discussion

7.4.1 WLR, Ambient vs. Anoxia Comparison

The WLR samples are prepared from cotton linters and TCF bleached flax pulp as part of the Turner paper reconstructions, see Chapter 3 and Chapter 4 for more details about this paper. Without gelatine size, gum Arabic or colourants, these samples present the simplest system in the sample set. Being an alkaline paper, with a pH below 9, hydrolysis, at least initially, is not expected to be a significant degradation pathway, and oxidative reactions should dominate. Therefore the WLR samples should be a good candidate for evaluating

the effect of anoxia on limiting the oxidation of cellulose, and are thus a logical, relatively simple starting point for the application of degradic footprinting to evaluate a conservation treatment.

Given that we are most interested in the display of heritage objects under controlled gallery conditions, accelerated light degradation with UV-filtered light at 25 °C and 50 % RH are the logical experimental conditions to apply to the samples. However, the WLR samples are effectively pure cellulose, lack chromophores capable of absorbing visible light, though some chromophores will be present from the TCF bleaching method. Therefore the samples of WLR, even those under ambient atmosphere, were not expected to degrade much, and thus the headspace above the samples was expected to be sparsely populated. This is the case, the raw, unaligned TICs in Figure 2 are sparsely populated. The large features in the TICs, particularly those after 30 min RT, are due to column bleed and from the headspace vial septa. It is the near base-line features that are significant.
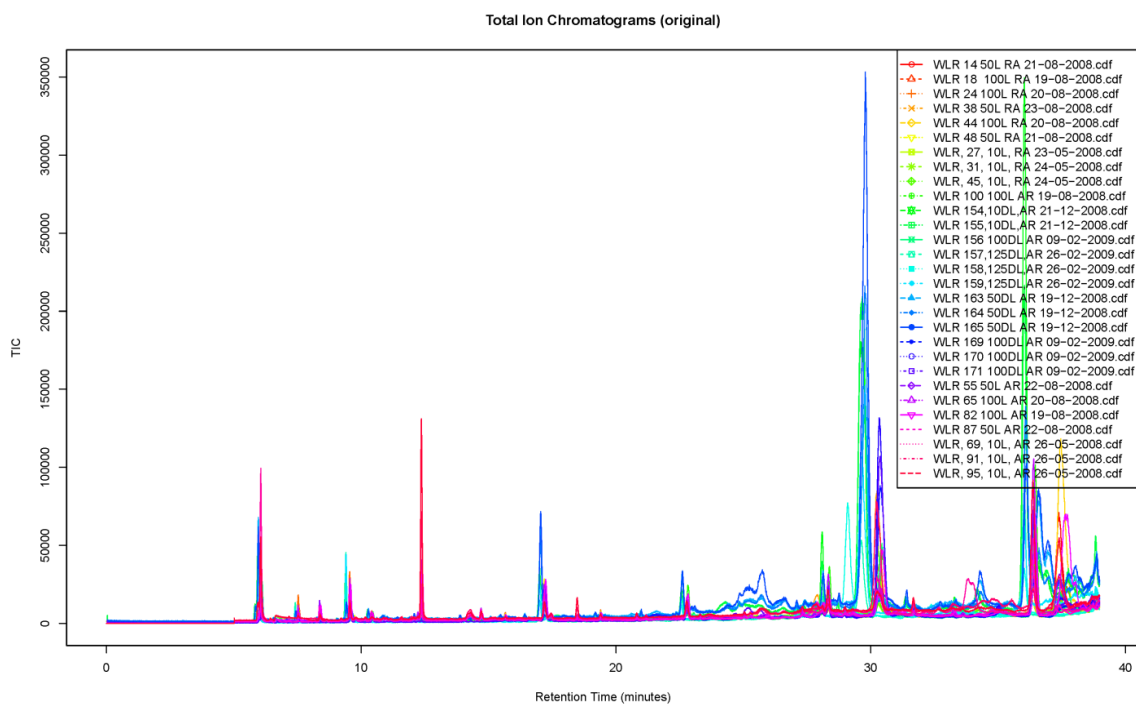
Figure 2 WLR, photodegraded, unaligned TICs.

7.4.1.1 Non-Sample Related Peaks

Significant efforts were made to remove any features that were determined to arise from either the column or the septa. This was done by manually pruning features from the peak intensity table from the aligned data sets. These features were identified by examining the chromatograms from empty vials and from column bleed test runs. When possible features were pruned by excluding all features from a particular RT, as was the case for the column bleed-related features which principally eluted after 30 minutes. The septa-related peaks are very strong, and dominate the chromatograms because the samples themselves did not

161

produce significant quantities of VOCs (the sample related peaks are near the base line). This problem was identified during the data generation stage, was investigated, and attempts were made to alleviate it.

- First the possibility of contamination from the trap or any other part of the gas flow system was tested by using 'no-vial' blanks where the autosampler is instructed to step through the sample introduction process without a vial in place, and without a vial-septum present the peaks disappeared confirming that they arose from the septa.
- Next, I proposed that the septa-related peaks arise from contaminants on the septa. So they were baked at 180 °C to desorb any VOCs in the septa prior to use; this practice did not significantly reduce the peaks, but it was continued for all of the samples.
- I then proposed that the peaks arise from the photodegradation of the septa, and so the outer surfaces of the caps and septa were protected from light with aluminium foil. However, this did not significantly reduce the peaks, but the practice was continued for all further samples.
- Next, I proposed that the peaks arose during sampling with the HT3 autosampler which uses a heated needle to minimise sample carryover between runs. It is neither possible to determine nor to adjust the temperature of this needle. At the time of experimental design it was thought that the needle would be at the oven temperature (75 °C), but the valve to which the needle was connected was maintained at 180 °C. Even if the needle was at 180 °C this temperature is well below the melting point of both PTFE and silicone and within the usable temperature range of the product, so it should not have caused degradation of the septa, but a needle at 180 °C might have released VOCs from the septa during the desorption process.

Because it was not possible to eliminate the peaks by changing the treatment of the vials and septa, attempted to mitigate their presence by modifying the GC-MS methods.

- I adjusted the split ratio to minimise the septa-related peaks, but this also minimised the sample-related peaks so it was abandoned.
- I explored the option of turning of the MS detection during the time intervals when I expected the peaks to evolve. This allowed me to better visualise the sample-related peaks, but the practice was soon abandoned because RT drift made the timing uncertain, and some sample-related peaks elute near or co-elute with the septa-related peaks resulting in a loss of data. I later found that this practice also makes these chromatograms incompatible for TIC alignment.
- I adjusted the chromatographic method to use a longer runtime and different temperature ramps and isotherms to increase the baseline separation, this improved the separation but did not eliminate the co-elution. It has the disadvantage, I later found, of making the data from the two different chromatographic methods incompatible for TIC alignment.

Finding no effective solution, I decided to return to the original GC-MS method and to remove the septa-related peaks during data analysis.

- I proposed that I could batch subtract these peaks from the chromatograms using averages of the integrated septa-related peaks generated from the blank runs. This was not effective because of the large variance in the samples.

- I proposed that I could deconvolute each individual mass chromatogram and then remove the septa-related peaks from the resulting peak lists. However, this practice was extremely time and processor intensive, ca. 2 h per chromatogram using AMDIS (449)on the computers that I had at my disposal. I decided not to pursue this route because it did not significantly change the manual interpretation of the chromatograms, and at the time of data generation (2008-2009) I did not have access to automated data handling software.

- With access to XCMS Online (443)and MetaboAnalyst (444), I have returned to the option of deconvolution before alignment and feature extraction, but neither package supports the importation of deconvoluted spectra from AMDIS (449), and I did not have access to the Metabolome Express package (450) which can be used to deconvolute and align mass chromatograms that can be uploaded onto MetaboAnalyst (444).

Having exhausted all conceivable options I decided that the best method would be to use the mass chromatograms from empty vials to identify features that definitely arise from the septa. The clearly siloxane-related features were then manually pruned from the aligned peak intensity tables generated by XCMS. However, because of co-elution and how the feature intensities were binned during TIC alignment it was not possible to remove all of the features arising from the septa without losing data from the samples. The features (as identified by deconvolution of the mass chromatograms) that could arise from both the sample and the septa (particularly the 73 m/z feature that can arise from siloxanes and from a variety of organic compounds) were retained in the peak intensity tables. This complicates the interpretation, but because they were present in all samples, their inclusion should not overly influence the chemometric methods, and on the contrary for the GSR and samples with colourants (where the co-elution was more significant), the exclusion of these features decreases the discriminating power of the chemometric methods: less separation between groups in PCA and PLS-DA, not as clear sub-grouping by colourant in HCA and SOM and reduced accuracy in RF class assignment. Therefore, it was decided that until I discover a better method to accurately and efficiently remove them from the mass chromatograms their presence was acceptable.

7.4.1.2 Data Treatment with XCMS

Below I will detail the data handling of the WLR sample set; this will serve as an example of the analyses applied to all of the sample groups, so that a more condensed summary of the results can be given for the remaining sample groups later in the chapter.

7.4.1.2.1 TIC Alignment

It is possible to focus on these small features and evaluate the chromatograms visually, but making sense from such evaluation is looking for a needle, not in a haystack, but in a stack of needles. Better is to apply an objective, machine-based method to first prepare each data set in exactly the same way and then to use statistical methods to mine the data: identifying significant features and patterns and building models to classify the samples into groups. To effectively do this the TICs must be processed and aligned. Figure 3 presents the TICs aligned using nonlinear peak grouping, based on 'well-behaved' peaks which serve as anchors selected by XCMS in each of the TICs.
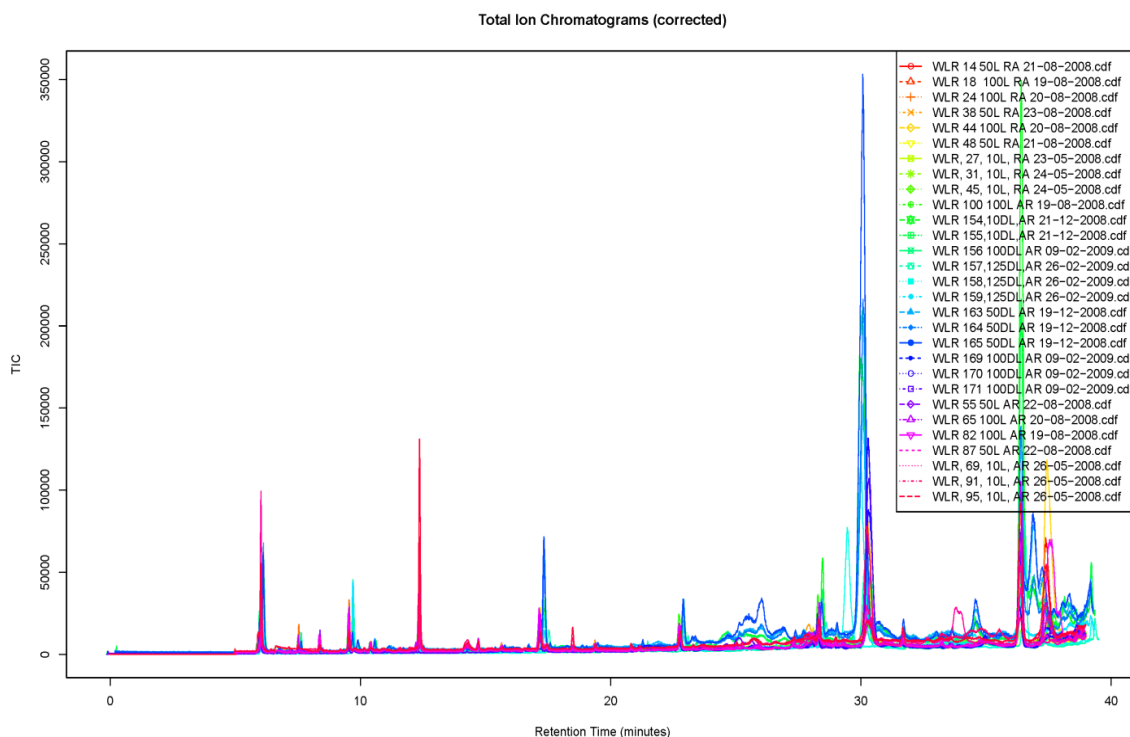
Figure 3 WLR, photodegraded, TICs aligned with non-linear retention time warping using 'well-behaved' peak groups. The quality of the alignment is typical for all of the sample groups and is acceptable for further analyses.

7.4.1.2.2 Extracted Ion Chromatograms (EICs)

A particularly useful output of XCMS processing is the generation of EICs and box plots of statistically significant features. Figure 4 presents the 40 m/z EIC and box plot at approximately 6 min RT (scan 357). This feature corresponds to argon in the headspace of the sample vial. Because the trap on the autosampler was not dry purged between loading and desorption, much of the argon in the samples was retained, and because it did not interact with the stationary phase of the column it was one of the first elutants. All of the ambient atmosphere samples have low intensity for this feature corresponding to the small amount of argon in the atmosphere. The standard deviation of these measurements for the ambient samples is quite small indicating that the sample introduction method is reproducible between samples. On the other hand the anoxic atmosphere samples have a range of different intensities at this feature.
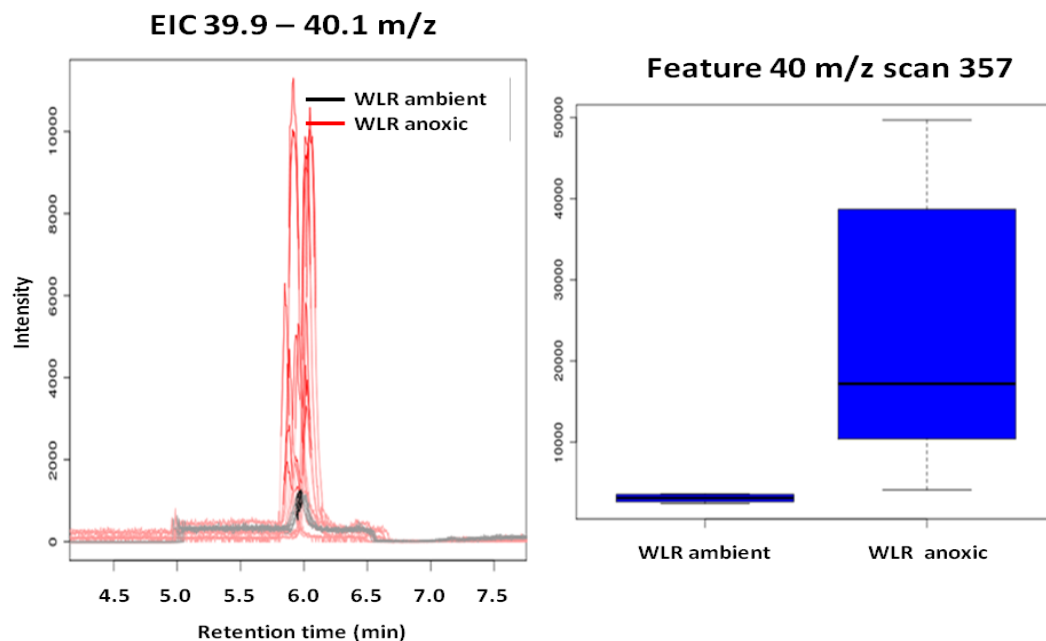
Figure 4 Extracted ion chromatograph and box and whisker plot of feature 40 m/z at ca. 6 min RT (identified as argon) for the WLR, photodegraded sample. The EIC on the left presents the overlaid EICs for all of the samples. We can see, that the ambient samples all have similar low intensities for this feature, this can be verified by the box and whisker plot on the right. The anoxic samples on the other hand have a wide range of intensities corresponding to a range of argon concentrations.

We can safely assume that given the same sample introduction method was used for every sample, we should have equal reproducibility for ambient and anoxic atmosphere samples. The reproducibility of sample handling, including sample introduction, of the autosampler was checked before each set of runs using the system diagnostic tools and vials containing furfural in methanol. Therefore, the greater variability for the anoxic samples is indicative of the variability of the quality of the seal, and thus this feature can be used for sample vial filling/sealing quality control.

Despite the fact that some anoxic vials, nearly all of the vials aged for 100 days, lost their argon, the 40 m/z feature is a strong classifier for the anoxic samples. Its inclusion in exploratory data analysis such as, multidimensional scaling, principal components analysis and clustering analysis proved to be useful for the interpretation of their outputs. However its inclusion, as is the case, in classification methods such as partial least squares discriminant analysis, random forest classification and support vector machines classification can overly influence the results. Bearing that in mind it would be better to repeat the analyses including and excluding this variable from the models and to then to compare and evaluate the results.

The assumption of inter-comparability of samples extends to all features of interest identified in the TICs; but the quality of the seal is less critical for the VOCs than for argon. This is due to the fact that paper itself acts as both a source and a sorbent of VOCs and releases them at elevated temperatures, while argon, being inert, does not interact with the paper and is able to escape through a poor seal and even diffuse through

the septum. The anoxic atmosphere samples aged for 100 days always have less argon than those aged for shorter periods of time, and it is likely that there was some loss of VOCs from the vials degraded for longer intervals. This factor must be recognised when comparing samples degraded for different time intervals, and perhaps the samples degraded for 100 days are less trustworthy for comparing different types of samples than those degraded for shorter intervals.

However, the validity of the sample inter-comparability assumption hinges on two factors. First that standard sample introduction and GC-MS methods are rigidly employed with no variations. Second that there are no malfunctions with the equipment (leaks in the gas lines, degradation of the trap or column, malfunction of the MS) that might lead to changes in the data. If even slightly different methods are used, for instance heating to 80 °C instead of 75 °C or purging for an extra 5 min, this will result in differences to the TICs, which may not be significant during visual examination, but which might be significant for statistical methods of analysis and therefore lead to false discoveries. Unfortunately, these experiments included a certain amount of adjustment and optimization of the methods, which at the time seemed to make the data generation step more efficient. Additionally, there were several malfunctions with the autosampler, GC and MS over the course of the two years that they were used for this research. Sometimes, the malfunctions did not generate a fault message to stop the automatic sample introduction thus leading to the loss of valuable samples. On another occasion a significant fault required major servicing of the instrument, which took time to arrange, thus generating a backlog of samples to be run and a change in the MS response. Thus, some of the visually estimated 'good quality' data is not of as good quality as I might have hoped, and it must be acknowledged that the above factors degenerate the quality of the data, however, much of the data is still useable. The results from the XCMS software include all samples from the alignment data set (some samples were excluded due to the fact the MS methods had been changed and as such that the peaks used for alignment were not present), this 'all-in' sample set can later be pruned to remove outliers identified in later data analysis. The decision to include a chromatogram or to prune it from the data set was made by first comparing the clustering of the samples in several chemometric methods, this will be explained below. Samples that appeared to be outliers were flagged and the their TICs and peak intensity tables examined by eye, and if there was something visibly odd about them they were excluded and the chemometric analyses repeated, and the results were compared to the initial 'all in' run. If the quality of the generated chemometric models, particularly those from unsupervised methods, improved then the excluded sample was pruned from the data set, if not the excluded sample was re-introduced and a new sample excluded.

7.4.1.2.3 Multidimensional Scaling

The first multivariate method to be applied to the data as part of XCMS is Kruskal's non-metric multidimensional scaling (MDS) (175). MDS was applied to all of the significant features identified in the aligned TICs of the paired data sets. Non-metric MDS is particularly useful for dimensional reduction and

interpretation of the large multivariate data sets generated by metabolomic analysis. The goal of MDS is to detect meaningful underlying dimensions in a set of data objects and provide a visual representation of the pattern of proximities between objects that allow the researcher to explain observed similarities or dissimilarities. It differs from other ordination methods, like PCA, in that it does not assume an underlying linear structure to the data (376, 451, 452).

MDS generates a two or three dimensional matrix using a distance measure (*e.g.* Euclidian) so that the ranked differences between objects are preserved and the resulting plot, which is similar to cluster analysis, can be evaluated visually (383, 452, 453). The orientation of the plot and the axes does not relate to underlying variables as in PCA. Simply the greater the distance between any two points on the plot corresponds to greater dissimilarity in the TICs. MDS is simply a quick way to scan the data for patterns and determine if further data analysis is warranted.
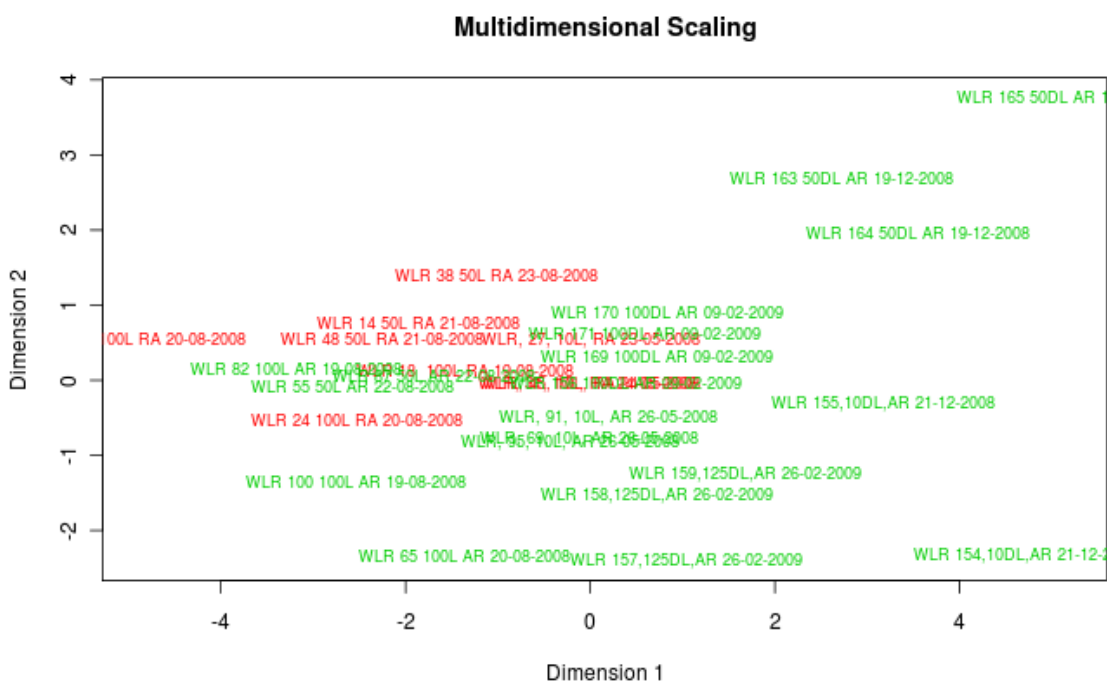
Figure 5 Multidimensional scaling analysis plot based on WLR, photodegraded, chromatographic data. It is possible to distinguish some pattern in the data with the samples degraded in ambient atmosphere (red) clustering to the left centre, and the samples degraded in argon (green) forming a second more dispersed cluster. Secondary clusters of samples degraded for the same duration can also be discerned in the plot.

Figure 5 is an MDS plot of the WLR samples; it reveals that there is a large spread in the anoxic atmosphere samples and that some anoxic samples, regardless of degradation time, cluster closer to the ambient atmosphere samples than to the rest of the anoxic samples. This is curious, and deserves to be further explored. Noting the sample names, it is apparent that most anoxic samples that cluster close the ambient samples have a sub-100 sample identification number.

WLR samples 1 – 100 were cut, inserted into vials, which were filled with argon and sealed all at the same time; such that all of the vials, regardless of time spent in the photodegradation chamber, had at least 100 days for the argon to leak from the vials. The 100-day samples went immediately into the degradation chamber while the 50 and 10-day samples were kept in a drawer until they were introduced into the degradation chamber. By sealing all of the vials at the same time, it was hoped to ensure the same starting headspace composition in all of the vials; however, just the opposite is true. Because of the argon leaking from the vials, the 100, 50 and 10 day samples each had a different starting point when introduced into the degradation chamber. To correct for this mistake a second set of WLR samples was prepared. These samples have an identification number greater than 100; and they were inserted into vials which were filled with argon and sealed just before being placed in the degradation chamber, such that they had the same headspace conditions at the start of the degradation period. This explains the observed differences in clustering, and helped to inform the pruning of all of the sub 100 WLR and GSR samples from their respective data sets, as described above, during further analysis with MetaboAnalyst.

7.4.1.3 Data Handling with MetaboAnalyst

MetaboAnalyst provides different data handling streams. A data treatment stream begins with alignment and peak matching between samples. Peaks are matched by both m/z and RT. The intensities of ions that meet both the user-specified m/z and RT tolerance windows (0.5 m/z and 5 s respectively) window are binned to give a single feature (176, 444).

The aligned chromatograms are then subjected to data integrity check, and to minimise downstream analysis problems, missing or zero values are replaced with a small value (one half of the minimum positive value in the original data) (176, 444). Interquartile range filtering is then applied to remove variables that are near constant between samples and therefore unlikely to be useful during data modelling. The filtered data is then treated with column-wise normalization. Column-wise normalisation aims to make each variable comparable within a sample. For the WLR samples, a log 2 transformation was selected over unit scaling, Pareto scaling or range scaling, because it preserves much of the data structure (376). Figure 6 presents the variable distribution of the original and the normalised data sets. Examining the intensity density plots (the lower section of Figure 6) we can see that before scaling most of the features have a low count intensity with some higher count intensity features. After scaling there is a multimodal Gaussian-like distribution of the variable intensity density. Note, however, the apparent bimodal distribution, this might be indicative of two sources of features.
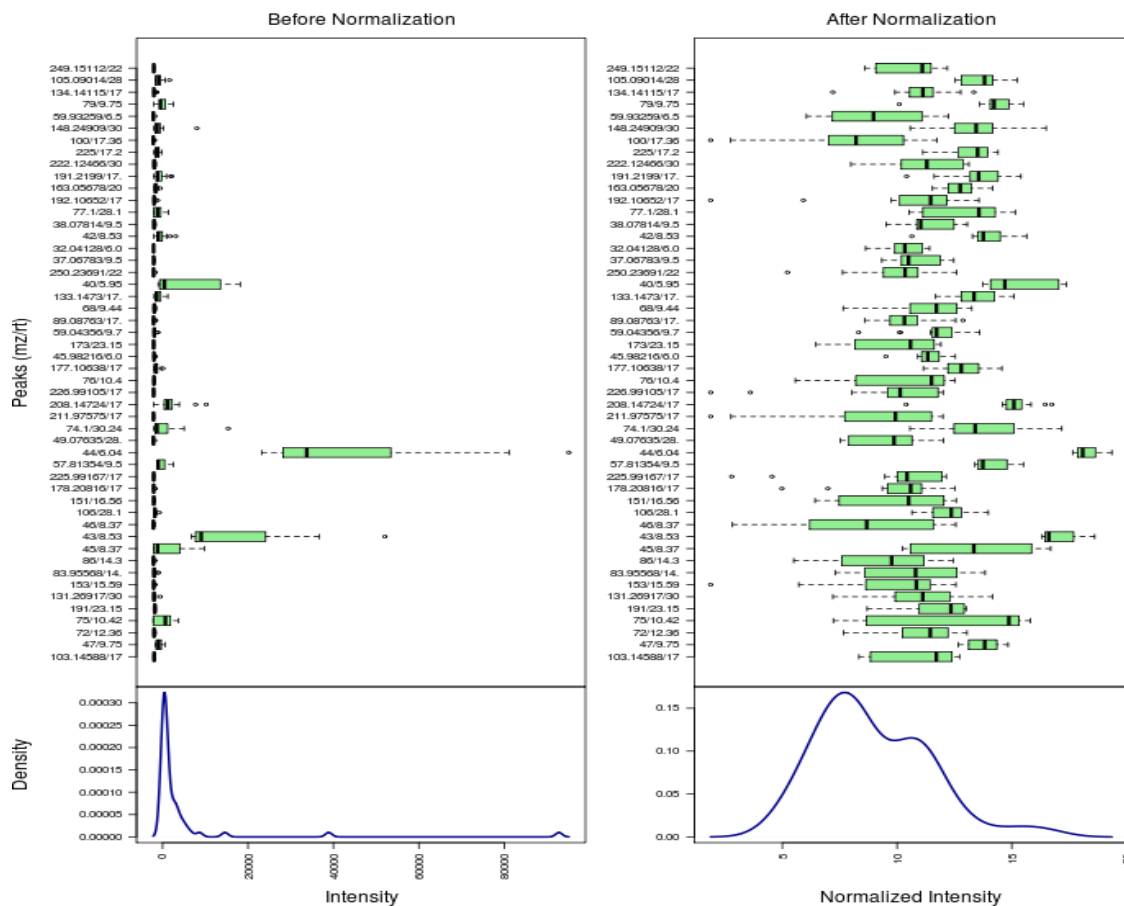
Figure 6 WLR, photodegraded, comparison of data before (left) and after (right) log 2 transformation column-wise scaling. The key point is the plot of the density of feature intensities. The goal of column-wise normalisation is to make the features within a sample, which can have a large range of intensities, more comparable. A more Gaussian-like distribution, like on the right, is desirable.

7.4.1.4 Statistical Analysis with MetaboAnalyst

After the data has been normalised, it is ready for the statistical analysis stream. The statistical analysis stream includes several paths: univariate methods, supervised and unsupervised multivariate methods, clustering methods, high-dimensional feature selection methods and supervised classification methods. The statistical analysis stream was iteratively applied to the data set to identify and exclude outlying samples and remove noise generating features (those associated with the septa and column) from the data set. The noise generating features were identified by deconvoluting randomly selected TICs and comparing them to empty vial and no vial blank runs. Ions that could definitely be associated with either the column or the septa were removed, but because non-deconvoluted TICs were used to generate the peak intensity tables and because ions of the same m/z within a RT window were binned it was impossible to exclude ions that could be associated with both the sample and the septa. An example of this is the 73 m/z ion that can arise from a number of sources including alcohols, ethers, esters, acids, and trimethylsilyl derivatives. It was decided that in the case of co-elution, the mixed-source ions should be retained, but models relying heavily on these ions should be approached with caution.

7.4.1.4.1 Univariate Analysis

7.4.1.4.1.1 Fold-Change Analysis

In fold-change analysis the goal is to compare the absolute value changes between groups, and for this purpose the non-normalised data is used (176, 383). Figure 7 presents the significant features identified by fold-change analysis. The fold-change threshold value was set to 2 (176, 444). In the plot, a log 2 transformation was used so that both up-regulated features (features that became larger between class 1 (ambient) and class two (anoxic)) and down-regulated features (those that became smaller between class 1 (ambient) and class two (anoxic)) could be symmetrically plotted. Fold-change analysis is a useful starting point to identify the regions of greatest change in the TICs, but this measure does not incorporate a measure of statistical significance, for that a Student t-test must be applied.

(m/z)/rt	Fold Change	log2(FC)
46/8.37	47.46	5.5686
45/8.37	30.179	4.9155
83.95568/14.71	28.01	4.8079
100/17.36	23.35	4.5453
59.93259/6.54	17.75	4.1497
86/14.3	13.699	3.776
211.97575/17.16	9.4203	3.2358
173/23.15	8.82	3.1408
40/5.95	0.11931	-3.0672
27.58659/6.06	7.9213	2.9857
49.07635/28.09	6.0499	2.5969
131.26917/30.17	0.23932	-2.063
148.24909/30.26	0.24306	-2.0406
77.1/28.1	3.7687	1.9141
151/16.56	3.4738	1.7965
74.1/30.24	0.34688	-1.5275
133.1473/17.2	0.37302	-1.4227
76/10.4	2.344	1.229
75/10.42	2.3379	1.2252
177.10638/17.2	0.44202	-1.1778
153/15.59	0.46406	-1.1076
103.14588/17.15	2.1485	1.1034
191/23.15	2.0991	1.0697
134.14115/17.19	0.4816	-1.0541
72/12.36	2.0556	1.0396

Figure 7 WLR, photodegraded, plot and table of significant features identified by log-fold-change analysis with a threshold set at 2. The fuchsia circles represent features above the threshold; note that the values are on log scale, so that both up-regulated and down-regulated features can be symmetrically plotted.

7.4.1.4.1.2 Student t-test

The student t-test is the most common univariate measure of statistical significance. Figure 8 presents the output of the individual application of the t-test to each feature in the TIC with a p-value threshold of 0.05 and the assumption that there is equal variance between the groups (176, 444). In the plot a $-\log 10$ transformation was applied to the p values such that the more significant features are plotted higher on graph. The student t-test, while a measure of statistical significance, does not consider the magnitude of change in the features, and as such it is good for identifying near-base-line features that could be important for evaluation of two different sample groups (383).

(m/z)/rt	p.value	-IOG10(p)	FDR
83.95568/14.71	2.05E-10	9.6876	1.07E-08
59.93259/6.54	1.27E-07	6.8961	2.26E-06
45/8.37	1.31E-07	6.8843	2.26E-06
46/8.37	1.30E-06	5.8866	1.69E-05
49.07635/28.09	9.17E-06	5.0376	9.54E-05
40/5.95	1.17E-05	4.9324	0.000101
86/14.3	1.40E-05	4.8527	0.000104
173/23.15	8.53E-05	4.0692	0.000554
100/17.36	0.000102	3.992	0.000588
77.1/28.1	0.000841	3.0752	0.004373
211.97575/17.16	0.002084	2.6811	0.009852
27.58659/6.06	0.005095	2.2929	0.022079
133.1473/17.2	0.010768	1.9678	0.041561
148.24909/30.26	0.011189	1.9512	0.041561
191/23.15	0.014414	1.8412	0.047489
131.26917/30.17	0.014612	1.8353	0.047489
103.14588/17.15	0.016549	1.7812	0.050621
75/10.42	0.018019	1.7443	0.052056
76/10.4	0.024645	1.6083	0.06745
105.09014/28.1	0.034936	1.4567	0.090833
72/12.36	0.0416	1.3809	0.10301
177.10638/17.2	0.045016	1.3466	0.1064

Figure 8 WLR, photodegraded, Plot and table of significant features identified by t-test with a threshold set at p=0.05. Fuchsia circles indicate significant variables; note that the –log10 of the p-values are plotted such that the more significant features (those with a smaller p-value) are plotted higher on the graph.

7.4.1.4.1.3 Volcano Plot

Simultaneous application of fold-change analysis and t-tests generates a volcano plot. It is a good way to visualise the most significant features and whether they are up- or down regulated. Figure 9 presents the volcano plot and a table of the significant features. The fold change threshold was set to 2, t-test p-value threshold 0.1 and equal variance was assumed (176, 444). Features above the horizontal line, the 0.1 p-value threshold are statistically significant. Features to the left of the left hand vertical line are up-regulated between ambient and anoxia samples, and the features to the right of the right hand vertical line are down-regulated between ambient and anoxic samples.

(m/z)/rt	FC	log2(FC)	p.value	-lOG10(p)
83.95568/14.71	28.01	4.8079	2.05E-10	9.6876
59.93259/6.54	17.75	4.1497	1.27E-07	6.8961
45/8.37	30.179	4.9155	1.31E-07	6.8843
46/8.37	47.46	5.5686	1.30E-06	5.8866
49.07635/28.09	6.0499	2.5969	9.17E-06	5.0376
40/5.95	0.11931	-3.0672	1.17E-05	4.9324
86/14.3	13.699	3.776	1.40E-05	4.8527
173/23.15	8.82	3.1408	8.53E-05	4.0692
100/17.36	23.35	4.5453	0.000102	3.992
77.1/28.1	3.7687	1.9141	0.000841	3.0752
211.97575/17.16	9.4203	3.2358	0.002084	2.6811
27.58659/6.06	7.9213	2.9857	0.005095	2.2929
133.1473/17.2	0.37302	-1.4227	0.010768	1.9678
148.24909/30.26	0.24306	-2.0406	0.011189	1.9512
191/23.15	2.0991	1.0697	0.014414	1.8412
131.26917/30.17	0.23932	-2.063	0.014612	1.8353
103.14588/17.15	2.1485	1.1034	0.016549	1.7812
75/10.42	2.3379	1.2252	0.018019	1.7443
76/10.4	2.344	1.229	0.024645	1.6083
72/12.36	2.0556	1.0396	0.0416	1.3809
177.10638/17.2	0.44202	-1.1778	0.045016	1.3466

Figure 9 WLR, photodegraded, plot and table from volcano plot. The fuchsia circles indicate significant features that exceed both the fold change and t-test threshold values.

7.4.1.4.1.4 Correlation Analysis

Correlation analysis can be used to identify which features correlate to a feature of interest or to identify if features show particular patterns under different conditions (176, 444). In Figure 10, correlation analysis was used to identify features that increase and decrease in intensity between ambient and anoxic atmospheres. Calculations were performed using the Pearson distance measure and the output includes the correlation coefficients, t-statistics, p-value and false discover rate (FDR) value for each feature. FDR is a statistical method for multiple hypothesis testing; it controls for the number of Type-I, false positive, errors (383). We can see that the most significant feature for anoxic atmosphere is the 40 m/z peak associated with argon, and the four other peaks positively associated with the anoxic samples. The rest of the plotted features anti-correlate with those of the anoxic samples. The key point here is that the samples in anoxic atmosphere have a sparsely populated headspace, and most of the constituents present can be associated with either the septa or column bleed. On the other hand, the samples in ambient atmosphere have a much more richly populated headspace with many more highly correlating features that can be derived from the paper. This in itself is a good indication that anoxia limits the degradation of paper in terms of VOC production.

Top 25 peaks associated with ambient – anoxic atmospheres
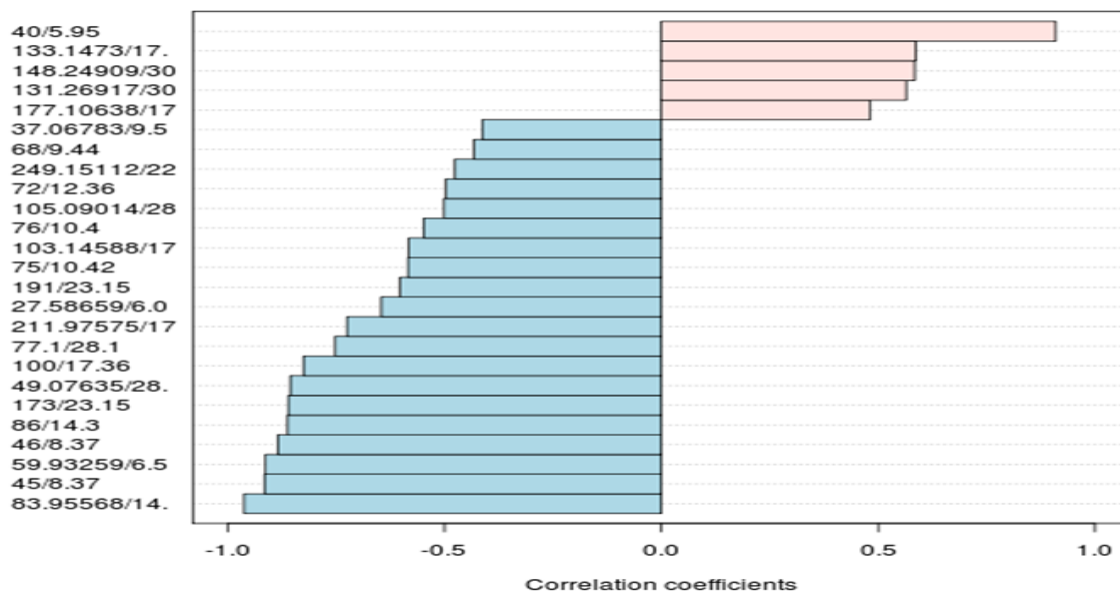
Figure 10 WLR, photodegraded, correlation analysis. The top 25 features correlating to anoxic atmosphere (red bars) and ambient atmosphere (blue bars) are identified with their correlation coefficients.

7.4.1.4.2 Multivariate Analysis

7.4.1.4.2.1 Principal Component Analysis

PCA is perhaps the most common unsupervised dimensional reduction method (453). The primary

assumption of PCA is that there is an underlying linear structure to the data. The goal of PCA is to identify a

set of hypothetical variables, components that account for the variance seen in the set of data objects, and

thereby reduce the dimensionality of the data (383). These new variables are linear combinations of the

original variables. Often PCA is used to simplify multivariate data into two or three variables for visualisation

of clustering. It can also be used to generate hypotheses about the correlation of the most significant

components to the underlying variables.

Figure 11 is a pair-wise score plot of the top five PCs; the green crosses are anoxic samples, and the red

triangles are ambient samples.
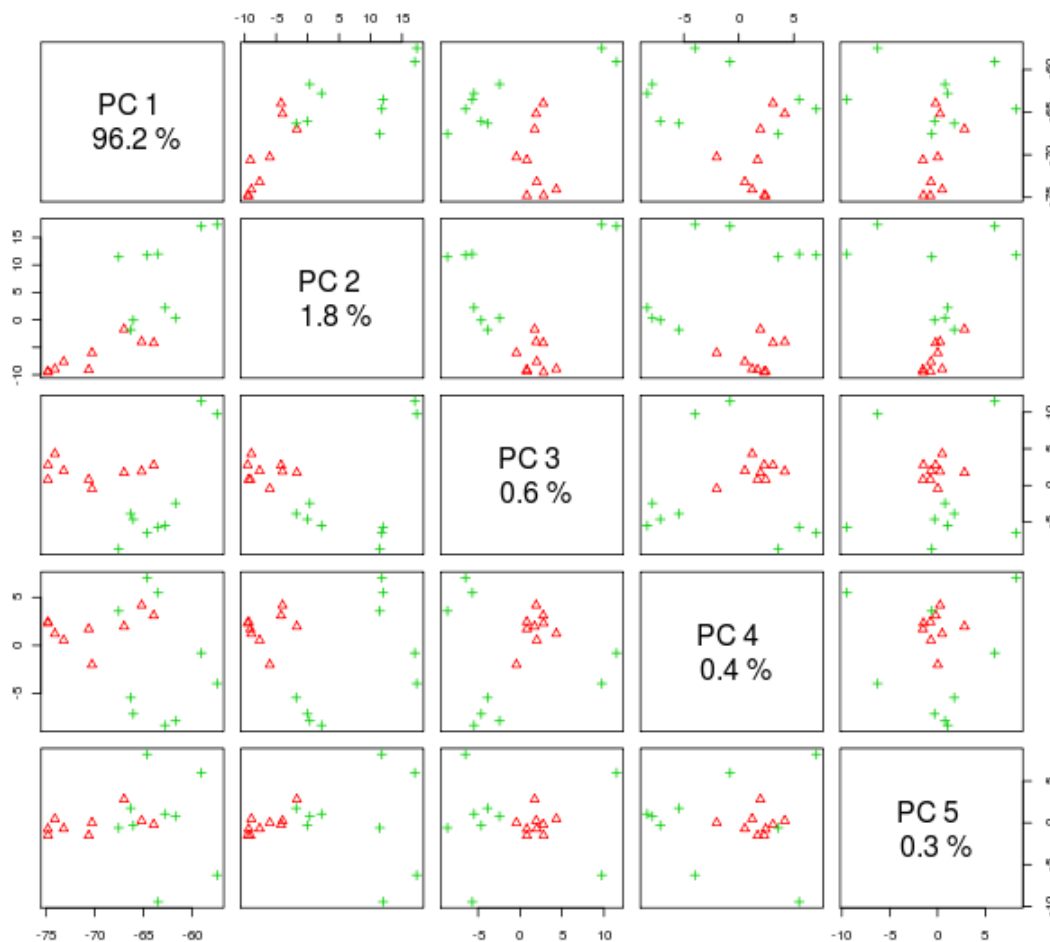
Figure 11 WLR, photodegraded, pair-wise PCA score plot. The red triangles are ambient samples and the green crosses are anoxic samples.

It can be seen that nearly all of the variance can be explained by the first component. If we look at the loading plot, Figure 12, we can see that PC1 essentially represents total volatile organic compounds (TVOC). PC2 can be described as anoxic character (most of the peaks that have positive loading values on PC2 were found to positively correlate with the 40 m/z (argon) feature and those with negative loading values on PC2 were found to anti-correlate with the 40 m/z feature).
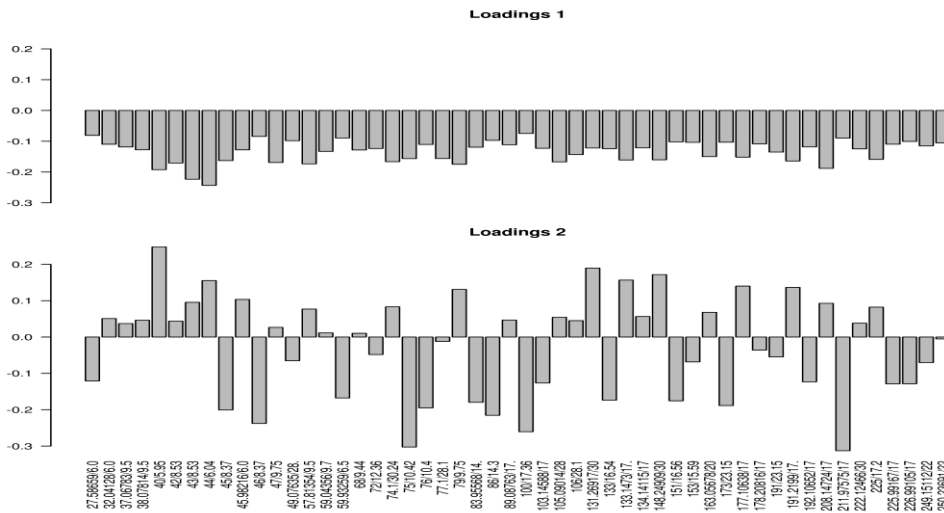
Figure 12 WLR, photodegraded, bar plot of the loading values of the features for PC1 and PC2.

PC1 and PC2 were used to generate a model that can explain 98% of the variance in the sample set, Figure 13.
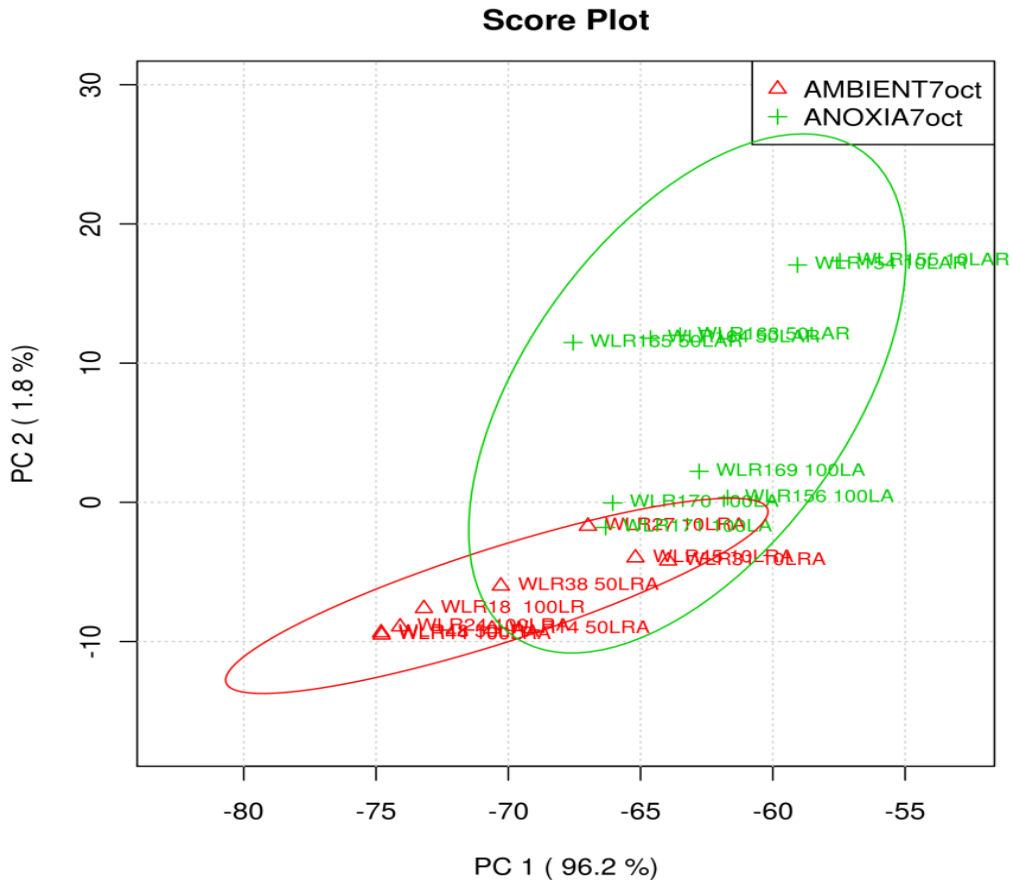
Figure 13 WLR, photodegraded, PC1 and PC2 score plot. The green crosses are anoxic samples, the red triangles are ambient samples, the degradation time is given as part of the name as described above. The ellipsoids are drawn to 95% confidence for identifications of sample outliers (454).

The first observation is that there are two distinct groups defined by the sample class, and within these groups there are clusters formed according to degradation time. Within the anoxic sample set the subgroups are separated on PC2; this indicates that with increasing degradation time more argon leaks from the vials (this leakage is probably due to diffusion across the septa) resulting in a lower PC2 score. In the ambient sample set separation of subgroups is primarily along PC1, indicating that with increasing degradation time, more VOCs are produced. That there is clustering of the 50-day and 100-day samples indicates that some VOCs might be lost due to diffusion across the septa or that we have reached a steady state, possibly due to oxygen depletion within the vials). We can also see that the scores for samples aged in anoxia for 100 days are quite close to the samples that were aged in ambient atmosphere for 10 days. A simple conclusion is that anoxia reduces emission of VOCs 10-fold. However, it must be stressed that this should not be translated into extension to the lifetime of the paper because while certain VOCs can contribute to autocatalytic degradation of paper, the lifetime of paper is dependent upon many other factors, and total VOC (TVOC) emission has not been correlated to DP loss, colour change, etc.; furthermore if VOCs are thought to diffuse across the septa of the ambient aged samples, then the same should be assumed for the anoxic samples. In fact if we consider the PC1 scores alone, we see that the anoxic samples degraded for 50 days and 100 days cluster in a similar fashion as do the ambient samples. If we consider PC2 alone we see that the 50-day samples have nearly the same score as the 10-day samples indicating that much of the argon is still present. These two factors indicate that the 50-days degradation interval is the one that should be used for further experiments to discriminate between ambient and anoxically aged materials. So then is it safe to conclude that anoxia gives a 5-fold benefit in terms of VOC emission? Probably not, but this point definitely deserves further research.

7.4.1.4.2.2 Partial Least Squares-Discriminant Analysis

PLS-DA can be an incredibly powerful tool to model data and identify significant features that can be used to predict sample classification. PLS-DA is a frequently used supervised classification method in metabolomics (383, 448). The aim of PLS-DA is to achieve the maximum separation with the fewest number of components, and better class separation (than for PCA) is achieved through the rotation of the components. The quality of the model is typically evaluated by the Q^2 value, but, however compelling, PLS-DA models can be over fitted, and careful validation by permutation testing to calculate a p-value is necessary (448, 455).

In this application, the generated PLS-DA model was optimised using leave one out cross validation (LOOCV) and the significance of the discrimination by the optimised model was tested using 2000-fold permutation test of separation distance based on the ratio of the between-group-sum-of-the-squares and the within-group-sum-of-the-squares (B/W-ratio) distance measure to calculate the p-value. A p-value less than or equal to 0.05 is considered excellent (176, 448), higher values can be useable if the observed statistic is not part of the distribution based on the permuted class assignments (176, 448, 455).
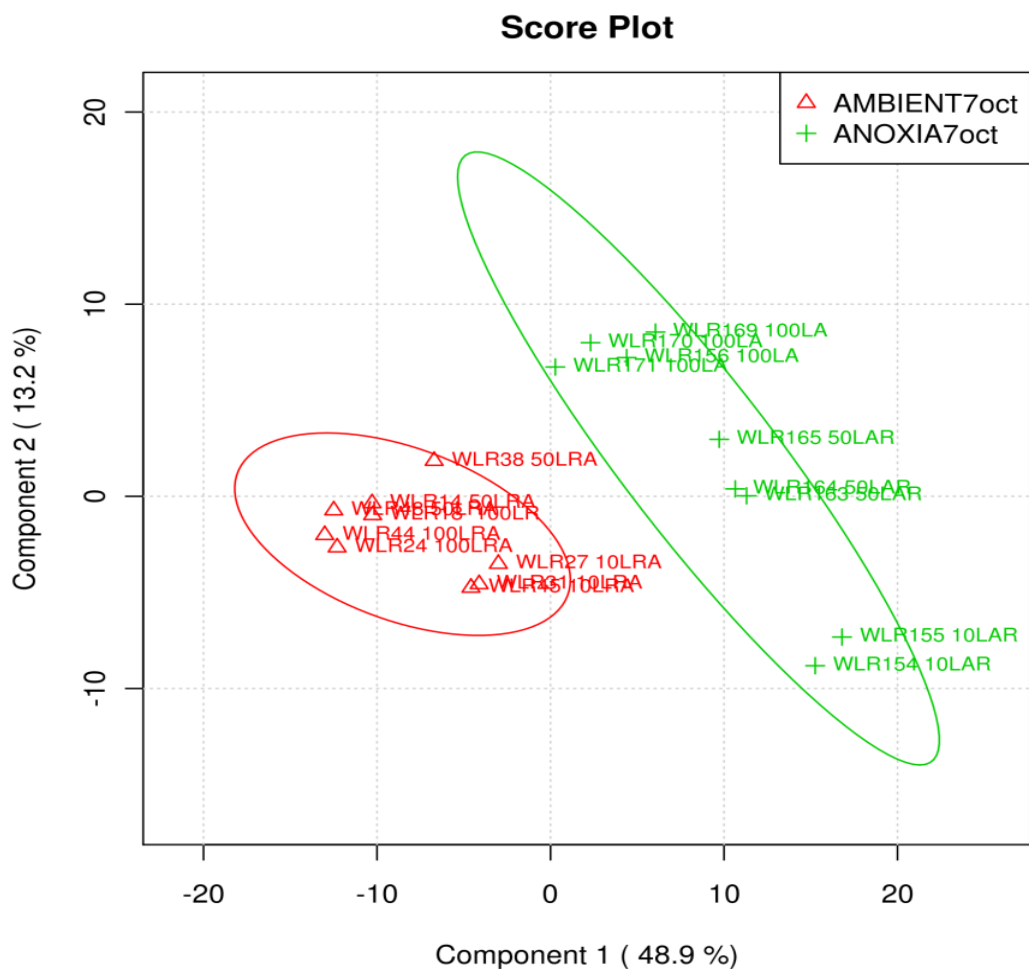
Figure 14 WLR, photodegraded, 2D score plot of the sample set on PC1 and PC2. The green crosses are anoxic samples and the red triangles are ambient samples. The circles are drawn to 95% confidence.

Figure 14 is a score plot of the first 2 PCs explaining 62% of the variability in the data in which good class and sub-group separation is observable. Examination of the loading plots, Figure 15, reveals a more complex situation than in PCA. While the 40 m/z (argon) feature does have a large positive PC1 loading value, there are many other features that have equal or larger negative loading values on PC1. Perhaps PC1 can be described as the anti-correlation between argon and TVOC. That is it accounts for not only the presence of argon at the time of analysis but also the presence of argon during some or all of the degradation duration. The presence of which, despite the slow leakage due to diffusion, should have affected the degradation pathway, and therefore would have lead to the generation of a different headspace profile from a sample that did not initially have a high concentration of argon. PC2 is less easy to explain; considering the score plot, Figure 14, it seems that it could be due to degradation time, but the loading of the features, Figure 15, indicates a more complex explanation is needed.
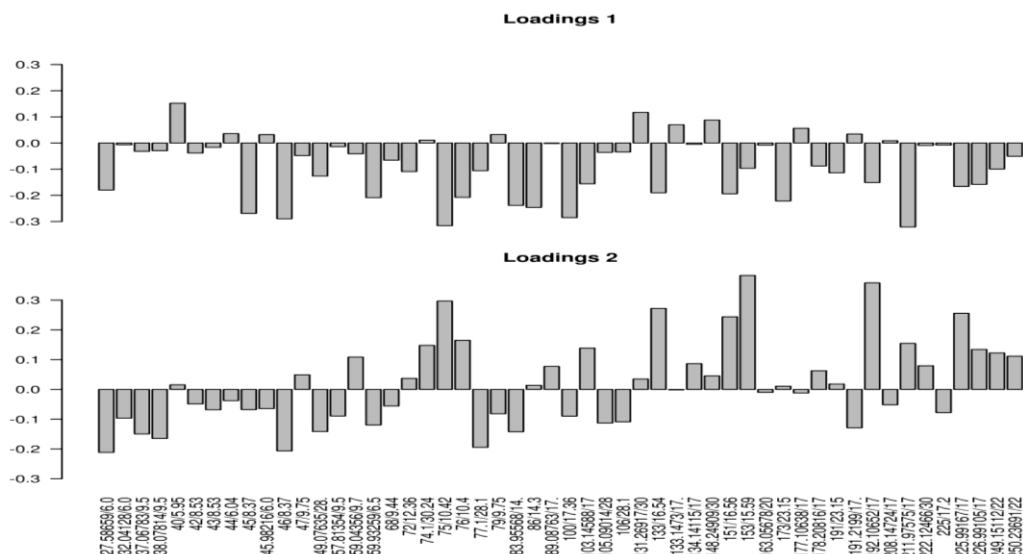
Figure 15 WLR, photodegraded, bar chart of PC1 and PC2 loading values from PLS-DA analysis.

The headspace is composed of the degradation products of sample/vial/septum system. The features that have positive loading values on PC2 tend to coincide with the large peaks in the TICs arising from the septa or column (Figure 2). We know that due to co-elution and how the data was processed, it was not possible to remove all of the non-sample features from the data sets. We know that the anoxically degraded samples have less populated headspaces (as determined by summing the intensities of all of the features) than ambient aged samples; so contributions to the headspace profile from non-sample sources should have greater significance for the anoxic samples than for the ambient samples. I propose that PC2 relates to a combination of the degradation time and the significance of the contribution of features that might arise from the septa. Another possibility could be that the PTFE-lined silicone samples underwent different degradation pathways depending on the atmosphere, and this resulted in a difference in the volatile degradome.
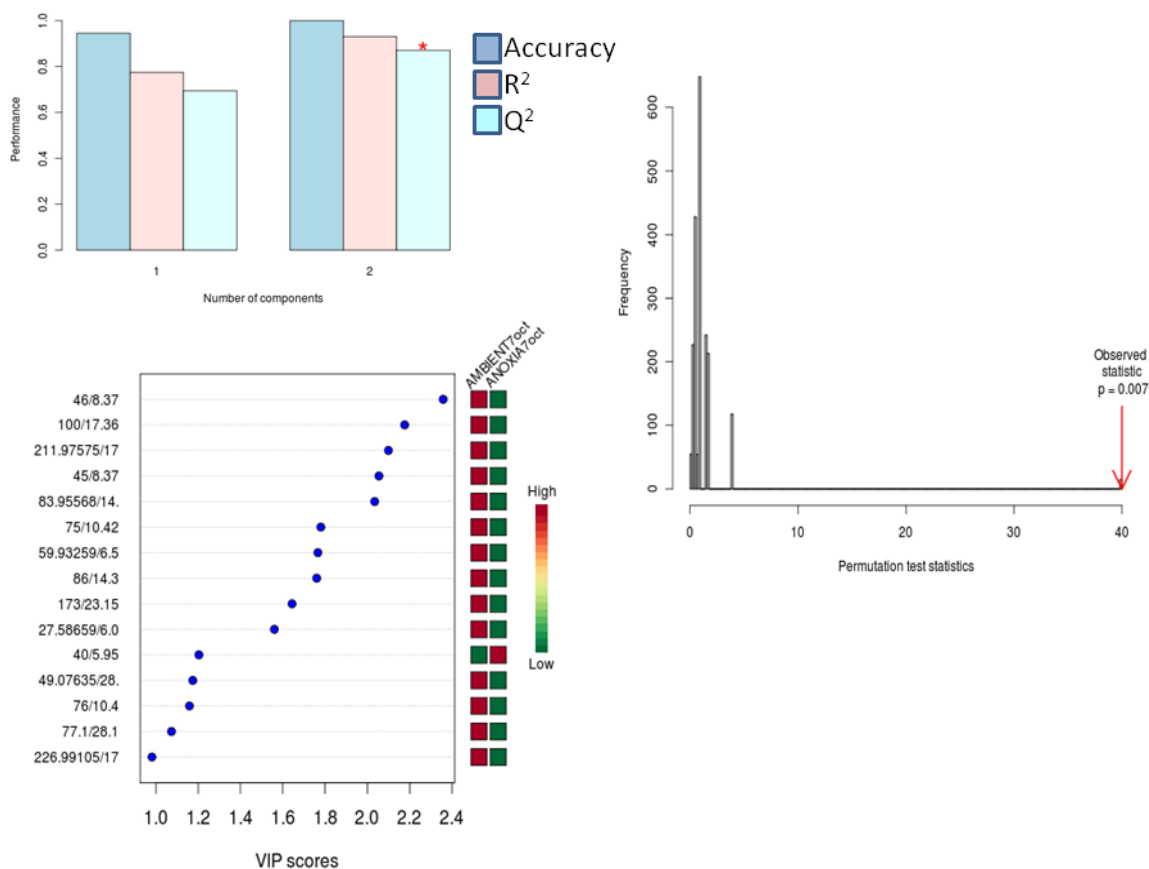
Figure 16 WLR, photodegraded, (clockwise from upper left) PLS-DA model optimization using LOOCV, results from 2000-fold permutation test using the optimized 2-component model determined by LOOCV. The top 15 significant features determined by variable importance in projection (VIP) from the PLS-DA model.

Figure 16 presents the model optimisation and permutation test results. By LOOCV it was found that only two components were necessary to have a prediction accuracy of 1.0 and a Q^2 value of nearly 0.9, which is excellent. The validity of the PLS-DA model was tested by 2000-fold permutation testing based on the optimal number of components as determined by cross-validation. Thus 2000, 2-component models were randomly constructed using the data after re-arranging the class assignment labels. If the labels are exchangeable under the null hypothesis, then the resulting tests yield exact significance levels. If the purpose of the permutation test is to either reject or not reject the null hypothesis, as is the case in this application, then we can sort the recorded differences, and then observe if constructed model is contained within the middle 95% of the permuted models. If it is not, we then we can reject the hypothesis of identical probability curves at the 5% significant level (383, 448, 456, 457). Here we have a calculated p-value of 0.007 indicating that the generated model is valid and can be used to discriminate between classes of samples.

In addition to class assignment, PLS-DA was used to identify significant features in the data set. The variable importance in projection (VIP) measure was used. VIP scores are the weighted sum of squares of PLS loadings which take into account the class predicting power of each feature in each dimension (176, 444). Figure 16 presents a plot of the top 15 VIP features. We can see that argon (40 m/z) with a VIP score of 1.25, does feature in this list, number 11, however, the PLS-DA model focuses on features that have high VIP

179

scores and correlate strongly for the ambient samples, indicating that this model does not rely upon the presence of argon to distinguish an anoxic sample from ambient samples (this would be the case if the 40 m/z feature had the highest VIP score with other features possessing much lower scores). Because discriminatory power of the model relies upon several features with a range of VIP scores then it is generally robust and can tolerate noisy data and even leaking septa to still achieve 100% sample classification.

7.4.1.4.3 Clustering Analysis

7.4.1.4.3.1 Hierarchical Clustering Analysis

Hierarchical clustering analysis (HCA) is an unsupervised method which is particularly useful when the number of sample clusters is not known *a priori*. The goal of HCA is to partition the samples into natural groups. Samples are grouped together on the basis of similarity, and a hierarchal structure of the data is generated using a distance measure and a linkage function. The relationships between samples are often represented by a dendrogram or a dendrogram and a heat map (201). HCA can be agglomerative or divisive; in agglomerative clustering, a bottom-up approach is used where samples are iteratively grouped into clusters, and in divisive clustering, a top-down approach in which the data set is divided is used (383).

Using MetaboAnalyst, agglomerative HCA was applied to the sample set. Several distance measures and linkage functions combinations were evaluated, and a Euclidian distance measure and a Ward linkage function generally produced the best results. Figure 17 presents the dendrogram and heat map from the HCA analysis. The heat map can be used to quickly screen the data set and build hypotheses on how the different features contribute to the classification of the samples. For instance the fourth variable from the left is the 40 m/z feature associated with argon, and samples that should be anoxic but have low intensities at this feature can quickly be identified and possibly removed from the sample set.
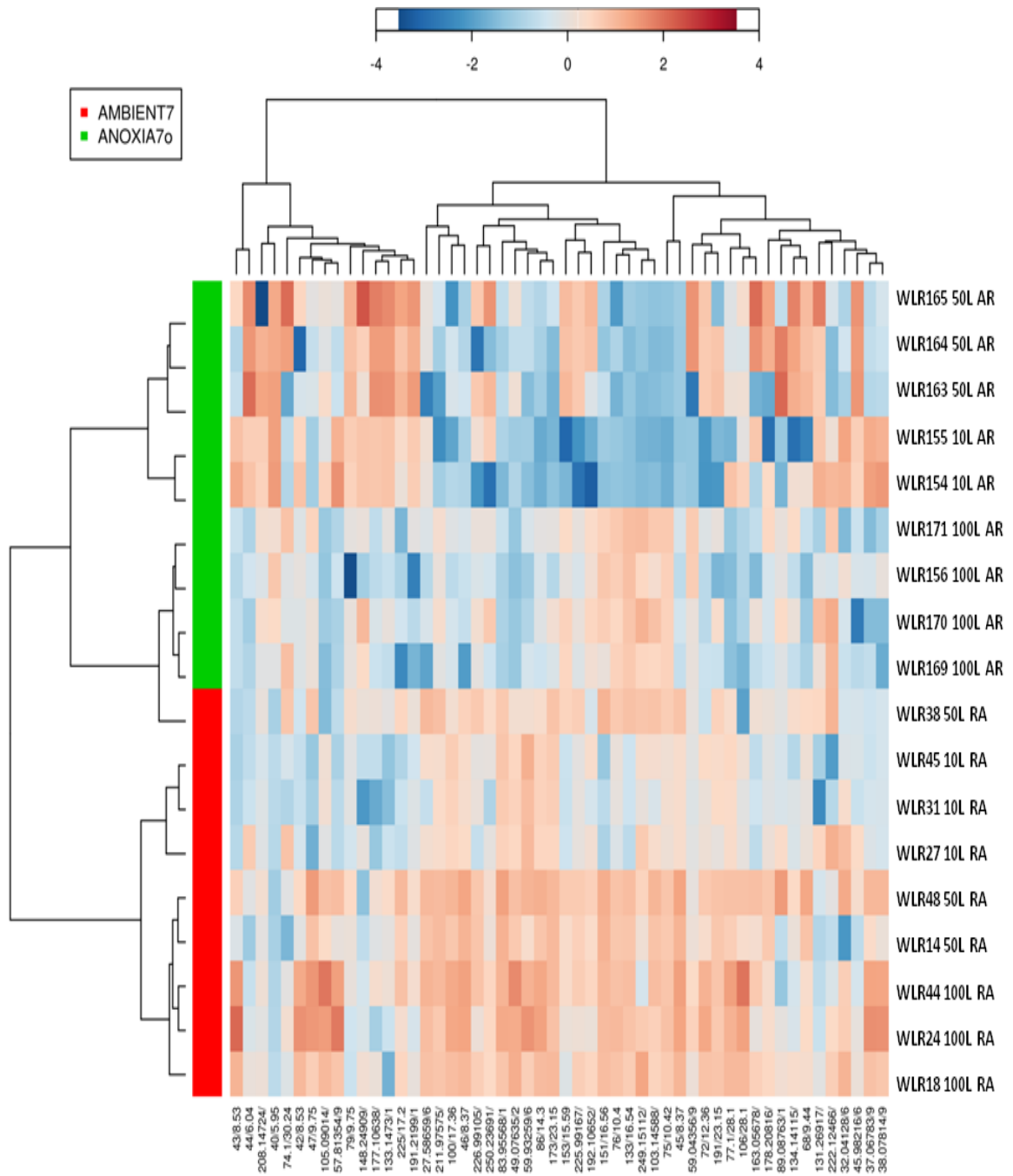
Figure 17 WLR, photodegraded, heat map and dendrogram generated from HCA analysis using Euclidian distance measure and Ward linkage. The red samples were aged in ambient atmosphere the green samples were aged in anoxic atmosphere. The colours in the heat map correspond to how strongly the feature correlates to the sample.

Remarkably, HCA gives near 100% accuracy in classification into ambient and anoxic aged sample groups; this is remarkable given that within each class the samples were aged for vastly different times. It also gives good clustering of the samples within each class into sub groups based on degradation time. The one outlier is WLR38 50L RA which was not included in the ambient branch of the dendrogram, but splits from the anoxic branch at the next juncture indicating that it is still ambient like. It is not clear why this sample is

grouped with the anoxic samples, however, it is also nearly an outlier in the PLS-DA model and was identified as an outlier by RF analysis.

7.4.1.4.3.2 K-Means Nearest Neighbour Clustering

K-means clustering is a supervised non-hierarchical, partitioning clustering method, where the number (k) of clusters is specified by the user. The clustering assignments are initially random, but over a series of iterations a sample is reassigned to a new cluster if its intensity values per feature are closer to the centroid of that cluster, so as to optimise the mean intensities per feature in each cluster (383). K-means clustering has not been widely applied to metabolomics (201), but it is a good method to confirm clustering observed in other models (201).
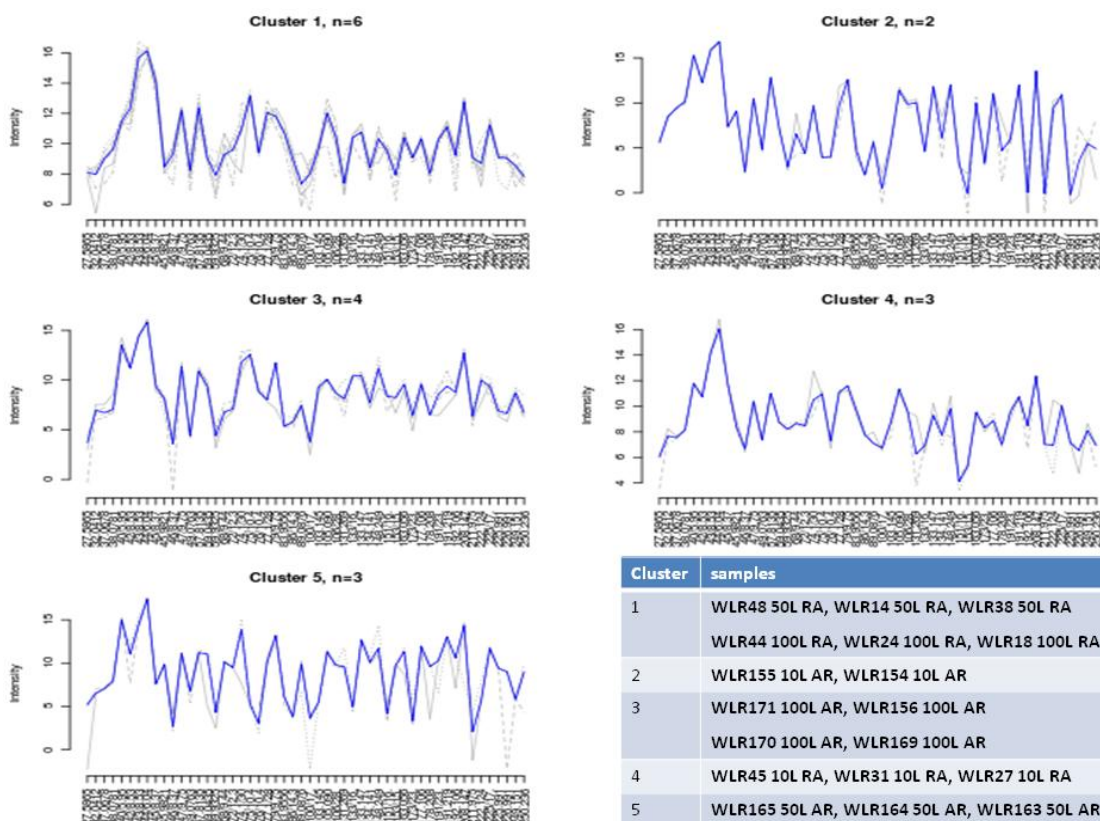
Figure 18 WLR, photodegraded, aggregated expression values from k-means clustering. In the graphs above, the x-axes are variable indices and the y-axes are relative indices. The blue lines represent the median intensities of the corresponding clusters. The cluster populations are given in the table on the lower right. Cluster 1 is composed of the samples degraded in air for 50 and 100 days, while each of the other clusters contain samples of a single atmosphere and degradation interval.

During data analysis, the effect of different numbers of specified clusters (2 - 6 clusters) was explored. A model specifying 2 clusters reliably separates the anoxic and ambient samples, but specifying 3, 4 or 6 clusters results in non-repeatable clustering, this is not surprising because k-means should produce a different clustering with each iteration (383). Based on the PCA and PLS-DA models presented above, it was proposed that there is a good argument for 5 clusters. Figure 18 presents the output from k-means clustering with 5 clusters. When 5 clusters are specified, k-means clustering reliably separates the data as

presented below. The position of a cluster will vary with each iteration, but the grouping of samples is repeatable, indicating that 5, as well as 2, are natural numbers of clusters for the data set.

7.4.1.4.3.3 Self-Organising Maps

Self-organising maps (SOM) analysis is the unsupervised counterpart to k-means clustering. SOM is based on an unsupervised neural network algorithm that can be used to identify trends and patterns in high-dimensional data. Similar to K-means clustering, SOM is based around a grid of interconnected nodes. Each node contains a model which starts with random values. Iterative training refines these models so that each node represents a different subset of the training set. Users need to specify the number of nodes via the x and y dimensions of the grid, the initialisation function (to create the first population of nodes) and the neighbourhood function which helps in sorting the subsets into specific nodes (176, 458).
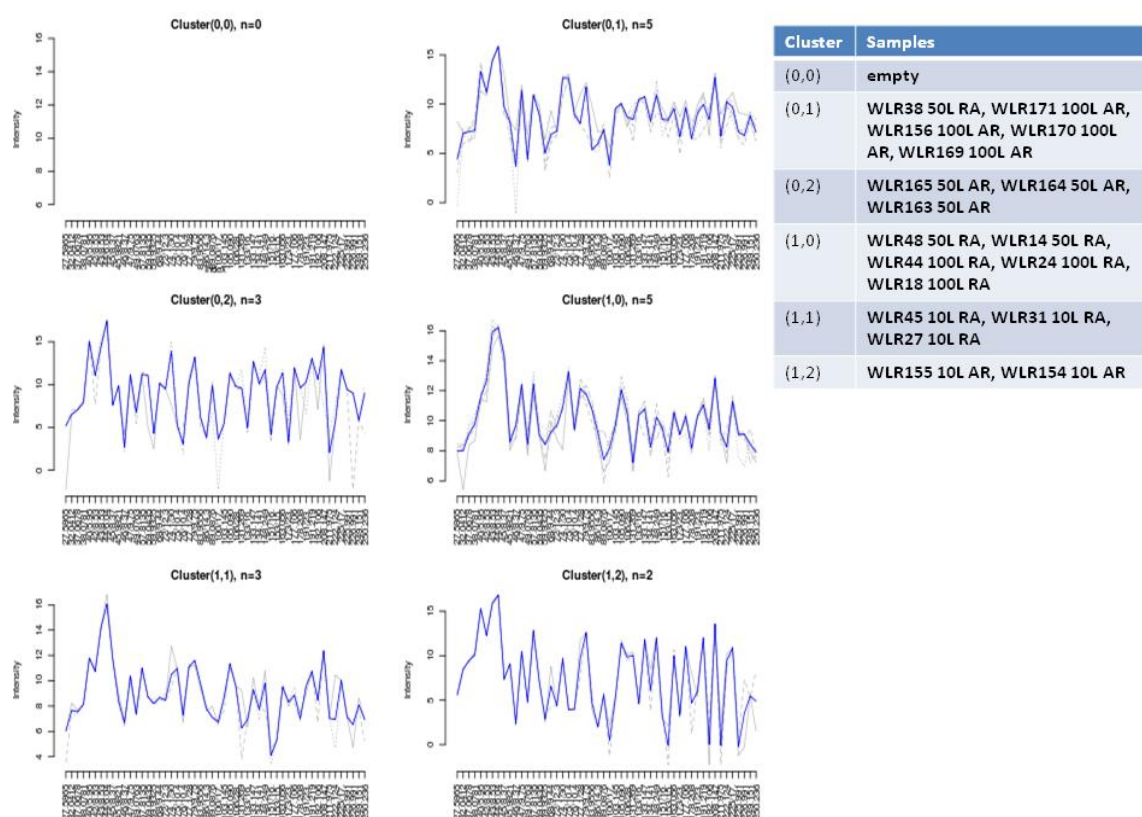
Figure 19 WLR, photodegraded, aggregated expression values from SOM clustering. In the graphs above, the x-axes are variable indices and the y-axes are relative indices. The blue lines represent the median intensities of the corresponding clusters. The cluster populations are given in the table on the upper right.

SOM analysis was iteratively run with different grid sizes, but on nearly every occasion only 5 clusters were formed regardless of the number of available cells, thus supporting the decision to use 5 clusters for k-means analysis and giving further weight to the PLS-DA model. Figure 19 presents the SOM results. A 2 x 3, 6-cell grid with a linear initialisation function and a Gaussian neighbourhood function was specified. The only difference between the SOM and K-means models is that WLR38 50L RA clusters with the 100L AR samples.

This is not entirely surprising given that the same samples cluster in the HCA model and it is bordering on being an outlier according to the PLS-DA model.

7.4.1.4.4 Supervised Learning Algorithms

7.4.1.4.4.1 Random Forest Analysis

RF analysis is a supervised machine learning algorithm that is good for high dimensional and multivariate data analysis. RF uses an ensemble of classification trees, each of which is grown by random feature selection from a bootstrap sample at each branch. Class prediction is based on the majority vote of the ensemble of classification trees.

RF also provides other useful information such as out-of-bag error (OOB), which is a variable importance measure. During tree construction, about one-third of the instances are left out of the bootstrap sample. This out-of-bag (OOB) data is then used as test sample to obtain an unbiased estimate of the classification error (OOB error). Variable importance is evaluated by measuring the increase of the OOB error when it is permuted (176).

Another important feature is outlier detection which is based on the proximity measures. The proximities are calculated by using all of the data, both the training set and the OOB set on a pre-grown classification tree. If the data object falls within the same classification as previous, then its proximity is increased by one. After all of the trees have been run, the proximities are normalised by dividing by the number of trees. Outliers are identified as being data objects within a class that have a low proximity relative to other objects in the same class (176, 201).
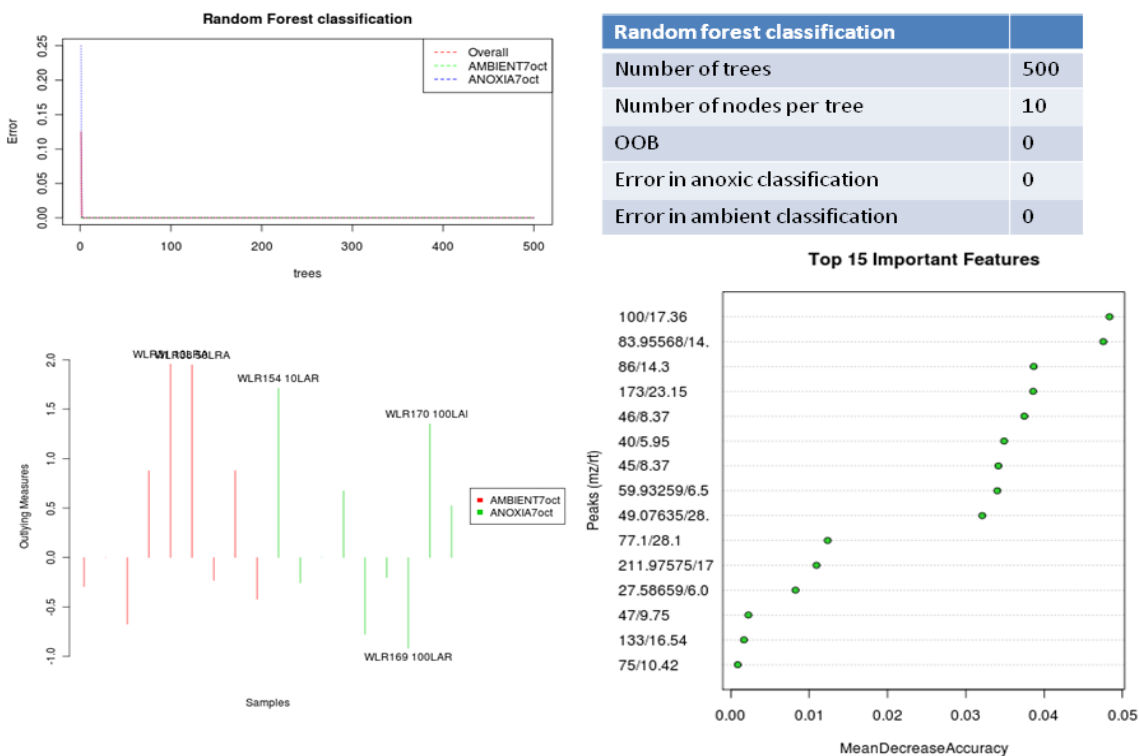
Figure 20 WLR, photodegraded, RF analysis (clockwise from the upper left) graphic representation of the classification error from the RF model, table presenting the details of the RF model including out of bag and classification errors, the top 15 important features identified by the RF model and possible outliers identified by the RF model.

Figure 20 presents the outputs from RF analysis in its final application to the photodegraded WLR samples. With MetaboAnalyst it is possible to specify the number of trees to be grown as well as the number of nodes per tree. It was found that the minimum values of 500 trees with 10 nodes per tree were all that were required to achieve total classification and OOB errors of 0.

The quality of this model is due to the reduced sample set used for its generation. Previous models had used all of the samples, but by iterative model building and exclusion of identified outliers, it was possible to improve the quality of not only the RF model, but of all of the above-described statistical models. In RF analysis the decision to retain or exclude an outlier from the sample set must be made by the user based on the number of outlying measures. In the results in Figure 20, none of the samples should be excluded because they have less than 2 outlying measures. If the decision is made to exclude a sample, then all of the above statistical tests should be repeated and the quality of all of the new models evaluated as a measure to determine whether or not to reinstate the sample.

The important features list identified by RF is very similar to the lists generated by the above models. The features are ranked by the mean decrease in accuracy when they are permuted. The last 3 features have a MDA value of less than 0.01 and therefore can be ignored.

7.4.1.4.5 Comparison of Statistical Methods

Having built several statistical models it is useful to compare them, particularly when related supervised and unsupervised methods were used. The PCA and PLS-DA models are remarkably similar. This is not surprising in that they both rely upon the generation of principal components, but the quality and agreement of the models helps to give confidence when interpreting them. The HCA, K-means and SOM are all in good agreement with unsupervised methods reinforcing the assumptions made in supervised methods. RF also found many of the same variables to be significant.

The significant features identified by each model are presented below in Table 9. We can see that many of the same variables are repeatedly selected by the different methods. If the top 25 variables identified by each model are tabulated, we find that 35 variables are used, and of those 35, 22 are used by at least 3 different models, see Table 10. Otherwise identical, the differences between the two sample populations arise from the atmosphere during degradation. The division into 5 distinct clusters is a result of differences in degradation time. Because the WLR samples do not contain, gelatine size, gum Arabic binding media or pigments, the features identified in the volatile degradome likely arise from the degradation of the paper substrate. If so, then it can be expected that many of them will be retained in more complex sample sets; because they relate to the paper substrate, they should be useable regardless of the applied colourant. Potentially useful if the chemometric methods are forced to select a reduced significant feature set based on features expressed by all samples with different applied colourants. In a profiling experiment these features, and their corresponding peaks in the TICs should be the focus of further analysis, and if possible these features should be connected to compounds and their presence in the headspace explained.

	Fold-change	T-test	Volcano	PLS-DA	RF	SVM
1	46/8.37	83.95568/14.71	83.95568/14.71	46/8.37	100/17.36	211.97575/17.16
2	45/8.37	59.93259/6.54	59.93259/6.54	100/17.36	83.95568/14.71	173/23.15
3	83.95568/14.71	45/8.37	45/8.37	211.97575/17.16	86/14.3	103.14588/17.15
4	100/17.36	46/8.37	46/8.37	45/8.37	173/23.15	75/10.42
5	59.93259/6.54	49.07635/28.09	49.07635/28.09	83.95568/14.71	46/8.37	76/10.4
6	86/14.3	40/5.95	40/5.95	75/10.42	40/5.95	133/16.54
7	211.97575/17.16	86/14.3	86/14.3	59.93259/6.54	45/8.37	249.15112/22.77
8	173/23.15	173/23.15	173/23.15	86/14.3	59.93259/6.54	40/5.95
9	40/5.95	100/17.36	100/17.36	173/23.15	49.07635/28.09	
10	27.58659/6.06	77.1/28.1	77.1/28.1	27.58659/6.06	77.1/28.1	
11	49.07635/28.09	211.97575/17.16	211.97575/17.16	40/5.95	211.97575/17.16	
12	131.26917/30.17	27.58659/6.06	27.58659/6.06	49.07635/28.09	27.58659/6.06	
13	148.24909/30.26	133.1473/17.2	133.1473/17.2	76/10.4	47/9.75	
14	77.1/28.1	148.24909/30.26	148.24909/30.26	77.1/28.1	133/16.54	
15	151/16.56	191/23.15	191/23.15	226.99105/17.2	75/10.42	
16	74.1/30.24	131.26917/30.17	131.26917/30.17	225.99167/17.19		
17	133.1473/17.2	103.14588/17.15	103.14588/17.15	103.14588/17.15		
18	76/10.4	75/10.42	75/10.42	131.26917/30.17		
19	75/10.42	76/10.4	76/10.4	151/16.56		
20	177.10638/17.2	105.09014/28.1	72/12.36	191/23.15		
21	153/15.59	72/12.36	177.10638/17.2	133/16.54		
22	103.14588/17.15	177.10638/17.2		148.24909/30.26		
23	191/23.15			72/12.36		
24	134.14115/17.19			68/9.44		
25	72/12.36			192.10652/17.18		

Table 9 WLR, photodegraded, significant features identified by each of the statistical models. The features are ranked in order of importance.

(m/z)/RT	Frequency	(m/z)/RT	Frequency
173/23.15	8	133.1473/17.2	3
211.97575/17.16	8	133/16.54	3
40/5.95	8	177.10638/17.2	3
100/17.36	7	105.09014/28.1	2
27.58659/6.06	7	151/16.56	2
45/8.37	7	249.15112/22.77	2
46/8.37	7	68/9.44	2
49.07635/28.09	7	106/28.1	1
59.93259/6.54	7	134.14115/17.19	1
75/10.42	7	153/15.59	1
77.1/28.1	7	192.10652/17.18	1
83.95568/14.71	7	225.99167/17.19	1
86/14.3	7	226.99105/17.2	1
103.14588/17.15	6	37.06783/9.56	1
76/10.4	6	47/9.75	1
191/23.15	5	74.1/30.24	1
72/12.36	5		
131.26917/30.17	4		
148.24909/30.26	4		

Table 10 WLR, photodegraded, significant features selected by the statistical models. Features are ranked by the numbers of times they were selected by a statistical model as being a significant feature.

7.4.2 GSR, Ambient vs. Anoxia Comparison

7.4.2.1 XCMS Processing

After WLR, the GSR samples are the next simplest sample subset. The TICs from the GSR samples are much more populated than those of the WLR samples with three times as many detected peaks in each TIC. The data was treated in XCMS identically as the WLR samples.

The aligned data was then explored with MDS, and significant grouping and sub-grouping of the samples, even without further treatment, is discernible in Figure 21. The MDS analysis, which uses all of the features identified in the TICs, suggests that there are 4 or 5 sub-groups: 10 DL RA, 50 DL RA and 100 DL RA, 10 DL Ar, 50 DL Ar, and 100 DL Ar.
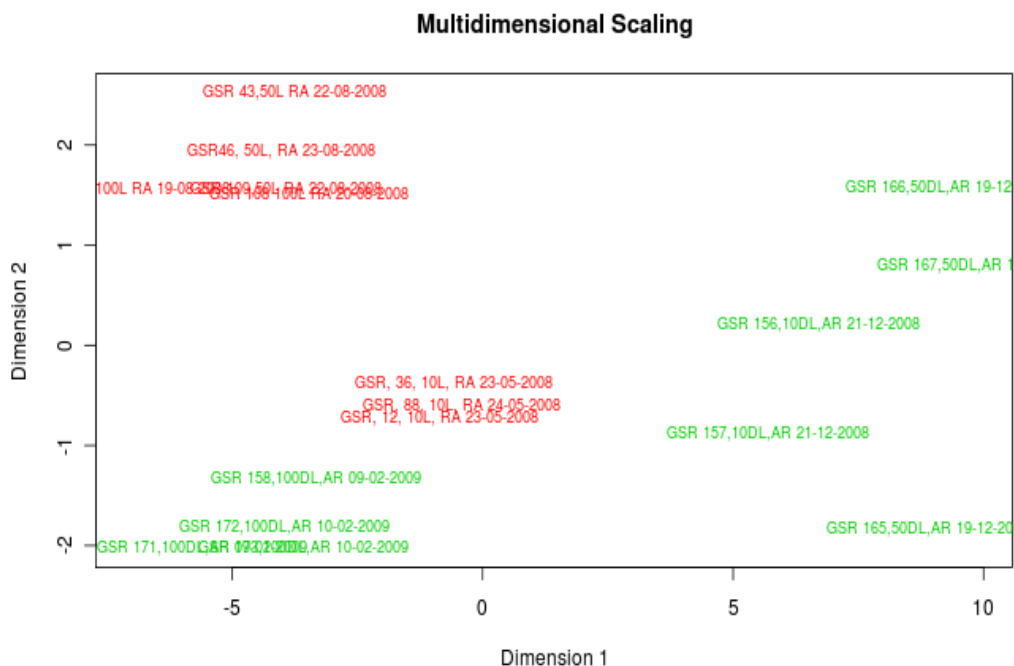
Figure 21 GSR, photodegraded, plot from MDS analysis. The grouping and sub-grouping of the samples is easily discernible, indicating that there is pattern in the data.

7.4.2.2 Data Processing and Analysis with MetaboAnalyst

After the data was treated by XCMS, it was extracted and imported into MetaboAnalyst for further treatment and statistical analysis. Figure 22 presents the results from column-wise normalisation by Pareto scaling. This method was found to give better results in minimising the effect of large peaks in the TICs and gave better separation in clusters during statistical analysis (376).
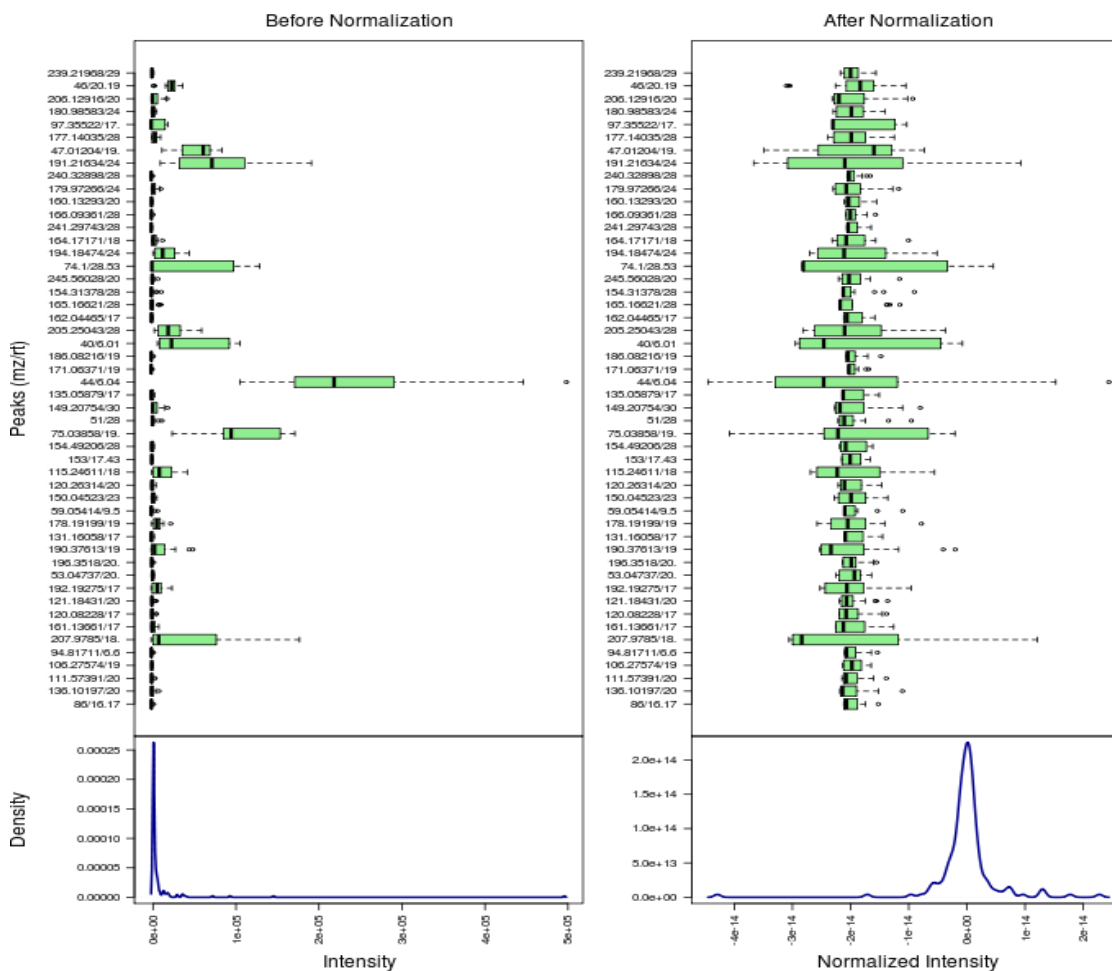
Figure 22 GSR. photodegraded, Comparison of data before (left) and after (right) Pareto scaling column-wise normalisation.

The normalised data was then iteratively subjected to statistical analysis, and outlying samples and noise generating variables were pruned from the data set using the same criteria and methods as for the WLR samples. The detailed results from PCA, PLS-DA and HCA will be presented below, but the results from the other analyses will be condensed into tables.

Table 11 presents the top 25 significant features identified by all the applied statistical methods. Table 12 orders the same features by the number of times they were identified by the different statistical methods.

Fold change	T-test	Volcano	PLS-DA	RF	SVM
97.35522/17.15	86/16.17	86/16.17	73.2/24.23	40/6.01	249.49417/20.07
97.26157/17.34	94.81711/6.65	94.81711/6.65	45.1/20.19	94.81711/6.65	192.19275/17.24
59.05414/9.56	40/6.01	40/6.01	249.49417/20.07	59.05414/9.56	191.21634/24.16
74.1/28.53	97.35522/17.15	97.35522/17.15	40/6.01	86/16.17	179.10892/28.51
179.10892/28.51	249.49417/20.07	249.49417/20.07	207.9785/18.6	49.07557/19.23	163.08506/18.6
154.31378/28.5	163.08506/18.6	163.08506/18.6	74.1/28.53	244.5/20.2	133.20784/28.26
58.08074/18.76	49.07557/19.23	49.07557/19.23	59.18667/24.23	68/9.44	117.19206/20.14
165.16621/28.53	75.15683/19.91	75.15683/19.91	44/6.04	75.15683/19.91	115.24611/18.76
86/16.17	58.08074/18.76	58.08074/18.76	75.15683/19.91	154.49206/28.31	103.22064/20.19
94.81711/6.65	73.2/24.23	154.49206/28.31	103.22064/20.19	60/11.04	97.26157/17.34
136.10197/20.13	154.49206/28.31	103.22064/20.19	133.20784/28.26	79/9.74	96.29564/17.18
207.9785/18.6	103.22064/20.19	102.14063/20.02	163.08506/18.6	53.04737/20.01	75.15683/19.91

40/6.01	102.14063/20.02	74.1/28.53	96.29564/17.18	150.04523/23.99	74.1/28.53
131.16058/17.12	74.1/28.53	61.04361/28.25	177.05489/18.57	97.26157/17.34	73.2/24.23
206.04781/28.28	61.04361/28.25	179.10892/28.51	43/20.18	135.05879/17.17	61.04361/28.25
225.37586/28.3	179.10892/28.51	97.26157/17.34	97.26157/17.34	212.9898/17.23	58.08074/18.76
177.85915/20.08	59.18667/24.23	167.08507/20.08	191.21634/24.16	59.18667/24.23	44/6.04
244.5/20.2	97.26157/17.34	206.04781/28.28	97.35522/17.15	61.04361/28.25	43/20.18
82.21926/17.16	46/20.19	59.05414/9.56	179.10892/28.51	206.04781/28.28	40/6.01
206.12916/20.16	167.08507/20.08	96.29564/17.18	61.04361/28.25	118.19679/19.95	221.3/30.17
96.29564/17.18	206.04781/28.28	207.9785/18.6	115.24611/18.76	208.2/17.19	177.05489/18.57
154.49206/28.31	59.05414/9.56	136.10197/20.13	46/20.19	211.99727/17.19	45.1/20.19
238.44518/28.28	96.29564/17.18	77.1/28.07	194.18474/24.18	177.14035/28.39	177.14035/28.39
221.91938/28.31	207.9785/18.6	177.14035/28.39	73.1/28.32	136.10197/20.13	89.15547/20.05
222.93514/30.19	136.10197/20.13	165.16621/28.53	47.01204/19.95	89.15547/20.05	47.01204/19.95

Table 11 GSR, photodegraded, significant features identified by statistical analysis. Features are identified by (m/z)/RT, and they are listed in descending order of importance for each method.

Feature [(m/z)/RT]	Frequency		Feature [(m/z)/RT]	Frequency
97.26157/17.34	8		77.1/28.07	2
40/6.01	8		47.01204/19.95	2
96.29564/17.18	7		44/6.04	2
75.15683/19.91	7		43/20.18	2
74.1/28.53	7		244.5/20.2	2
61.04361/28.25	7		191.21634/24.16	2
179.10892/28.51	7		167.08507/20.08	2
97.35522/17.15	6		165.16621/28.53	2
94.81711/6.65	6		82.21926/17.16	1
86/16.17	6		79/9.74	1
58.08074/18.76	6		73.1/28.32	1
249.49417/20.07	6		68/9.44	1
207.9785/18.6	6		60/11.04	1
177.14035/28.39	6		53.04737/20.01	1
163.08506/18.6	6		238.44518/28.28	1
103.22064/20.19	6		225.37586/28.3	1
73.2/24.23	5		222.93514/30.19	1
59.18667/24.23	5		221.91938/28.31	1
206.04781/28.28	5		221.3/30.17	1
136.10197/20.13	5		212.9898/17.23	1
59.05414/9.56	4		211.99727/17.19	1
46/20.19	4		208.2/17.19	1
45.1/20.19	4		194.18474/24.18	1
177.05489/18.57	4		192.19275/17.24	1
154.49206/28.31	4		154.31378/28.5	1
133.20784/28.26	4		150.04523/23.99	1
115.24611/18.76	4		135.05879/17.17	1
102.14063/20.02	4		131.16058/17.12	1
49.07557/19.23	3		118.19679/19.95	1
89.15547/20.05	2		117.19206/20.14	1

Table 12 GSR, photodegraded. Significant features and the number of occurrences.

The statistical methods identified many more significant features in the GSR photodegraded samples than in the WLR; though interestingly many of the same features occur in both sample types. These two observations are not surprising in that the GSR samples contain gelatine which can undergo photo-oxidative degradation to produce VOCs (303, 379, 380, 459-462), and the primary constituent of the sample is paper in either case, so both a more populated and diverse headspace and a certain overlap in VOC samples are expected. Another point is that the GSR samples produced many more high-m/z features than the WLR samples. These high-m/z compounds, which were not present in the otherwise identical WLR paper, probably originate from the gelatine, were often selected as being significant and dominated the models. Furthermore the compounds giving rise to these features often co-eluted with compounds previously

190

identified as arising from the septa or the column. Therefore, the decision was made to set an upper limit of 250 m/z for inclusion in the statistical models. This decision does not exclude compounds giving rise to those features (remember that with electron impact ionisation MS there is significant fragmentation leading to lower m/z features), but by forcing the models to focus on lower m/z features the lighter VOCs become more significant.

7.4.2.2.1 PCA Analysis

Figure 23 presents a pair-wise overview of the first 5 PCs generated by PCA. By eliminating the high m/z compounds and using Pareto scaling, the quality of the PCA plot was significantly improved, so that two PCs were required to explain 77% of the variability and with three PCs 84% can be explained.
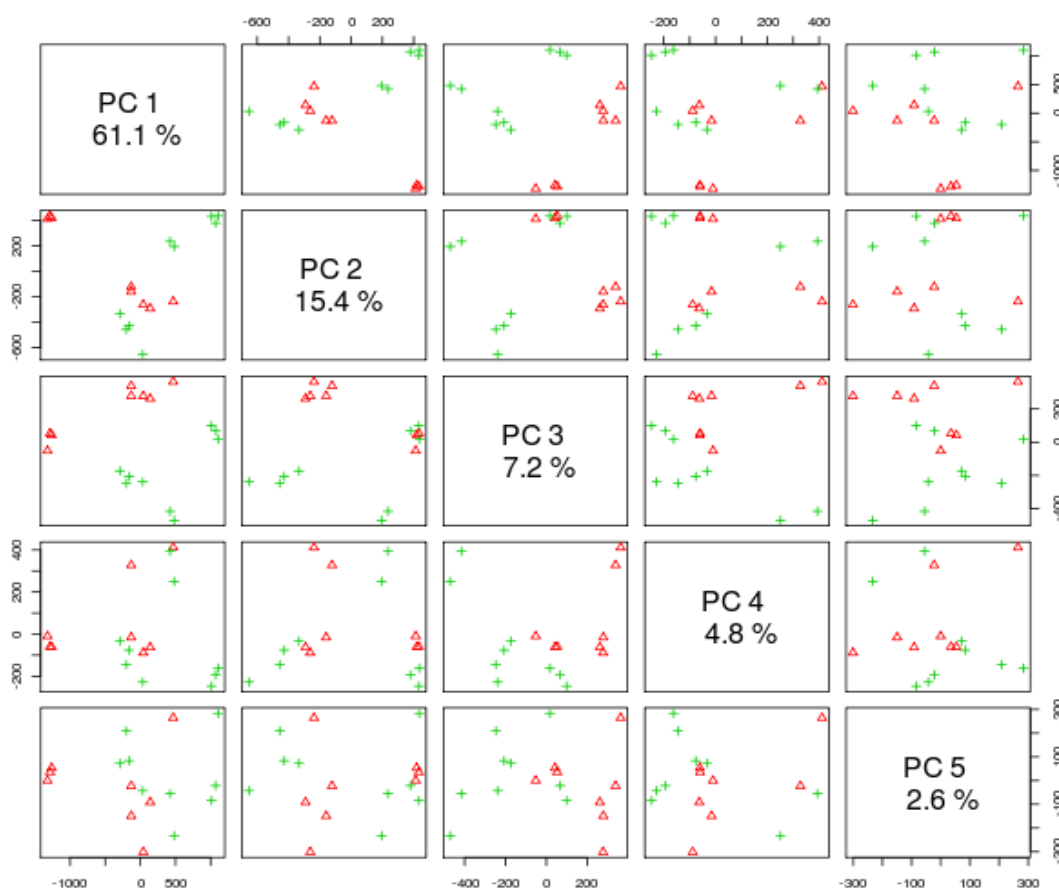
Figure 23 GSR, photodegraded, pair-wise PCA score plot.

Figure 24 presents the 2D and 3D score plots for the first 3 PCs. Good grouping and sub-grouping of the samples is apparent in the 2D model. The loading plots are more difficult to interpret than those for the WLR samples. Figure 25 is a score plot of PC1 and PC2. We can see that many of the same features dominate PC1 and PC2. PC1 has positive correlations to many features but is dominated by a 73 m/z feature at 24.25 min RT and 45 m/z and 43 m/z features at 20.2 min RT. These features correspond to the fragmentation of

191

carboxyl acids (462), and based on the higher m/z features at the same RT, to the degradation of amino acids, possibly proline. PC2 has some of the same features anti-correlating strongly. The 40 m/z feature has a strong anti-correlation on PC3 and neither correlates nor anti-correlates strongly to PC1 and PC2.
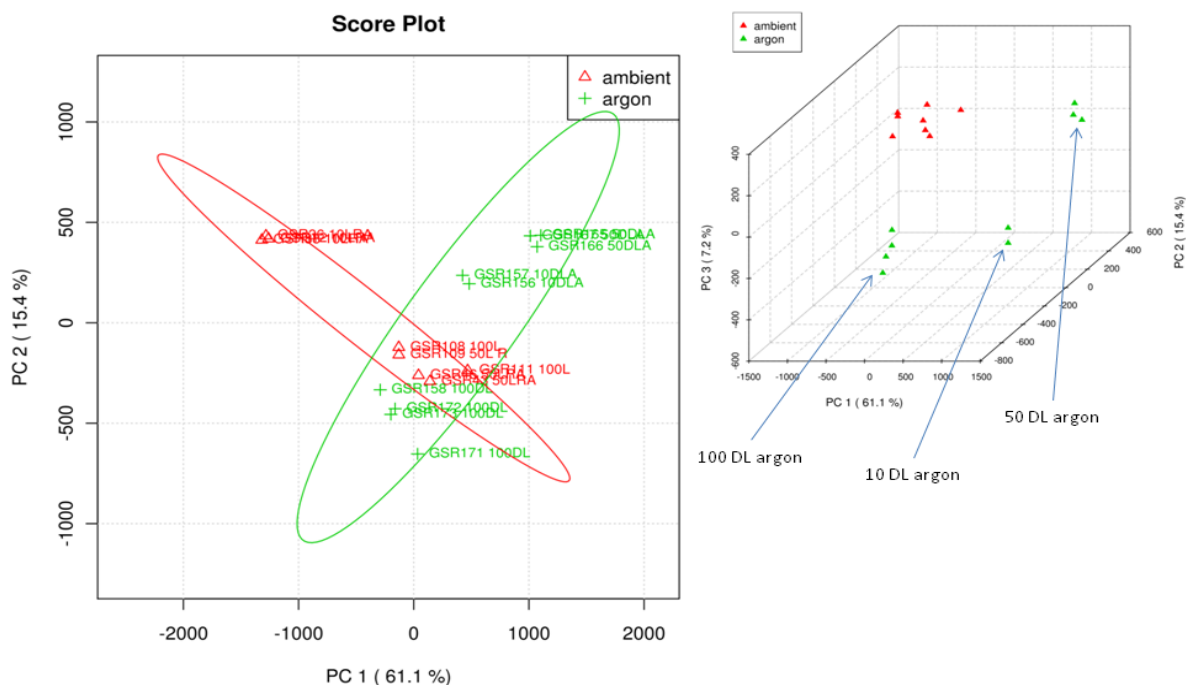
Figure 24 GSR, photodegraded, PCA (on the left) 2D score plot on PC1 and PC2. The green crosses are anoxic samples, the red triangles are ambient samples, the degradation time is given as part of the name as described above. The circles are drawn to 95% confidence. 3D score plot on PC1, PC2 and PC3 (on the right). The green crosses are anoxic samples, the red triangles are ambient samples.

Therefore the observed separation in the 2D score plot on PC1 and PC2,Figure 24 (left) does not arise from the presence or absence of argon in the vial at time of sampling, but rather to the distribution of VOCs in the headspace. In the 3D plot, Figure 24 (right) excellent sub-grouping of the anoxic samples is evident. With respect to the clustering, as noted with the WLR samples the samples degraded for 50 days and 100 days in ambient conditions tend to cluster together, while the samples degraded in anoxia have a wider spread. That the 50 and 100 day ambient samples cluster together could be indicative of oxygen consumption after ca. 50 days leading to a slowing of oxidative processes and resulting in the 100 day ambient samples being more similar to the 50 day ambient samples. Likewise the separation, particularly on PC3 in the anoxic samples could be due to the slow diffusion of argon from the vials. Again if argon can diffuse from the vials, it is likely that light VOCs can also diffuse across the septa. If so then this would explain why the 100 day argon and 100 day ambient samples cluster together.
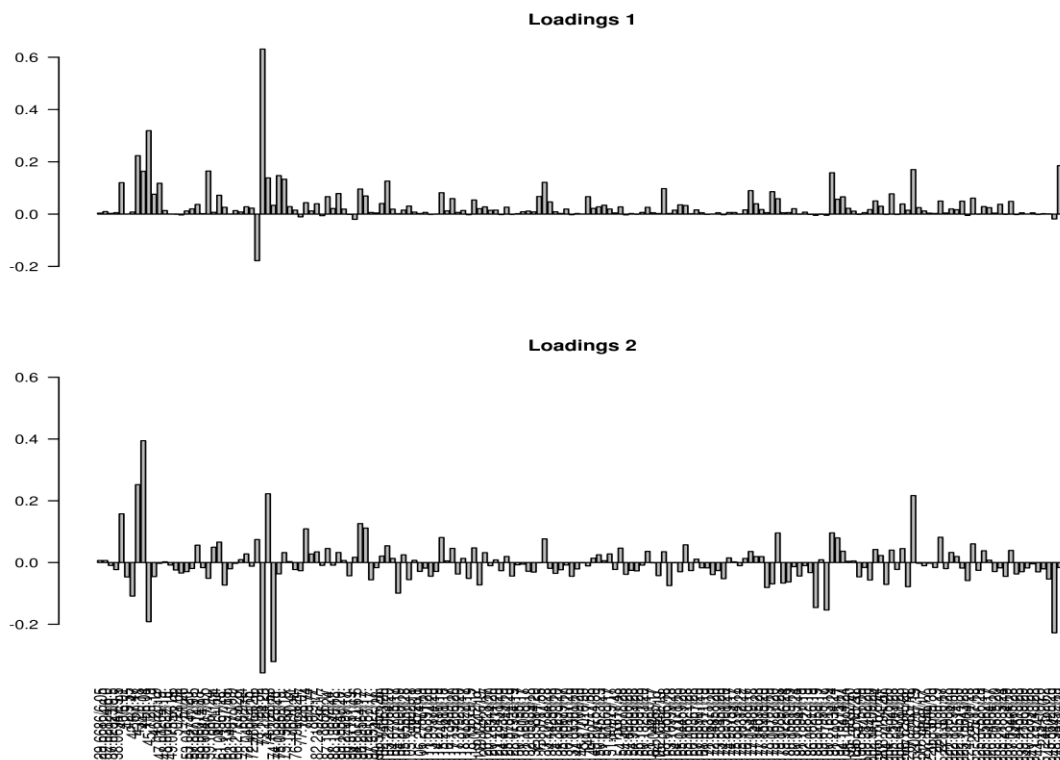
Figure 25 GSR, photodegraded, PCA bar plot of the feature loadings onto the first two PCs.

7.4.2.2.2 PLS-DA Analysis

The PLS-DA model built for the GSR photodegraded samples was optimised to two components using LOOCV to yield a Q^2 value of 0.81 and the significance of the separation distance tested using 2000 permutations generating a p-value of 0.0075 indicating that the model is statistically significant. Figure 26 is a score plot on the first 2 PCs. A clear separation between sample classes and degradation sub-groups is visible. PLS-DA identified significant features using VIP analysis, see Table 11 above. As with PCA these features tend to occur at retention times 6, 17, 18, 20, 24, 28 min.

At this point in time it is unclear as to why the 10-day anoxic and 100-day anoxic samples are clustering close to each other. The distance between the 10-day ambient and the other ambient aged samples is also difficult to interpret. Slightly better sub-group separation is achieved when a third PC is applied, but if a third PC is introduced to the optimised model the p-value becomes 0.1, which indicates a poorer quality model. This is a sign that many of the features can be used to generate an apparently good model, but one that results in a type-I (false positive) error. It is likely that including samples from 10, 50 and 100 days erodes the quality of the model by providing too many correlating features. Deconvolution prior to alignment might have generated better quality data, and it should be used in the future for samples with complex volatile degradomes.
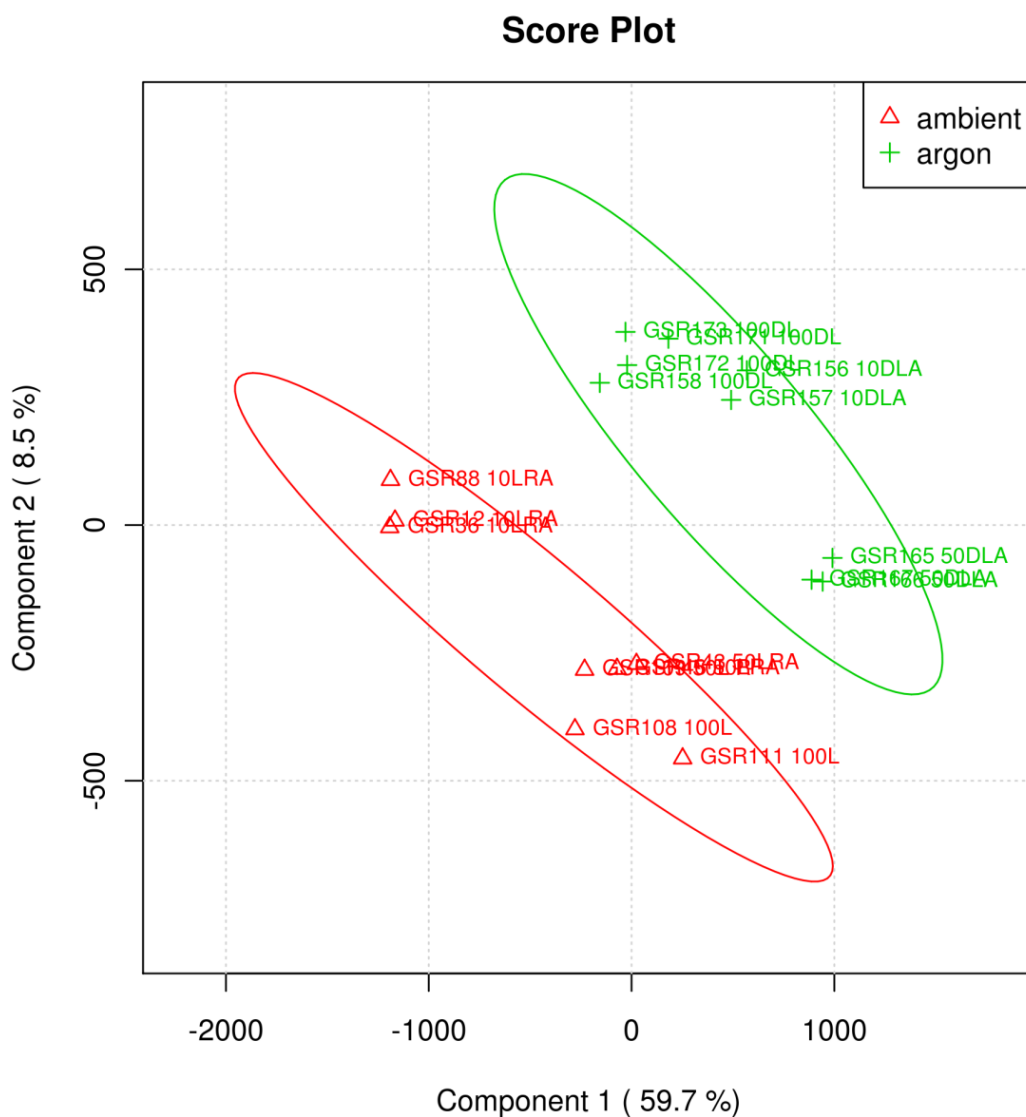
Score Plot

Figure 26 GSR, photodegraded. PLSDA 2D score plot of the sample set, the green crosses are anoxic samples and the red triangles are ambient samples. The circles are drawn to 95% confidence.

7.4.2.2.3 HCA Analysis

HCA analysis was conducted using Euclidian distance measure and Ward linkage. Figure 27 is a dendrogram from the HCA analysis with a heat map of the correlation values for all of the features in the TICs.

We can immediately see that something is odd for the samples aged for 10 days in the ambient atmosphere. They anti-correlate to almost every feature, except for a low correlation to 44 m/z at 6 min RT; moderate correlations to 60 m/z at 11 min RT, 86 m/z at 16 min RT; and high correlations to 94.8 at 6.5 min RT and 73 m/z at 28.3 min RT. I will attempt to explain this in light of what is known about the samples below.

The 44 m/z feature at 6 min RT is due to CO_2, and could be attributed to the background from air, but since we know that CO_2 can also be produced by reaction of acids with the alkali reserve in the paper then we can

advance a hypothesis that the 44 m/z feature is due to CO_2 generated by the neutralisation of acids formed during oxidation of the paper or from the autoxidation of aldehydes.
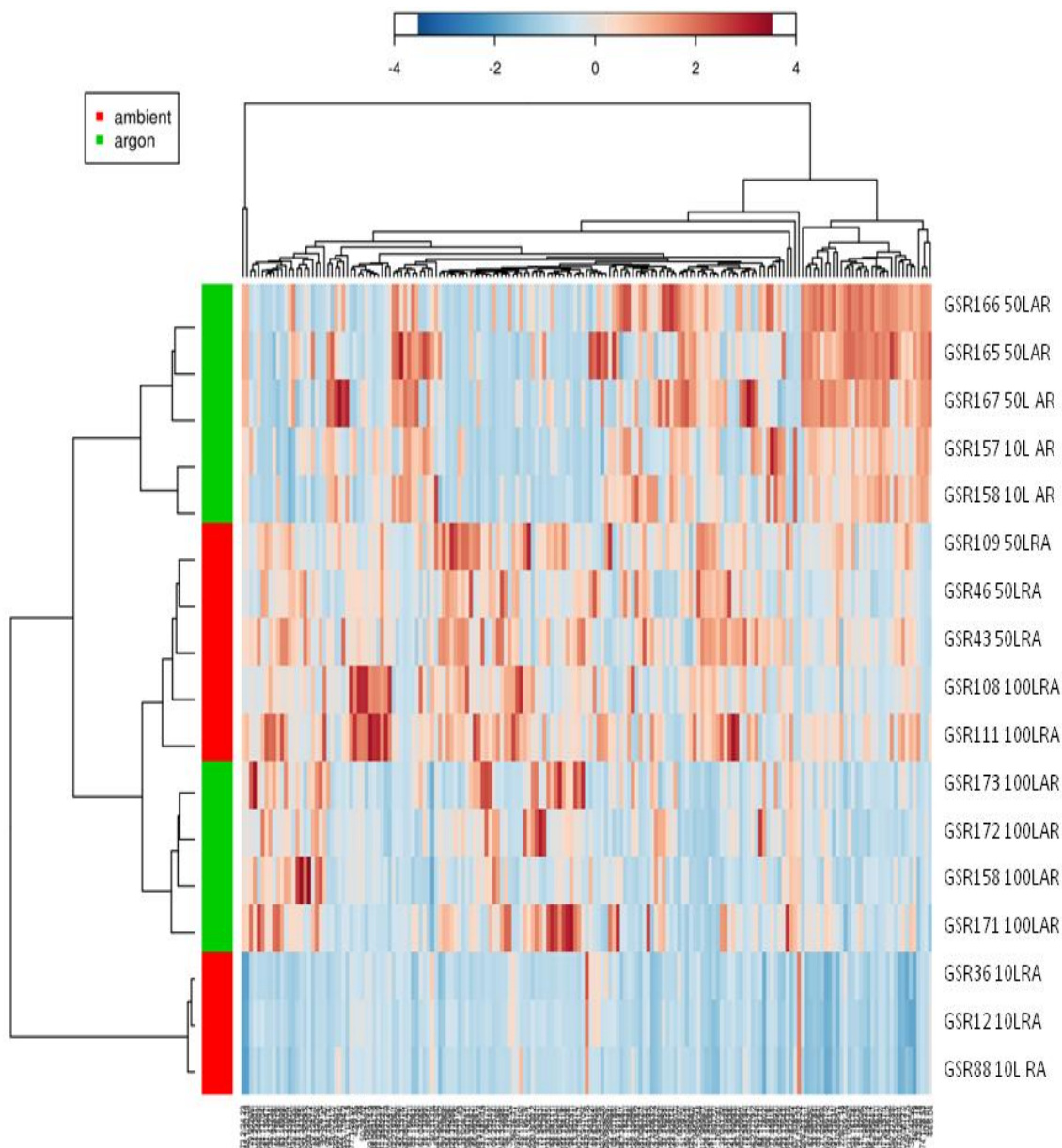
Figure 27 GSR, photodegraded, heat map and dendrogram generated from HCA analysis using Euclidian distance measure and Ward linkage. The red samples were aged in ambient atmosphere, the green samples were aged in anoxic atmosphere. The colours in the heat map correspond to how strongly the feature correlates to the sample.

Thus a low correlation for the samples photodegraded for 10 days ambient atmosphere could be expected, and a higher correlation should be seen for samples with longer degradation times. Indeed this is the case, except only for samples aged in anoxia, and not for those aged in room atmosphere, and then only for the samples degraded for 50 days. Because if one examines the 100-day photodegraded anoxic samples it is apparent that both the 44 m/z and 40 m/z features at 6 min corresponding to CO_2 and Ar, respectively, have low correlation values, indicating a low population. This helps explain why the groups in the 2D PCA score

195

plot, Figure 24 above, cross. During degradation the Ar, and presumably other gases, such as CO_2 and light VOCs, escaped by diffusion across the septa or by slow leak at the septa-vial junction resulting in a more 'ambient-like' final headspace profile.

If we assume that the vials were sealed well[29], then the leakage should be due to diffusion. If by diffusion, then it would have been relatively slow[30] and so we can assume a period of 'anoxia' followed by an extended period of hypoxia ending with an argon concentration slightly above ambient levels (ascertained by comparing peak intensities) and an unknown oxygen concentration. Hypoxia has been shown to limit yellowing of paper (an oxidation reaction) (463), so even though the argon diffused out from the vials, there was still an unknown degree of protection by anoxia/hypoxia resulting in a changed volatile degradome for the samples photodegraded for 100 days in anoxia, and thus these were clustered separately from the ambient samples by HCA, but also by K-means clustering, and why PLS-DA and RF always identified them as being members of the anoxic class.

So what of the other differences? In general we see that the ambient aged samples have many more highly correlating peaks than the anoxic samples. This indicates that there are many more significant compounds in the volatile degradome. If we look at the heat map the upper right hand corner is a hotspot of high correlations for the 10 and 50 day anoxic samples. Aside from the 40 m/z and 44 m/z features, which have already been discussed, many of these features correspond to the peaks that co-eluted with the septa-related peaks. From the heat map we can see that they correlate higher with the 50 day samples than with the 10 day samples indicating that their concentrations increase with a longer degradation interval and thus are unlikely to arise from the septa (the intensities of the septa-related features at the same RT that were pruned from the data set were relatively constant with respect to degradation time). If we then look at the feature correlation dendrogram we see that many of these features (aside from the 40 m/z and 44 m/z) show low differentiation and correlate with each other, possibly indicating a common source. These features are not significant for the WLR samples and therefore it is likely that they derive from the gelatine, either the amino acids or associated lipids. That they are not significant for the ambient samples indicates that these features are unique for the samples photodegraded in anoxia. Examining the deconvoluted TICs it is likely that these features relate to the photodegradation of lipids and amino acids in the gelatine (276, 303, 379-381, 460, 464). But why do not the same features correlate strongly for the 100 day anoxic samples? Simply they are not in concentrations that are significantly different from the 50 and 100 day ambient samples, but why is this? Two possibilities, either they leaked from the sample as proposed above, or perhaps, over the course of the degradation interval, they reacted with other VOCs or was oxidised by

---

[29] These samples were the second batch of samples photodegraded for 100 days, and with experience I became better at sealing crimp caps, so this assumption is plausible.

[30] Again this is plausible because both PTFE and silicone are permeable to oxygen, and probably Ar and CO_2 as well, though Chromacol was not able to provide data on this. However, they did advise that using headspace vials as degradation vessels exceeded normal use and thus they could not guarantee their septa.

reaction with oxygen that might have leaked into the vials. It is likely a combination of both factors: based on the 40 m/z feature, undoubtedly some gases were able to leak form the vials but the headspace around the sample is also a dynamic system with VOCs evolving and being consumed by degradation reactions. If oxygen is present, as is the case for the ambient samples and seems likely for the 100 day anoxic samples, then it can lead to the oxidation VOCs from collagen and materials derived thereof (303, 461).

Returning to the initial question, why do the correlation matrices of 10 day ambient samples look odd? Generally, the lack of correlation and the large distance in the MDS and HCA as well as the groupings in PCA and PLS-DA makes me suspicious of the samples. Since few features have high correlation values, it seems that the simplest hypothesis is that something went wrong during the data collection stage, either in the headspace extraction or with the MS. Either option is possible because on several occasions a fault with the mass flow controller on the HT3 would stop the vial purging process, but not always stop the triggering of the GC. The other possibility is that the MS, which developed several faults during the research period, faulted so that it was no longer detecting but not able to trigger a fault with the GC and HT3 and thus stop the extraction and loading of the volatile degradome. Because an automated method was used for overnight and over the weekend runs, these faults were often not detected until after the entire sample set had been completed. This resulted in the loss of many samples. After each automated sequence, the TICs of all of the samples were visually examined and compared to the blank samples, any TICs that appeared odd based on what was known about the samples were noted and examined in detail. It could be that the 10 day ambient samples, which were not expected to significantly degrade and thus produce VOCs, slipped through this screening process.

7.4.2.2.4 K-means, SOM and RF

These three methods help to inform the above analyses and hypotheses. Non-hierarchal clustering of the data was explored using k-means clustering. Unlike the WLR samples, if 2 clusters were forced on the data, the samples photodegraded for 10 days in the ambient atmosphere formed a single cluster, while all the other samples were in a second. This indicates that these samples are more different from all of the other samples than the anoxic samples from the ambient samples. This is supported by the HCA which places them on a branch apart from all other samples, and is further evidence that something went wrong during data acquisition. If 5 clusters are specified then the samples photodegraded for 50 and 100 days in the ambient atmosphere are grouped together and with the rest of the samples from groups based on their atmosphere and degradation time. If 4 clusters are specified then the samples photodegraded for 100 days in anoxia cluster together with the samples photodegraded for 50 and 100 days in the ambient atmosphere, while the other degradation periods each have their own clusters. If 6 clusters are specified, the grouping is much the same as with 5 clusters, but with a non-repeatable single sample in a lone cluster, indicating that this is an un-natural number of clusters for the data set.

SOM repeatedly identifies 4 clusters (the samples photodegraded for 100 days in anoxia cluster together with the samples photodegraded for 50 and 100 days in the ambient atmosphere, while the other degradation periods each have their own clusters), regardless of the number of available cells. This indicates that there are 4 natural clusters in the data. Though it must be noted that the median values of the intensities for the cluster with all of the samples photodegraded for 50 and 100 days in the ambient atmosphere and samples photodegraded for 100 days in anoxia is not as good a fit, thus indicating that there is still large variability within each cluster.

Because the samples photodegraded for 50 and 100 days in the ambient atmosphere and those for 100 days in anoxia cluster together in both k-means and SOM clustering, a hypothesis that light degradation in head space vials for longer than 50 days is not recommendable, is supportable. First because of the diffusion problem hypothesised above, but also because of oxygen depletion. If photo-oxidation is occurring in the ambient samples, then oxygen must be consumed at some point. If the rate of consumption is greater than the rate of diffusion of oxygen across the septa, then oxygen depletion is a real possibility, however, while examination of the TICs for an oxygen related feature (m/z =32 with a RT value near 6 min), does identify a possible candidate, there is no correlation with degradation time and the intensity values are too noisy to interpret.

As with the WLR sample set, RF proved to be invaluable in identifying outliers and pruning them from the sample set to improve the quality of the other statistical analyses. To achieve this, RF analyses were repeatedly conducted and the sample with the greatest outlier value removed from the set. The final result was the 17-sample set used for the above analyses[31]. Considering this final reduced sample set it was possible to achieve 100% accuracy in sample classification with an OOB error of 0 using a forest of 500 trees of 15 nodes.

7.4.3 Samples with Applied Watercolour Paints

After demonstrating the successful application of principles of degradomics for WLR and GSR photodegraded samples, it is time to examine the samples with watercolour paints. A set of samples with 12 different watercolour paints on GSR, see Table 1 above, as well as blank WLR and GSR samples, in two different atmospheres was constructed to determine if non-targeted degradic footprinting could be used to answer the following questions:

- Discriminate between samples with and without paint,

---

[31] The six anoxic GSR samples degraded for 10 and 50 days with identification numbers less than 100 were pruned beucase they has been sealed at the same time as the 100 day samples,and allowed to remain in a drawer until placed in the ageing chamber. This resulted in an unknown amount of argon leaking from the vials before the degradation experiments were started. This was corrected for by repeating the degradation experiments with newly filled and sealed samples.

- Discriminate between samples containing the same pigment with and without photo-initiating extenders,
- Discriminate between samples containing unrelated organic pigments,
- Discriminate between samples containing madder lake pigments with essentially the same chromophores but different preparation conditions or different amounts of associated transition metals,
- Discriminate between samples of modern and historic pigments within the same pigment type,
- Above all of this, whether the effect of atmosphere during degradation could be distinguished for each pigment type and for painted samples in general, and from this construct hypotheses as to how anoxic display affects the degradation of watercolour drawings.

The samples were degraded for varying periods of time, and the data was generated as described above. XCMS was used to process each pigment type separately. The strategy of TIC alignment and RT correction using peak groups worked well for each pigment except TTB13. For TTB13 it was necessary to either use Obiwarp RT correction algorithms or to turn off RT correction in XCMS analysis.

Regardless of the method of RT correction, the EICs and MDS plots generated by XCMS were useful for evaluating the quality of the data; revealing that despite the fact that many of the anoxic samples had lost most of their argon,[32] there was still good separation between samples classes visible in the MDS plots indicating that there were indeed differences in the volatile degradomes between samples aged in different atmospheres for different durations. Figure 28 is typical of the MDS plots from the samples with applied watercolour paints.

---

[32] For half of the samples with pigments screw cap headspace vials were used on recommendation of the Chromacol representative. These vials, while easier to seal, did not provide as tight a seal as the crimp cap vials. In every case, the same type of vial was used for a given sample type, thus allowing for intra-sample group comparison.

Multidimensional Scaling
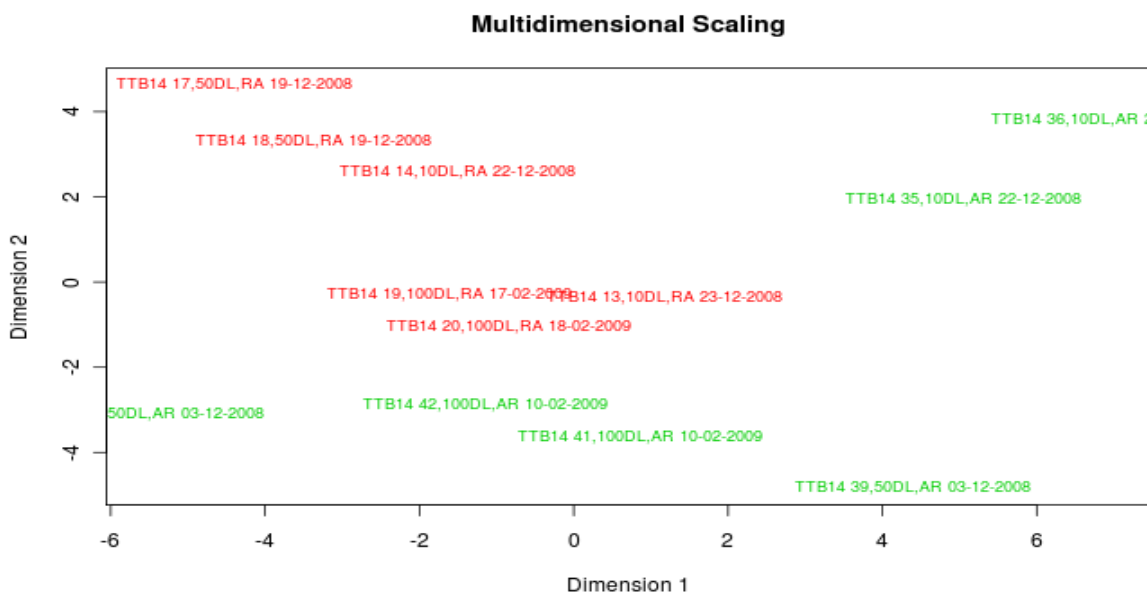
Figure 28 TTB14, photodegraded, MDS plot following XCMS analysis. The samples labelled in red were aged in ambient atmosphere and the samples labelled in green were aged in anoxic atmosphere.

In Figure 28 we can see a clear, relatively close group of the samples photodegraded in ambient atmosphere and a more dispersed group of the samples degraded in anoxia. Similar results were observed for all pigmented samples sets, indicating that it is possible to discriminate between atmosphere subgroups within a specific pigment sample set, therefore it is possible to distinguish the effect of anoxia on the degradation pathways of all samples regardless of applied colourant, and importantly this could potentially be used to build a method for evaluating the degradation of a watercolour drawing in an anoxic frame.

7.4.3.1 XCMS Processing

Initially I attempted an inclusive approach using all of the degradation times for all of the samples, however it proved impossible to align the TICs with either peak groups or Obiwarp algorithms. It is likely that there are too great differences between the TICs to allow for alignment. We can see that within the TTB14 sample set, the degradation time subgroup with the greatest MDS distance between atmosphere subgroups is the sample degraded for 50 days, Figure 28. This was the case for all of the sample sets, as demonstrated above for WLR and GSR. The sub-set degraded for 50 days was selected as the best candidate for discriminating both between atmosphere sub-groups and pigment sample sets and it was possible to align the TICs using the Obiwarp algorithm in XCMS. Figures 29 and 30 present the overlaid TICs before and after alignment respectively.
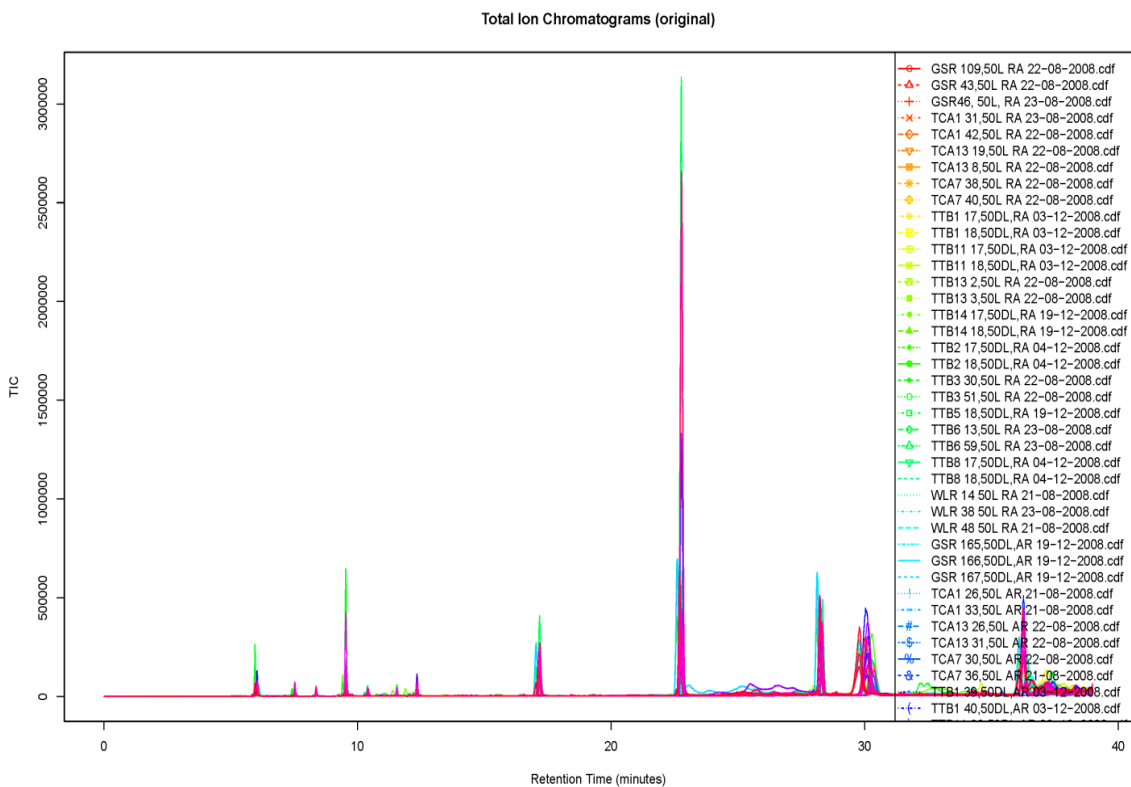
Figure 29 Samples with watercolour paints, 50 days photodegradation, overlaid TICs without retention time correction.
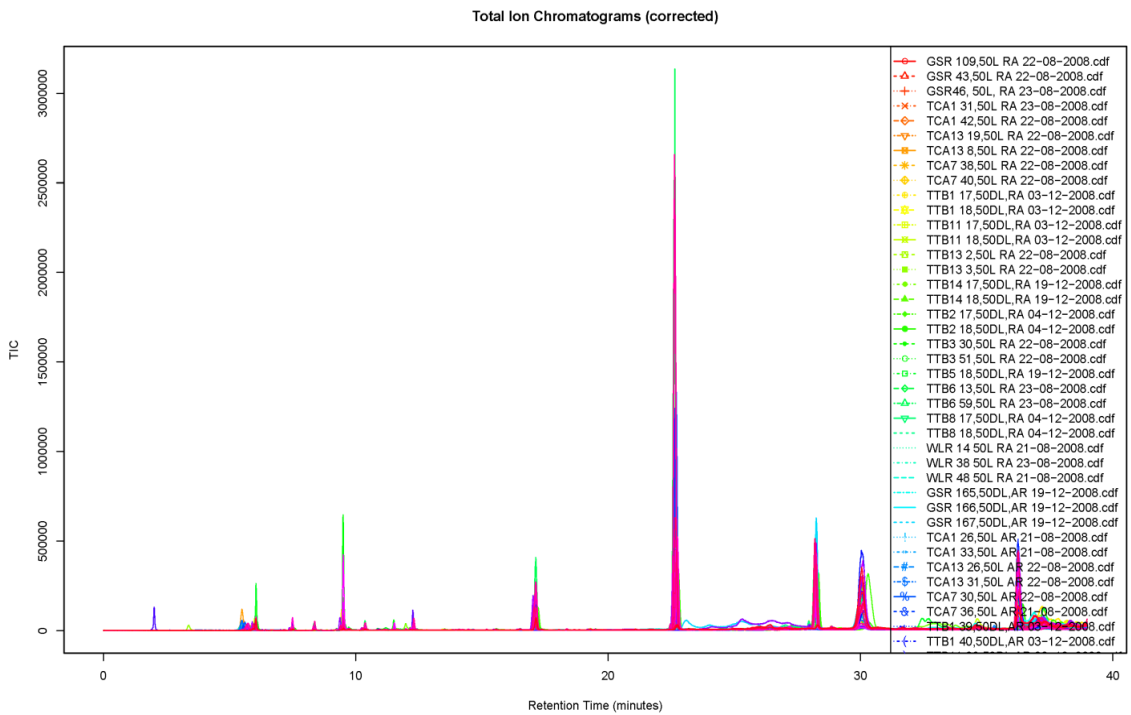
Figure 30 Samples with watercolour paints, 50 days photodegradation, overlaid TICs with retention time correction using Obiwarp.

While Obiwarp improves the alignment above 15 min RT, it introduces new errors in the sub-10-min RT interval, this is visible in Figure 30 as less overlap of peaks. Why this occurs is not clear, but it is could due to a need to optimise the Obiwarp parameters. Optimisation of these parameters is time consuming, and potentially without benefit, because Obiwarp performs less well on very dissimilar samples. Furthermore, the RT deviation was not significant in the sub-30-min RT interval, Figure 29, and it was decided to use no retention time correction in XCMS, while maintaining all other XCMS parameters, and to complete the alignment using a linear correction method in MetaboAnalyst (446). Linear RT correction is less resource intensive, and if there are no significant RT deviations, then linear RT correction often performs as well as Obiwarp (446).

7.4.3.2 MetaboAnalyst Processing and Statistical Analysis

The peak intensity table from XCMS was imported into MetaboAnalyst and the TIC alignment tuned using linear correction (5 s RT window and 0.5 m/z window). Zero value correction and data filtering was performed as for WLR and GSR, and then features with RT >30 min or m/z >250 were removed from the data set. The resulting reduced data set was then subjected to different column-wise normalisation methods to optimise the statistical analyses (376, 465); auto-scaling was found to perform best with regard to PCA and PLS-DA analyses, while the results from the clustering, significant feature detection and classification remained much the same regardless of whether Pareto-scaling or auto-scaling was used (376). Figure 31 presents a plot of the feature intensity distribution before and after auto-scaling, which was the selected data pre-treatment method because it optimised the PCA and PLS-DA methods.
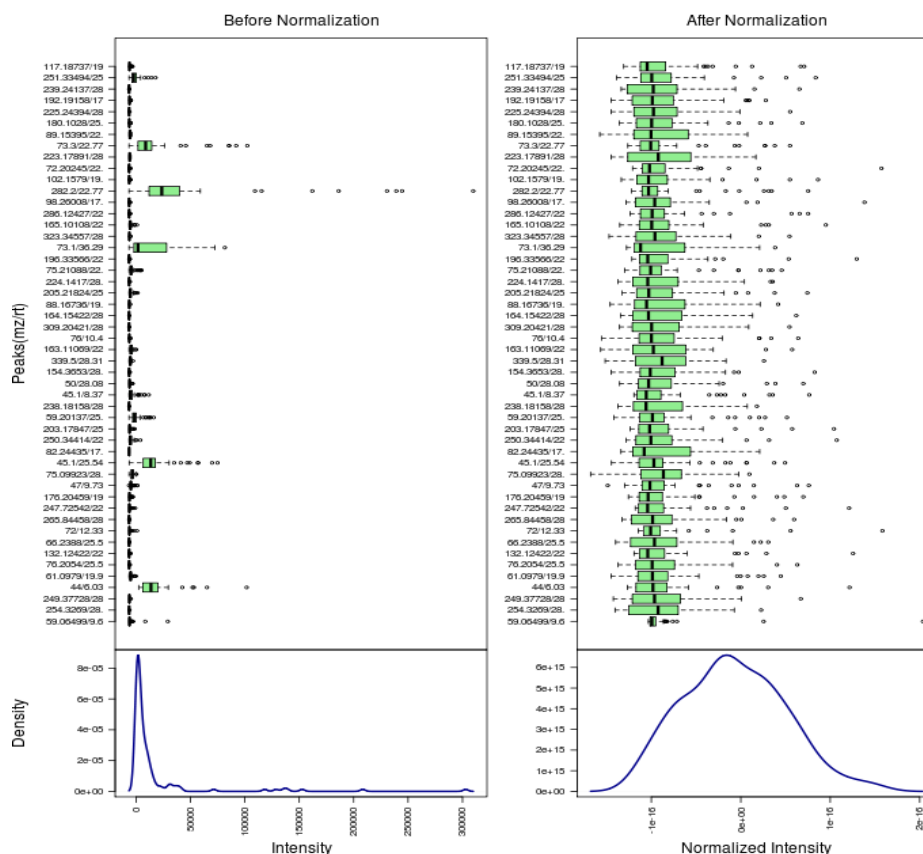
Figure 31 Samples with watercolour paints, 50 days photodegradation, relative feature intensity distribution before and after normalisation by auto-scaling.

Considering the diversity of the sample set, the normalised data was then explored using the same statistical tools as for WLR and GSR with remarkable success. The significant features identified by the various statistical methods are summarised in Tables 13 and 14. Several of the same significant features identified for both WLR and GSR sample sets also occur in the watercolour paint set indicating that these features are particularly good at discriminating between samples aged in different atmospheres regardless of applied colourant type. However, the reduced size of this sample set, when compared to the WLR and GSR significant features see Tables 9-12 above, is immediately obvious. The reduction in the number of significant features is likely due to two factors: first, selection of a single degradation period (previous statistical models were trained to discriminate between ambient and anoxic aged samples regardless of degradation time, the population of VOCs might be dependent upon degradation time thus a larger significant feature set should be required to discriminate between atmospheres), and second the inclusion of a variety of colourants in the sample set (the models generated for the watercolour containing samples must select significant features that are able to discriminate across all the sample types, regardless of applied colourant; because of the diversity of the sample set it seems likely that there are fewer features that are accurate class predictors for all of the samples, and that these features likely derive from the

common sources in every sample, that is: the argon feature (though due to vial leakage it is not present in every anoxic sample),the paper substrate, the gelatine size and gum Arabic binding media[33]).

Fold change	T-test	Volcano	PLS-DA	RF	SVM
40/5.94	40/5.94	40/5.94	40/5.94	40/5.94	96.30775/17.17
73.1/36.29	96.30775/17.17	51.00848/28.09	96.30775/17.17	45.1/8.37	82.24435/17.17
78.1/28	51.00848/28.09	77.1/28.09	51.00848/28.09	51.00848/28.09	73.1/36.29
49.0816/28.09	77.1/28.09	49.0816/28.09	77.1/28.09	96.30775/17.17	40/5.94
82.24435/17.17	49.0816/28.09	73.1/36.29	49.0816/28.09	68/9.42	192.19158/17.17
52.09321/28.09	73.1/36.29	82.24435/17.17	73.1/36.29	87.22144/22.76	119.11359/17.18
77.1/28.09	82.24435/17.17	52.09321/28.09	82.24435/17.17	78.1/28	120.11729/17.16
51.00848/28.09	52.09321/28.09	106/28.08	52.09321/28.09	50/28.08	
239.24137/28.29	106/28.08	50/28.08	106/28.08	72/12.33	
106/28.08	50/28.08	239.24137/28.29	50/28.08	49.0816/28.09	
50/28.08	239.24137/28.29	78.1/28	239.24137/28.29	52.09321/28.09	
	78.1/28		78.1/28	77.1/28.09	
	120.11729/17.16		120.11729/17.16	37.08497/9.53	
	87.22144/22.76		87.22144/22.76	212.99996/17.17	
	238.18158/28.25		238.18158/28.25	44/6.03	
	119.11359/17.18		119.11359/17.18	106/28.08	
			74.1/32.29	151/16.56	
			68/9.42	112.27242/22.73	
			112.27242/22.73	227/17.17	
			212.99996/17.17	239.24137/28.29	
			237.12519/28.28	120.11729/17.16	
			195.20921/22.77	73.1/36.29	
			192.19158/17.17	238.18158/28.25	
			149.28146/30.11	103.26701/22.75	
			118.1219/17.17	75/10.4	

Table 13 Samples with watercolour paint, 50 days photodegradation, significant features identified by statistical analysis, arranged by statistical method and ordered from most to least significant.

Feature	Frequency		Feature	Frequency
40/5.94	8		112.27242/22.73	3
73.1/36.29	8		68/9.42	3
106/28.08	7		192.19158/17.17	2
239.24137/28.29	7		74.1/32.29	2
49.0816/28.09	7		118.1219/17.17	1
50/28.08	7		149.28146/30.11	1
51.00848/28.09	7		151/16.56	1
52.09321/28.09	7		195.20921/22.77	1
77.1/28.09	7		227/17.17	1
78.1/28	7		237.12519/28.28	1
82.24435/17.17	7		37.08497/9.53	1
96.30775/17.17	6		44/6.03	1
120.11729/17.16	5		45.1/8.37	1
119.11359/17.18	4		72/12.33	1
212.99996/17.17	4		75/10.4	1
238.18158/28.25	4		103.26701/22.75	1
87.22144/22.76	4			

Table 14 Samples with watercolour paint, 50 days photodegradation, significant features identified by statistical analysis ordered by frequency of occurrence.

It must be remembered that the significant features are those that are best at classifying the samples as being degraded in ambient or anoxic conditions. However, the rest of the features, while less useful for

---

[33] In this sample set, the WLR samples are often sub-clustered based on their anti-correlation to significant features that were identified in the GSR samples and the pigment containing samples sub-cluster based on feature sets unique to each pigment type.

discriminating between ambient and anoxic conditions are good for sub-classification of samples into pigment types. It is these features, not in the significant features lists, that are responsible for the clustering of the samples in the applied multivariate and clustering methods.

7.4.3.2.1 MDS Analysis with XCMS

The 2D MDS plot generated by XCMS, Figure 32, reveals exciting grouping of the samples not just into anoxic and ambient clusters but also according to pigments; as an unsupervised method MDS uses all of the features in the mass chromatogram to calculate the distance measures between samples. It seems that the samples containing Prussian blue without extenders (TCA7 and TTB6) in the lower right are more alike (regardless of atmosphere during the experiment) and dissimilar to the samples with organic pigments. Samples containing TTB3, gamboge, also tend to cluster together separately from the madder-derived colourants; this is expected because gambogic acid, the main chromophore in gamboge is distinct from the anthraquinone chromophores in madder lakes. The madder-derived colourants also seem to fall into two clusters with further partitioning by degradation atmosphere. This clustering of the madder lakes could be due to transition metal content which, as we have seen in Chapter 5, affects the chemiluminometric yield, which has been used as a measure of oxidative activity (37).

In the centre-left of the MDS plot there is a dense cluster of samples with many overlaid points. This could indicate that the samples are very similar (identical), however, the more likely explanation, knowing the samples, is that for this sample set, 2 dimensions are not adequate to explain the differences between the samples (451, 452, 466). Though not applied in this case, a stress-test of the MDS analysis could be used to confirm this hypothesis.
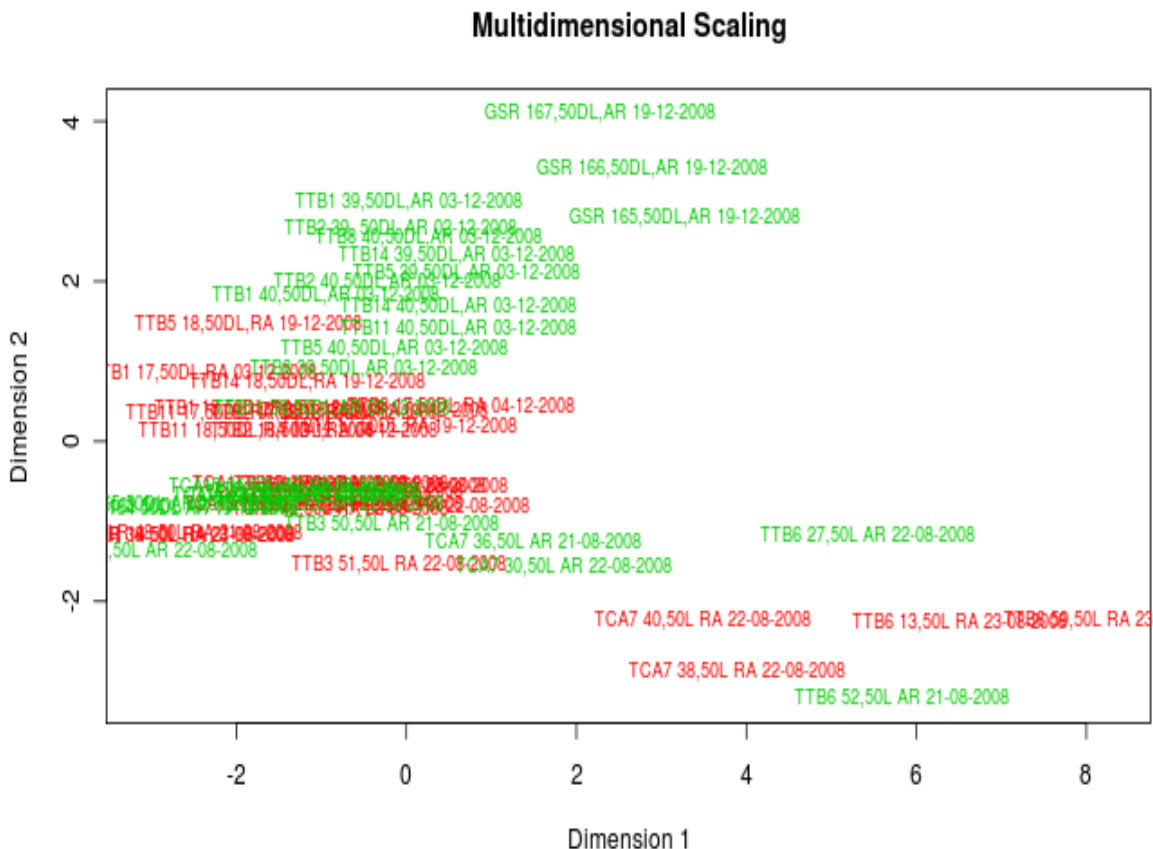
Figure 32 Samples with watercolour paint, 50 days of photodegradation, plot from multidimensional scaling analysis. Some clustering is apparent, but the overlaid sample points near the centre-left indicate that 2 dimensions are not adequate to describe the differences between the samples.

7.4.3.2.2 PCA Analysis

As the next multivariate analytical tool, PCA was used to explore the data. PCA performed less well with this sample set than with the WLR and GSR sample sets above. Figure 33 represents the score plot on the first 2 PCs which explain nearly 58% of the total variance. Examination of this score plot reveals a similar clustering pattern as visible in the MDS plot. The anoxic samples, except TCA7 and TTB6, tend to separate along PC2 while the ambient samples tend to separate along PC1. If we consider the loadings onto the PCs, Figure 34; PC1 can be described as TVOC with almost all of the features having a loading score of roughly -0.1 (a notable exception is the 40 m/z feature from Ar which has a PC1 score near zero). PC2 is more difficult to define; the features with high loading values, including the 40 m/z argon feature, were found to have high correlations to the anoxic sample class during correlation analysis; thus it can be described as maintenance of anoxic atmosphere during degradation, or perhaps, seal quality, because many of the anoxic samples with low scores on PC2 were the ones in screw cap vials that were found to leak faster than the crimp cap vials.

206
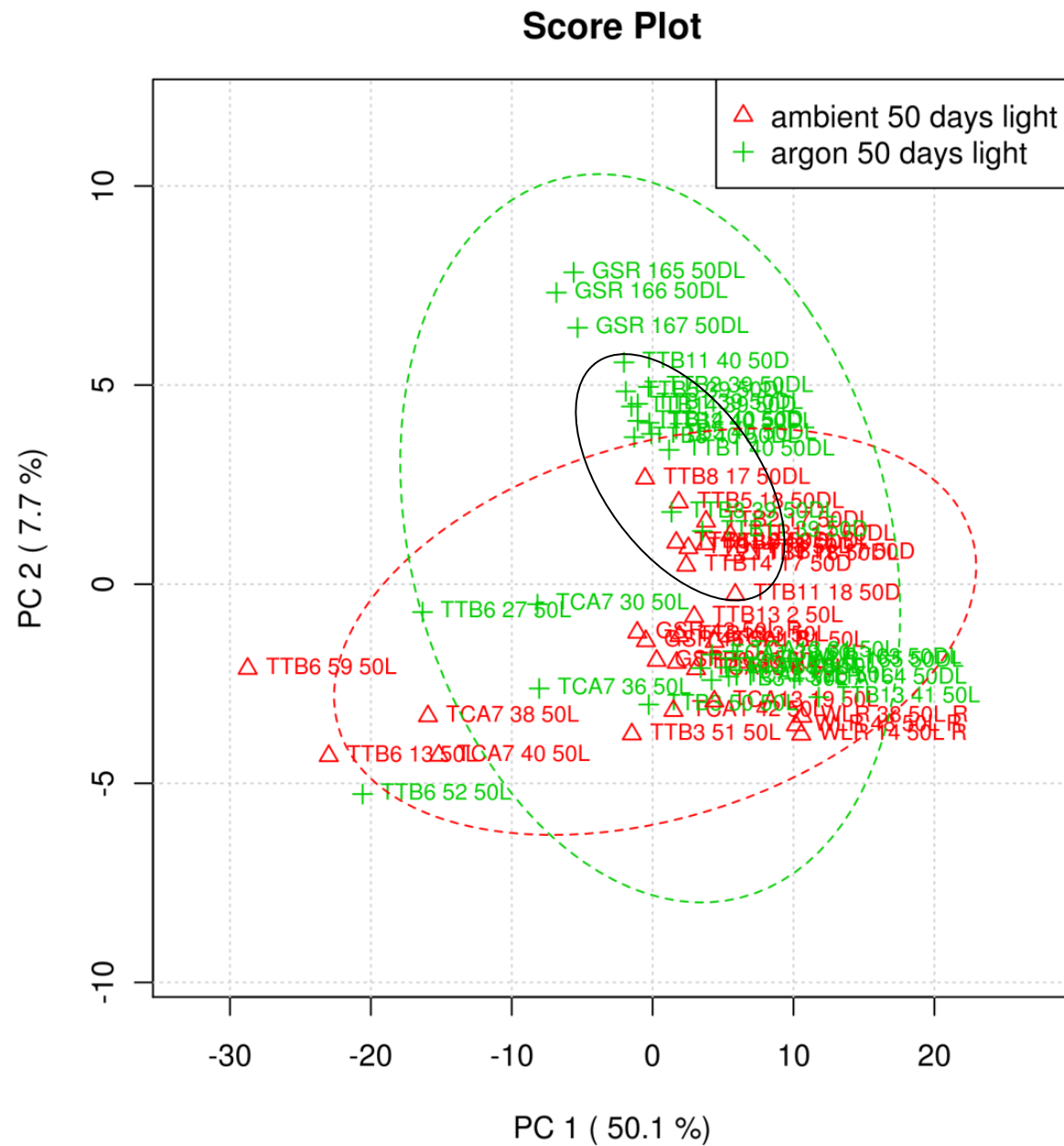
Score Plot

Figure 33 Samples with watercolour paint, 50 days of photodegradation. Score plot from PCA analysis. 58% of the variance can be explained by the first 2 principal components. The green and red ellipsoids are drawn with 95% confidence. The black ellipsoid on the figure indicates the cluster of madder lake pigments with low associated transition metal contents.
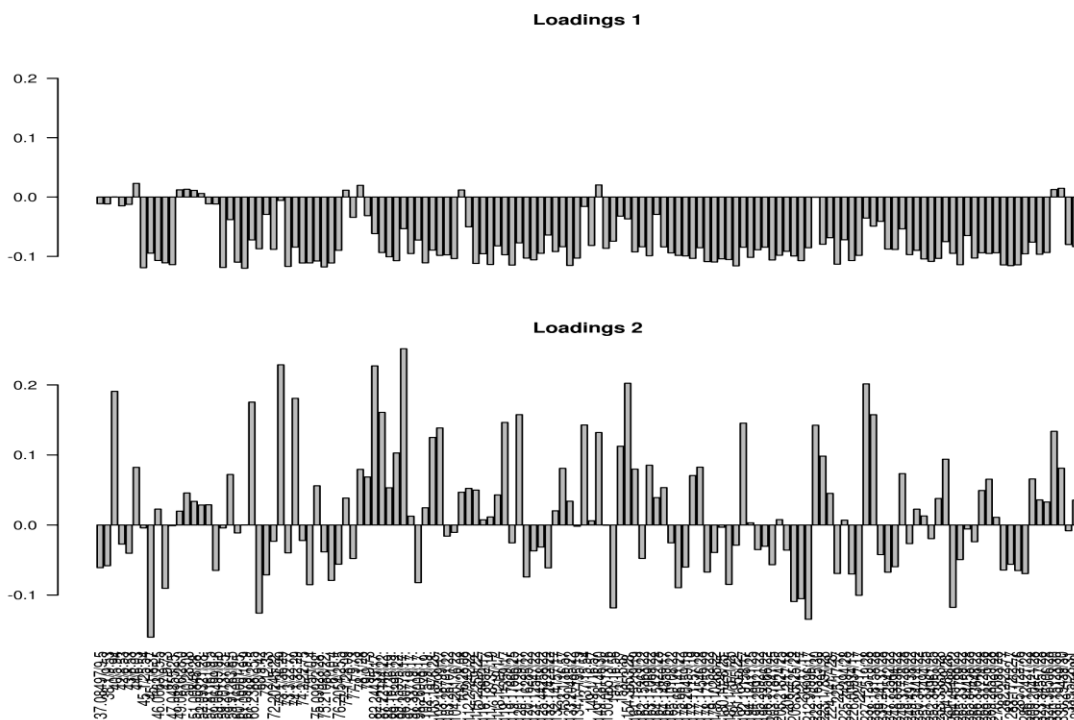
Figure 34 GSR Samples with watercolour paint, 50 days of photodegradation. Bar plots of the loading values onto PC1 and PC2. PC1 can be interpreted as TVOC, and PC2 with strong loadings from the 40m/z feature and features that correlate to this feature, can be described as anoxic character.

Further examination reveals subgroup clustering:

- There is a cluster of Prussian blue-containing pigments (TTB6 and TCA7) in the lower left indicating that they are significantly different from all the other samples. In fact they have the most populated VOC profiles of all of the samples studied[34] indicating that they promote the degradation of the paper and production of volatiles. This possibility was ruled out by Ware (127), however his research was based on mechanical properties of paper. Chemiluminometric (CL) analysis following irradiation with visible light of samples containing Prussian blue pigments TCA7 and TTB6 shows decreased CL intensity in the region associated with peroxide decomposition relative to samples without colourant, see Chapter 5. This has been interpreted as increased decomposition of peroxides via Fenton-like reactions by transition metals (37).

- The madder containing pigments also seem to separate into clusters, which might be explained by the presence of transition metals in the lake pigment which, with the chromophores, can have a pro-oxidative or anti-oxidative effect, see Chapter 5 (8).

---

[34] This was calculated by summing the intensities of all of the features in the TICs.

- o TTB13 was found to have significantly more copper than other madder lakes, and samples with this colourant had a much higher oxidative activity as measured by chemiluminometry. If the copper is present as a copper oxide, as proposed by Hansen and Townsend (232, 233), then this could act as a photoactivated catalyst for VOC decomposition, or if present in a coordination compound with a chromophore, it could participate in photo-Fenton-like advanced oxidative reactions thus changing the volatile degradome (8, 37).

- We also see that the gamboge samples (TTB3) as well as the orange madder (TCA 13) and the Antwerp blue (TCA 1) tend to cluster apart from the madder lakes, hinting that they are significantly different from these samples. As an unsupervised method PCA uses all of the features in generation of the score plots, therefore the observed clustering and sub-grouping of the samples is due to the entire feature set, and not just the reduced set of significant features that are best for class identification by supervised methods.

  - o The positioning of TTB3 apart from the madder lakes is expected as it is an unrelated chromophore and should therefore generate a different degradic profile.

  - o The separate clustering of the TCA13 samples could indicate that this orange madder is from a synthetic, rather than natural, source, and possibly that it is 1,2-dihydroxy-3-nitro-9,10-anthraquinone (C.I. Mordant Orange 14).

  - o The positioning of the Antwerp blue samples apart from the other Prussian blue samples is interesting. This could be due to several factors. On the one hand XAS studies suggest that the Prussian blue pigment in TCA1 is the same as that in TCA7, see Chapter 6, but because of the presence of white pigment extenders, ZnO and $BaSO_4$ (identified by SEM-EDX), there is much less Prussian blue in the colourant, and therefore reduced Fenton-reactivity is expected. On the other hand, ZnO is photoactive and can act as a type-1 reactive oxygen species (ROS) generator to form super oxide anions which can lead to the advanced degradation of paper (42, 392) but also to the photo-initiated decomposition of VOCs, Chapter 5. For pure ZnO, UV radiation is required to drive the reaction, but the presence of coloured metal oxides, as well as other chromophores such as organic dyes (and presumably Prussian blue) can push the activation spectrum into the visible range via electron transfer between the coloured species and ZnO. Returning to the CL data, see Chapter 5, for TCA1-containing samples the CL peak associated with peroxides has a value intermediate between the other Prussian blue-containing samples and samples without colourants. Without direct measurement of peroxides or their decomposition products it is difficult to

interpret this intermediate value, however, a hypothesis based on competing peroxide decomposition (by Prussian blues and peroxide formation via ROS generation (by ZnO) can be proposed. Examining the TICs of the TCA1 samples reveals that they are less populated than the other Prussian blue-containing samples, it seems possible that the ZnO, possibly in conjunction with the Prussian blue, is acting as a photocatalyst to decompose VOCs in the samples (461).

- The final observation that can be drawn from the score plot is that there is still a significant overlay of data points near the centre of the plot indicating that a number of samples are not well explained with only two PCs. Figure 35 is a 3D score plot along the first 3 PCs; better separation can be seen, but still only 64% of the variance can be explained thus indicating that more PCs are needed, and that perhaps PCA is not the best method to explore the data.
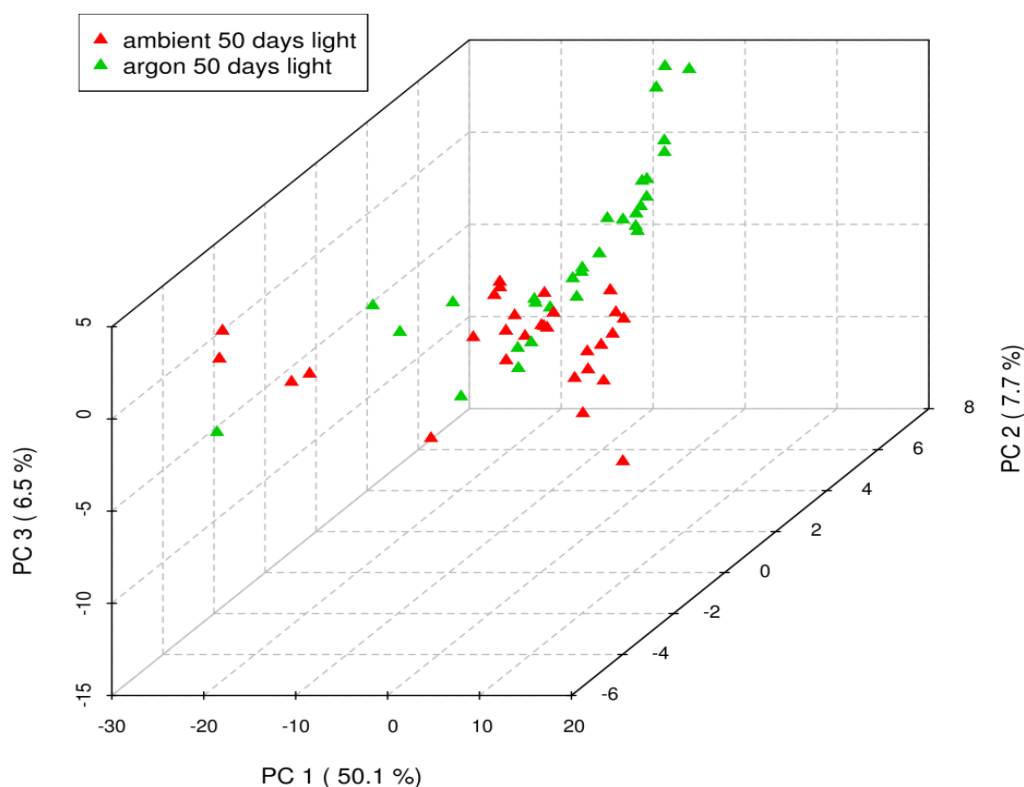
Figure 35 PCA score plot for the first three PCs explaining 64% of the variance in the population of samples with watercolour paint, photodegraded for 50 days.

7.4.3.2.3 PLS-DA Analysis

A PLS-DA model was optimised to 2 PCs using LOOCV; this model has an accuracy score in excess of 0.8, R^2 of approximately 0.5, and a Q^2 value of around 0.3. The significance of class discrimination was tested with a 2000-permutation test yielding a p-value of 0.0445 indicating that it is statistically significant.

Figure 36 is a score plot from the first two PCs generated by PLS-DA analysis; on the whole, slightly better class separation as well as tighter sub-group clustering than in the PCA model is observable. The first two PCs are very similar to those generated by PCA, but with PC1 corresponding to anoxic character and PC2 to TVOC.
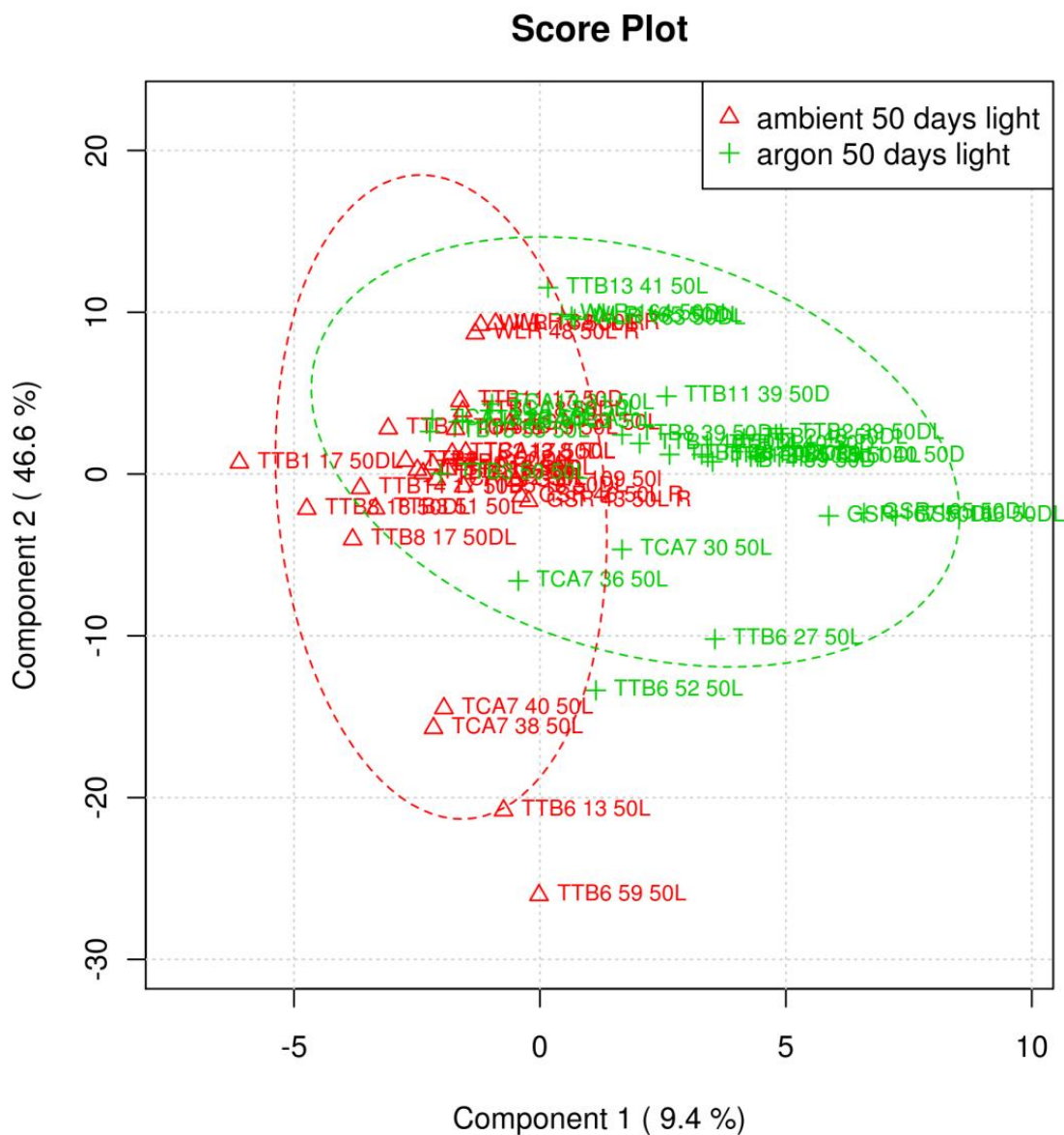
Figure 36 PLS-DA score plot for the first two PCs explaining 56% of the variance in the population of samples with watercolour paint, photodegraded for 50 days. The ovals are drawn with 95% confidence.

The separation of the samples with organic colourants degraded in anoxia is based almost entirely on PC1, which is related to the anoxic character. If we can consider the Ar feature as a good indicator of leak rate, then we can evaluate the origin of this class separation. In fact, the samples TCA7 36 50L AR, TTB3 50 50L AR, TCA7 30 50L AR, TCA13 31 50L AR, TTB3 4 50L AR, TCA1 33 50L AR, TCA13 26 50L AR, TCA1 26 50L AR and TTB13 55 50L AR all have Ar features within the ambient distribution indicating that at the time of

measurement most of the argon had leaked from the vials. The explanation for this error is due to the fact that these samples were aged in screw cap vials which leaked. So the sub-group separation seen for the organic samples might not be real, i.e. the samples that seem to be more ambient in character might actually be that. This is belied by the fact that the samples in the leaky vials do not overlay with their ambient counterparts and that during single colourant statistical analyses good separation is observed between sample classes even for the leaky vial samples. Be that as it may, the sub-group cluster should be considered with some scepticism unless it parallels similar sub-grouping in the ambient samples, which would not have been affected to the same degree by leaky vials. In that case we can consider the separation of TCA1 from TCA7 and TTB6 samples as real (confirming the ability to distinguish between samples with and without extenders, and interestingly, sample TTB13 41 50L AR, which looks like an outlier, placed near the WLR Ar samples, has retained its Ar, indicated by a large 40 m/z feature, and its separation from the other madders is therefore real. However, like PCA, PLS-DA suffers from over-reduction of dimensionality, the question about the apparent separation of historic madder lakes from other organic colourants would better be answered using cluster analyses which does not rely upon PC generation and are better able to preserve the sub-group topography after dimension reduction.

7.4.3.2.4 HCA Analyses

As an unsupervised method, HCA analysis is perhaps the most useful tool in discriminating class differences and sub-grouping in the sample set. Agglomerative HCA with a Euclidian distance measure and Ward clustering algorithm was applied. Figure 37 is a dendrogram created by HCA analysis, and immediately we can see that the samples with Prussian blue (TCA7 and TTB6) are all closely related but unrelated to the rest of the samples forming a separate subgroup with a distance measure of nearly 150 a.u. Thus we can distinguish between organic and inorganic samples. TCA7 and TTB6 are both relatively pure soluble Prussian blues, see Chapter 6 for more details. Despite the fact that the Ar had leaked from the anoxic TCA7 samples and one of the anoxic TTB6 samples, HCA was able to correctly group by pigment and atmosphere. Thus we are able to distinguish between a historic and a modern Prussian blue, and distinguish between samples of each pigment that have been aged in different atmospheres indicating that even partial anoxia or anoxic conditions during part of the light degradation regime will generate measurable differences in the volatile degradome.
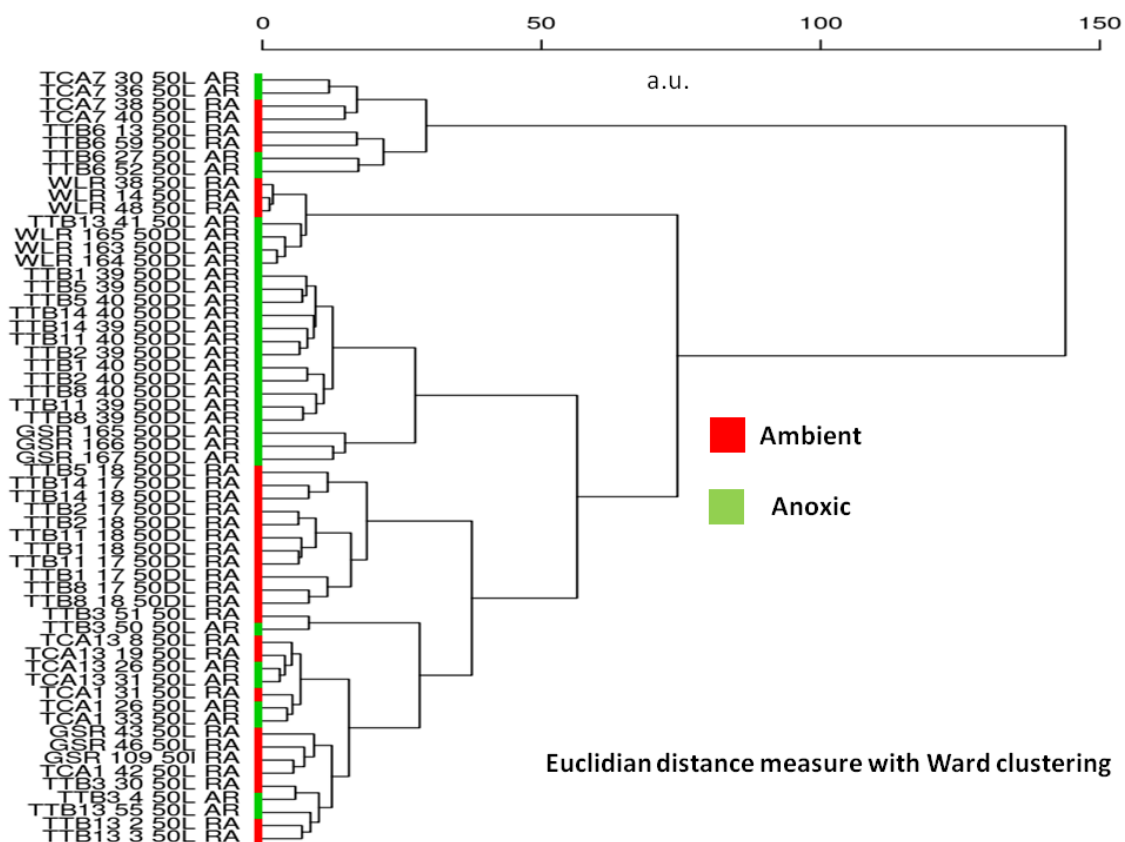
Figure 37 HCA dendrogram created with a Euclidian distance measure and Ward clustering algorithm for the population of samples with watercolour paint, 50 days light degradation. Samples labelled in red were degraded in ambient atmosphere, and samples labelled in green were degraded in anoxic atmosphere.

If we consider the heat map view of the dendrogram, Figure 38, we can see that the Prussian blue samples have the most highly correlating features of the sample set. This is more easily observed using heat map-dendrogram generated using the top 25 features as identified by PLS-DA VIP analysis, Figure 39. This indicates that the headspace is highly populated, with a much greater TVOC yield (calculated by summing the intensities of all of the features) than GSR alone. This in turn indicates that the presence of Prussian blue leads to accelerated oxidative degradation of either the gum binding medium or the paper.

Next we see that the WLR samples, both ambient and anoxic, form a distinct branch from the remaining samples at about 75 a.u., Figure 37. This is likely due to the fact that they alone have not been treated with gelatine size. Looking closer we see good sub-grouping by atmosphere, but we can also see that the ambient samples are more similar to each other (smaller intra-group distance measure) than the anoxic samples. A reason for this could be the quality of the seal, with small differences being detectable. Strangely a sample of TTB13 is grouped with the anoxic WLR samples. This sample had a particularly good seal (judging by the
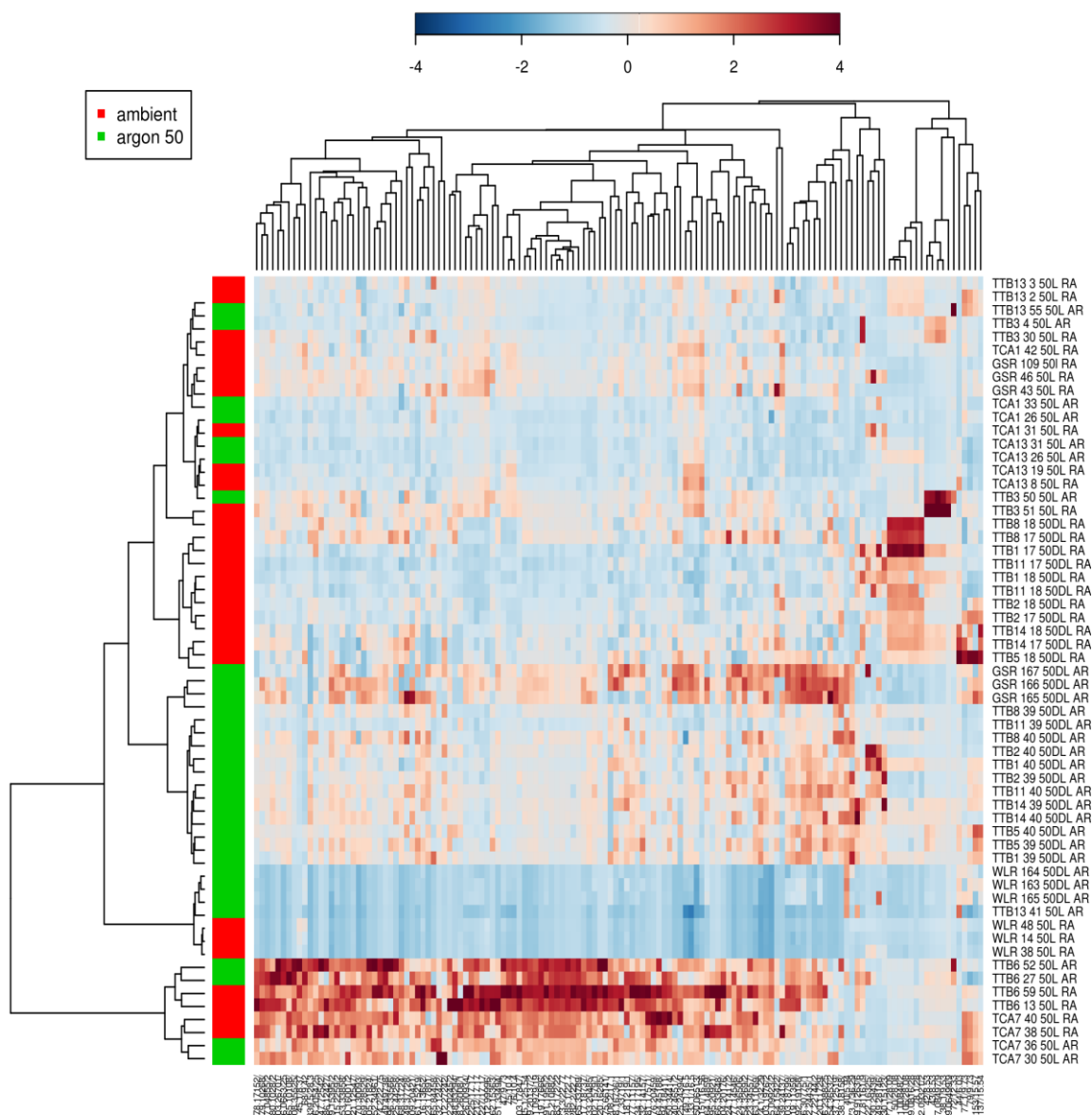
Figure 38 HCA heat map created with a Euclidian distance measure and Ward clustering algorithm, for samples with watercolour paint, photodegraded for 50 days.

intensity of the Ar feature) and it has a moderate anti-correlation to most features, indicating a headspace with low TVOC content. Its clustering with the WLR samples is likely an artefact of agglomerative clustering; once two samples are grouped, it is impossible for the pairing to be changed. The anoxic WLR samples also anti-correlate to most features, except the argon feature, and thus a grouping with TTB13 41, which shares the same traits, is possible.

Proceeding down the dendrogram we find that the anoxic madder lake and GSR samples branch with a distance measure of about 60 a.u., Figure 37. Within this cluster, the GSR samples form a distinct sub-group at about 30 a.u. This is expected because these samples lack both gum Arabic and pigments. In Figure 38, it

is possible to see a difference in correlation patterns between the anoxic GSR and madder lake samples. The differences between the different sample types are clearer in Figure 39; here we can see a correlation 'hot spot' for
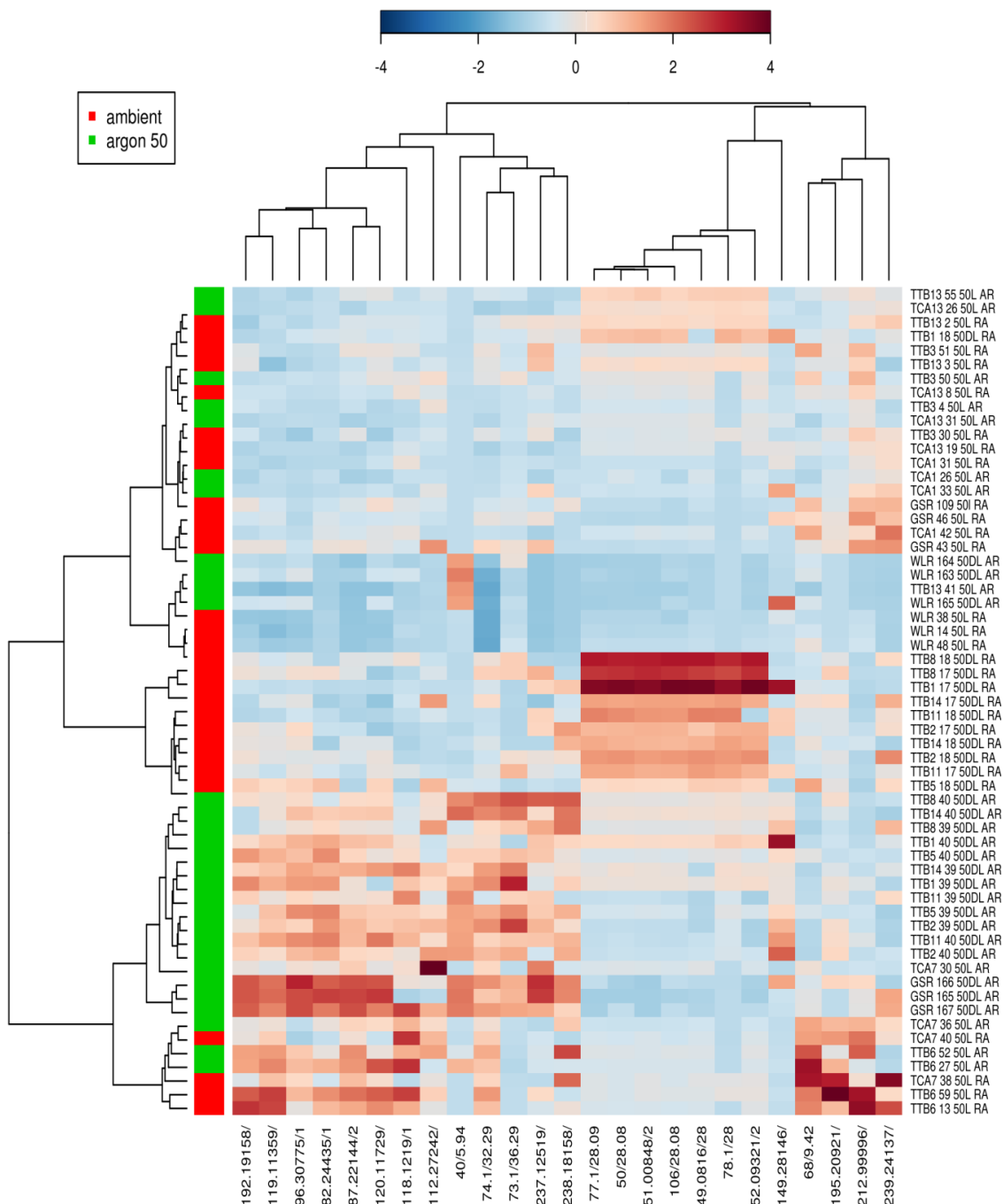
Figure 39 HCA dendrogram created with a Euclidian distance measure and Ward clustering algorithm, for samples with watercolour paint, photodegraded for 50 days. The top 25 features as identified by PLS-DA VIP analysis were used as a reduced variable set.

GSR, these features relate to nitrogen-containing compounds and are likely amino acid degradation products. There is relatively good pairing of duplicate samples within the anoxic madder lake cluster. It is remarkable that there is only minor shuffling of samples given that the samples are so similar. This indicates that there were significant differences in the volatile degradomes between madder lake types, and that with further method development, we should be able to reliably distinguish between different madder lakes. The next important observation is that the anoxic madder lakes typically anti-correlate with features with which the ambient madder lakes have positive correlations, see Figure 38 and particularly Figure 39. These features with the RT of approximately 28 min, correspond to aromatic compounds. Their presence in the ambient samples could be indicative of oxidative degradation of the anthraquinone chromophore or of photo-tendering (degradation) of the gelatine, particularly amino acids with aromatic residues (phenylalanine, proline, hydroxyproline, histidine and tyrosine). In either case anoxia seems to limit this degradation phenomenon.

Examining the ambient madder lake cluster, Figure 38, we see even better duplicate pairing, the only mistake in clustering being with TTB1 and TTB11 which are grouped together. Given that the samples of each colourant used for both atmospheres were prepared as the same paint out, it is likely that the shuffling observed in the anoxic samples is related to the quality of the seal on the headspace vial. Interestingly, unlike the anoxic samples, the ambient GSR samples do not fall in this cluster.

The next grouping, at relative distance measure of 40 a.u., is what I have termed the 'odd-one-out' cluster. The sample types in this grouping are chemically unrelated to each other, comprising the ambient and anoxic TTB3, TTB13, TCA1 and TCA13, as well as the ambient GSR samples, see Table 1 for a description of these samples. If we examine the heat map in Figure 39, we can see that within this grouping the sample types tend to cluster together, and that generally each sample type is just different enough from the madder lake samples to warrant their separation, but not so radically different, such as the Prussian blue and WLR samples, to need a separate branch in the dendrogram. In agglomerative clustering, the samples must cluster, and for lack of more closely related samples, these odd samples find similarity in their near differences from the rest of the sample set. Can we explain the origins of these differences?

TTB13 is thought to be a madder lake from *R. cordifolia, it* has some features in common with the other madder lakes, which are thought to be from *R. tinctorum* sources. The common features are expected as the chromophores have a common hydroxyl-substituted anthraquinone structure, and the features with the RT of approximately 28 min could be from the chromophores. However, the features do not correlate as well for the TTB13 as for the other madder lakes, and some key diagnostic features anti-correlate for TTB13. Aside from possibly coming from a different madder source, TTB13 also has significant quantities of copper. In Chapter 5 it was proposed that this leads to increased oxidative activity. If this is the case, then contrary to what we might expect (i.e. to see more VOCs), this should lead to reduced VOCs due to their catalytic decomposition at the chromophore-metal complex.

The TCA13 samples are also a madder pigment, but they have even lower correlations to the features attributed to the chromophores. I propose that the TCA13 is from a synthetic source and is possibly 1,2-dihydroxy-3-nitro-9,10-anthraquinone (C.I. Mordant Orange 14). This could be confirmed with further MS studies of the raw pigment in the future.

TTB3 is gamboge, and while an organic pigment, its primary chromophore, gambogic acid, is unrelated to the anthraquinones of madder lakes. In Figure 39 it is possible to distinguish several features with very strong correlation values in the sub-10-min RT region and anti-correlations to the features assigned to the madder lake pigments.

The TCA1, Antwerp blue, samples do not correlate strongly with any feature. This is a bit of a mystery, a possible explanation is the presence of ZnO as an extender. As noted above the ZnO in conjunction with Prussian blue, could act as a photocatalyst for the decomposition of VOCs in the headspace. This hypothesis has not been tested, but it is intriguing, and should be evaluated with further research. I propose to do this using a CATLAB (Hiden Analytical). Pellets of Prussian blue mixed with varying amounts of ZnO could be placed in the reactor and irradiated with visible light. The VOC decomposing photo catalytic activity could then be evaluated using a light alkane (hexane perhaps) as a model VOC. This could be supplemented with confocal Raman studies on paper immobilised pigment mixtures, (LabRAM, Horiba), using a reaction cell and gas phase analysis with a photo acoustic FTIR attachment (Gasera), here methane could be used as a model VOC. The heritage degradomics reactor, Chapter 8, could also be fitted with an online gas analysis instrument, perhaps a FAIMS (LoneStar, Owlstone) and again using a light alkane as the model VOC.

Two questions remain for these 'odd' samples. Why do the anoxic samples cluster with the ambient samples, and why are the ambient GSR samples included in this cluster?

The first question is simple to address. The screw caps used to seal these samples leaked. Though it must be noted that despite the leaking seals, using MDS it was still possible to distinguish separate ambient and anoxic clusters in the data sets for all pigment types. The fact that the ambient atmosphere samples, as well as the anoxic samples, grouped apart from the madder lakes could be interpreted as an indication of real separation, but the fact the argon was able to escape means that the VOCs could have also escaped, and thus the leaking seal could also explain why this separate grouping exists altogether. This would need to be evaluated by repeating the experiment using crimp cap vials, a more intense light source and shorter degradation time.

The inclusion of the ambient GSR samples, which were in crimp cap vials that did not leak, is likely due to interaction of two variables (atmosphere and pigment) for the ambient samples. This hypothesis was tested using analysis of variance between groups (ANOVA) which identified two groups based on presence of madder lake pigment and atmosphere for the ambient samples, but only a single group for the anoxic samples. Thus the ANOVA results support the separation of the GSR RA samples from both GSR AR as well as

the ambient madder lakes. The existence of two groups for the anoxic samples, and a single group for the ambient samples is supported by the CL data, see Chapter 5, which found that after irradiation in a nitrogen there was nearly identical CL activity for all samples, but after irradiation in air, different CL activities were observed for TTB13 containing samples, samples containing other madder lakes and GSR samples.

The inclusion of ambient GSR samples in the 'odd-one-out' cluster is not due to a chemical similarity to the other members of the cluster, but is likely an artefact of agglomerative clustering.

7.4.3.2.5 SOM Analysis

Kohonen self-organising map analysis was then applied to the sample set with good success using an 8 x 8 matrix of square cells with a linear initialisation and Gaussian neighbourhood function (177, 444). Kohonen neural networks are particularly useful because they map objects from m-dimensional space to a reduced n-dimensional space in an unsupervised fashion. Each square in the matrix represents a model to describe a data set. The initially random models are refined by iterative training to modify the weight of the model to increase the quality of the fit of the median intensity of the samples in the cluster. The topological features of the data are preserved in how the clusters are grouped together by the neighbourhood function (458). Groups of clusters that share a border are more similar than groups of clusters with empty cells separating them. The greater the distance between two clusters, the greater the difference between the occupants. Figure 40 is a heat map translated from MetaboAnalyst's SOM analysis output. For ease of interpretation metadata about the pigment type, number of samples from each atmosphere type, whether a sample was found to be leaky or mislabelled has been included in each cell of the heat map plot.
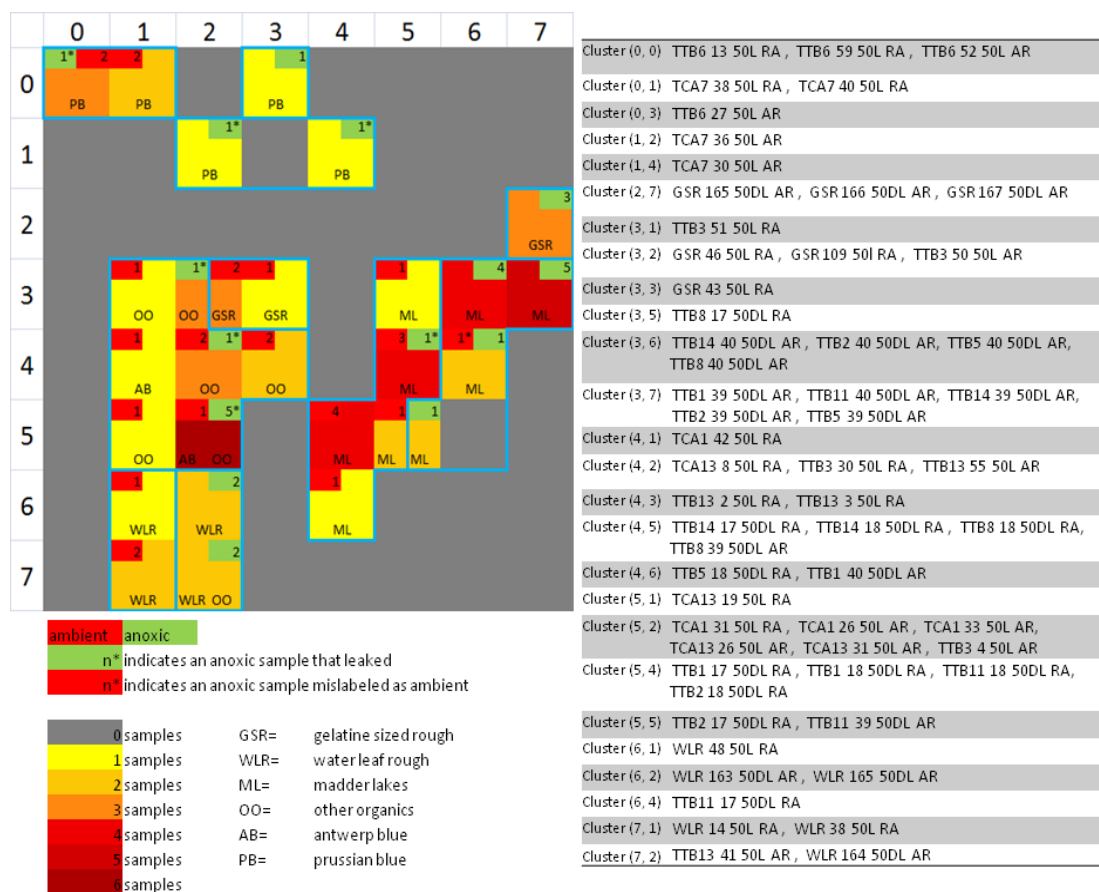
Figure 40 Heat map from SOM analysis, for samples with watercolour paint, photodegraded for 50 days. The cluster occupants are given in the table on the right, and the number of occupants per cluster is indicated by the colour coding. The number of ambient and anoxic samples per cluster is indicated by the red and green rectangles in the upper left and right corners of each cluster. The type of pigment is given in the main body of the cluster. If two pigment types are present in a cluster they are both listed. The blue lines define groupings based on prior knowledge of the pigment composition of each sample in the set.

In Figure 40, we can see three main groupings of clusters that can be described as Prussian blue (upper left) madder lakes (centre right) and 'odd-one-out' plus WLR left. These main clusters can be further divided according to atmosphere and pigment type so that the GSR, WLR, madder lakes and Prussian blues (ambient and anoxic) can be defined as separate groups; these groups, based on prior knowledge about the pigments in the samples, have been indicated using blue lines drawn onto the heat map. Generally, SOM analysis supports the HCA and PCA results giving greater confidence in the interpretation detailed above.

7.5 Conclusions

Based on the above experimental results, it can be concluded that non-targeted degradic footprinting is a valid tool for discriminating between samples aged in ambient and anoxic atmospheres and consequently hypotheses generation. Several different statistical methods were used to analyse the data, construct models and build and test hypotheses. More than any single chemometric method, it was the combination of approaches that informed the research. The strong points of different methods were exploited to

overcome the weaknesses of others, and the resulting models were compared and used to refine each other. Starting with the simplest sample set (WLR RA vs. WLR AR) and moving to the most complex sample set (samples with watercolour paints) there is good agreement between all of the applied multivariate and clustering methods indicating that the observed clustering in the data is real. The feature selection methods, whatever the selection method, generally identify the same features within a sample set, and several features are retained between sample sets indicating that they are robust markers for discriminating between samples aged in ambient and anoxic atmospheres. Patterns in these features can be evaluated by correlation analysis, and their significance tested by *in silico* 'knocking out' experiments, as in genetic function analyses, where a gene function is turned off or on, where the feature, and correlating features are excluded from a statistical model and the included/excluded models compared.

Using an entirely non-targeted approach:

- For anoxic samples, it was possible to use the 40 m/z feature associated with argon to evaluate the quality of the seal. As a simple spot check of argon concentration, only univariate analysis is needed;
- It is possible to distinguish between samples photodegraded for different durations, for this multivariate analyses excel, as they can make use of the entire volatile degradome and still distinguish between samples that started the degradation process in anoxia but from which the argon had leaked by the time of analysis from those that were in air for the entire degradation interval;
- It was found that the reliability of the seal was much lower for samples photodegraded longer than 50 days;
- For a single sample type, it is possible to discriminate between samples photodegraded in anoxia and those aged in standard air.
- It is possible to distinguish between closely related pigments and moreover the effect of those pigments on the volatile degradome that derived from the pigment-substrate interaction
    - Modern and historic soluble Prussian blues clustered separately.
    - Prussian blue with ZnO and BaSO$_4$ extenders (Antwerp blue) clustered apart from the pure Prussian blues.
    - Organic pigments from different sources, gamboge vs. madder lakes, cluster separately.
    - Madder lakes from *R. cordifolia* cluster apart from madder lakes from *R. tinctorum.*
    - Despite having the same chromophores, within the *R. tinctorum* cluster there was good separation of madder lakes by colour, which corresponds to both

> preparation conditions and the presence of different ratios of associated transition metals.

- Marker features of interest relating to specific pigment-atmosphere-degradation interval combinations were identified. If profiling experiments are conducted these marker features can be used to evaluate the effect of anoxic display on the object and if they can be correlated to specific material properties: DP, colour change, change in pH etc., then they can be used to predict the lifetime extension, if any, of anoxia for WOPs.

The data quality could be improved by deconvolution prior to TIC alignment, however care must be taken to use apply the same parameters to all samples prior to other data treatment steps. Deconvolution should resolve many of the problems with co-elution and help to identify the constituents of the volatile degradome. This in turn can be used for targeted degradic profiling of the samples.

Despite the difficulties with the data generation stage, we can begin to piece together the differences in chemistry between the ambient and anoxic samples. Generally, features associated with organic acids such as 45 m/z and 73 m/z correlate highly to the ambient sample class. This indicates that acids are being produced by oxidation of paper or gelatine. Samples with madder lakes that were aged in anoxia were found to have high correlations with features associated with aromatic compounds, while the same samples aged in anoxia anti-correlated to the same features. These features could derive from the oxidative degradation of the anthraquinone chromophores, which seems to be inhibited by anoxic conditions.

Samples with gelatine that were aged in anoxia tend to correlate well with high-m/z features at RT of 17 and 28 min. These features, and their fragment ions, contain nitrogen and therefore come from gelatine. However, the samples photodegraded in ambient air do not correlate with these same features but do correlate with nitrogen containing features corresponding to amines, amides and furans at typically shorter RTs. It is possible that the compounds responsible for the features observed in the anoxic samples are further oxidised in the ambient samples to generate lighter VOCs.

It is not clear why samples with Prussian blue (TCA7 and TTB6) have such highly populated headspaces, but it is indicative of accelerated degradation of the paper, gelatine or gum Arabic. Prussian blue undergoes reductive fading upon irradiation with visible light (127). To be reduced, a suitable reducing agent must be in contact with the pigment. Based on the CL data from Chapter 5 we can propose that the irradiation of the samples produces peroxides which can react with reduced Prussian blue (127) in a Fenton-like reaction to produce hydroxyl radicals that can then lead to the accelerated degradation of samples (278, 388, 467-469) leading to a more populated headspace.

TCA1 and TTB13 are both known to contain photo-active metal-containing species, ZnO and Cu^{n+} respectively. Both ZnO and copper ions in association with organic dyes, have been used as photocatalysts for advanced oxidative processes for VOC and dye removal respectively (396, 470). It is possible that the

presence of these photo-active compounds in association with a pigment or a chromophore can lead to a similar photo-driven decomposition of VOCs resulting in a reduced headspace population and general anti-correlation observed for these samples (42, 393-395, 397, 471). However, this would need to be substantiated by catalytic activity testing.

Taken as a whole, while the experiment can be considered successful, it raised many more questions than it answered. Non-targeted degradic footprinting is an exciting new method that can be used to generate new hypotheses to re-think the degradation of WOP. Using chemometrics it was possible to answer all of the experimental questions and discriminate between sample groups. The existing data set can be further mined by deconvolution and the profiling experiments conducted *in silico*, but the use of different sample vial types can also lead to confusing variability in the data set. A single vial, septa and closure type should be used for all samples. Instead of PTFE-lined silicone septa, perhaps Al-lined butyl septa should be used for future research. This should eliminate many of the septa-derived peaks that co-elute with sample peaks. It is recommended that portions of the research be repeated using Al-lined butyl, or Viton, rubber septa on crimp cap vials. If a more intense light source is used degradation times can be significantly reduced, and this will help to limit the leaking of the vials during the experimental process.

Chapter 8 Heritage Degradomics Reactor

8.1 Introduction

Much of heritage science research involves accelerated degradation studies to develop models of the degradation behaviour of heritage objects. Typically a reductionist approach is used in experimental design: a simplified model material is developed and subjected to either thermal-, photo- or pollutant- based degradation regimes (241). The degradation is then periodically interrupted for sampling and analysis, or several 'identical' samples are sequentially removed and analysed. Such studies,[35] while informative and useful, can be criticised on several factors, primarily: the reproducibility in the alignment of the measurement area, intra- and inter-sample inhomogeneity, the low time-resolution for kinetic studies and/or the oversimplification of the experimental conditions (degradation is a complex phenomenon often with synergistic effects between light, heat, humidity, and pollutant concentrations.

A better experimental solution would be one that:

- Gave greater control over the environmental conditions, including temperature, relative humidity and atmosphere composition,
- Combined accelerated thermal degradation with accelerated light degradation,
- Did not require the sample to be repositioned between measurements,
- Allowed for the simultaneous collection of spectrometric data from multiple spectral regions in real time
- Allowed for the characterisation of the volatile degradome
- Could be reconfigured for *in situ* applications on a heritage object or as a laboratory reaction cell.

Such a solution, which combines accelerated degradation with simultaneous spectroscopic and evolved gas measurements, can be used to study the degradation of materials in higher time resolution, give greater confidence in the reproducibility of the measured spot and allow for the correlation between VOC emissions and spectroscopic measurements. Those capabilities are key to developing new non-destructive methods that can be applied to heritage objects and to developing 'sniff tests' for evaluating both individual objects and storage environments.

---

[35] These methods have been used in the generation of the data used for this Thesis. The author's firsthand experience of the limitations of reproducibility in replicate and/or punctuated measurements of the degradation of materials served as the "what if" departure point in the design of the heritage degradomics reactor (HDR).

Micro-fadeometry (11, 404, 406, 428, 472-474) and the field and the laboratory emission cell (FLEC) (435, 475, 476) each partially address this issue. A micro-fadeometer can be used to measure the rate of photodegradation reactions of heritage materials with improved time and spatial resolution, as well as to evaluate the effects of museum lighting on heritage objects (11, 404, 406, 428, 472-474). A FLEC has been used to study VOC emissions from paper (435).

However, the above instruments have limitations to their application. Micro-fadeometry is able to accelerate photodegradation in the museum environment, however, unless the instrument is built into a glove box as has been done by some researchers (474), there is no control over the atmosphere, nor is there an integrated method to control the temperature beyond ambient conditions, and a FLEC is a sampling device for collecting the VOC emissions from a material, while the gas composition and humidity can be controlled, the temperature is not controllable beyond ambient conditions (475). Thus neither instrument represents a complete solution. Each offers only a single analytical method, and neither provides full environmental control.

Parallels to the above formulated problem can be found in the development of novel heterogeneous catalysts. During catalytic development, researchers would like to have real-time data about the structure-activity relationship of a catalyst as well as the products of the catalytic reactions under real catalytic conditions (477, 478). However, not until recent years have there been significant advances in the development of reaction cells and spectroscopic methodology to allow for *in situ* analyses of catalytic processes under true catalytic conditions. These methods are often referred to as *operando* spectroscopy. Rather than produce a short review of *operando* spectroscopy here, readers are directed to Tinnemans *et al* (478) and Bañares (477) who provide good general reviews of the field; therein readers can find a discussion of the development of the methodology and references to its specific application to the study of catalytic systems. However, the key points of *operando* methodology can be summarised here: ***real materials, real time*** and ***real conditions***.

In response to the perceived limitations of standard accelerated degradation methods, micro-fadeometry, the FLEC and other available instrumentation and methods, and inspired by the goals of *operando* spectroscopy of catalyst materials, a prototype *operando-* reactor was designed and constructed for application to heritage science.

The heritage degradomics reactor (HDR) was conceived as a multi-purpose experimental platform to address some of the shortcomings identified in micro-fadeometry and accelerated degradation-based studies of the degradation of heritage materials. From the start it was imagined as a tool to study the degradation pathways of heritage materials and tie into the method of heritage degradomics that I was developing in parallel. The HDR is a low-cost, modular system. It combines thermal-, light-, modified atmosphere- and pollution- based accelerated degradation (or any combination of the above) capabilities with fibre optic

reflectance (FORS-) spectroscopy/micro-fadeometry for near UV to NIR (350 to 2000 nm) applications as well as an interface for evolved gas analysis. Additionally, the constructed HDR prototype can be considered a single cell in a scalable array of HDR units that could potentially be used for parallel Arrhenius-type or combinatorial experiments.

Presented below are the concept, reasoning, and design of the first prototype of the HDR, as well as two case studies that serve to illustrate applications of the HDR to the study of the degradation of model materials as well as *in situ* studies of heritage objects. These case studies were selected not only on the basis of the successful application of the HDR, but also because they illustrate areas of needed improvement in the HDR design to increase its usability.

8.2 The Heritage Degradomics Reactor

Therefore the HDR prototype was constructed at relatively low-cost and has been tested as a proof of concept for *operando*-type experiments. See Figure 1 for an exploded diagram of the HDR. Because of the simplicity and low cost of a single HDR, it is possible to imagine an array of HDRs which could be termed (HyDRA) after the mythical beast which it would resemble with its multiple optics heads. This array could be used for conducting Arrhenius-type or combinatorial-type experiments in parallel at a fraction of the cost (measured in terms of equipment, energy, time and sample consumption) as compared to conducting the same experiments as per standard practice.

8.2.1 Instrument Design and Operation Description

The HDR is a modular experimental platform that can separate into optics and temperature control subassemblies, Figure 1.[36] Both subassemblies can be used together to form an accelerated degradation/emission cell for laboratory tests on expendable samples, or the optics head can be used alone and function as an emission cell and/or a controlled atmosphere micro-fadeometer for *in situ* studies on heritage objects.

---

[36] Most of the machining of the subassemblies was performed at the workshop of the chemistry department at the University of Ljubljana. I completed the machining, assembled and aligned the optics, and built the first version of the temperature controller at Tate according to my designs. An improved temperature controller was built by colleagues at the Jagiellonian University.
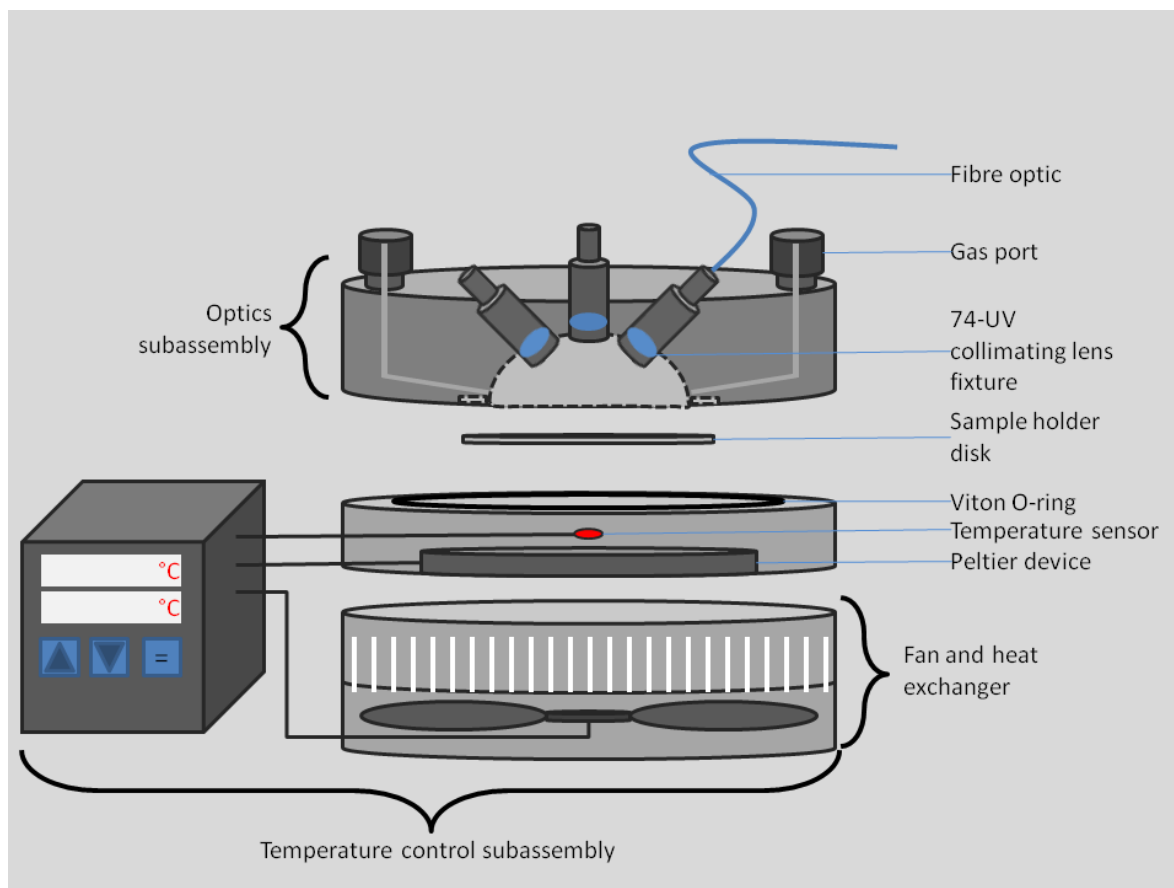
Figure 1 An exploded diagram of the HDR identifying key subassemblies.

8.2.1.1 Optics Sub-Assembly

The body of the optics subassembly is machined from aluminium with matte black hard anodizing. A hemispherical chamber machined into the body serves as the sample compartment of the HDR. A recessin the lower surface accepts the sample holder disk, a thin section of aluminium machined to allow for illumination and VOC emission, Figure 1.

8.2.1.1.1 Optical Elements

The optics are comprised of three custom fabricated Ocean Optics 74-Vis collimating lens fixtures, which are fixed in a collinear -45°/ 0°/45° geometry into the sample compartment. The 74-Vis collimating lens fixtures employ a fused silica bi-convex lens allowing for near UV through NIR (350 – 2000 nm) light to be transmitted. The lenses are potted into the lens fixtures with a VOC resistant epoxy, thus guaranteeing a gas-tight seal around the lens and thereby the possibility of reliably establishing a modified atmosphere within the sample chamber. The arrangement of the lens fixtures allows for different combinations of light sources and spectrometers to be connected to the optics subassembly, such that light degradation and spectra at different wavelength ranges can be evaluated simultaneously, via dual diffuse reflectance collection with the illumination at 0 ° and observation at -45° and 45° or simultaneous diffuse reflectance and specular reflectance collection with the light source at 45° and spectrometers at 0 ° and -45°. While not

tested, it should be possible to integrate inline filters into the system to evaluate wave-length dependent fading and/or conduct fluorescence studies with the HDR.

8.2.1.1.2 Gas Ports and Emission Studies

Two, 60° opposed, gas ports enter the sample compartment at an acute angle to the sample plane. These can be used to supply a specific atmosphere (RH control, oxygen concentration, pollutant dosing) to the sample chamber. The position of the gas ports and their angle of entry were selected to maximise turbulent mixing in the sample chamber to better extract VOCs from the sample surface.

The HDR can be operated in continuous flow or static modes. In continuous flow the sample chamber is constantly purged and the effluent analysed in real-time , for instance via gas phase photo acoustic FTIR (PA-101 Gasera Ltd. Finland) (216), Lone Star FAIMS (Owlstone Nanotech, United Kingdom) (217) or MS 200 tof-MS (Kore Technology, United Kingdom) (479), or concentrated onto a thermal desorption tube (TDT) for later analysis by thermal desorption gas chromatography-mass spectrometry (TD-GC-MS) (480, 481). In static mode, the atmosphere in the sample chamber is exchanged and then sealed before the beginning of an experiment; after the experiment the accumulated VOCs can be flushed from the sample chamber and collected on a TDT for TD-GC-MS analysis or analysed on line via a desired gas phase analytical method (475, 480-482).

8.2.1.2 Temperature Control Sub-Assembly

The temperature control subassembly consists of a polished aluminium block into which a peltier device (TEC1-12708) is embedded. A heat sink and fan are attached to the opposite face of the peltier device. A Viton o-ring is set into the aluminium surface to provide a good seal with the optics sub-assembly, Figure 1.

The peltier device is controlled by a temperature controller (RE71, Lumel) with a relay allowing for binary (heating/cooling) control. A PT-100 sensor embedded in the aluminium block provides temperature feedback to the RE71 controller, and a PID algorithm maintains the temperature at the set point with very low oscillations, typically on the order of ±0.5 °C, and with better tuning of the PID algorithm, even this small oscillation can be eliminated.

8.2.2 Laboratory Reactor Configuration

In the laboratory reactor configuration, a sample of paper, or other flat material, such as textile, is placed at the centre of the aluminium surface of the temperature control sub-assembly and held in place by the sample holder disk. The optics sub-assembly is then mounted and secured in place with eight evenly torqued bolts. Once the body is assembled the fibre optic cables and gas lines can be connected to suit the desired application.

When in this configuration the HDR can be used to simultaneously age and analyse both the spectroscopic changes to the sample as well as emitted VOCs. Because the degradation regime is not interrupted for

measurements, there is no need to re-align the sample, nor is there risk of accumulated VOCs being vented during opening. Moreover, spectroscopic data can be correlated to evolved gas data thus aiding to fill a knowledge gap between chemical changes as measured by VOC emissions and physical changes, such as colour change.

See Figure 2 for images of the HDR in two different laboratory applications. In the image on the left, the HDR is being used to photo-degrade a sample of paper with real time analysis of the evolved VOCs by FAIMS combined with simultaneous colour measurement. In the image on the right, the HDR is being used with a thermal desorption tube to evaluate the total evolved VOCs during the photodegradation of a sample of paper, and as before, colorimetry was conducted on the degradation spot.
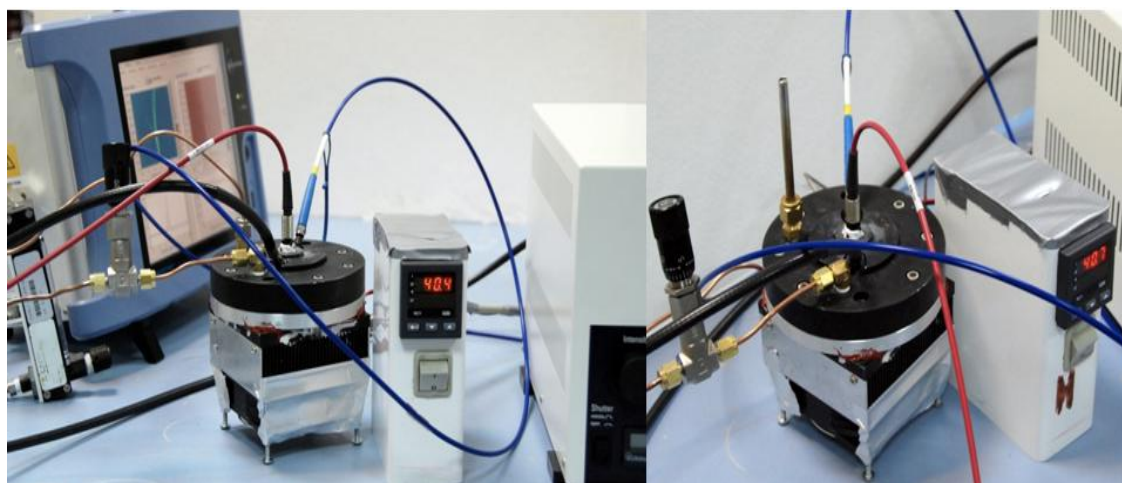
Figure 2 Two different configurations of the HDR as a laboratory reactor. On the left, a LoneStar FAIMS unit is used for real time evolved gas analysis with simultaneous light degradation and colorimetry. On the right, the HDR is fitted with a thermal desorption tube for total evolved gas analysis by TD-GC-MS, again with simultaneous light degradation and colorimetry.

8.2.3 In Situ Analysis Configuration

During *in situ* analysis only the optics sub-assembly is used. In this configuration a flat object is placed on a sheet of Melinex or glass and the areas of interest are identified and documented, as in normal conservation practice. The anodized sample holder disk is then placed as a mask on the object, and the optic subassembly is positioned on the object. Once positioned the fibre optic cables and gas lines can be installed. See Figure 5 in the *in situ* experimental section below.

In this configuration the object is not heated above ambient conditions, as such the HDR can be considered to function as a controlled atmosphere micro-fadeometer or as a FLEC with added lighting control and spectroscopy.

8.3 Case Studies

8.3.1 Real Time Gas Analysis and Colorimetry with HDR-FAIMS-FORS

8.3.1.1 Introduction

It has been estimated that in some countries nearly all books printed between 1850 and 1990 are on acidic paper (483, 484), and if immediate conservation measures are not taken, these materials are in immediate risk of being lost. Moreover, through the emission of VOCs (179, 435), these papers can increase the rate of degradation of other papers in their immediate environment (92, 220, 485). In this regard volatile organic acids are a particular concern as they can catalyse cellulose hydrolysis (92, 485, 486). However, the VOCs emitted from paper can also provide information about its chemical and physical properties. Volatile aldehydes have proven useful in diagnosing degraded paper and correlate to pH, (155, 205, 220, 225). The VOC profile can be correlated to paper type (9, 179, 435). Łojewski *et al.* have correlated chromatographic studies with spectroscopic studies (225), and other researchers have used NIR spectroscopy and colorimetry to non-destructively evaluate paper properties (23, 24, 26, 318, 487). Thus VOCs from paper can be considered both a threat and an information source (436). Several research projects have aimed to develop methods to interpret the smell of an old book, and other heritage materials, and use the generated information to inform conservation decisions (171, 488).

In most of the above cited studies, the evolved VOCs were pre-concentrated on solid phase micro extraction (SPME) fibres or TDT before being analysed by GC-MS. GC-MS analysis is time consuming and expensive, and the technique is not amenable to real-time measurement. However, a new technology, field asymmetric ion mobility spectroscopy (FAIMS) has been proposed as a method that can be used for rapidly surveying the VOCs emitted by books.[37] According to the manufacturer's website (217), once trained on a known sample set, FAIMS can be used to detect multiple gasses in complex mixtures down to ppb levels. However, until recently, FAIMS technology has only found application in military, home land security and industrial applications, and as such there is a paucity of publications on the application of the technique. The lack of publications makes it difficult to evaluate the potential of FAIMS for application to heritage science, however it was proposed that the HDR, which had previously been successfully interfaced with thermal desorption tubes (TDT) to collect and analyse by GC-MS the VOCs emitted from paper samples, would be a suitable interface with a FAIMS unit. If a well-characterised paper was analysed with both TD-GC-MS and FAIMS the resulting data sets could be compared and correlated.

Model paper 3 (P3) was selected was selected for this purpose (489). Previous TD-GC-MS analyses of P3 identified a complex mixture of hundreds of VOCs (205, 225), but with major contributions to the TIC from

---

[37] The British Library purchased a FAIMS unit for this purpose, and the AHRC funded project Heritage Smells will evaluate the applicability of the technique. Independent research along the same line is being conducted by the author at Jagiellonian University in Krakow.

acetic acid, furfural, and vanillin. As these compounds are detectable by FAIMS, it was proposed that the FAIMS unit could be used to generate a fingerprint P3 and this stored fingerprint could be used to identify similar papers. Additionally, it was proposed that the HDR-FAIMS-colorimetry could be used to follow the degradation of P3 during simultaneous light and thermal degradation.

Presented below are the preliminary results from the first attempt at HDR-FAIMS-colorimetry integration. I must admit that the results are less than successful in generating usable data on VOC evolution in real time with FAIMS, but are more than successful in demonstrating FAIMS has potential to fingerprint paper as well as illustrating a problem in the HDR design.

8.3.1.2 Materials

8.3.1.2.1 Paper

P3, supplied by the Center for Paper and Board Research (TNO, Delft, Netherlands) was used. This unsized paper was prepared from a mixture of 30% ground wood and 70% bleached sulphite pulps from softwood sources. The paper was prepared with kaolin filler and alum, and it has an ash content of 2.0% by weight. It tests positive for lignin with phloroglucinol. It has a pH of 5.9 by the cold extraction method, and water content of ca. 4.5% after storage at 23 °C and 50% RH (489).

Samples, 4 cm to a side (16 cm^2 external surface area), were cut and weighed on an analytical balance prior to their characterisation.

8.3.1.2.2 Gases

Dried and compressed nitrogen, as supplied by a nitrogen generator, was used in this study. Prior to introduction to the sample chamber, the gas was passed through an activated carbon and molecular sieve filter to remove any VOCs and reduce the water content that might be present. The relative humidity of the gas stream was monitored by an RH sensor integrated into the FAIMS unit and was found to be ca. 1.3% during the measurements. The gas flow was controlled by a micrometer-driven needle valve at the entrance to the HDR and a flow meter at the exit to the FAIMS unit. The gas pressure was kept at 1 bar and the flow rate at 1 l/min throughout the experiment.

8.3.1.2.3 Light Source

Two light sources were used in this experiment.

A Leica EL6000 mercury metal halide light source was integrated into the HDR via a liquid light guide with a 4 mm core fitted into the 45° lens fixture. This high intensity source is normally used for fluorescence microscopy and has a UV component and a significant IR component. This light source was used for photodegradation of the sample and was operated at full power which saturates the power meter, and

indicates that the output is well in excess of 200,000 lux. Due to the fact that the EL6000 has a noticeable flicker, a second, stabilised light source was used for colorimetry.

An Ocean Optics LS-1 tungsten halogen source, interfaced via a 200-micron fibre optic to the 0° lens fixture. This light source was operated continuously during fading and colorimetric measurements, while the EL6000 was shuttered to prevent saturation of the spectrometer.

8.3.1.3 Methods

8.3.1.3.1 Colorimetry

The diffuse reflectance spectra of the samples were recorded with an Avaspec 2048 spectrometer (Avantes), at 45 ° via a 200-micron core, solarisation resistant fibre optic. The total reflectance of the system was calibrated with a Spectralon diffuse reflectance white standard before each measurement. The integration time was 1000 ms; the boxcar width was set to 1 and the scan averaging was set to 1 scan.

The CIE 1976 colour parameters L*, a*, b* at D65 and 2° observer were calculated by AvaSoft 7.0 control software (Avantes) at 5 min intervals and exported to Excel for analysis. The CIE ΔE* values were calculated from the measured CIE values according to the following formula:

$$CIE \; \Delta E^* = \; \sqrt{((L_1 - L_o)^2 + (a_1 - a_o)^2 + (b_1 - b_o)^2)}$$

Equation 1

8.3.1.3.2 Evolved Gas Analysis

The HDR was interfaced with a LoneStar FAIMS (Owlstone Nanotech) via 1/8 inch copper tubing. Gas flow was maintained at 1 l/min at a pressure of 1 bar. The RH, as measured by the sensor integrated in the LoneStar, was relatively constant at 1.3 ±0.5 % giving a stable signal. The instrument was operated in dispersion field (DF) matrix mode with a full dispersion field sweep from 0 to 100% with 26 lines collected per sweep. Both positive and negative ion spectra were collected. The background was recorded by purging the empty HDR sample chamber with dry nitrogen and recording the relative ion peak (RIP) value. Once the background was established the paper was loaded into the HDR, and the flow rate and pressure were allowed to stabilise at 1 l/min and 1 bar before spectra were recorded. Readers are directed to the Owlstone Nanotech website where they can find information and animations describing FAIMS and how it can be used for gas analysis (217).

8.3.1.3.3 Accelerated Degradation

The samples were loaded into the HDR at 40 °C. Prior to the initiation of the degradation regime, the HDR was purged with the dry gas stream for 5 min to allow for the gas flow rate to the FAIMS to stabilise. During the gas flow stabilisation period the reference spectra for colorimetry were collected. After stabilisation the HDR was ramped up to 50 °C and the shutter on the EL-6000 light source was opened. It should be noted

here that the light was of sufficient intensity that definite browning of the paper was observable after 10 min.

8.3.1.4 Results and Discussion

8.3.1.4.1 Colorimetry

Integration of FORS and colorimetry with the HDR is relatively simple as the optics subassembly can be positioned on a white standard for the collection of calibration spectra before it is mounted on the temperature control subassembly. Once mounted above the sample a reference spectrum can be collected for either colorimetric analysis or conversion to absorbance-like spectra.
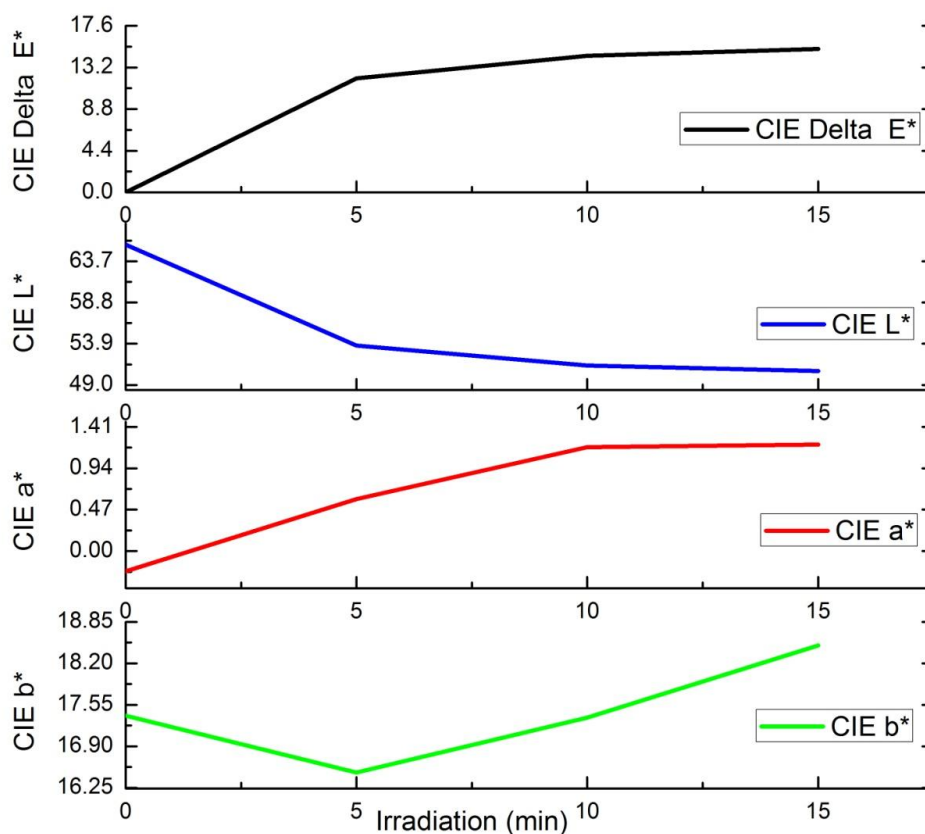
Figure 3 Colour change of P3, sample 2, during light degradation at 50 °C under 1 l/min flow of nitrogen.

Table 1 Colorimetric data from light degradation of P3, sample 2

Heating to 50 °C (min)	Irradiation (min)	CIE L*	CIE a*	CIE b*	CIE Δ E*
5	0	65.67	-0.23	17.38	0
10	5	53.67	0.59	16.49	12.06
15	10	51.3	1.18	17.35	14.44
20	15	50.64	1.21	18.48	15.14

Table 1 and Figure 3 present the colorimetry results from P3, sample 2. Previous experiments using the HDR at higher temperatures indicated that heating of the lens fixtures and optical fibres can result in a change to the measured colour values. To account for this, the sample was placed in the sample compartment of the HDR, which had been pre-heated to 50 °C, and the optics subassembly was mounted. The temperature of the HDR was allowed to stabilise for 5 min under a flow of nitrogen at 1 l/min before the reference colour coordinates of the sample P3, sample 2, were collected. This thermally-corrected reference was then used for colour change calculations.

I proposed that this thermal conditioning could affect the colour of the sample. This was tested by taking an identical sample of paper P3 and recording the reference spectrum at ambient temperature using a HunterLAB ColorQuest XE Colorimeter (HunterLAB, USA) with a 1-cm mask. The sample was then heated in air to 50 °C on the temperature control subassembly of the HDR for 5 min. After heating the sample was removed from the HDR and allowed to cool to ambient temperature and the colour coordinates were again recorded with the colorimeter. The measured CIE ΔE* of 0.1 was considered to be insignificant.

The effect of simultaneous light and thermal degradation was then evaluated. The HDR was maintained at 50 °C with the 1 l/min flow of nitrogen, the optimal flow rate for the LoneStar, and the shutter of the EL-6000 light source was opened for 5 min. At 5-min intervals the shutter was closed and the colour coordinates were recorded. Manual operation was necessary as it was not possible to integrate the control software for the light source and the spectrometer. The recorded colour coordinates were exported to Excel and the CIE ΔE* was calculated from the reference spectrum. The CIE b* values were seen to initially decrease after 5 min of irradiation indicating a loss of yellowness, therefore bleaching of the carbonyl chromophores (49, 50, 490, 491). Further light exposure led to a nearly linear increase in CIE b* values indicating yellowing of paper and the formation of new chromophores. The CIE L* and CIE a* mirror each other in their respective decrease and increase, indicating a general darkening of the paper. Levelling off of the CIE ΔE* value at 15.14 was observed after 15 min photodegradation at 50 °C under anoxic conditions. That much of the observed colour change was observed in the first 5 min of photodegradation argues for the need to reduce the light intensity and to increase the sample rate so that better kinetic resolution of the degradation can be observed.

8.3.1.4.2 Evolved Gas Analysis

The evolved VOCs were characterised concurrently with the colour measurements. To accomplish this, the effluent gas port on the HDR was connected to an Owlstone Nanotech, LoneStar FAIMS unit via 45-cm of 1/8-inch copper tube, and brass Swagelok fittings. The Dispersion field (DF) matrices from a full dispersion field sweep from 0 to 100% with 26 lines collected per sweep were recorded. Each measurement required ca. 70 s to complete.
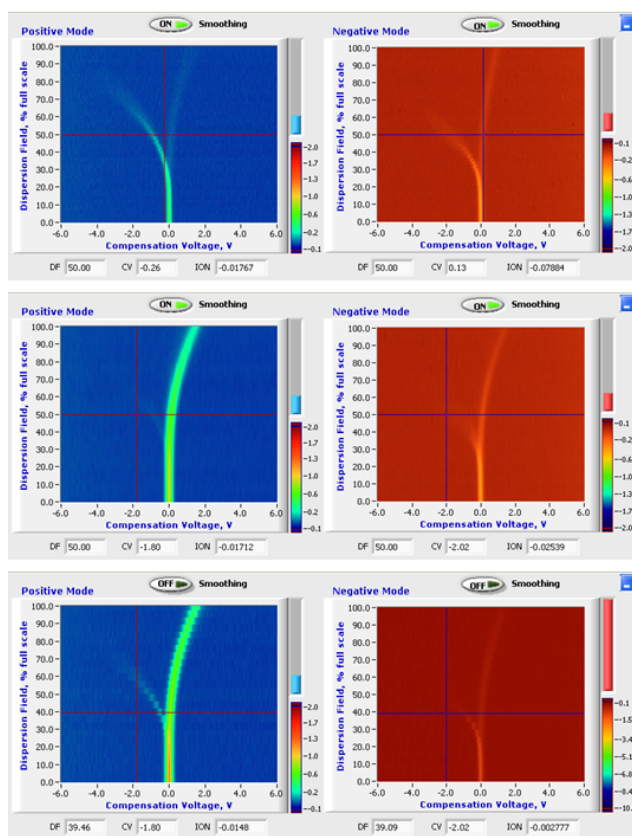
Positive and negative DF matrices generated by FAIMS from an empty HDR at 50 °C. The signal is typical of the RIP resulting from dry nitrogen.

Positive and negative DF matrices generated by FAIMS from P3, sample 2 after 15 min irradiation at 50 °C. under dry nitrogen. Both the positive and the negative matrices are distinguishable from the RIP.

Positive and negative DF matrices generated by FAIMS from an empty HDR after 2 h of 1 l/min flow of nitrogen following the test of P3, sample 2. There is still a clear presence of contaminants.

Figure 4 DF matrices generated by FAIMS from the sample P3, sample 2. The first pair of DF matrices are of the relative ion peak (RIP). The RIP is analogous to the background in a FAIMS measurement. The second pair of DF matrices are from photo- and thermal- degraded P3. The third pair of DF matrices are from carry over following the degradation experiment.

Prior to loading the sample into the HDR, a blank was generated by recording several DF matrices from the empty HDR held at 50 °C, with irradiation, and 1 l/min flow of nitrogen at 1 bar pressure through the unit. The top pair of positive and negative matrices in Figure 4 are typical of the blank sets generated from the HDR. The 'blank' DF matrices from the HDR were then compared to the DF matrices from the FAIMS unit in self-purge mode under the same operating conditions and were found to be similar and typical of the relative ion peak (RIP) observed with the FAIMS when dry nitrogen is used as the carrier gas. Therefore, the blank matrices could be used as the zero point reference for evaluating matrices from the paper samples.

The sample P3, sample 2, was then loaded into the HDR for the colorimetry experiments described above, and the DF matrices were recorded during 20 min of thermal and photodegradation experiment. After loading the sample into the HDR it took approximately 3 min to establish a stable gas flow of 1 l/min at 1 bar pressure through the HDR. Once a stable flow was established the DF matrices were continuously recorded as above. An immediate significant difference was observable in the matrices indicating a different population of gasses. Figure 4 presents (middle pair of matrices) the final DF matrices after 20 min at 50 °C and 15 min under irradiation.

However, after the initial 3 sets of DF matrices, the shape and intensity of the DF matrices did not change with further thermal and light degradation. Several hypotheses were proposed to explain this:

- The FAIMS detector was saturated.
- The VOC signature of the sample was not changing significantly during the degradation period.
- An emitted VOC had a near-constant concentration in the gas phase during the measurement period, and this particular VOC had a high proton affinity. Therefore it is selectively ionised and detected by FAIMS.
- There was a cold spot in the experimental set up resulting in the condensation and carryover of VOCs.

The fact that P3 has a strong vinegar odour indicates that acetic acid is present in ppm quantities (435, 492). This fact supports the first hypothesis, that the FAIMS detector was saturated by a VOC. However, this hypothesis was easily ruled out by the fact that the gain control on the DF matrix viewer needed to be set to quite a high value for the ion count from the signal to be discernable from the background. A flow rate of 1 l/min through the HDR effectively reduced the concentration of the VOCs to low enough levels such that detector saturation was not a problem.

The second hypothesis, that P3 was not changing significantly during the degradation regime, can also be eliminated. The observed colour change is indicative of chemical changes to the material. It could be that the sample was changing significantly, but that the high gas flow rate diluted these changes to below the detectable limit of the FAIMS instrument.

The third hypothesis, that a particular VOC is emitted at a constant rate under the experimental conditions, and that this VOC is selectively detected by FAIMS has not been excluded. Because FAIMS can be an incredibly sensitive technique to detect particular gasses in complex mixtures it finds most of its applications in the detection of explosives and chemical warfare agents. However, each gas molecule in the mixture competes for ionisation with all other gas molecules. Those with higher proton affinities are selectively ionised and detected by FAIMS, but the detectability of a compound is affected by the makeup of the background gas. If the compound of interest is vastly different from the normal composition of the background then isolation of the compound's signal is moderately simple, however if the compound of interest is chemically similar to the background gases, the job is much more difficult. The first half of this hypothesis is currently being tested by degrading a sample with the HDR for different time intervals and collecting the emitted VOCs on TDT for evaluation by GC-MS. The second half of the hypothesis will be tested in the future by collecting the FAIMS spectra of single organic compounds, and mixtures thereof, and comparing the resulting spectra for selective ionisation. However, this process of method development has only just begun.

The final hypothesis, e.g. the presence of cold spots in the experimental setup, was thought to be the most likely. The copper tubing, since it is not heated, was proposed as the source of the problem. Indeed, this was confirmed by removing the sample and repeating the blank measurement of the HDR; the DF matrices were identical to those collected when the sample was in the HDR. The copper tubing was then exchanged for a length of PTFE tubing and the resulting DF matrices were similar to the pre-run blank. In an attempt to evaluate the degree of carryover, the copper tubing was reconnected to the HDR and the unit purged with nitrogen. The lower pair of DF matrices in Figure 4 were taken after 2 h of flushing the HDR with nitrogen. There is still a clear presence of carryover, though differences can be discerned in the matrices: some small wisps visible in the negative mode for P3, sample 2, have disappeared indicating the absence of some VOCs from the gas mixture and the positive mode has slightly more RIP character. After 12 h of flushing, the DF matrices were similar to the RIP indicating that the carryover had been purged from the system.

8.3.1.5 Conclusions from Real Time Gas Analysis Studies

The HDR has been demonstrated as a suitable experimental platform for analysis of the degradation of paper samples.

1. Simultaneous light and thermal degradation under modified atmosphere is possible, though care must be taken not to use too intense irradiation as this can result in the pyrolysis or combustion of the sample.
2. The HDR can be used to generate VOCs from a sample for analysis by TD-GC-MS or in real-time with appropriate instrumentation, for instance FAIMS, gas phase PA-FTIR, TOF-MS.
3. During real-time gas analysis cold spots in the experimental setup can result in condensation and carryover during and between measurements. The sample transfer line needs to be redesigned.
4. FAIMS has the potential to be used to fingerprint papers, but, the method will require much development, both of the experimental protocol as well as generation of libraries of known samples and VOC blends.

8.3.2 *In-Situ* Light Fastness Testing of Modern Watercolour Drawings under Ambient and Anoxic Conditions

8.3.2.1 Introduction

Many colourants have been found to fade more slowly in anoxia than in ambient conditions, however, some colourants have been found to have the opposite behaviour, see Chapter 1 for a review. Therefore before anoxic treatment is applied to an object it is important to evaluate the object's light fastness in both ambient and anoxic conditions. This is typically done in one of two ways: the object and a micro-fadeometer are loaded into a glove box in which anoxia is established or the object is cased in an anoxic frame and the colour change is measured through the glass. In either method a sufficiently large glove box or anoxic case

are required to test the object. This can typically be arranged for smaller objects, but large or irregularly shaped objects can present problems. In the latter example, when the object is loaded into an anoxic test frame, the glass between the object and the micro-fadeometer can introduce errors in the measurements (due to surface reflections and refraction of the incident light) that can affect the reproducibility and reliability of the data.

A better solution would be to evaluate the light fastness *in situ* on the object by generating a localised modified atmosphere at the micro-fadeometry measurement spot. I proposed that the optics subassembly of the HDR could be applied *in situ* on an object to generate the desired atmosphere and conduct micro-fadeometry. To evaluate this, a test object was produced using known modern materials, and the light-fastness of the watercolour tested with the HDR. See Figure 5 for an image of the HDR being used on a watercolour drawing. If a suitable masking material is used, the HDR can be placed on an object without damaging the surface. Presented below are the results of this experiment.
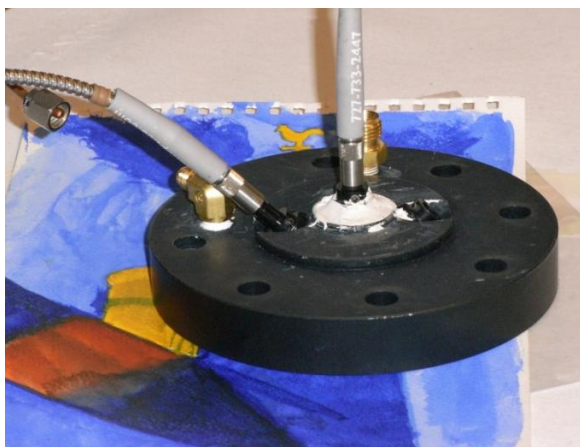
Figure 5 Image of the HDR optics subassembly positioned on a test object.

8.3.2.2 Materials

8.3.2.2.1 Watercolour Paint and Paper

The object selected for analysis is a contemporary watercolour drawing prepared with a Winsor and Newton (UK), Cotman watercolour set on Canon 100 double-sized, watercolour paper on the cold press surface. The pans of colours were wetted with tap water and applied in the wet-on-dry technique with no mixing and little over painting so that large areas of pure colour were available for testing. The colours used in the object are summarised in Table 2.

Table 2 Description of the watercolours used in the test object

Colour Name	Chemical Description	Colour Index Name	Colour Index Number	ASTM Light Fastness Rating
burnt sienna	synthetic iron oxide	PR101	77491	I
intense blue	copper phthalocyanine	PB15	74160	II
lemon yellow hue	benzimidazolone yellow H6G	PY175	11784	not tested

8.3.2.2.2 Gases

During anoxic measurements, zero grade argon, BOC, was humidified to 50 ± 5% by mixing dry and wet gas streams. The RH level of the final gas stream was monitored in-line in a mixing chamber with a TinyTag View 2, TV-4506, fitted with external T and RH probes. Once the RH had stabilised in the mixing chamber, the gas flow was directed to the sample chamber of the HDR via a piece of 1/8-inch copper tubing. The gas flow was regulated with a needle valve at the probe head to achieve a flow of gasses from the HDR sample chamber of ca. 1 ml/s as measured by a bubble flow-meter installed at the sample chamber's gas outlet. The sample chamber was purged with a flow of humidified argon for 30 min prior to initiation of the fading tests.

For ambient atmosphere measurements, no gas lines were attached to the HDR, and the gas ports to the HDR sample chamber were left open to allow for air exchange. During the measurement period the humidity of the standard room atmosphere remained at 50 ± 5%, as measured by a TinyTag View 2, TV-4506 (Gemini Data Loggers, UK).

8.3.2.2.3 Light Source

An Ocean Optics (USA) HPX 2000 35 W xenon source was attached to the optics head at 0° via a 400-μm core, solarisation resistant optical fibre. An extended hot mirror was placed in the filter holder between the source and the SMA fibre adapter. The light source was allowed to warm up for 30 min before use, and a shutter was used to block the light when necessary.

The spot size was estimated at 1.5 mm in diameter by fading a sample of Light Check Ultra(493) and measuring the observed damage spot via microscopy with a graduated reticule.

The output from the 74-Vis lens was measured with a light meter fitted with a cosine corrector. The measured value was found to be ca. 100,000 lux, although that is likely an underestimate of the value as the light meter is designed to measure fill light and not a point source.

8.3.2.3 Methods

8.3.2.3.1 Colorimetry

The diffuse reflectance spectra of the samples were recorded with an Avaspec 2048 spectrometer (Avantes, USA) at 45 ° via a 200-μm core, solarisation resistant fibre optic. The total reflectance of the system was

calibrated with a Spectralon diffuse reflectance white standard before each measurement. The integration time was 300 ms and 10 scans were averaged per measurement.

The CIE 1976 colour parameters L*, a*, b* at D65 and 2° observer were calculated by AvaSoft 7.0 control software, Avantes. Time series measurements were recorded with a 120-s interval and exported to Excel for analysis. The colour change of each sample was measured under each atmosphere two times, once for 60,000 s (1,000 min) exposure and once for 16,200-s (270 min) exposure. The CIE ΔE* values were calculated from the measured CIE values according to Equation 1 above. Due to noise in the data sets, particularly in some anoxic fading curves, the final CIE ΔE* value for each measurement was calculated to be the average of the last 10 CIE ΔE* values for each data set.

8.3.2.4 Results and Discussion

The pigments selected for this study are rated as permanent or highly permanent by the manufacturer, and their high permanence values make colour change difficult to evaluate in a work of art. However, a literature review indicates that burnt sienna (73) and phthalocyanine blue (2, 494) have both been identified as being less lightfast in the absence of oxygen than in air, and as such were of interest for the Anoxic Frames Project at Tate. The fading behaviour of benzimidazolone yellow H6G under anoxic conditions has not been evaluated; however as a common synthetic organic substitute for the variable, metal-chromate based 'lemon yellow' pigment, its fading behaviour is of interest for the project with regard to contemporary art.

Because such long measurement periods were required, the stability of the system was a real concern. The drift was evaluated by recording the observed colour change of a Spectralon white standard over the same interval. The measured drift was on the order 0.2 ΔE* in 60,000 s. Three measurements of 16,200 s were then recorded, yielding an average ΔE* 0.13 and standard deviation of 0.04, see Figures 6 and 7 below. Therefore any colour change observable in a colourant that is less than or approximately equal to this value cannot be discerned from the drift in the source.

Having established the measure of colour change attributable to the drift in the source, the colourants identified on the object were evaluated. The object was examined under a microscope and areas of pure colourant without mixing or over painting were selected for measurement. In preparation for measurement, the object was placed on a sheet of Melinex and the sample disk holder was placed on the object over an identified area of interest. The optics subassembly was then placed on the disk and the fibre optics attached.

Measurements under ambient atmosphere were conducted with the gas ports on the HDR left open to allow for air exchange during the measurements. During anoxic experiments humidified argon was supplied via gas lines, which were attached to the subassembly prior to its placement on the object. Argon was selected for establishing anoxia for several reasons: it is inert and does not interact with the object; if proper health and safety considerations are taken, it poses no risk for human life; and it is more dense than air so it is able to form a blanket over the exposed object surface in the sample chamber so that anoxia could be reliably

239

established. During both the anoxic and standard room atmosphere measurements, the relative humidity of the supplied gases remained within 50 ± 5% RH.
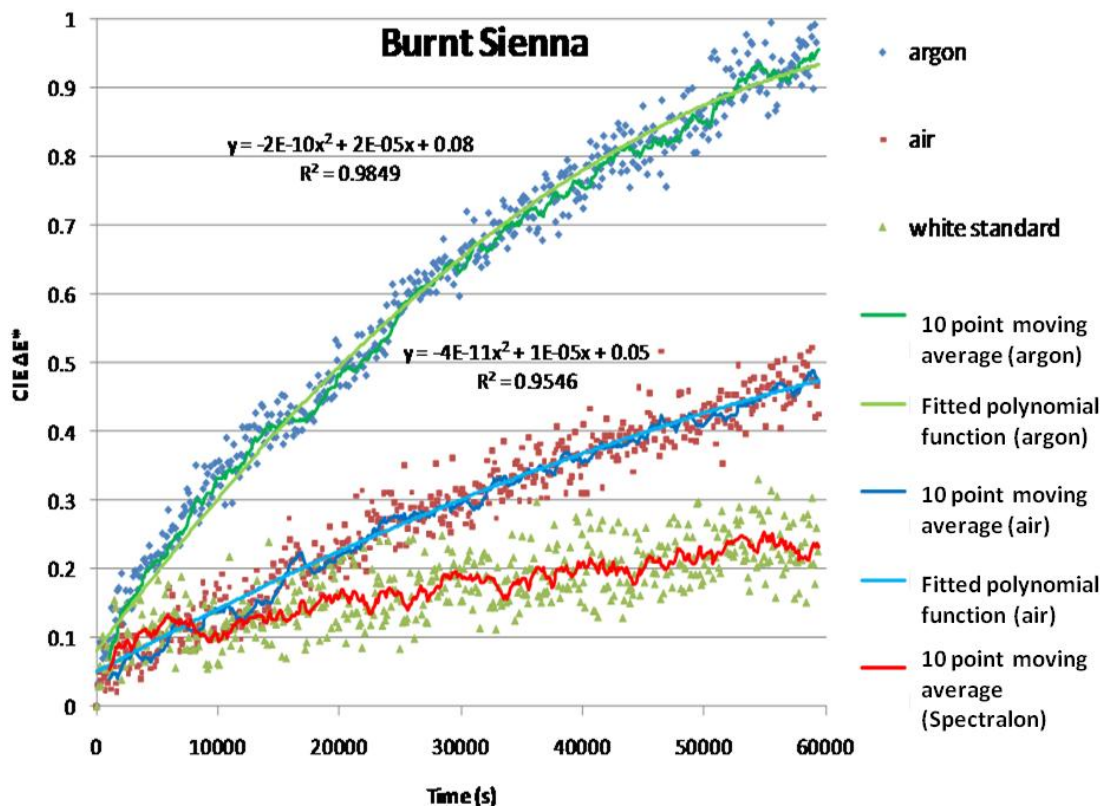
Figure 6 Fading of burnt sienna under argon and ambient atmosphere. The observed colour change of a Spectralon white standard has been included as a reference to evaluate the stability of the system during the measurement interval.

Figure 6 presents the colour change results of burnt sienna after 60,000 s (16.66 h) of light degradation under both argon and standard atmosphere. A clear difference between anoxic degradation (CIE ΔE^* = 0.94) and light degradation under sambient atmosphere (CIE ΔE^* = 0.47) is easily discerned, and curves can be fitted to the data with very high confidences. Furthermore the observed colour changes are significantly greater than that observed on the Spectralon white standard (CIE ΔE^* = 0.23).

The experiments run under ambient atmosphere tended to exhibit less noise than those conducted under argon. The noise was particularly bad for the first two overnight experiments (brilliant blue and lemon yellow hue under argon). The noise was initially attributed to dimensional changes in the paper due to small differences in the RH between the argon and the ambient atmosphere. A change to the experimental set up prior to the overnight measurement of burnt sienna under argon, where the gas lines were secured to the lab bench with cable holders significantly reduced, but did not eliminate, the noise. Thus the noise observed in the previous anoxic experiments was likely due to amplification of ambient vibrations and their transmission to the optics head via the rigid copper gas lines. This new secured set up was used for all further measurements under argon atmosphere.
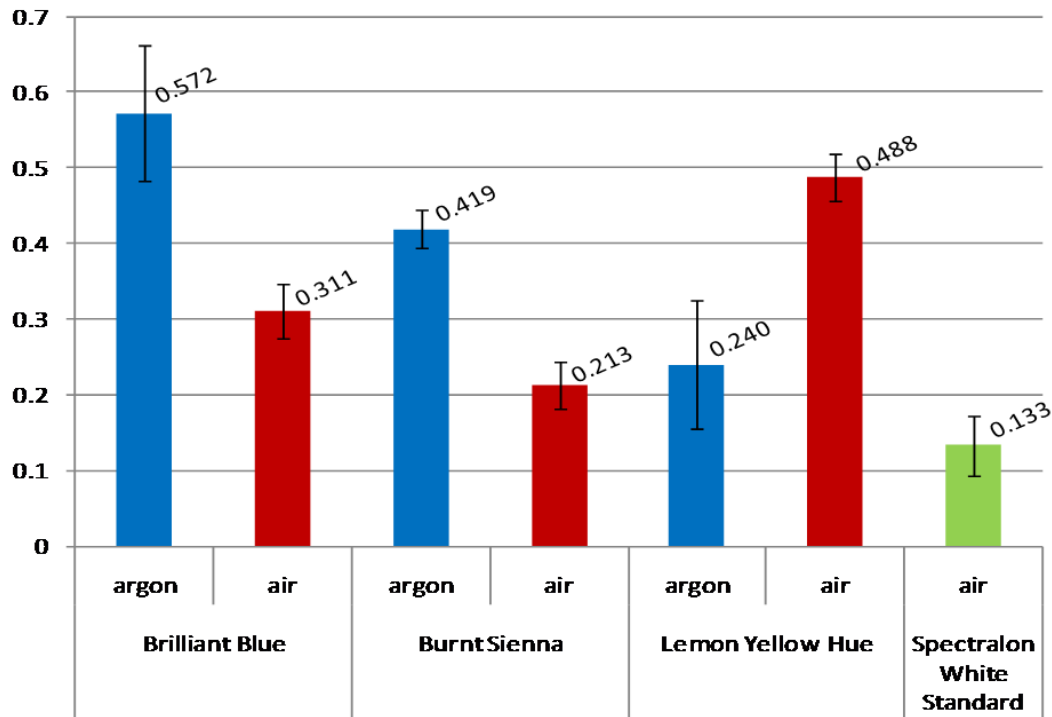
Figure 7 The average final CIE ΔE* measurements for the three colourants under anoxic and ambient atmospheres after 16,200 s degradation (450,000 lux h). The observed colour change of Spectralon has been included as a reference, and is attributable to drift in the light source and spectrometer.

While the ambient atmosphere measurements did not suffer from the same level of vibration-induced noise, they were still prey to the incidental events that resulted in jump-like steps, spikes, and breaks in the data. Such events were fairly common over the course of the Anoxic Frames Project and had been interpreted as arising from fluctuations in the power supply to the light source and 'impact events' which corresponded to the time when the cleaning staff were in the laboratory. Over the course of the research, several methods were developed to correct for most of these events with either smoothing, trimming the spike from the data series or by applying an offset factor.

Though longer measurement intervals lead to greater observable colour change, it was decided that they were too expensive in terms of consumed bulb lifetime. Furthermore, the risk of complications due to vibrations and other disturbances outweighed the benefits of greater observed change. Therefore it was determined that it would be better to repeat all of the measurements with a shorter interval of ca. 16,200 s (4.5 h), since two measurements (ambient and anoxic for a given sample) could be made in a single day. Figure 7 and Table 3 present the average CIE ΔE* after 4.5 h for the three colourants under two atmospheres and compares these to the average CIE ΔE* of the Spectralon white standard.

Table 3 Average CIE ΔE* at 16,200 s (450,000 lux h).

		CIE ΔE* at 16,200 s	Standard deviation
brilliant blue	argon	0.57	0.09
	air	0.31	0.04
burnt sienna	argon	0.42	0.02
	air	0.21	0.03
lemon yellow hue	argon	0.24	0.08
	air	0.49	0.03
Spectralon white standard	air	0.13	0.04

Even at this shorter time interval the differences in fading behaviour can still be discerned for all of the samples. Brilliant blue (copper phthalocyanine) and burnt sienna both faded significantly faster in anoxia than in ambient atmosphere. This is in good agreement with the literature (2, 73, 494). Lemon yellow hue, benzimidazolone yellow H6G, faded twice as fast in standard atmosphere than in argon, thus indicating some small but measurable benefit of anoxia for the colourant.

Most of the observed colour changes are larger than that attributed to the drift in the light source, as estimated by the CIE ΔE* of the Spectralon white standard. However, the changes in burnt sienna under air and lemon yellow hue under argon are both close to within one standard deviation of the observed changes in the white standard, and could be interpreted as being below the threshold of observable change.

8.3.2.5 Conclusions from *In Situ* Lightfastness Testing

The optics head of the HDR can be used for *in situ* applications on works of art on paper.

1. The larger spot size (1.5 mm in diameter compared to the 0.25 – 0.5 mm diameter spot size of a typical micro-fadeometer) results in reduced intensity and thereby requires a longer measurement period. This is particularly pronounced for colourants with high permanence, which can require several hours for a colour change to become discernable from the system drift.

2. Care must be taken during measurements, particularly during long-duration experiments, to limit sources of mechanical noise. The gas lines and fibre optic cables should be secured to the lab bench to avoid amplification of vibrations which can disturb the optics subassembly.

3. If the object surface is smooth enough, the optics subassembly, once fitted with secured gas lines, can be used to establish an anoxic environment above the sample surface by purging the sample chamber with argon. Thus the effect of anoxia on the fading of colourants can be evaluated *in situ* on an object thus the HDR capabilities beyond those of a standard micro-fadeometer.

4. While more repetitions are required to verify the results, it appears that burnt sienna and copper phthalocyanine fade faster under anoxic conditions than, and Benzimidazolone Yellow H6G receives a small benefit from anoxia.

8.4 General Conclusions about HDR

Based on my use of the instrument, while there is much room for improvement, I can say that the basic design of the HDR is sound, and it can be reconfigured for different *operando*-type experiments involving real-time spectroscopic and evolved gas analysis of degradation reactions and in *in situ* studies. Nevertheless, several points can be improved to increase the functionality of the instrument and reduce cross contamination between samples.

1. An important improvement would will be the use of stainless steel as opposed to aluminium. As this instrument was intended to be a proof of concept rather than a finished product, aluminium was selected as it was significantly cheaper and easier to machine than stainless steel. However, aluminium must be hard anodized to seal the surface; if this process is not carefully executed a porous, rather than sealed surface can result. This was the case with the present HDR, and the anodizing has to be removed from the sample compartment by abrasive polishing.

2. In the next iteration, CNC machining of the optics subassembly will be used to improve the accuracy of the alignment of the optics subassembly. Other lens assemblies, such as fast achromats could be substituted for the collimation lens systems to allow for better focus and smaller spot size. A useful addition might be a bore scope, so that the illuminated spot can be imaged and its position confirmed.

3. There is also a need to install pins into the temperature control subassembly to align both the sample holder disk and the two subassemblies. This can be done on the present HDR prototype to increase the usability of the instrument.

4. The efficiency of the temperature control system needs to be evaluated. In the present HDR a single-stage peltier device is used with a simple heat exchanger and fan. This gives an effective temperature range of 10 °C below ambient to 75 °C. This may be helped by the application of thermal insulation to the optics subassembly, this will be evaluated in the future.

5. In the next prototype, a multi-stage peltier device will be used along with a more efficient heat exchanger to increase the temperature range to sub 0 °C to in excess of 100 °C. This will allow for exploration of freeze-thaw cycles as well as higher temperature degradation regimes.

6. If an array of reactors is constructed, thermal insulation between separate cells will be needed to retain independent heating and cooling efficiency.

7. The main application of the HDR to evolved gas analysis is both aided and hampered by cold spots in the instrument design. When fully assembled, the temperature control subassembly is controllably heated to the set point, but the optics sub-assembly is slightly cooler than the set point, and the gas transfer lines can be as cold as ambient temperature. When thermal desorption tubes are used to collect the evolved VOCs, it is desirable for them to be as cool as possible to inhibit break through. In this application, the HDR design excels in that the TDT is kept at nearly room temperature. However, if the HDR is to be used for real-time measurements during thermal degradation studies, a new sample transfer line must be developed. The present configuration, which uses copper tubing, creates a cold spot in the transfer line resulting in condensation of analytes and non-usability of the HDR for analyses. A low cost solution to make the HDR usable would be to use an inert, low thermal mass material, such as PTFE tubing, as the transfer line, and to minimise the distance between the HDR and the detector. A better solution would be to use a heated and insulated PTFE or deactivated stainless steel transfer line. These can be purchased ready-made with a temperature controller or produced with little difficulty in the laboratory.

8. The copper tubing also creates problems for *in situ* measurements as it seems to amplify vibrations in the room and transfer them to the optics subassembly resulting in more noise in the colour measurements. To address this problem, PTFE tubing could be used for the gas supply line, as it is less rigid than copper.

Despite the identified problems with the HDR design, it can be considered a moderate success. With some small modifications it should become much more useable for both *in situ* and laboratory applications. The low cost of the unit and the ability to generate concurrent and coincident data sets without interrupting the accelerated degradation regime make the HDR an interesting alternative to the standard practice of punctuated data collection during accelerated degradation. The next stage will be to implement the above identified changes and produce a new HDR prototype for further testing as well as to continue to utilise the present prototype for TD-GC-MS and *in situ* studies. If the next prototype proves to be more successful in limiting vibration and carryover, a small HyDRA will be produced and tested.

Chapter 9 Conclusions

Heritage science is an applied science with a specific target audience: heritage institutions and practitioners, and heritage science research should be conducted with a goal of knowledge transfer to museum (library, archive, etc.) practice. Therefore in drawing conclusions from this body of research it is useful to step back and consider a larger context. Where does anoxic research fit within the operation of a heritage institution? What pressures are there for anoxia? What prejudices must be overcome for anoxic display to become a tool used by conservators, curators and collection managers? These questions were always on my mind during my PhD research, and because I was based at Tate Britain, I had ample opportunities to discuss them with my colleagues in several departments.

What follows is a brief synopsis of the research and the conclusions drawn from each chapter. I will attempt to place this research within a larger context and propose how the results of this PhD can be translated into changes in practice.

9.1 Effect on Reduced Oxygen Atmosphere Display on Watercolour Drawings

With the research tools and methods I developed I was able to evaluate the effect of anoxic display on watercolour drawings.

- If we consider the paper substrate alone, chemiluminometry and viscometry are very good analytical methods. With chemiluminometry we can detect the formation of peroxides and charge-transfer complexes between molecular oxygen and the glycosidic bonds in cellulose as a result of irradiation of paper in air. The peroxides can decompose to form radicals which can then participate in the radical-based oxidation of paper. If the paper is irradiated in an oxygen-free environment the charge transfer complex is not formed and production of peroxides is reduced. That this corresponds to a reduction in the degradation of paper can be confirmed with viscometry. Therefore it can be concluded that anoxic display would be beneficial for the paper substrate.

- Chemiluminometry has also proven to be a powerful tool for evaluating the interaction between pigments and paper. In the case of madder lakes both pro-oxidative and anti-oxidative interactions were observed. It appears that for some of the madder lakes studied, transition metals, particularly copper, associated with the laking process can lead to catalytic pro-oxidative degradation of the paper substrate when the samples are irradiated under air. It was proposed that the anthraquinone-metal complex acts as a renewable photo-Fenton catalyst able to decompose peroxides. Madder lakes prepared with aluminium tend to show a protective anti-oxidative effect possibly acting as radical scavengers. The pro-oxidative effect was not observed when the samples

were irradiated under argon, thus indicating a beneficial effect of anoxic display. A pro-oxidative effect was also observed for samples with Prussian blue. When Prussian blue is irradiated with 400 nm or 700 nm visible light the Fe^{3+} centres are photo-reduced to Fe^{2+}. These Fe^{2+} centres can then act as a Fenton catalyst to decompose peroxides, and in turn be oxidised to re-form Prussian blue. The radicals formed by the decomposition of the peroxides can then oxidise the cellulose leading to accelerated loss of degree of polymerisation as measured by viscometry. As above, Irradiation of the samples in argon inhibits the formation of charge transfer complexes and new peroxides. However, long-lived, stable peroxides formed frior to the application of anoxia can still be decomposed toradicals by photoreduced PB thus leading to degradation ofthe paper substrate. Therefore, anoxic display would not give the same protection to sections of a WOP that have been paintedwith PB as compared to the unpainted sections.

- Because Prussian blue is known to fade faster in anoxia than in air, the fading and reversion of Prussian blue was a particular concern for the AFP. Using XANES we were able to probe electronic transitions of PB during irradiation with visible light under air, nitrogen and helium. We found identical transitions regardless of atmosphere, indicating that the fading PB in anoxia is identical to that in air and thus offers no hazard for a watercolour containing PB.

- Using non-targeted degradic footprinting significant differences were observed between samples photo degraded under argon and those under air. Based on the TICs, generally the headspace of samples degraded in anoxia was less populated than of those degraded in air. Several chemometric models were constructed that were able to cluster samples according to degradation atmosphere, duration of degradation and applied pigment. In most cases the models were able to correctly assign samples to the anoxic class even when the argon had leaked from the vials by the time of analysis. Based on the VOC profiles it was possible to begin to propose degradation pathways for the samples. Importantly, this method is in principle non-destructive and should be transferable to museum practice. A sample of a VOC sorbent, such as carbon cloth, which had been enclosed with the object/mount system in an anoxic frame, can later be used as a sample pre-concentrator in a solid-phase-extraction-thermal desorption GC-MS technique. Further research will need to be conducted to detail a degradation pathway model, correlating specific VOCs to paper properties, but once constructed degradic profiling should prove to be a useful way of evaluating the degradation of a WOP in an anoxic frame, a MC frame, or any other display/storage environment.

- With real-time sampling, and the ability to simulate complex multi-parameter degradation environments, the HDR should prove to be a useful laboratory tool to develop degradation models of WOP.

- The *in situ* operation mode of the HDR extends the capabilities of micro-fadeometry to include evaluation of the effect of modified atmospheres on fading rates without sampling or placing the object in a glove box. It has proven effective for generating a localised anoxic environment and non-

destructively evaluating the fading of colourants on a WOP under argon and air. This tool will be useful for institutions to quickly evaluate the effect of anoxia on a particular WOP.

9.2 Why Anoxia? Why Now?

Heritage institutions are charged with the twin duties of caring for and providing access to the objects in their collections. For a vast body of objects in a collection the balance between access and preservation is struck with reasonable ease, however, for objects that are deemed to be light sensitive these duties can seem mutually exclusive, and balancing optimum preservation and optimum access can be an acute challenge for heritage institutions.

WOP particularly watercolour drawings, are a good example of objects that challenge the preservation/access balance. For WOP, after the identity of the artist, the visual impact of the object is one of the key value-defining parameters. Damage to an object can then be broadly defined as any process that alters an object's visual impact. Thus the goal of preservation of an object is to limit changes to the visual impact of an object, hopefully while ensuring continued access to the object.

At many heritage institutions the best practice is to err on the side of caution and limit access (in terms of display, loans out and, in some cases, access to objects for scholarly study) in favour of their preservation. While this practice is generally good for the object and will help to preserve it for future generations, it is difficult to justify for high-profile, national treasures when there is a public and perhaps politically perceived obligation to display such objects as much as possible to justify their acquisition (495, 496). Furthermore, the role of museums in society is changing, and public accountability through access to objects is a common theme in the UK in particular, as can be seen by the by the conference proceedings of the 2008 IIC meeting *Conservation and Access* (497), and this provides a stimulus to develop new display methods that allow for greater access through display without jeopardizing the long-term preservation of the objects in question.

Fiscal pressures in the form of budget cuts and rising energy costs provide a stimulus for heritage institutions to try to do more with less (495). This can translate into cuts in services and core activities, but under good institutional management it can also spur innovation so that deliverables can still be met. Good examples of this are micro-climate (MC) frames and show cases (498, 499), of which anoxic frames can be considered a subset. Through low air exchange rates MC frames offer better humidity control and protection from exogenous pollutants than room- or building- wide heating ventilation air conditioning (HVAC) systems (498-501). MC frames tailor the environmental control to each object, enhancing the objects' preservation and allowing for looser environmental (temperature and relative humidity) control in the gallery space thereby reducing institutional operating costs by decreasing dependence on HVAC systems (498). Thus MC frames give better value for money by focusing energy expenditures on where it counts most, the objects.

9.2.1 A Solution in Sight?

MC frames offer only a partial solution. While they allow looser gallery-level environmental control, they do nothing to limit light damage of objects. An ideal solution would offer all of the benefits of MC frames as well as address light damage issues so that heritage institutions can display specific objects longer in long-term displays, under higher light levels and looser environmental control. As extensions of MC framing, anoxic and modified atmosphere frames may offer such a solution. While MC frames are now a standard part of the conservation/preservation tool box, there is much resistance to – or at minimum serious concern about - the adoption of anoxic framing policies at many institutions. Based on the discussions at the symposium, *Anoxia and Microfading the Impact on Collection Care*, Tate Modern 12 – 13 September 2011, the resistance to anoxic display, at least for WOP, seems to arise from 3 factors: risk perception, an unclear cost-benefit relationship and a lack of a clear decision guide for end users. Overcoming these three factors will be the next challenge for anoxic research.

9.2.1.1 A Risky Situation?

Anoxic display is seen by some museum professionals, particularly those responsible for collection care decisions, as imposing undue risk to an object.[38] Certainly anoxic display of a WOP exposes it to hazards, and thereby risks, just as does standard display practice. But does anoxic display expose a WOP to new hazards that it would not otherwise encounter during normal display practice?

If we return to the object D03635, Figure 1, we can see the effect of long-term display in standard atmosphere on a watercolour drawing. This object was part of the First Loan Exhibition, and was nearly constantly displayed in natural light (likely including near- ultraviolet light transmitted by window glass) from 1869 to 1931 (169). In his 1909 catalogue, Finberg noted that, where not protected by the passepartout the blue in the sky was faded to expose a warm brown wash (170). The fugitive blue in the sky is likely indigo, and the blue colourants elsewhere in the drawing, such as in water near the shore, which has not faded, are likely Prussian blue. The observed damage to this painting is considered to be normal degradation behaviour, albeit an extreme example, and for this and other WOPs during standard display the risk has been identified (502), and measures, such as reduced light exposure through rotated display and light level control, can be taken to reduce the risk damage. A certain amount of change to an object during normal display can be accepted as a calculated risk (503).

---

[38] Since 2006, I have been a member of anoxic research groups at two national museums in two different countries. I have also given several workshops on modified atmosphere framing solutions and worked as a private consultant regarding the display of WOP and textile objects in anoxia. Through this work I have had first-hand exprience with the different attitudes regarding anoxic framing. For many institutions and private persons decisions about object care represent sensitive information; out of discretion this section lacks specific references to personal communications; rather it is written based on a generalisation of my personal experiences and conversations with curators, conservators, collection managers, private collectors, etc.

Under anoxic conditions there are many unknowns (each colourant in the WOP will behave differently), and therefore the risk is more difficult for a practitioner to evaluate. If we can identify the differences between anoxic and standard display we can begin to evaluate the differences in risks associated with anoxic and standard display environments.

Figure 1 Duniquoich Hill, with Inveraray Castle and Loch Fyne; Figures on the Shore and in Boat, J.M.W. Turner, Tate, D03635, circa 1801-1810 © Tate 2011.

9.2.1.1.1 Oxygen Concentration

The obvious difference is in oxygen concentration; by definition, anoxic environments should have no oxygen, but in practice they may well include low levels of oxygen. Anoxia can be established by gas displacement (typically with argon or nitrogen), oxygen scavenging (leaving a reduced pressure atmosphere comprised largely of nitrogen and argon) or much less commonly by vacuum. The first of these is difficult to maintain, and it is also extremely difficult to prove whether it has been maintained over the middle and longer term, and not trivial to measure low-to-zero oxygen concentration in an enclosure even in the short term. The absence of oxygen has been perceived to be a hazard for some colourants leading to the risk of new fading behaviours for individual colourants, and differential fading for the object.

This is the case. One of the main purposes of anoxic display is to generate an environment where fugitive colourants fade at a slower rate. Unfortunately not all colourants are affected to the same extent, and some colourants, Prussian blue for instance, are perceived to fade faster in anoxia. The result is differential or selective fading of an object, but it must be stressed that differential fading already happens during standard display (that is the accepted risk which is generally not foreseeable in detail). Anoxic display will minimise the fading of most colourants and thereby generate a differential fade on a different vector than standard display (3) .

9.2.1.1.2 Relative Humidity (RH)

RH has been shown to affect the rate of degradation of the paper substrate (504, 505) and fading of colourants (506), and measures can be taken to control the water vapour partial pressure so as to establish a constant relative humidity (RH) in the anoxic cassette giving as good or better protection from RH extremes and fluctuations as when compared to standard display (499). In fact, like an MC frame the RH level in an anoxic cassette can be tailored to the object, rather than for the room, thus giving the potential for better preservation of the WOP.

9.2.1.1.3 Volatile Organic Compounds (VOCs)

The core requirement of anoxia is a hermetically-sealed microclimate to exclude atmospheric oxygen. As noted in Chapter 1, encapsulation of paper creates a sealed microclimate that is adverse to the long-term preservation of the objects. Several researchers have linked sealed degradation to the evolution and accumulation of acidic species as well as other VOCs within a microenvironment (33, 34, 86, 213, 238, 250, 499, 507, 508).

Like other encapsulation methods anoxic framing leads to the accumulation of VOCs in the headspace around the object-mount system, and some of these VOCs can participate in degradation reactions leading to auto catalytic degradation (32-34, 92, 205, 225, 322, 433). Therefore these VOCs must be mitigated through the use of VOC sorbents, such as activated carbon cloth (171), or a VOC scavenger such as $KMnO_4$, but more work is needed to identify the best sorbents/scavengers and how much of the material is needed for an anoxic cassette.
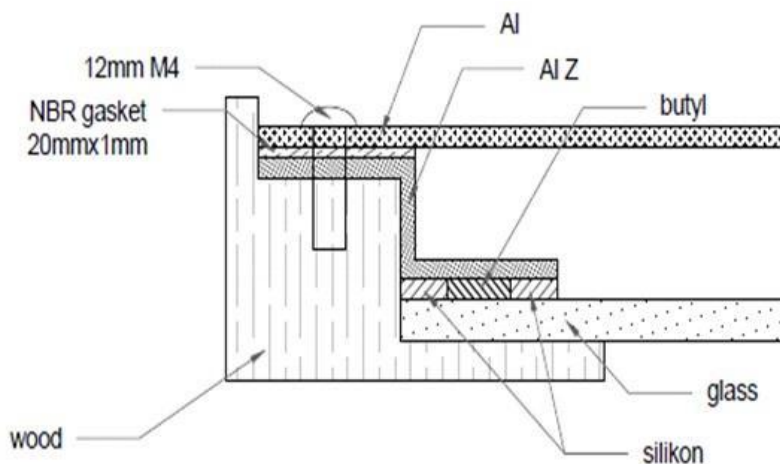
Figure 2 A cross section view of a variant of the anoxic cassette design I developed for the AFP. The frame is an aluminium z-section (Al Z) with welded corners. The glass is permanently fixed to the frame section with a combination of butyl mastic and neutral cure silicone adhesive, such as what is used for argon-filled, double-glazed structural glass. The aluminium back is secured with machine screws at 25 mm on centre spacing and sealed with a NBR (acrylonitrile and butadiene co-polymer) gasket. Decorative elements, such as a wooden frame, can be used to conceal the anoxic cassette.

However, unlike a standard glazed and backed wooden frame, which also produces and traps VOCs, all of the materials used in the construction of an anoxic cassette can be inert and low off-gassing, see Figure 2. Therefore most of the VOCs in the headspace of an anoxic frame should be from the object/mount system; quite the opposite was found for a standard Turner frame at Tate during the ProPaint project (499), where the high levels of acetic and formic acids were attributed to emission from the framing materials and a low air exchange rate (213, 499). Therefore through the use of inert materials, though better sealed, an anoxic frame will provide a better environment (in terms of VOCs) for a WOP than the standard glazed and backed wooden frames used at many institutions (213, 499, 501, 509).

9.2.3 At What Cost?

More than ever, in today's fiscal climate heritage institutions must make every penny count. Is anoxic display a more efficient use of resources than standard display? What are the trade-offs?

9.2.3.1 Price

One of the proposed benefits of anoxic frames, as well as MC frames is the reduction in the dependency on HVAC systems. This benefit is potentially huge in terms of percent of the yearly operating budget of a heritage institution, but to achieve it, all of the sensitive objects must put into a MC or anoxic frame. Until recently anoxic frames, such as those used for the *American Charters of Freedom* (57, 58), were prohibitively expensive and used only for high-value objects at the largest of institutions. I have implemented the design in Figure 2 for less than £50 additional materials cost (in Poland, in 2010) for an A2 sized object.[39] At this price, anoxic frames are affordable for nearly every institution and for entire collections. Suddenly, the potential cost-saving benefit of being able to reduce HVAC dependence seems achievable.

9.2.3.2 Access

Anoxic display has been proposed to increase the (viewing) access to objects. By limiting the fading of colourants and degradation of the paper substrate a WOP can be displayed for longer periods at higher light levels, but to achieve the full benefit the object should remain in its frame when in storage. When framed, it is not possible to access and interact with a WOP in the same way as when it is unmounted. As a heritage scientist interested in WOP, I visit prints and drawings rooms to examine objects, and I often want to see the reverse of WOPS, to examine them in transmitted and raking light, smell them, and if possible to touch them. A WOP in an anoxic frame limits access to an object for scholarly research, or necessitates additional costs if such access is granted to staff and researchers even once.

9.2.3.3 Storage and Display Costs

Anoxic frames, particularly for A1 and larger objects can be heavy. This will change the requirements for object mounts and decorative frame dimensions (possibly necessitating the re-think of gallery-wide uniform

---

[39] This assumes that the mount, decorative frame and glazing can be re-used.

framing policies, or the production of new standard frames). It might also affect the number of art handlers required to mount and demount an object, potentially raising the costs of exhibition changes (510).

If WOPs are to be stored in anoxic frames, then this will increase the cost of storage space. WOPs in anoxic frames will need to be stored like easel paintings on compact storage racks rather than in Solander boxes for instance.

9.2.4 Calculated Risk

Anoxic display is not inherently more risky than standard display; in fact I would argue that it is less risky. However, new risk evaluations for anoxic display of WOP need to be developed. This might be possible in terms of object classes, but it will likely need to be done on an object-by-object basis. In this scenario the more that is known about an object the easier it will be to evaluate the risk to an object, but it is not necessary to know the identities of the colourants in a WOP to evaluate it for anoxic display. The colour usage pattern can be mapped and weighted according to an object-specific scale based on their usage and contribution to the visual impact of the object.[40] Within these mapped regions, sample locations can be identified, and micro-fadeometry used to identify the least lightfast colourants and assign a fading rate, either in terms of unit colour change per unit time or in relation to the Blue Wool scale, to each colour region. These three factors: colour usage, visual impact contribution, and fading rate can then be used to calculate the risk of continuing standard display and the benefit of anoxic display.

A point that must be remembered, anoxic encasement is perhaps the easiest conservation treatment to reverse. If rapid and undesirable colour change is observed in an object once placed in an anoxic frame, it can be halted simply by returning the object to air. The risk of anoxic display is really minimal compared to standard display, if it is assumed that objects are display are inspected at least casually, and regularly.

9.2.5 The Forest for the Trees

Making the decision to change the display practice for an object, or a gallery of objects, is a great responsibility and it is not easy to make. First there are all the different reactivities of each component in each object, and many other factors need to be considered: the perceived value/significance of an object, its condition, intended display practice, loan policies etc (502). With all of the details, it quickly becomes a problem of not being able to see the forest for the trees. I attempted to simplify this problem by constructing several decision trees to help guide conservators and curators through the process of deciding whether an object should go into anoxic display and/or storage or not. A draft of these trees can be found in Appendix B at the end of this Thesis. The decisions are based on the chemical and physical properties of the objects but roughly weighted by object value/significance and display practice. I tested rough drafts of these

---

[40] For instance in D03635, Figure 1, I would weight the indigo of the sky higher (it is widely used and a change to this colour would significantly affect the visual impact of the object) than the Prussian blue used sparingly in the water.

decision trees at the NET-Heritage Project's - *International Workshop Heritage Science Education in a Changing World* on 6 April 2011 (511). I was able to guide users through their application, but they were not the self-help guides which I had hoped for. Many in that audience were not accustomed to regarding their daily work as a series of evidence-based judgements, that is, as object-by-object risk assessment. Yet the trend in conservation practice is towards adopting such collections-based decision making. I plan on reworking them into a more user-friendly, multi-page format as part of planned publication on anoxic display of WOPs.

9.3 Is Anoxia Safe?

Considering the data presented in the preceding chapters and briefly summarised above, it is possible to conclude that anoxic display will reduce the formation of reactive oxygen species, including peroxides, which can participate in photo- and autoxidation reactions of the paper substrate, gelatine size, binding media, and some colourants. This translates to a reduction in the rate of loss of DP of samples with and without pigment; however, this reduction is not the same for all pigmented samples and not to the same degree for pigmented samples as with paper alone. In no cases was irradiation of samples in anoxia observed to lead to greater degradation of paper (in terms of loss of DP or production of peroxides) than irradiation of identical samples in air in a sealed vessel. Therefore it can be concluded that anoxic display will be beneficial for WOP in terms of retention of mechanical properties.

However, photodegradation in a sealed environment, even in anoxia, leads to the production and accumulation of VOCs. Some VOCs, particularly organic acids, can have an autocatalytic effect on the degradation of paper, and therefore need to be mitigated. VOC sorbents such as carbon cloth have proven useful to reduce VOC levels in MC frames (171, 213, 499), but further research is needed to optimise the selection of VOC sorbents (213, 499). The VOCs can also be used as diagnostic tools to inform about the condition of the object (9, 173, 436). The degradic footprinting method used in this research should be transferable to museum practice by using the VOC sorbents as a solid phase extraction material for the headspace in the anoxic frames. Once specific VOCs have been correlated to paper properties (9, 204, 205, 220), this will be a non-destructive method to evaluate the condition of a WOP in an anoxic frame.

The developed heritage degradomics reactor can be used *in situ* to evaluate the effect of anoxia on the fading of colourants and the VOC profile of a WOP and thereby serve as a tool to screen an object for anoxia. If no colourants are found to irreversibly fade faster in anoxia than in air, and the object is not found to release large quantities of organic acids, then anoxic display will not be detrimental for the object and will lead to a measureable beneficial effect. If the object is found to be acidic then de-acidification, prior to any form of enclosed display or storage (including standard glazed and backed frames and Solander boxes) is recommended.

9.4 Innovative Character of the Research

The research for this Thesis began with a very general question, what is the effect of reduced oxygen display on WOP in Tate's collection? Tate's collection of WOP spans more than 500 years of art history and every imaginable artist's material. To make the project more manageable, the focus was narrowed to mid-19th century watercolours with an emphasis on the works of J.M.W. Turner. Answering even this reduced question has proven to be a challenge, and it has required much innovation:

- Preparation of model materials

  - Through collaboration with several researchers at Tate and abroad, but particularly Charlotte Caspers (167) and Chris Bingham at Ruscombe Mill, I have prepared reconstructions of some of Turner's paper, Chapter 4. This paper was then used to reconstruct some of Turner's painting techniques and paintings using watercolour paints prepared according to historical recipes with his studio pigments (166). These materials and reconstructions have featured in the AFP research which was summarised in a short paper "De/re-constructing Turner for research projects at Tate" published in *Sources and Serendipity* (166). Through my work in reconstructing a Turner paper I have contributed a chapter to the book, *How to Paint Like Turner* (348).

- Anoxic frame design and construction

  - I developed a low-cost, low form factor anoxic frame design for WOP. This design was presented as a conference paper and a short workshop at the conference *Showcases Inside Out* (512) and at the NET-Heritage Project's - *International Workshop Heritage Science Education in a Changing World* as a workshop (511). I have successfully tested this design in an accelerated photo-degradation chamber, during land and air transport and during gallery mounting, display and demounting. In all cases it was able to maintain anoxic conditions.

- Chemiluminometry

  - I developed a *recto* irradiation and *verso* observation method, which allows for chemiluminometry to be used on coloured samples. With this method I was able to study the photo-oxidation of watercolours, Chapter 5, under standard and anoxic atmospheres. My work on chemiluminometry of madder lakes has been published as an article in *Polymer Degradation and Stability* (8). My work with the chemiluminometry of Prussian blue contributed to a UK and US patent (405), and it will now be prepared as a publication in *Polymer Degradation and Stability*.

- X-ray absorption Spectrometry (XAS)

  - Through collaboration with Dr. Sven Schroeder, University of Manchester, and the Pigmentum Project, Oxford University, I successfully applied for beam time at Daresbury Synchrotron Radiation Source and Diamond Light Source to characterise a library of historic Prussian blue pigments and the fading of Turner's PB applied as a watercolour, Chapter 6. My work with Prussian blue contributed to a UK and US patent (405), and it will now be prepared as a publication in a suitable journal.

- Heritage Degradomics

  - In collaboration with the PaperVOC project, University of Ljubljana, Slovenia, I developed the concept of heritage degradomics, Chapter 2, which transfers metabolomics methods to the study of heritage materials. An introduction to this method was published as article in *Analytical Chemistry* (9) as well as conference papers (173, 436).

- Non-targeted degradic footprinting of watercolour drawings

- I applied a heritage degradomics method, non-targeted degradic footprinting with headspace-gas chromatography-mass spectrometry, to the volatile degradomes of watercolour drawings, Chapter 7. I was then able to construct several chemometric models able to discriminate between samples photo-degraded in anoxia and in air as well as between different pigment classes and between related pigments, such as different madder lakes.

- Design and construction of reaction cells

  - For the synchrotron beam times two reaction cells were specially designed and constructed. I significantly contributed to the design of the cell used at Diamond Light Source, and machined the components for its construction at Tate. The designs and applications of these cells will be prepared as a publication for a suitable journal.

  - I designed, constructed and tested an *operando* reaction cell for multi-parameter accelerated degradation studies, Chapter 8. This reaction cell, termed heritage degradomics reactor (HDR), can be used for thermal, photo, pollution, or combinations of all three degradation studies with control over temperature, light level, RH, and atmospheric composition. The degradation spot is measured in real time with simultaneous UV-Vis-NIR spectrometry and gas phase analysis. The HDR can be scaled up to a reactor array for combinatorial-type experiments or parallel Arrhenius-type experiments. It can also be used to study *in* situ the fading of a WOP under a modified atmosphere without the need to sample the object or place it in a glove box.

9.5 Further Research

This PhD has raised many new questions and highlighted exciting lines of research, some of which I am actively pursuing already.

9.5.1 Heritage Degradomics

I plan to further develop heritage degradomics by refining the data generation and handling methods. This will lead to a better model of the degradation of WOP and identification of degradation markers that can be used to evaluate a WOP in any display or storage environment. I will also plan to extend the degradomics method to other materials including silk, wool and synthetic polymers. I have established collaborations to continue this research.

9.5.2 HDR

I plan to have a new HDR machined out of stainless steel and to use silco steel fittings and PTFE gas lines to reduce carry over and vibrations. Once an inert probe is constructed this instrument should prove to be very useful for degradomics research

9.5.3 Prussian Blue

I will explore the photo-catalytic reactivity of PB and PB with ZnO in collaboration with researchers at Jagiellonian University Krakow, Poland; however, I have not designed the experiments. I would like to apply for beam time at a synchrotron facility to collect better data in the EXAFS region during the fading of PB. Some of the changes that were observed in this region are curious, and deserve further investigation. With complete spectra it should be possible to use computational tools.

9.5.4 Micro-Fading and Identification of Faded Organic Colourants

I am presently working on optimising the design and application of micro-fadeometry to colourants on a number of substrates. Some of this work has been published in *Review of Scientific Instruments* (474). I am also beginning pre-normative work trying to relate micro-fadeometry to standard photodegradation methods. In the near future I intend to begin to use atmospheric pressure inlet (API)-mass spectrometric techniques, possibly coupled to capillary electrophoresis (CE), to identify faded and unfaded colourants on WOP.

9.6 Beyond this Thesis

9.6.1 Application of Chemometrics in Conservation Science

The application of chemometric methods to conservation science is gaining in popularity, and it is beginning to re-shape the field. The SurveNIR project (23, 230) is perhaps the best example of how chemometrics can be used in heritage science to develop a non-destructive spectroscopy/chemometric based alternative to destructive sampling methods. The SurveNIR instrument employs near infrared spectroscopy (NIR) and advanced chemometric models based on the correlation of NIR spectral features to a database of measured paper properties, and it can be used to non-destructively survey a collection of WOP giving information about paper properties that could, until now, only be gained by destructively sampling the object (23, 26, 229, 230). However, while the SurveNIR instrument uses chemometric models to predict paper properties from NIR spectra, it does not give end-users access to those chemometric tools to answer other questions. For this two things are needed, a good statistics software package and the knowhow to use it and interpret the results. The former is a matter of resources and preference. As an average computer not accustomed to a command line prompt, I prefer software packages with a graphic user interface (GUI), and several are available like *XLSTAT* (ADDINSOFT), *Unscrambler* (Camo) and *Grams AI* (Thermo).These offer competitive

pricing and in the case of the last two, templates to directly import spectral data from many analytical instruments easing the data handling step. *MetaboAnalyst* (444), which I made extensive use of for this Thesis, gives users access to the powerful statistical programming language and environment *R* (R-Project), with a GUI and a set of recommendations to guide a novice user through the application of many multivariate and machine learning methods to the analysis of mass spectrometric data, and it is free to remotely use running on a server at the University of Alberta (444). However, software without knowhow is not useful. The knowhow is coming from how new heritage scientists, myself included, are being trained. Most of the recent heritage science PhD theses that I have read incorporate multivariate statistical analysis into their work. This is not to say that statistics was not used before in heritage science, but that the new users are more comfortable with the application of chemometrics and the use of statistical software. It is the combination of the availability of good, easy to use software and conservation scientists that are comfortable using it that is changing the face of conservation science.

9.6.2 Chemometrics for Degradation Studies

The tools and the knowhow exist, how can they be applied to degradation studies? Let's take the example of the degradation of WOP in an anoxic or MC frame. The first step in the process, determining if a non-targeted headspace approach can be used to discriminate between WOP photodegraded in different atmospheres is covered in Chapter 7. It was found that based on the volatile degradome it was possible to discriminate between the two sample groups, several supervised and unsupervised chemometric methods were employed and, they were in a remarkably good agreement. Many of these methods identified significant features that were best in discriminating between sample classes. The training sets for the chemometric models were composed of samples degraded for different intervals and with various applied colourants, thus forcing the statistical methods to select features that performed well regardless of the ageing time or applied colourant. I propose that this reduced feature set relates to the materials common across the samples: paper substrate, gelatine size and gum Arabic binding media. While on the other hand the entire degradome can be used for finer clustering, pigment type for instance.

These features can now serve as the starting point for the next stage in the process, identifying the compounds that gave rise to these features, and propose degradation pathways for their evolution in the volatile degradome. This will involve degradic profiling experiments to see how the populations of these features change with different degradation time and conditions.

Parallel to this research would be work to correlate features, or compounds giving rise to those features, to paper properties. Some research has already been done towards this goal (183, 184, 204-206, 294, 513). But a comprehensive study with well characterised model materials such as what was performed for the SurveNIR project (23-25, 230) will be needed.

A method of sample collection and introduction will need to be built. Because the proposed frame design will be hermetically sealed, a VOC sorbent will need to be enclosed with the object. Carbon cloth is a good candidate for this role, and conveniently it can be used for solid phase extraction of the volatile degradome. The method I imagine would be at the time of encasement, a known area of carbon cloth would be included in the anoxic frame, a sample of that cloth, again with known area would be taken and placed in a sealed vial in cold storage. Whenever the frame is opened a second sample, of known area, can then be collected and placed in a sealed vial. The two samples, the initial carbon cloth blank and the carbon cloth that had been exposed in the sealed frame can then be heated and the re-emitted VOCs analysed by HS-GC-MS. An internal standard could be included for normalisation of the resulting chromatograms which could be normalised by the area of the carbon cloth. After this point the chromatograms could then enter the data handling pipeline used in this research. Once processed the data can be related to the constructed chemometric models and the condition of the object evaluated.

9.6.3 Other Materials?

The research approach of heritage degradomics as outlined in this Thesis can be used to study the volatile degradomes of many other materials, heritage and otherwise. The application to WOPs, particularly watercolours that have a layered composite structure and use multiple colourants can almost be seen as a worst case scenario. An obvious subject of study would be the degradation of modern polymeric materials as used in sculpture. These, often high value, objects can be difficult to conserve and can degrade spectacularly quickly. The POPART project (514) is addressing the preservation of plastics in art; their work will provide a good starting point for a degradomics study of the same materials.

Considering all of the above factors, I expect heritage degradomics to be increasingly applied to understand the degradation of heritage materials and to inform the preservation of heritage objects.

References

1.   Lockett K, McKenzie B. Anoxic framing investigations at Tate to date. In: Rayner J, Kosek J, Christensen B, editors. Art on Paper: Mounting and Housing. London: Archetype Publications; 2005. p. 67-74.
2.   Townsend JH, Thomas J, Hackney S, Lerwill A. The benefits and risks of anoxic display for colorants. In: Saunders D, Townsend JH, Woodcock S, editors. Conservation and Access; London: IIC; 2008. p. 76-81.
3.   Thomas J, Townsend JH, Strlič M, Hackney S. A Review of Anoxia as Applied to Works of Art on Paper. Studies in Conservation.accepted for publication.
4.   Korenberg C. The photo-ageing behaviour of selected watercolour paints under anoxic conditions. British Museum Technical Research Bulletin. 2008;2:49-57.
5.   Kirby J. Fading and colour change of Prussian blue: occurrences and early reports. National Gallery technical bulletin. 1993;14:62-71.
6.   Kirby J, Saunders D. Fading and colour change of Prussian blue. National Gallery Technical Bulletin. 2004;25:73-99.
7.   Rowe S. The effect of insect fumigation by anoxia on textiles dyed with Prussian blue. Studies in conservation. 2004;49(4):259-70.
8.   Thomas J, Townsend JH, Hackney S, Strlič M. A chemiluminescence study of madder lakes on paper. Polymer Degradation and Stability. 2010;95:2343-9.
9.   Strlič M, Thomas J, Trafela T, Cséfalvayová L, Cigić Kralj I, Kolar J, et al. Material degradomics: on the smell of old books. Analytical Chemistry. 2009;81(20):8617-22.
10.   Whitmore P, Pan X, Bailie C. Predicting the fading of objects: identification of fugitive colorants through nondestructive lightfastness measurements. Journal of the American Institute for Conservation. 1999;38:395-409.
11.   Lerwill A. Modified micro-fading spectrometry: an investigation into the display of traditional watercolour pigments in anoxia. Nottingham: Nottingham-Trent University; 2011.
12.   Major W. The degradation of cellulose in oxygen and nitrogen at high temperatures. Tappi. 1958;41(9):530-7.
13.   Arney JS, Novak CL. Accelerated aging of paper, the influence of acidity on the relative contribution of oxygen-independent and oxygen-dependent processes. Tappi. 1982;65(3):113-5.
14.   Arney JS, Jacobs AJ. Newsprint deterioration, the influence of temperature on the relative contribution of oxygen-independent and oxygen dependent processes in the total rate. Tappi. 1980;63(1):75-7.
15.   Arney JS, Jacobs AJ. Accelerated aging of paper, the relative importance of atmospheric oxidation. Tappi. 1979;62(7):89-91.
16.   Malešič J, Kolar J, Strlič M, Kocar D, Fromageot D, Lemaire J, et al. Photo-induced degradation of cellulose. Polymer Degradation and Stability. 2005;89(1):64-9.
17.   Malešič J, Kolar J, editors. Photo-induced degradation of cellulose. 14th Triennial Meeting of ICOM-CC; 2005.
18.   Kolar J, Strlič M, Malešič J, Lemaire J, Fromageot D. Photooxidative degradation. In: Strlič M, Kolar J, editors. Ageing and Stabilisation of Paper. Ljubljana: National and University Library Ljubljana; 2005. p. 149-62.
19.   ISO. ISO 5351/1:1981 Cellulose in dilute solutions -- Determination of limiting viscosity number -- Part 1: Method in cupri-ethylene-diamine (CED) solution. ISO; 1981.
20.   Evans R, Wallis AFA, editors. Comparison of cellulose molecular weights obtained by high performance size exclusion chromatography and viscometry. 4th International Symposium on Wood Chemistry; 1987 1987; Raleigh.

21.	Strlič M, Kolar J, Zigon M, Pihlar B. Evaluation of size-exclusion chromatography and viscometry for the determination of molecular masses of oxidised cellulose. Journal of Chromatography A. 1998;805(1-2):93-9.

22.	Strlič M, Kolar J. Size exclusion chromatography of cellulose in LiCl/N,N-dimethylacetamide. Journal of Biochemical and Biophysical Methods. 2003;56(1-3):265-79.

23.	Strlič M, Cassar M, Kolar J, Lichtblau D, Anders M, Trafela T, et al., editors. NIR/Chemometrics approach to characterisation of historical paper and surveying of paper-based collections. ICOM-CC 15th Triennial Conference; 2008; New Delhi: James and James.

24.	Lichtblau D, Strlič M, Trafela T, Kolar J, Anders M. Determination of mechanical properties of historical paper based on NIR spectroscopy and chemometrics – a new instrument. Appl Phys A. 2008;92:191–5.

25.	Havermans J, Aziz HA, Penders N. NIR as a tool for the identification of paper and inks in conservation research. Restaurator. 2005;26(3):172-80.

26.	Trafela T, Strlic M, Kolar J, Lichtblau Da, Anders M, Mencigar DP, et al. Nondestructive analysis and dating of historical paper based on IR spectroscopy and chemometric data evaluation. Analytical Chemistry. 2007;79(16):6319-23.

27.	Sinnott ML. Carbohydrate Chemistry and Biochemistry Structure and Mechanism. Cambridge: RSC Publishing; 2007.

28.	Strlič M, Kolar J, editors. Ageing and Stabilisation of Paper. Ljubljana: National and University Library; 2005.

29.	Dwan A. Paper complexity and the interpretation of conservation research. Journal of the American Institute for Conservation. 1987;26(1):1-17.

30.	Strlič M, Kolar J, editors. Evaluating and enhancing paper stability - the needs and recent trends. 5th EC Conference Cultural Heritage Research; 2002; Cracow.

31.	Margutti S, Conio G, Calvini P, Pedemonte E. Hydrolytic and oxidative degradation of paper. Restaurator. 2001;22(2):67-83.

32.	Łojewska J, Miskowiec P, Łojewski T, Proniewicz LM. Cellulose oxidative and hydrolytic degradation: In situ FTIR approach. Polymer Degradation and Stability. 2005;88(3):512-20.

33.	Zervos S, Moropoulou A. Cotton cellulose ageing in sealed vessels. kinetic model of autocatalytic depolymerization. Cellulose. 2005;12(5):485-96.

34.	Calvini P, Gorassini A, Merlani A. Autocatlytic Degradation of Cellulose Paper in Sealed Vessels. Restaurator. 2007;28(1):47-54.

35.	Baranski A, Lagan JM, Lojewski T. Acid-catalysed degradation. In: Strlic M, Kolar J, editors. Aging and Stabilisation of Paper. Ljubljana :National and University Library of Slovenia; 2005. p. 93-109.

36.	Potthast A, Rosenau T, Kosma P. Analysis of oxidised functionalities in cellulose. Advances in Polymer Science. 2006;205:1-48.

37.	Šelih VS, Strlič M, Kolar J, Pihlar B. The role of transition metals in oxidative degradation of cellulose. Polymer Degradation and Stability. 2007;92:1476-81.

38.	Kelly GB, Williams JC, Mendenhall GD, Ogle CA. The Use of Chemiluminiscence in the Study of Paper Permanence. In: Kelly GB, Eby RK, editors. Durability of Macromolecular Meterials, Advances in Chemistry Series. Washington DC: American Chemical Society; 1979. p. 117-25.

39.	Kolar J. Mechanism of autoxidative degradation of cellulose. Restaurator. 1997;18(4):163-76.

40.	Kolar J, Strlič M, Novak G, Pihlar B. Aging and stabilization of alkaline paper. Journal of Pulp and Paper Science. 1998;24(3):89-93.

41.	Malešič J, Kolar J, Strlič M. Effect of pH and carbonyls on the degradation of alkaline paper: Factors affecting ageing of alkaline paper. Restaurator. 2002;23(3):145-53.

42.   Daniels V. Discolouration of paper induced by pigments containing zinc. Restaurator. 1990;11(4):236-43.

43.   Dufour J, Havermans J. Study of the photo-oxidation of mass-deacidified papers. Restaurator. 2001;22(1):20-40.

44.   Barclay LRC, Grandy JK, MacKinnon HD, Nichol HC, Vinqvist MR. Peroxidations initiated by lignin model compounds: investigating the role of singlet oxygen in photo-yellowing. Can J Chem-Rev Can Chim. 1998;76(12):1805-16.

45.   Wang J, Heitner G, Manley RJ. The photodegradation of milled-wood lignin .2. The effect of inhibitors. Journal of Pulp and Paper Science. 1996;22(2):J58-J63.

46.   Griffiths J, Hawkins C. Involvement of singlet oxygen in sensitized photodegradation of cellulose. Polymer. 1976;17(12):1113-4.

47.   Baugh PJ. Photodegradation and photooxidation of cellulose1981.

48.   Buschlediller G, Zeronian SH. Photodegradation of oxidized cotton cellulose. Journal of Applied Polymer Science. 1993;47(8):1319-28.

49.   Bukovský V, Trnková M. The influence of secondary chromopores on the light induced oxidation of paper. Part 2, The influence of light on groundwood paper. Restaurator. 2003;24(2):118-32.

50.   Bukovský V, Trnková M. The influence of secondary chromophores on the light induced oxidation of paper. Part I: The influence of light on cellulose and secondary chromophores. Restaurator. 2003;24(1):18-35.

51.   Forsskåhl I, Maunier C. Photocycling of chromophoric structures during irradiation of high-yield pulps. In: Heitner C, Scaiano JC, editors. Photochemistry of Lignocellulosic Materials. Washington DC: American Chemical Society; 1993. p. 156-66.

52.   Russell WJ, Abney WdW. Action of light on watercolours. London: HMSO, 1888.

53.   Bunsen R, Roscoe H. Photo-chemical researches. Part IV. Philos Trans R Soc Lond. 1859;149(879-926).

54.   Chevreul M. Recherches chimiques sur la teinture. Mémoires de l'Académie Royale des Sciences de l'Institut de France. 1837;16:41-166.

55.   Brommelle NS. The Russell and Abney Report on the action of light on water colours. Studies in conservation. 1964;9(2):140-9.

56.   Kangay JR. Effect of oxygen concentration and moisture on the stability of leather at elevated temperatures. Journal of Research of the National Bureau of Standards. 1940;25(149).

57.   Nicholson C, Ritzenthaler ML. The Declaration of Independence, The United States Constitution and Bill of Rights: scientific basis and practice of encasement. In: Rayner J, Kosek J, Christensen B, editors. Art on Paper: Mounting and Housing. London: Archetype Publications; 2005. p. 75-80.

58.   NBS. Preservation of the Declaration of Independence and the Constitution of the United States. Washington, D.C.: National Bureau of Standards, 1951 Contract No.: 505.

59.   Arney JS, Jacobs AJ, Newman R. The influence of oxygen on the fading of organic colorants. Journal of the American Institute for Conservation. 1979;18(2):108-17.

60.   Kühn H. The effect of oxygen, relative humidity and temperature on the fading rate of watercolours: reduced light damage in a nitrogen atmosphere. In: Thomson G, editor. Museum Climatology; London: International Institute for Conservation; 1967. p. 79-85.

61.   Kenjo T. Basic experiments concerning deterioration of glue and discoloration of pigments, and discussion on the actual condition of wall panel paintings on the basis of their results. Hozon kagaku. 1974;12:83-94.

62.   Kenjo T, Toishi K. A basic study of the prevention of decoloration and discoloration of pigments. I. Shikizai Kyokaushi. 1964;37(4):133-7.

63.   Schwen G, Schmidt G. Some experiments on the effect of dye, fibre, and atmosphere on light fastness. Journal of the Society of Dyers & Colourists. 1959;75:101-5.

64.   Calderon M, Barkai-Golan R. Food Preservation by Modified Atmospheres. Boston: CRC Press; 1990.

65.   Story K. Approaches to Pest Management in Museums. Washington DC: Conservation Analytical Laboratory, Smithsonian Institution; 1985.

66.   Gilberg M. Inert atmosphere fumigation of museum objects. Studies in Conservation. 1989;34(2):80-4.

67.   Selwitz CM, Maekawa S. Inert gases in the control of museum insect pests. Los Angeles: The Getty Conservation Institute; 1998.

68.   Maekawa S, Preusser FD, Lambert P. A hermetically sealed display and storage case for sensitive organic objects in inert atmospheres. Biodeterioration of Cultural Property 2; Yokohama: International Congress of Biodeterioration of Cultural Properties; 1993. p. 374-85.

69.   Valentín N, Preusser FD. Nitrogen for biodeterioration control on museum collections. The Third Meeting of the Pan American Biodeterioration Society; Washington: The Pan American Biodeterioration Society; 1989.

70.   Maekawa S, Elert K. The use of oxygen-free environments in the control of museum insect pests. Los Angeles: The Getty Conservation Institute; 2003.

71.   Maekawa S, editor. Oxygen-Free Museum Cases. Los Angeles: J. Paul Getty Trust; 1998.

72.   Arai H, Kenjo T. A closed system for preventing fungal growth in cultural properties. In: Agrawal OP, Dhawan S, editors. International Conference on Biodeterioration of Cultural Property: Macmillian India; 1991.

73.   Kenjo T. Studies on the long-term conservation of cultural properties. I. effects of differnt concentrations of oxygen on pigments used for cultural properties. Kobunkazai no kagaku. 1980;25:103-7.

74.   Shenton H. Strategic developments in collection storage of libraries and archives -- architectural, technical, political. Liber Quarterly. 2005;15(3/4).

75.   Jensen G. Hypoxic Air Venting for Protection of Heritage. Oslo: Riksantikvaren and Historic Scotland, 2006.

76.   Willemsen E, Luyten R, Castelijns W, Beentjes G. Innovation in Low-O, Technology: A solution for Conservation, Protection and Treatment Restaurator. 2011;32:13-26.

77.   Pinzari F, Pasquariello G, De Mico A. Biodeterioration of Paper: A SEM Study of Fungal Spoilage Reproduced Under Controlled Conditions. Macromolecular Symposia. 2006;238(1):57-66.

78.   Pinzari F, Colaizzi P, Montanari M, Valenti P. Effects of anoxia on cultural heritage deteriorating fungi: possible side effects for the stored objects. NOOX 3; London: The British Library and the Natural History Museum; 2003. p. poster.

79.   Hwang KO, Lucia LA. Fundamental insights into the oxidation of lignocellulosics obtained from singlet oxygen photochemistry. J Photochem Photobiol A-Chem. 2004;168(3):205-9.

80.   Destine JN, Wang J, Heitner C, Manley RSJ. The photodegradation of milled-wood lignin .1. The role of oxygen. Journal of Pulp and Paper Science. 1996;22(1):J24-J30.

81.   Thomas J. Final report on STSM for the Pilot study for the application of chemiluminometry to evaluate anoxic display of watercolours. London: Tate and University of Ljubljana, Faculty of Chemistry and Chemical Technology, 2008.

82.   Farquhar RL, Pesant D, McLaren BA. Canadian Textile Journal. 1956;73(3):51-6.

83.   Barański A, Łagan JM, Łojewski T. The Concept of Mixed-Control Mechanisms and its Applicability to Paper Degradation Studies. e-Preservation Science. 2006;3:1-4.

84.   Wise A, Granowski C, Gourley B. Out of the box: measuring microclimates in Australian-made Solander boxes. In: Rayner J, Kosek J, Christensen B, editors. Art on Paper: Mounting and Housing. London: Archetype Publications; 2005. p. 55-8.

85.	Thickett D. Print frame microclimates. In: Rayner J, Kosek J, Christensen B, editors. Art on Paper: Mounting and Housing. London: Archetype Publications; 2005. p. 48-54.

86.	Havermans J. Ageing behaviour of encapsulated paper. Restaurator. 1999;20(2):108-15.

87.	Shahani CJ, Harrison G. Spontaneous formation of acids in the natural aging of paper. In: Daniels V, Donnithorne A, Smith P, editors. Works of art on paper: books, documents and photographs: techniques and conservation; Sep; Baltimore, MD: International Institute for Conservation; 2002. p. 189-92.

88.	Kosek J, Jacobs D. What happens to enclosed paper? In: Rayner J, Kosek J, Christensen B, editors. Art on Paper: Mounting and Housing; London: Archetype Publications; 2005. p. 29-37.

89.	Lattuati-Derieux A, Bonnassies-Termes S, Lavedrine B. Identification of volatile organic compounds emitted by a naturally aged book using solid-phase microextraction/gas chromatography/mass spectrometry. Journal of Chromatography A. 2004;1026(1-2):9-18.

90.	Dupont A-L, Egasse C, Morin A, Vasseur F. Comprehensive characterisation of cellulose- and lignocellulose-degradation products in aged papers: Capillary zone electrophoresis of low-molar mass organic acids, carbohydrates, and aromatic lignin derivatives. Carbohydrate Polymers. 2007;68(1):1-16.

91.	Thomas J. Evaluation of reduced oxygen display and storage of watercolours. London: University College London; 2010.

92.	Dupont AL, Tétreault J. Cellulose degradation in an acetic acid environment. Studies in Conservation. 2000;45(3):201-10.

93.	Leschine SB. Cellulose degradation in anaerobic environments. Annual Reviews Microbiology. 1995;49:399-426.

94.	Kobiakova VI, Dobrusina SA. The Behaviour of Paper Treated in a Carbon Dioxide Modified Atmosphere. Restaurator. 2003;24(2):81-7.

95.	Malshe VC, Elango S. Alkylated phenolic antioxidants for paints Surface Coatings International part B: Coatings Transactions. 2005;88(2):145-8.

96.	Stadtman ER. Protein oxidation and aging. Free Radical Research 2006;40(12):1250-8.

97.	Kato Y, Uchida K, Kawakishi S. Oxidative degradation of collagen and its model peptide by ultraviolet irradiation. Journal of Agricultural and Food Chemistry. 1992;40:373-9.

98.	Popescu C, Budrugea P, Wortmann F-J, Miu L, Demco D, Baias M. Assessment of collagen-based materials which are supports of cultural and historical objects. Polymer Degradation and Stability. 2008;93:976-82.

99.	Hansen E. Protection of objects from environmental deterioration by reducing their exposure to oxygen. In: Maekawa S, editor. Research in Conservation: Oxygen-Free Museum Cases. Los Angeles: Getty Conservation Institute; 1998. p. 7-15.

100.	Strlič M, Kralj I, Rabin I, Kolar J, Pihlar B, Cassar M. Autoxidation of lipids in parchment. Polymer Degradation and Stability. 2009 in press.

101.	van de Weerd J, van Loon A, Boon JJ. FTIR Studies of the Effects of Pigments on the Aging of Oil. Studies in Conservation. 2005;50:3-22.

102.	Mallégol J, Gonon L, Lemaire J, Gardette J-L. Long-term behaviour of oil-based varnishes and paints 4. Influence of film thickness on the photooxidation. Polymer Degradation and Stability. 2001;72:191-7.

103.	Thomson G. Oxygen Starvation in paint and other films. National Gallery Technical Bulletin. 1978;2:66-70.

104.	Volz HG, Kaempf G, Fitzky HG, Klarean A. Photostabilization and Photodegradation of Coatings. In: Pappas SP, Winslow HP, editors. ACS Symposium Series 151. Washington D.C.: American Chemical Society; 1981. p. 163-82.

105.	Shashoua Y. Inhibiting the Inevitable; Current Approaches to Slowing the Deterioration of Plastics. Macromolecular Symposia. 2006;238(1):67-77.

106.   Hamid SH, editor. Handbook of Polymer Degradation. 2nd ed. London: CRC Press; 2000.
107.   Grosjean D, Grosjean E, Williams EL. Fading of artists' colorants by a mixture of photochemical oxidants. Atmospheric Environment Part A General Topics. 1993;27(5):765-72.
108.   Giles CH. The fading of coloring matters. Curator. 1966;9(2):95-102.
109.   Giles CH, Baxter G, Rahman S. Studies of high fastness to light in colouring matters in hydrophilic substrates. Textile Research Journal. 1961;31(10):831-44.
110.   Giles CH, McKay RB. The light fastness of dyes: a review. Textile Research Journal. 1963;33(7):528-77.
111.   Giles CH, Shah CD, Watts WE. Oxidation and reduction in light fading of dyes. Journal of the Society of Dyers and Colourists. 1972;88(12):433-5.
112.   Duff DG, Sinclair RS, Stirling D. Light-induced color changes of natural dyes. Studies in conservation. 1977;22(4):161-9.
113.   Cox-Crews P. The fading rates of some natural dyes. Studies in Conservation. 1987;32(2):65-72.
114.   Imada K, Harada N, Takagishi T. Fading of azo reactive dyes by perspiration and light. Journal of the Society of Dyers & Colourists. 1994;110(7-8):231-4.
115.   Saunders D, Kirby J. Light-induced colour changes in red and yellow lake pigments. National Gallery Technical Bulletin. 1994;15:79-97.
116.   Ajax RL, Conlee CJ, Upham JB. The effects of air pollution on the fading of dyed fabrics. Journal of the Air Pollution Control Association. 1967;17(4):220-4.
117.   Whitmore PM, Cass GR, Druzik JR. The fading of traditional natural colorants due to atmospheric ozone. The American Institute for Conservation of Historic and Artistic Works, preprints of papers presented at the fourteenth annual meeting, Chicago, Illinois, 21-25 May 1986. Washington, DC: American Institute for Conservation of Historic and Artistic Works; 1986. p. 114-24.
118.   Yoshizumi K, Kadakura T, Kashiwagi M, Saito M. Effects of atmospheric SO2 and NO2 on the fading of dyed fabrics by traditional dyestuffs. In: Rama Rao N, Ganorkar MC, editors. 1st international colloquium on the role of chemistry in archaeology 15-18 November, 1991. Andhra Pradesh: Birla Institute of Scientific Research; 1991. p. 131-6.
119.   Saito M, Goto S, Kashiwagi M. Effect of the concentration of NO2 gas to the fading of fabrics dyed with natural dyes. Kobunkazai no kagaku. 1994;39:67-74.
120.   Grosjean D, Salmon LG, Cass GR. Fading of organic artists' colorants by atmospheric nitric acid: reaction products and mechanisms. Environmental science and technology. 1992;26(5):952-9.
121.   Yun Y, Salmon LG, Cass GR. The ozone fading of traditional Chinese plant dyes. Journal of the American Institute for Conservation. 2000;39(2):245-57.
122.   Beltran V, Druzik J, Maekawa S. An extended investigation of the influence of oxygen on colour fading. In: Bridgland J, editor. ICOM-CC 15th Triennial Meeting New Delhi; New Delhi, India: Allied Publishers Pvt. Ltd.; 2008.
123.   Buss JJB, Crews PC. Influence of nitrogen gas and oxygen scavengers on fading and color change in dyed textiles. The Textile Specialty Group postprints of papers delivered at the Textile Subgroup Session: American Institute for Conservationannual meeting2001. p. 55-67.
124.   Kigawa R, Miyazawa Y, Kuchitsu N, Sano C, Yamano K, Miura S. Anoxia treatment by various kinds of oxygen scavenger: evaluation of effects on pigments. Hozon kagaku. 1998(37):23-33.
125.   Lønnve J. Consequences of oxygen free storage on inorganic pigments In: Fjæstad M, Åkerlund M, Bergh J-E, editors. Syrefria mikroklimat Förebyggande konservering. Stockholm: Riksantikvarieämbetet; 2003. p. 43-7.

126.   Petersson K. Påverkan på indigofärgat bomullstyg i syrefritt mikroklimat In: Fjæstad M, Åkerlund M, Bergh J-E, editors. Syrefria mikroklimat Förebyggande konservering. Stockholm: Riksantikvarieämbetet; 2003. p. 35-42.

127.   Ware M. Cyanotype: the history, science and art of photographic printing in Prussian blue Bradford: Science Museum and National Museum of Photography, Film & Television; 1999.

128.   Bleuzen A, Escax V, Ferrier A, Villain F, Verdaguer M, Münsch P, et al. Thermally Induced Electron Transfer in a CsCoFe Prussian Blue Derivative: The Specific Role of the Alkali-Metal Ion. Angewandte Chemie. 2004;43:3728-31.

129.   Etaiw SEH, Ibrahim AMA. Unusual chromic behaviour of the solid supramolecular 3D polymers [(Me3Sn)nFe(CN)6]∞ (n=3/4). Journal of Organometallic Chemistry. 1996;522:77-86.

130.   Dostal A, Kauschka G, Reddy SJ, Scholz F. Lattice contractions and expansions accompanying the electrochemical conversions of Prussian blue and the reversible and irreversible insertion of rubidium and thallium ions Journal of Electroanalytical Chemistry. 1996;406:155-63.

131.   Sheu H-S, Jen S-H, Kang T-W, Jang L-Y, Lee J-F. Cation driven charge transfer in (Co, Fe) Prussian blues. Journal of the Chinese Chemical Society. 2002;49:813-8.

132.   Saunders D, Spring M, Higgitt C. Colour change in red lead-containing paint films. In: Vontobel R, editor. ICOM-CC Meeting; Sep; Rio de Janeiro: London; 2002. p. 455-63.

133.   Masel R. Principles of adsorption and reaction on solid surfaces. New York: Wiley; 1996.

134.   Gupta D. Fastness properties of natural dyes. Part II: effect of chemical structure on light fastness. Coulourage. 1999;46(8):41-6.

135.   Cristea D, Vilarem G. Improving light fastness of natural dyes on cotton yarn. Dyes and Pigments. 2006;70:238-45.

136.   Gupta D. Fastness properties of natural dyes. Part I: introduction and review of literature. Coulourage. 1999;46(7):35-8.

137.   Padfield T, Landi S. The light-fastness of the natural dyes. Studies in Conservation. 1966;11(4):181-96.

138.   Cumming JW, Giles CH, McEachran A. A study of the photochemistry of dyes on proteins and other substrates. Journal of the Society of Dyers & Colourists. 1956;72:373-80.

139.   Cox-Crews P. The influence of mordant on the light fastness of yellow natural dyes. Journal of the American Institute for Conservation. 1982;21(2):43-58.

140.   Van Beek HCA, Heertjes PM. Fading by light of organic dyes on textiles and other materials. Studies in conservation. 1966;11(3):123-32.

141.   Buss JJB, Crews PC, editors. Influence of nitrogen gas and oxygen scavengers on fading and color change in dyed textiles. American Institute for Conservation Annual Meeting; 2001: American Institute of Conservation.

142.   Van Beek HC, Heertjes PM. Fading by light of organic dyes on textile and other materials. Studies in Conservation. 1966;11(3):123-32.

143.   Görner H. Oxygen Uptake and Involvement of Superoxide Radicals upon Photolysis of Ketones in Air-saturated Aqueous Alcohol, Formate, Amine or Ascorbic Acid Solutions. Photochemistry and Photobiology. 2006;82(3):801-8.

144.   Görner H. Photoinduced oxygen uptake for 9,10-anthraquinone in air-saturated aqueous acetonitrile in the presence of formate, alcohols, ascorbic acid or amines. Photochem Photobiol Sci. 2006;5(11):1052-8.

145.   Leaver IH. Photoxidation and photoreduction of dyes in polymers. In: Allen NS, McKellar JF, editors. Photochemistry of Dyed and Pigmented Polymers: Elsevier Science & Technology; 1980.

146.   Černič Letnar M, Muck T. The quality of graphic art paper the influence of paper permanence and durability on graphic art. Restaurator. 2003;24(4):240-52.

147.   Irving J. Construction paper: a brief history of impermanence. The Book & Paper Group Annual [Internet]. 1997; 16.
148.   Purinton N, Irving J. Argon-filled containers for the display of paper. In: Rayner J, Kosek J, Christensen B, editors. Art on Paper: Mounting and Housing. London: Archetype Publications; 2005. p. 81-5.
149.   Ahlgren C. Motverkande av bläckfrätning från järngallbläck på papper – försök med förvaring i syrefri miljö. In: Fjæstad M, Åkerlund M, Bergh J-E, editors. Syrefria mikroklimat Förebyggande konservering. Stockholm: Riksantikvarieämbetet; 2003. p. 26-34.
150.   Ellis MH. The porous pointed pen as artistic medium. In: Fairbrass S, editor. Conference Papers Manchester 1992; Leigh, Worcester: IPC; 1992. p. 11-8.
151.   Ellis MH, McGlinchey CW, Chao E. Daylight fluorescent colors as artistic media. In: Stratis H, Salvesen B, editors. The Broad Spectrum; London: Archetype; 2002.
152.   Pfingstag G. Colorants in inks for writing, drawing and marking. Journal of the Society of Dyers and Colourists. 1993;109(5/6):188-92.
153.   Ellis M. Drawings in fibre-tipped pen - new conservation challenges. In: Richmond A, editor. Modern Works, Modern Problems?; Leigh, Worcester: IPC; 1994. p. 114-21.
154.   Strlič M, Thomas J, Trafela T, Cséfalvayová L, Kralj I, Kolar J, et al. Material degradomics: on the smell of old books. Analytical Chemistry. 2009;in press.
155.   Strlič M, Kralj I, Kolar J, De Bruin G, Pihlar B. Non-Destructive Evaluation of Historical Paper Based on pH Estimation from VOC Emissions. Sensors. 2007;7:3136-45.
156.   Bower P. Blues and Browns and Drabs: The Evoloution of Coloured Papers. In: Stratis H, Salvesen B, editors. The Broad Spectrum. London: Archetype; 2002.
157.   Bower P. All the Colours of White: The Changing Nature of White Papers. In: Stratis HK, Salvesen B, editors. The Broad Spectrum. London: Archetype 2002.
158.   Bower P. Turner's papers: a study of the manufacture, selection and use of his drawing papers 1787-1820. London: Tate Gallery; 1990.
159.   Bower P. Turner's later papers: a study of the manufacture, selection and use of his drawing papers 1820-1851. London: Tate Publishing; 1999.
160.   Bower P, editor. A brush with nature: an historical and technical analysis of the papers and boards used as supports for landscape oil sketching. Works of art on paper: books, documents and photographs: techniques and conservation; 2002 Sep; Baltimore, MD: International Institute for Conservation.
161.   Townsend JH. The Analysis of Watercolor Materials, in Particular Turner's Watercolours at the Tate Gallery (1790s to 1840s). In: Stratis H, Salvesen B, editors. The Broad Spectrum. London: Archetype; 2002.
162.   Townsend JH. Turner's Painting Techniques. 4th edition ed. London: Tate Publishing; 2005.
163.   Hunter D. Papermaking The History and Technique of an Ancient Craft. New York: Dover; 1978.
164.   Fairbanks Harris T, Wilcox S, editors. Papermaking and the Art of Watercolor in Eighteenth-Centry Britain. London: Yale University Press; 2006.
165.   Clarke M. A.T.S.R. Art Technological Source Research. 2010 [cited 2011 4 February]; Available from: http://www.clericus.org/atsr/index.htm.
166.   Townsend JH, Thomas J, Caspers C, Pis Marcos M, Brookes A, Ormsby B, et al. De/re-constructiong Turner for research projects at Tate. In: Hermens E, Townsend JH, editors. Sources and Serendipity. London: Archetype; 2010. p. 159-62.
167.   Caspers C. Reconstructing British 19th-century Watercolour Paint [SRAL Thesis (unpublished)]. Maastricht: University of Amsterdam; 2008.
168.   Tate. Colour and Line Turner's Experiments. 2007 [cited 2011 22 November]; Available from: http://www.tate.org.uk/britain/exhibitions/turnercolourandline/default.shtm.

169.   Warrell I. R.N. Wornum and the first three loan collections: a history of the early display of the Turner Bequest Outside London. Turner Studies. 1991;2(1).
170.   Finberg AJ. A Complete Inventory of the Drawings of the Turner Bequest London: The National Gallery; 1909.
171.   PaperVOC project: VOCs in paper-based cultural heritage collections - source of information or risk? 2009 [17 November 2011]; Available from: http://www.science4heritage.org/papervoc/.
172.   Thomas J, Lerwill A, Townsend JH, Hackney S. A review of anoxia for the storage and display of works of art on paper. In: Townsend JH, editor. Conservation Science 2007; Milan: Archetype; 2007. p. 227-33.
173.   Thomas J, Strlič M. Heritage 'degradomics': an introduction. MaSC 2009 Meeting; London: User's Group for Mass Spectrometry and Chromatography; 2009.
174.   Trafela T, Strlič M, Kralj Cigić I, Kolar J, Pihlar B. Volatile 'degradic' fingerprinting of historical paper MaSC 2009 Meeting; London: User's Group for Mass Spectrometry and Chromatography; 2009.
175.   Smith CA, Want EJ, O'Maille G, Abagyan R, Siuzdak G. XCMS: Processing mass spectrometry data for metabolite profiling using nonlinear peak alignment, matching and identification. Analytical Chemistry. 2006;78:779-87.
176.   Xia J, Psychogios N, Young N, Wishart DS. MetaboAnalyst: a web server for metabolomic data analysis and interpretation Nucleic Acids Research. 2009;37:652-60.
177.   Xia J, Wishart DS. Web-based inference of biological patterns, functions and pathways from metabolomic data using MetaboAnalyst. Nature Protocols. 2011;6:743-60.
178.   Donetzhuber A, Johansson B, Johansson K, Lövgren M, Sarin E. Analytical characterization of the gas phases in paper and board products. Nordic Pulp and Paper Research Journal. 1999;14(1):48-60.
179.   Lattuati-Derieux A, Bonnassies-Termes S, Lavedrine B. Characterisation of compounds emitted during natural and artificial ageing of a book. Use of headspace-solid-phase microextraction/gas chromatography/mass spectrometry. Journal of Cultural Heritage. 2006;7(2):123-33.
180.   Gibson LT, Robertson C. Analysing smelly old books. Advances in Paper Conservation Research Conference; British Library. London: British Library; 2009. p. 40-2.
181.   Isinay E, Yüzay S. Development of electronic nose method for evaluation of residual solvents in low-density polyethylene films Packaging Technology and Science. 2006;20(2):99-112. Epub 1 June 2006.
182.   Forsgren G. Taint and odour related quality monitoring of two food packaging board products using gas chromatography, gas sensors and sensory analysis. Nordic Pulp and Paper Research Journal. 1999;14(1):5-16.
183.   Ziegleder G. Odorous compounds in paperboard as influenced by recycled material and storage. Packaging Technology and Science. 2001;14:131-6.
184.   Asensio E, Nerín C. Evaluation of a screening method for classifying virgin and recycled paper and board samples. Packaging Technology and Science. 2009. Epub 5 March 2009.
185.   . Conference Proceedings. Advances in Paper Conservation Research Conference; 2009; British Library. London: British Library.
186.   Goodacre R, Roberts L, Ellis D, Thorogood D, Reader S, Ougham H, et al. From phenotype to genotype: whole tissue profiling for plant breeding. Metabolomics. 2007;3(4):489-501.
187.   Goodacre R, Vaidyanathan S, Dunn WB, Harrigan GG, Kell DB. Metabolomics by numbers: acquiring and understanding global metabolite data. Trends in Biotechnology. 2004;22(5):245-52.
188.   Kell DB, Brown M, Davey HM, Dunn WB, Spasic I. Metabolic footprinting: the medium is the message. Nature Reviews Microbiology. 2005;3:557-65.

189.   Brown M, Dunn WB, Ellis DI, Goodacre R, Handl J, Knowles JD, et al. A metabolome pipeline: from concept to data to knowledge Metabolomics. 2005;1(1):39-51.
190.   Hollywood K, Brison D, Goodacre R. Metabolomics: Current technologies and future trends. Proteomics. 2006;6(17):4716-23.
191.   Mapelli V, Olsson L, Nielsen J. Metabolic footprinting in microbiology: methods and applications in functional genomics and biotechnology. Trends in Biotechnology. 2008;26:490-7.
192.   Katajamaa M, Oresic M. Data processing for mass spectrometry-based metabolomics. Journal of chromatography A. 2007;1158(1-2):318-28.
193.   Dettmer K, Aronov PA, Hammock BD. Mass spectrometry-based metabolomics Mass Spectrometry Reviews. 2007;26:51-78.
194.   Bundy J, Davey MP, Viant MR. Environmental metabolomics: a critical review and future perspectives. Metabolomics. 2009;5:3-21.
195.   Viant M. Applications of metabolomics to the environmental sciences. Metabolomics. 2009;5:1-2.
196.   Shepherd T, Dobson G, Verrall SR, Conner S, Griffiths DW, McNicol JW, et al. Potato metabolomics by GC–MS: what are the limiting factors? Metabolomics. 2007;3(4):475-88.
197.   Ward JL, Beale MH. Proceedings from the 4th International Plant Metabolomics Conference. Metabolomics. 2006;2(4):269-334.
198.   Tholl D, Boland W, Hansel A, Loreto F, Röse USR, Schnitzler J-P. Practical approaches to plant volatile analysis. The Plant journal : for cell and molecular biology. 2006;45(4):540-60.
199.   Want EJ, Nordström A, Morita H, Siuzdak G. From Exogenous to Endogenous: The Inevitable Imprint of Mass Spectrometry in Metabolomics. Journal of Proteome Research. 2007;6(2):459-68.
200.   Nordström A. Data mining for metabolomics. In: Griffiths WJ, editor. Metabolomics, Metabonomics, and Metabolite Profiling Cambridge: RSC; 2008.
201.   Boccard J, Veuthey J-L, Rudaz S. Knowledge discovery in metabolomics: an overview of MS data handling. Journal of Separation Science. 2010;33(3):290-304.
202.   Bonaduce I, Brecoulaki H, Colombini MP, Lluveras A, Restivo V, Ribechini E. Gas chromatographic-mass spectrometric characterisation of plant gums in samples from painted works of art. Journal of chromatography A. 2007;1175(2):275-82.
203.   Organic Mass Spectrometry in Art and Archaeology. Chichester: John Wiley & Sons; 2009.
204.   Strlič M, Cigić Kralj I, Kolar J, de Bruin G, Pihlar B. Non-Destructive Evaluation of Historical Paper Based on pH Estimation from VOC Emissions. Sensors. 2007;7:3136-45.
205.   Łojewski T, Sawoszczuk T, Łagan JM, Zięba K, Barański A, Łojewska J. Furfural as a marker of cellulose degradation. A quantitative approach. Applied Physics A. 2010.
206.   Ziegleder G, Stojacic E, Lustenberger M. Cause and Detection of Off-odours in Unprinted Paperboard *. Food Technology. 1995;8(6):36-9.
207.   Uchida Y, Inaba M, Kijima T. Evaluation of Aqueous Washing Methods of Paper by the Measurement of Organic Acid Extraction. Restaurator. 2007;28(3):169-84.
208.   Balazic A, Habicht S, Smodis M, Kolar J, Strlic M, editors. Extending the useful life of paper - evaluation of the effect of various preservation actions. Museum Microclimates; 2007 2008; Copenhagen: The National Museum of Denmark.
209.   Burke J. Anoxic microenvironments: a simple guide. SPNHC leaflets. 1996;1(1):1-4.
210.   Carrió V, Stevenson S. Assessment of materials used for anoxic microenvironments. In: Townsend JH, Eremin K, Adriaens A, editors. Conservation Science 2002: papers from the conference held in Edinburgh, Scotland, 22-24 May 2002. London: Archetype Publications Ltd.; 2003. p. 32-8.

211.   Passaglia E. The characterization of microclimates and the degradation of archival records: a research program. Washington D.C.: U.S. Department of Commerce, National Bureau of Standards, Institute for Materials Science and Engineering, 1987.

212.   Ryhl-Svendsen M, Grinde L, Christoffersen LD, editors. The microclimate inside archival boxes in rooms with fluctuating relative humidityand temperature. ICOM-CC 15th Triennial Conference; 2008; New Delhi: James and James.

213.   Grøntoft T, Odlyha M, Mottner P, Dahlin E, Lopez-Aparicio S, Jakiela S, et al. Pollution monitoring by dosimetry and passive diffusion sampling for evaluation of environmental conditions for paintings in microclimate frames. Journal of Cultural Heritage. 2010.

214.   Thomas J, Lerwill A, Caspers C, Brookes A, Townsend JH, Hackney S. Evaluation of anoxic environments for the display and storage of works of art on paper. Durability of Paper and Writing 2; 7-9 July 2008; Ljubljana2008.

215.   ASTM. ASTM E1655 - 05 Standard Practices for Infrared Multivariate Quantitative Analysis. ASTM International; 2005.

216.   Gasera. Gas Analyzers. 2011 [cited 2011 22 November]; Available from: http://www.gasera.fi/products/photoacoustic-gas-analyzers/f10/.

217.   Owlstone. Lonestar Portable Gas Analyzer. 2011 [cited 2011 22 November]; Available from: http://www.owlstonenanotech.com/site.php?lonestar.

218.   Canhoto O, Pinzari F, Fanelli C, Magan N. Application of electronic nose technology for the detection of fungal contamination in library paper. International Biodeterioration & Biodegradation. 2004;54(4):303-9.

219.   Xu Y, Cheung W, Winder CL, Goodacre R. VOC-based metabolic profiling for food spoilage detection with the application to detecting Salmonella typhimurium-contaminated pork. Analytical and Bioanalytical Chemistry. 2010;397(6):2439-49.

220.   Fenech A, Strlič M, Cigić Kralj I, Levart A, Gibson LT, de Bruin G, et al. Volatile aldehydes in libraries and archives. Atmospheric Environment. 2010;44(17):2067-73.

221.   Pedersoli Jr. JL, Ligterink FJ. Spectroscopic characterization of the fluorescence of paper at the wet-dry interface. Restaurator. 2001;22(3):133-45.

222.   Vives JMG, Escoda JRM, Guerra RA, Hernandez LA. A method for the non-destructive analysis of paper based on reflectance and viscosity. Restaurator. 2001;22(4):187-207.

223.   Jerosch H, Lavédrine B, Cherton J-C. Study on the Correlation Between SEC and Mechanical Tests of Different Paper Types for Degradation State Evaluation. Restaurator. 2002;23(4):222-39.

224.   Jerosch H, Lavedrine B, Cherton JC, editors. The use of size exclusion chromatography (SEC) for the evaluation of paper degradation caused by nitrogen oxides in comparison with other methods. Works of art on paper: books, documents and photographs: techniques and conservation; 2002 Sep; Baltimore, MD: International Institute for Conservation.

225.   Łojewski T, Zięba K, Knapik A, Bagniuk J, Lubańska A, Łojewska J. Evaluating paper degradation progress. Cross-linking between chromatographic, spectroscopic and chemical results. Applied Physics A. 2010.

226.   Workman JJJ. Infrared and Raman spectroscopy in paper and pulp analysis. Applied Spectroscopy Reviews. 2001;36(2-3):139-68.

227.   Gurnagul N, Howard RC, Zou X, Uesaka T, Page DH, editors. The Mechanical Permanence of Paper: A Literature Review. Effects of aging on printing and writing papers; 1994 Jul; Philadelphia, PA: CONSHOHOCKEN.

228.   Mark R, Murakami K, editors. Handbook of physical and mechanical testing of paper and paperboard New York: Dekker; 1983.

229.   Lichtblau D, Anders M, editors. Characterization of Paper by Near Infrared Spectroscopy. Durability of Paper and Writing; 2004; Ljubljana, Slovenia: National and University Library, Ljubljana, Slovenia.

230.   SurveNIR. SurveNIR Near Infrared Tool for Collection Surveying. 2008 [cited 2011 22 November]; Available from: http://www.science4heritage.org/survenir/

231.   Eastaugh N. A report on the dye analysis of Turner's pigments. Surbiton: 1990.

232.   Hansen NW. Some Painting Materials of J.M.W. Turner. Studies in conservation. 1954;1(4):162-73.

233.   Townsend JH. The materials of J M W Turner: pigments. Studies in Conservation. 1993;38(4):231-54.

234.   Ormsby BA, Townsend JH, Singer BW, Dean JR. British Watercolour Cakes from the Eighteenth to the Early Twentieth Century. Studies in Conservation. 2005(50):45-66.

235.   Kocar D, Pedersoli JL, Strlic M, Kolar J, Rychly J, Matisova-Rychla L. Chemiluminescence from paper II. The effect of sample crystallinity, morphology and size. Polymer Degradation and Stability. 2004;86(2):269-74.

236.   Feller RL. Accelerated Ageing: Photochemical and Thermal Aspects. Los Angeles: Getty Conservation Institute; 1994.

237.   Porck H. Rate of Paper Degradation the predictive value of artificial aging tests. Amersterdam: European Commission of Preservation and Access, 2000.

238.   Shahani CJ, editor. The evolution of a new accelerated ageing test for paper. Durability of Paper and Writing; 2004; Ljubljana, Slovenia: National and University Library, Ljubljana, Slovenia.

239.   Bégin PL, Kaminska E. Thermal accelerated ageing test method development. Restaurator. 2002;23(2):89-105.

240.   Bansa H. Accelerated ageing of paper: Some ideas on its practical benefit. Restaurator. 2002;23(2):106-17.

241.   Feller R. Accelerated aging. Los Angeles: J. Paul Getty Trust; 1994.

242.   Calvini P, Gorassini A. On the rate of paper degradation: lessons from the past. Restaurator. 2006;27(4):275-90.

243.   Zervos S, Moropoulou A. Methodology and criteria for the evaluation of paper conservation interventions. Restaurator. 2006;27(4):219-74.

244.   ASTM. ASTM D6819-02(2007) Standard Test Method for Accelerated Temperature Aging of Printing and Writing Paper by Dry Oven Exposure Apparatus. ASTM International; 2007.

245.   Matisová-Rychlá L, Bukovský V, Rychlý J, Pleteníková M. Chemiluminescence - A Novel Method in the Research of Degradation of Paper. I. The Effect of Light on Stacked Sheets of Paper. Macromolecular Symposia. 2007;247:340-9.

246.   Buchbauer G, Jirovets L, Wasicky M, Nikiforov A. On the Odour of Old Books. Journal of Pulp and Paper Science. 1995;21(11):398-400.

247.   Carter H, Bégin P, Grattan D. Migration of volatile compounds through stacked sheets of paper during accelerated ageing. Part 1: Acid migration at 90º C. Restaurator. 2000;21(2):77-84.

248.   Bülow A, Bégin P, Carter H, Burns T. Migration of volatile compounds through stacked sheets of paper during accelerated ageing: Part II - Variable temperature studies. Restaurator. 2000;21(4):187-203.

249.   Giles CH, Shah CD, Johari DP, Sinclair RS. Effect of gaseous diffusion in the substrate on the light fastness of dyes. Journal of the Society of Dyers and Colourists. 1972;58(2):59-61.

250.   Havermans J, editor. Encapsulation and ageing of paper. Durability of Paper and Writing; 2004; Ljubljana, Slovenia: National and University Library, Ljubljana, Slovenia.

251.   Hill DJT, Le TT, Darveniza M, Saha T. A study of the degradation of cellulosic insulation materials in a power transformer. Part III: Degradation products of cellulose insulation paper. Polymer Degradation and Stability. 1996;51(2):211-8.

252.   Emsley AM. Kinetics and mechanisms of degradation of cellulosic insulation in power transformers. Polymer Degradation and Stability. 1994;44(3):343-9.

253.   Isenberg IH. Pulp and Paper Microscopy 3ed. Appleton: The Institute of Paper Chemistry; 1967.

254.   Calvini P, Gorassini A, Merlani AL. Autocatalytic Degradation of Cellulose Paper in Sealed Vessels. Restaurator. 2007;28(1):47-54.

255.   ASTM. ASTM D778-97(2002) Standard Test Methods for Hydrogen Ion Concentration (pH) of Paper Extracts (Hot- Extraction and Cold-Extraction Procedures). ASTM International; 2002.

256.   TAPPI. TAPPI T529 Surface pH Measurement of Paper TAPPI; 2004.

257.   Strlič M, Pihlar B, Mauko L, Kolar J, Hočevar S, Ogorevc B. A new electrode for micro-determination of paper pH. Restaurator. 2005;26(3):159-71.

258.   Strlič M, Kolar J, Kočar D, Drnovsek T, Šelih V, Susič R, et al. What is the pH of Alkaline Paper? e-Preservation Science. 2004;1:35-47.

259.   Dupont AL. Degradation of cellulose at the wet/dry interface: I. The effect of some conservation treatments on brown lines. Restaurator. 1996;17(1):1-21.

260.   Dupont AL. Degradation of cellulose at the wet/dry interface: II. An approach to the identification of the oxidation compounds. Restaurator. 1996;17(3):145-64.

261.   Schuster G, Schmidt S. Chemiluminescence of organic compounds. Advances in Physical Organic Chemistry. London: Academic Press Inc; 1982.

262.   Blakey I, Goss B, George G. Chemiluminescence as a Probe of Polymer Oxidation. Australian Journal of Chemistry. 2006;59(8):485-.

263.   Dekker M, editor. Luminescence techniques in solid-state polymer research. New York1989.

264.   Strlič M, Kolar J, Pihlar B, Rychlý J, Matisová-Rychlá L. Chemiluminescence during thermal and thermo-oxidative degradation of cellulose. European Polymer Journal. 2000;36(11):2351-8.

265.   Malešič J, Kolar J, Strlič M, Kočar D, Fromageot D, Lemaire J, et al. Photo-induced degradation of cellulose. Polymer Degradation and Stability. 2005;89:64-9.

266.   Rychlý J, Matisová-Rychlá L, Bukovský V, Pleteníková M, Vrška M. The Progress of Ageing of Lignin-containing Paper Induced by Light and its Relation to Chemiluminescence – Temperature Runs. 2006:178-92.

267.   Rychlý J, Ebringerova A, Matisová-Rychlá L. Chemiluminescence accompanying the oxidation of hemicelluloses. Polymer Degradation and Stability. 2008;93(9):1674-80.

268.   Rychlý J, Matisová-Rychlá L, Strlič M. Kinetic aspects of chemiluminescence response to periodic changes of temperature during thermal treatment of cellulose ´1. Polymer International. 2000;49:981-6.

269.   Rychlý J, Strlič M, Matisová-Rychlá L, Kolar J. Chemiluminescence from paper I. Kinetic analysis of thermal oxidation of cellulose. Polymer Degradation and Stability. 2002;78:357-67.

270.   Strlič M, Kolar J, Pihlar B, Rychlý J, Matisová-Rychlá L. Initial degradation processes of cellulose at elevated temperatures revisited — chemiluminescence evidence. Polymer Degradation and Stability. 2001;72(1):157-62.

271.   Kočar D, Strlič M, Kolar J, Pihlar B. Peroxide-related chemiluminescence of cellulose and its self-absorption. Polymer Degradation and Stability. 2008;93:263-7.

272.   Kočar D, Pedersoli JL, Jr., Strlič M, Kolar J, Rychlý J, Matisová-Rychlá L. Chemiluminescence from paper II. The effect of sample crystallinity, morphology and size. Polymer Degradation and Stability. 2004;86:269-74.

273.   Kočar D, Strlič M, Kolar J, Rychlý J, Matisová-Rychlá L, Pihlar B. Chemiluminescence from paper III: the effect of superoxide anion and water. Polymer Degradation and Stability. 2005;88.

274.   Rychlý J, Matisová-Rychlá L, Lazar M, Slovak K, Strlič M, Kočar D, et al. Thermal oxidation of cellulose investigated by chemiluminescence. The effect of water at temperatures above 100 °C. Carbohydrate Polymers. 2004;58:301-9.

275.   Konoma F, Cai X, Osawa Z. Chemiluminescence from the thermal and photo-oxidation of several wood pulps. Polymer Degradation and Stability. 2000;69(1):105-11.

276.   Millington KR, Deledicque C, Jones MJ, Maurdev G. Photo-induced chemiluminescence from fibrous polymers and proteins. Polymer Degradation and Stability. 2008;93(3):640-7.

277.   Šelih V, Strlič M, Kolar J, Pihlar B. The role of transition metals in oxidative degradation of cellulose. Polymer Degradation and Stability. 2007;92:1476-81.

278.   Strlič M, Kolar J, Šelih V, Kočar D, Pihlar B. A comparative study of several transition metals in Fenton-like reaction systems at circum-neutral pH. Acta Chim Slov. 2003;50:619-32.

279.   Kolar J, Strlič M, editors. Iron Gall Inks: on manufacture, characterisation, degradation and stabilisation. Ljubljana: National and University Library; 2006.

280.   Strlič M, Menart E, Cigić IK, Kolar J, de Bruin G, Cassar M. Emission of reactive oxygen species during degradation of iron gall ink. Polymer Degradation and Stability. 2010;95(1):66-71.

281.   Matich A. Analysis of Food Volatiles Using SPME In: Pawliszyn J, editor. Applications of solid phase microextraction. Cambridge: RSC; 1999.

282.   Augusto F, Leite e Lopes A, Alcaraz Zini C. Sampling and sample preparation for analysis of aromas and fragrances. Trends in Analytical Chemistry. 2003;22(3):160-9.

283.   Gudat A, Firor R. The determination of extractables and leachables in pharmaceutical packaging materials using headspace GC/MS. 2006.

284.   Zhouyao Zhang JP. Analysis of organic compounds in environmental samples by headspace solid phase microextraction. Journal of High Resolution Chromatography. 1993;16(12):689-92.

285.   Zelda P. Determination of residual solvent in pharmaceutical preparations by static headspace GC. Journal of High Resolution Chromatography. 1992;15(5):329-31.

286.   Wang X, Jiang T, Yuan J, Cheng C, Liu J, Shi J, et al. Determination of volatile residual solvents in pharmaceutical products by headspace liquid-phase microextraction gas chromatography-flame ionization detector. Analytical and Bioanalytical Chemistry. 2006;385(6):1082-6.

287.   Suresh Chandra R. Analysis of organic solvents in printing inks by headspace gas chromatography - mass spectrometry. Journal of High Resolution Chromatography. 1991;14(9):587-9.

288.   Services UCLL. Systematic Identification of Conserved Metabolites in GC/MS Data for Metabolomics and Biomarker Discovery. Analytical Chemistry. 2007.

289.   Lommen A, Weg GVD, Engelen MCV, Bor G. An untargeted metabolomics approach to contaminant analysis: Pinpointing potential unknown compounds. Analytica Chimica Acta. 2007;584:43-9.

290.   Herebian D, Hanisch B, Marner F-J. Strategies for gathering structural information on unknown peaks in the GC/MS analysis of Corynebacterium glutamicum cell extracts. Metabolomics. 2005;1(4):317-24.

291.   Cbe SFC. Metabolomics, Metabonomics and Metabolite Profiling: RSC Publishing; 2008.

292.   Metabolomics The Frontier of Systems Biology. Tokyo: Springer; 2005.

293.   Pedro MK. Multivariate accelerated shelf-life testing : a novel approach for determining the shelf-life of foods. Journal of Chemometrics. 2006(November):76-83.

294.   Ziegleder G. Volatile and odorous compounds in unprinted paperboard. Packaging Technology and Science. 1998;11:231-9.

295.   Kolb B, Ettre LS. Static Headspace-Gas Chromatography: Theory and Practice. second ed. New Jersey: John Wiley and Sons Inc.; 2006. 349 p.

296.   Coleman IWM, Gordon BM. Hyphenated gas chromatography. In: Meyers RA, editor. Encyclopedia of Analytical Chemistry. Chichester: John Wiley and Sons Ltd.; 2000.

297.   Penton Z. Optimization of conditions in static headspace GC. Journal of High Resolution Chromatography. 1992;15(12):834-6.

298.   RESTEK. A technical guide for static headspace analysis using GC. www.restekcorp.com.

299.   Wenzl T, Lankmayr EP. Reduction of adsorption phenomena of volatile aldehydes and aromatic compounds for static headspace analysis of cellulose based packaging materials. Journal of Chromatography A. 2000;897(1-2):269-77.

300.   Supelco. Purge-and-trap system guide. Sigma Aldrich; 1997.

301.   Venema A. Dynamic headspace capillary gas chromatography: a versatile analytical technique. Journal of High Resolution Chromatography & Chromatography Communications. 1987;11(1):128-31.

302.   Zhouyao Zhang JP. Sampling volatile organic compounds using a modified solid phase microextraction device. Journal of High Resolution Chromatography. 1996;19(3):155-60.

303.   Strlič M, Cigić Kralj I, Rabin I, Kolar J, Pihlar B, Cassar M. Autoxidation of lipids in parchment. Polymer Degradation and Stability. 2009;94(6):886-90.

304.   Ezquerro O, Tena MT. Determination of odour-causing volatile organic compounds in cork stoppers by multiple headspace solid-phase microextraction. Journal of Chromatography A. 2005;1068(2):201-8.

305.   Ezquerro O, Pons B, Tena MT. Direct quantitation of volatile organic compounds in packaging materials by headspace solid-phase microextraction-gas chromatography-mass spectrometry. Journal of Chromatography A. 2003;985(1-2):247-57.

306.   Ezquerro O, Pons B, Tena MT. Evaluation of multiple solid-phase microextraction as a technique to remove the matrix effect in packaging analysis for determination of volatile organic compounds. Journal of Chromatography A. 2003;1020(2):189-97.

307.   Ezquerro O, Pons B, Tena MT. Development of a headspace solid-phase microextraction-gas chromatography-mass spectrometry method for the identification of odour-causing volatile compounds in packaging materials. Journal of Chromatography A. 2002;963(1-2):381-92.

308.   Strlič M, Menart E, Cigić Kralj I, Kolar J, de Bruin G, Cassar M. Emission of reactive oxygen species during degradation of iron gall ink. Polymer Degradation and Stability. 2010;95(1):66-71.

309.   Koeningsberger DC, Prins R, editors. X-ray Absorption: principles, applications and techniques of EXAFS, SEXAFS and XANES: Wiley; 1988.

310.   Solomon E, Hedman B, Hodgson K, Dey A, Szilagyi R. Ligand K-edge X-ray absorption spectroscopy: covalency of ligand–metal bonds. Coord Chem Rev. 2005;249:97-129.

311.   Westre T, Kennepohl P, DeWitt J, Hedman B, Hodgson K, Solomon E. A Multiplet Analysis of Fe K-Edge 1s → 3d Pre-Edge Features of Iron Complexes. Journal of the American Chemical Society. 1997;119(27):6297-314.

312.   Rehr J, Ankudinov a. Progress in the theory and interpretation of XANES. Coord Chem Rev. 2005;249(1-2):131-40.

313.   Wilke M, Hahn O, Woodland AB, Rickers K. The oxidation state of iron determined by Fe K-edge XANES—application to iron gall ink in historical manuscripts. Journal of Analytical Atomic Spectrometry. 2009;24:1364-72.

314.   Gaur A, Shrivastava BD, Joshi SK. Copper K-edge XANES of Cu(I) and Cu(II) oxide mixtures. Journal of Physics: Conference Series. 2009;190:1-4.

315.   Jerosch H, Lavédrine B, Cherton J-C. The use of size exclusion chromatography (SEC) for the evaluation of paper degradation caused by nitrogen oxides in comparison with other methods. In: Daniels V, Donnithorne A, Smith P, editors. Works of art on paper: books, documents and photographs: techniques and conservation: contributions to the Baltimore Congress, 2-6 September 2002. London: International Institute for Conservation of Historic and Artistic Works; 2002. p. 108-13.

316.   Dupont AL, editor. The role of gelatine/alum sizing in the degradation of paper: a study by size exclusion chromatography in lithium chloride/N,N-dimethylacetamide using multiangle light

scattering detection. Works of art on paper: books, documents and photographs: techniques and conservation; 2002 Sep; Baltimore, MD: International Institute for Conservation.

317.	Havlínová B, Jančovičová V, Brezová V, Čeppan M, Turanová M. Study of ageing of arylmethane dyes by UV-VIS spectroscopy. Restaurator. 2006;27(1):24-34.

318.	Missori M, Righini M, Storace MS, Congiu Castellano A, Selci S, editors. The Effect of Artificial Aging and Sizing on Discolouration of Paper Studied by UV-Vis-NIR Spectroscopy in Comparison to Ancient Paper. Durability of Paper and Writing; 2004; Ljubljana, Slovenia: National and University Library, Ljubljana, Slovenia.

319.	Clementi C, Nowik W, Romani A, Cibin F, Favaro G. A spectrometric and chromatographic approach to the study of ageing of madder (Rubia tinctorum L.) dyestuff on wool. Analytica Chimica Acta. 2007;596:46-54.

320.	Fardim P, Ferreira MMC, Durán N. Multivariate calibration for quantitative analysis of eucalypt kraft pulp by nir spectrometry. Journal of Wood Chemistry and Technology. 2002;22(1):67-81.

321.	Łojewska J, Miśkowiec P, Proniewicz LM, editors. Oxidative and Hydrolytic Path of Paper Degradtion Studied by In-Situ FTIR Transmission Spectroscopy. Durability of Paper and Writing; 2004; Ljubljana, Slovenia: National and University Library, Ljubljana, Slovenia.

322.	Łojewska J, Lubańska A, Łojewski T, Miśkowiec P, Proniewicz LM. Kinetic approach to degradation of paper in situ FTIR transmission studies on hydrolysis and oxidation. e-Preservation Science. 2005;2:1-12.

323.	Krill J. English Artists' Paper: Renaissance to Regency. 2nd revised ed. New Castle: Oak Knoll Press; 2001.

324.	Barrett TD. Early European papers/contemporary conservation papers a report on research undertaken from fall 1984 through fall 1987. The Paper Conservator 1989;13:7-108.

325.	Green SB. Conservation the Papermaker's Perspective. The Paper Conservator. 1986;10:55-63.

326.	Barrett T. Old and new fibers for fine papermaking. Counter. 1995;2:7-9.

327.	Stephens CH, Barrett T, Whitmore PM, Wade JA, Mazurek J, Schilling M. Composition and condition of naturally aged papers. Journal of the American Institute for Conservation. 2008;47(3):2001-215.

328.	McCrady E. The Great Cotton-Rag Myth. Alkaline Paper Advocate. 1992;5(5).

329.	Erhardt D, Tumosa CS, Mecklenburg MF. Chemical and Physical Changes in Naturally and Accelerated Aged Cellulose. In: Cardamone JM, Baker MT, editors. Historic Textiles, Papers, and Polymers in Museums. Washington D.C.: American Chemical Society; 2001. p. 23-37.

330.	Brandis L, Lyall J. Properties of paper in naturally aged books. Restaurator. 1997;18(3):115-30.

331.	Burns T, editor. `A serious and universal evil': the early scientific study of paper deterioration. Works of art on paper: books, documents and photographs: techniques and conservation; 2002 Sep; Baltimore, MD: International Institute for Conservation.

332.	Fredricks PS, Lindgren BO, Theander O. Chlorine oxidation of cellulose. IV.Kinetics and mechanisms of the reactions of methyl-beta-D-glucopyranoside with chlorine in acid aqueous solution. 1971.

333.	Ghosh P, Datta C. Oxidation of jute fibre using different oxidising agents. Indian Journal of Technology. 1987;25(12):681-90.

334.	Rath H, Klink H. Changes of cellulose by chlorine bleach. Melliand Textilberichte international. 1950;31:832-5.

335.	Marina Bicchieri ASGPCC. Analysis of degraded papers by non-destructive spectroscopic techniques. Journal of Raman Spectroscopy. 2006;37(10):1186-92.

336.   Varma AJ, Chavan VB. A study of crystallinity changes in oxidised celluloses. Polymer Degradation and Stability. 1995;49(2):245-50.

337.   Thygesen A, Thomsen AB, Schmidt AS, Jorgensen H, Ahring BK, Olsson L. Production of cellulose and hemicellulose-degrading enzymes by filamentous fungi cultivated on wet-oxidised wheat straw. Enzyme and Microbial Technology. 2003;32(5):606-15.

338.   Eronen P, Österberg M, Jääskeläinen A-S. Effect of alkaline treatment on cellulose supramolecular structure studied with combined confocal Raman spectroscopy and atomic force microscopy Cellulose. 2009;16(2):167-78.

339.   Jähna A, Schrödera MW, Fütingb M, Schenzel K, Diepenbrocka W. Characterization of alkali treated flax fibres by means of FT Raman spectroscopy and environmental scanning electron microscopy Spectrochimica Acta Part A: Molecular and Biomolecular Spectroscopy. 2002;58(10):2271-9.

340.   Cates DH, Eggert C, Yang JL, Eriksson K-EL. Comparison of effluents from TCF and ECF bleaching of kraft pulps. Tappi. 1995;78(12):93-8.

341.   Hernádi A. Thermally induced changes in structure and optical properties of TCF pulp. Papiripar. 2001;45(4):135-9.

342.   Gustavsson R, Swan B. Evaluation of the degradation of cellulose and delignification during oxygen bleaching. TAPPI. 1975;58(3):120-3.

343.   Ouchi A, Sakai H, Oishi T, Hayashi T, Ando W, Ito J. Oxidative total chlorine free photochemical bleaching of cellulosic fabrics. Green Chemistry. 2003;5(5):516-23.

344.   Saito T, Isogai A. TEMPO-mediated oxidation of native cellulose. The effect of oxidation conditions on chemical and crystal structures of the water-insoluble fractions. Biomacromolecules. 2004;5(5):1983-9.

345.   Saito T, Okita Y, Nge TT, Sugiyama J, Isogai A. TEMPO-mediated oxidation of native cellulose: Microscopic analysis of fibrous fractions in the oxidized products. Carbohydrate Polymers. 2006;65(4):435-40.

346.   Elsakhawy M. Effect of bleaching sequence on paper ageing. Polymer Degradation and Stability. 2005;87(3):419-23.

347.   Ek M, Gellerstedt G, Henriksson G, editors. Pulp and Paper Chemistry and Technology Pulping Chemistry and Technology. Berlin: De Gruyter; 2009.

348.   Moorby N, Warrell I, editors. How to Paint Like Turner. London: Tate; 2010.

349.   Tate. Colour and Line Turner's Experiments. United Kingdom: Tate Britain; 2007. p. 2 May 2007 – 30 April 12.

350.   Barrett T, editor. Evaluating the effect of gelatin sizing with regard to the permanence of paper. The Institute of Paper Conservation: conference papers; 1992; Manchester: Institute of Paper Conservation.

351.   Baty J, Barrett T. Gelatin size as a pH and moisture content buffer in paper. Journal of the American Institute for Conservation. 2007;46:105-21.

352.   Barrett T, Mosier C. The role of gelatin in paper permanence. Journal of the American Institute for Conservation. 1995;34:173-86.

353.   Barrett T, Mosier C. The role of gelatin in paper permanence II. The Book & Paper Group annual. 1994;13:5-8.

354.   Nguyen TP, Delatour A, Bouvet S, Rouchon-Quillet V, editors. Effects of Gelatine Sizing on Iron Gall Ink Corroded Paper. Durability of Paper and Writing; 2004; Ljubljana, Slovenia: National and University Library, Ljubljana, Slovenia.

355.   Strlič M, Kolar J, editors. Durability of Paper and Writing 2 Book of Abstracts. Ljubljana: Faculty of Chemistry and Chemical Technology; 2008.

356.   Johnston-Feller R, Feller RL, Bailie CW, Curran M. The Kinetics of Fading: Opaque Paint Films Pigmented with Alizarin Lake and Titanium Dioxide. Journal of the American Institute for Conservation. 1984;23(2):114-.

357.   Allen NS. Action of light on dyed and pigmented polymers. In: Allen NS, Edge M, Horie CV, editors. Polymers in conservation: proceedings of an international conference organized by Manchester Polytechnic and Manchester Museum, Manchester, 17-19 July 1991. Cambridge: Royal Society of Chemistry (Great Britain); 1992. p. 192-213.

358.   Bamford CH, Dewar MJS. Photosensitisation and tendering by vat dyes. Journal of the Society of Dyers and Colourists. 1949;65:674-81.

359.   Egerton GS, Morgan AG. The photochemistry of dyes IV—The role of singlet oxygen and hydrogen peroxide in photosensitized degradation of polymers. Journal of the Society of Dyers and Colourists. 1971;87(8):268-77.

360.   Strlič M, Kolar J, Šelih V-S, Kočar D, Pihlar B. A comparative study of several transition metals in fenton-like reaction systems at circum-neutral pH. Acta Chim Slov. 2003;50:619-32.

361.   Bors W, Michel C, Stettmaier K. Structure-activity relationships governing antioxidant capacities of plant polyphenols. Methods in Enzymology. 2001;335:166-80.

362.   Cai Y, Sun M, Xing J, Corke H. Antioxidant Phenolic Constituents in Roots of Rheumofficinale and Rubia cordifolia: Structure–Radical Scavenging Activity Relationships. Journal of Agricultural and Food Chemistry. 2004;52:7884-90.

363.   Habtemariam S. Antioxidant activity of Knipholone anthrone. Food Chemistry. 2007;102(4):1042-7.

364.   Perron N, Brumaghim J. A Review of the Antioxidant Mechanisms of Polyphenol Compounds Related to Iron Binding. Cell Biochemistry and Biophysics. 2009;53:75-100.

365.   Yen G-C, Chuang D-Y, Duh P-d. Antioxidant activity of anthraquinones and anthrone. Food Chemistry. 2000;70:437-41.

366.   Aguiar A, Ferraz A. Fe(3+)- and Cu(2+)-reduction by phenol derivatives associated with Azure B degradation in Fenton-like reactions. Chemosphere. 2007;66(5):947-54.

367.   Comini LR, Montoya SCN, Sarmiento M, Cabrerea JL, Arguello GA. Characterizing some photophysical, photochemical and photobiological properties of photo sensitizing anthraquinones. Journal of Photochemistry and Photobiology A: Chemistry. 2007;188(2-3):185-91.

368.   Montoya SCN, Comini LR, Sarmiento M, Becerra C, Albesa I, Arguello GA, et al. Natural anthraquinones probed as Type I and Type II photosensitizers: singlet oxygen and superoxide anion production. Journal of Photochemistry and Photobiology B: Biology. 2005;78(1):77-83.

369.   Habtemariam S, Dagne E. Prooxidant action of knipholone anthrone: Copper dependent reactive oxygen species generation and DNA damage. Food and Chemical Toxicology. 2009;47:1490-4.

370.   Ma J, Ma W, Song W, Chen C, Tang Y, Zhao J, et al. Fenton degradation of organic pollutants in the presence of low-molecular-weight organic acids: cooperative effect of quinone and visible light. Environmental science & technology. 2006;40(2):618-24.

371.   Ma J, Song W, Chen C, Ma W, Zhao J, Tang Y. Fenton degradation of organic compounds promoted by dyes under visible irradiation. Environmental science & technology. 2005;39(15):5810-5.

372.   Cardon D. Le monde des teintures naturelles. Paris: Belin; 2003.

373.   Cardon D. Natural Dyes. London: Archetype; 2007.

374.   Zlatkevich L, editor. Luminescence techniques in solid-state polymer research. New York: Marcel Dekker Inc.; 1989.

375.   Strlič M, Kolar J, Pihlar B, Rychly J, Matisova-Rychla L. Chemiluminescence during thermal and thermo-oxidative degradation of cellulose. European Polymer Journal. 2000;36(11):2351-8.

376.   van den Berg RA, Hoefsloot HCJ, Westerhuis JA, Smilde AK, van der Werf MJ. Centering, scaling, and transformations: improving the biological information content of metabolomics data. BMC Genomics [Internet]. 2006; 7.

377.   Kočar D, Luiz Pedersoli JJ, Strlič M, Kolar J, Rychly J, Matisova-Rychla L. Chemiluminescence from paper: II. The effect of sample crystallinity, morphology and size. Polymer Degradation and Stability. 2004;86(2):269-74.

378.   Kočar D, Strlič M, Kolar J, Rychly J, Matisova-Rychla L, Pihlar B. Chemiluminescence from paper III: the effect of superoxide anion and water. Polymer Degradation and Stability. 2005;88(3):407-14.

379.   Abrusci C, Marquina D, Santos A, A., Corrales T, Catalina F. A chemiluminescence study on degradation of gelatine biodegradation by bacteria and fungi isolated from cinematographic films. Journal of Photochemistry and Photobiology A: Chemistry. 2007;185(2-3):188-97.

380.   Abrusci C, Martín-Gonzalez A, A., Catalina F, Bosch P, Corrales T. Chemiluminescence study of commercial type-B gelatines. Journal of Photochemistry and Photobiology A: Chemistry. 2004;163(3):537-46.

381.   Millington KR, Maurdev G, Jones MJ. Thermal chemiluminescence of fibrous proteins. Journal Of Applied Polymer Scienc. 2007;92:1504-12.

382.   Millington KR, Zhang H, Jones MJ, Wang X. The effect of dyes on photo-induced chemiluminescence emission from polymers. Polymer Degradation and Stability. 2010;95(1):34-42.

383.   StatSoft. Electronic Statistics Textbook. Tulsa: StatSoft; 2011. Available from: WEB: http://www.statsoft.com/textbook/.

384.   Shen L, Ji HF, Zhang HY. Photophysical and photochemical properties of anthraquinones: A DFT study. Theochem-J Mol Struct. 2008;851(1-3):220-4.

385.   Singh A, Koppenol WH. Introduction: interconversion of singlet oxygen and related species. Photochemistry and Photobiology. 1978;28(45):429-33.

386.   Hider BC, Liu ZD, Khodr HH. Metal chelation of polyphenols. Methods in Enzymology. 2001;335:190-203.

387.   Xu X-R, Li H-B, Wang W-H, Gu J-D. Degradation of dyes in aqueous solutions by the Fenton process. Chemosphere. 2004;57(7):595-600.

388.   Aplin R, Feitz AJ, Waite TD. Effect of Fe (III)-ligand properties on effectiveness of modified photo-Fenton processes. Water Science & Technology. 2001;44(5):23-30.

389.   Griffiths J, Hawkins C. Involvement of singlet oxygen in the sensitized photodegradation of cellulose. Polymer. 1976;17(I):1113-4.

390.   Rabek J, Rånby B. The role of singlet oxygen in the photooxidation of polymers. Photochemistry and Photobiology. 1978;28:557-70.

391.   Hon N-s. Photooxidative Degradation of Cellulose: Reactions of the Cellulosic Free Radicals with Oxygen. Journal of Polymer Science Polymer Chemistry Edition. 1979;17:441-54.

392.   Daniels V. Oxidative damage and the preservation of organic artefacts. Free radical research communications. 1989;5(4-5):213-20.

393.   Egerton GS. The mechanism of the photochemical degradation of textile materials. Journal of the Society of Dyers and Colourists. 1949;65(12):764-80.

394.   Baruah S, Jaisai M, Imani R, Nazhad M, Dutta J. Photocatalytic paper using zinc oxide nanorods. Science and Technology of Advanced Materials [Internet]. 2010; 11.

395.   Markham MC, Laidler KJ. A kinetic study of Photo-oxidations on the Surface of Zinc Oxide in Aqueous Suspensions. Journal of Physical Chemistry. 1953;57(3):363-9.

396.   Rehman S, Ullah R, Butt AM, Gohar ND. Strategies of making TiO(2) and ZnO visible light active. Journal of Hazardous Materials. 2009;170:560-9.

397.   Hung-Wei C, Thanamuthu R, Shen-Ming C. Preparation, characterization and electrocatalytic behaviour of zinc oxide/zinchexacyanoferrate andruthenium oxide hexacyanoferrate hybrid film-modified electrodes. Electrochimica Acta. 2008;53:2862-9.

398.   Argemi M, Gonzalo D, Pugès M, Maspoch ML, Mourey W, Alonso M. Long-term conservation of heritage in transformed atmospheres. In: Mourey W, Robbiola L, editors. Metal 98: proceedings of the International Conference on Metals Conservation = Actes de la conférence internationale sur la conservation des métaux: Draguignan-Figanières, France, 27-29 May 1998. Ottawa: James & James Ltd.; 1998. p. 245-7.

399.   Gilberg M, Grattan D, editors. Oxygen-free storage using Ageless oxygen absorber. Preventive conservation practice, theory and research; 1994; Washington, DC.

400.   Hadgraft N, Welch S. Vacuum-packing and its implications for library, archive and related materials. Paper Conservation News. 1999;89:12-4.

401.   Linnie MJ. Use of a low-oxygen atmosphere for the control of insect pests. Collection forum. 2000;14(1-2):57-65.

402.   Maekawa S. Oxygen-free environments for conservation in museums. OPD restauro: rivista dell'Opificio delle pietre dure e laboratorio di restauro di Firenze. 2001;13:131-42.

403.   Ware M. A blueprint for conserving cyanotypes. Topics in photographic preservation. 2003;10:2-18.

404.   Lerwill A, Townsend JH, Liang H, Thomas J, Hackney S. A portable micro-fading spectrometer for versatile lightfastness testing. e-Preservation Science. 2008;5:17-28.

405.   Hackney S, Townsend JH, Thomas J, Lerwill A, inventors; Trustees of the Tate Gallery, Hackney, S., Townsend, J. H., Thomas, J., Lerwill, A., assignee. A method for preserving objects containing pigment. UK patent WO 2010029314 (A1) 2010.

406.   Lerwill A, Townsend JH, Liang H, Hackney S, Thomas J, editors. Design for a versatile microfadometer for lightfastness testing and pigment identification. SPIE Europe, Optical Metrology, O3A: Optics for Art, Architecture, and Archaeology; 2007; Munich.

407.   Eastaugh B. The Pigmentum Project: The Pigmentum Collection. 2006 [updated 2011; cited 2011 November 14]; Available from: http://pigmentum.org/about/collection/.

408.   Janssens K, Rouchon-Quillet V, Remazeilles C, Eveno M, Wattiaux A, editors. Evaluation of Relative Fe2+ and Fe3+ Contents of Original Manuscript Fragments by Means of μ-Xanes and Mössbauer Spectrometry. Durability of Paper and Writing; 2004; Ljubljana, Slovenia: National and University Library, Ljubljana, Slovenia.

409.   Gütlich P. Photoswitchable coordination compounds. Coord Chem Rev. 2001;219-221:839-79.

410.   Christophe, Champion G, Cafun J-D, Arrio M-A, Bleuzen A. Structural rearrangements induced by photoexcitation in a RbCoFe Prussian blue derivative. Angewandte Chemie (International ed in English). 2007;46(8):1287-9.

411.   Verdaguer M, Girolami GS. Magnetic Prussian Blue Analogues. ChemInform. 2005;36(28).

412.   Balmaseda J, Reguera E, Rodríguez-Hernández J, Reguera L, Autie M. Behavior of transition metals ferricyanides as microporous materials. Microporous and Mesoporous Materials. 2006;96(1-3):222-36.

413.   Dostal A, Kauschka G, Reddy SJ, Scholz F. Lattice contractions and expansions accompanying the electrochemical conversions of Prussian blue and the reversible and irreversible insertion of rubidium and thallium. Journal of Electroanalytical Chemistry. 1996;406:155-63.

414.   Kaye S, Long J. The role of vacancies in the hydrogen storage properties of Prussian blue analogues. Catalysis Today. 2007;120:311-6.

415.   Itaya K, Uchida I, Neff V. Electrochemistry of Polynuclear Transition Metal Cyanides: Prussian Blue and Its Analogues. Accounts of Chemical Research. 1986;19:162-68.

416.   Neff V. Electrochemical oxidation and reduction of thin films of prussian blue. Journal of the Electrochemical Society. 1978;1125:886-7.

417.   Kulesza P. Solid-state electrochemistry of iron hexacyanoferrate (Prussian blue type) powders evidence for redox transitions in mixed-valence ionically conducting microstructures. Journal of Electroanalytical Chemistry. 1990;289:103-16.

418.   Gu Z-Z, Einaga Y, Sato O, Fujishima A, Hashimoto K. Photo- and Dehydration-Induced Charge Transfer Processes Accompanied with Spin Transition on $CoFe(CN)_5NH_3 \cdot 6H_2O$. Journal of Solid State Chemistry. 2001;159:336-42.

419.   Roque J, Reguera E, Balmaseda J, Rodríguez-Hernández J, Reguera L, del Castillo LF. Porous hexacyanocobaltates(III): Role of the metal on the framework properties. Microporous and Mesoporous Materials. 2007;103(1-3):57-71.

420.   Herren F, Fischer P, Ludi A, Haelg W. Neutron diffraction study of Prussian Blue, Fe4[Fe(CN)6]3.xH2O. Location of water molecules and long-range magnetic order. Inorganic Chemistry. 1980;19(4):956-9.

421.   Buser H, Schwarzenbach D, Petter W, Ludi A. The crystal structure of Prussian blue $Fe_4[Fe(CN)_6]_3 \cdot xH_2O$. Inorganic Chemistry. 1977;16(11):2704-9.

422.   Kravzov J, Rios C, Altagracia M, Monroynoyola A, Lopez F. Relationship between physiochemical properties of Prussian blue and it efficacy as antidote against thallium poisoning. Journal of Applied Toxicology. 1993;13(3):213-6.

423.   Christensen PA, Harriman A, Neta P, Richoux M-C. Photo-oxidation of water using Prussian blue as catalyst. Journal of the Chemical Society, Faraday Transactions I. 1985;81:2461-6.

424.   Holmes SM, Whelpley AS, Girolami GS. Nanocomposite of a chromium Prussian blue with TiO2. Redox reactions and the synthesis of Prussian blue molecule-based magnets. Polyhedron. 2007;26(9-11):2291-8.

425.   Smith PJ. Photofading of pigments and photosensitizer material. Journal of the Society of Dyers and Colourists. 1991;107(7/8):282.

426.   Samain L, Silversmit G, Sanyova J, Vekemans B, Salomon H, Gilbert B, et al. Fading of modern Prussian blue pigments in linseed oil medium. Journal of Analytical Atomic Spectrometry. 2011;26:930-41.

427.   Kigawa R, Miyazawa Y, Yamano K, Miura S, Nochide H, Kimura H, et al. Practical methods of low oxygen atmosphere and carbon dioxide treatments for eradication of insect pests in Japan. In: Kingsley H, Pinniger D, Xavier-Rowe A, Winsor P, editors. Integrated pest management for collections: proceedings of 2001, a Pest Odyssey. London: James & James Ltd.; 2001. p. 81-8.

428.   del Hoyo J, Mecklenburg MF. The use of micro-fading spectrometry to evaluate the light fastness of materials in oxygen-free environments. Spectroscopy Letters. 2011;44:113-21.

429.   Roque J, Reguera E, Balmaseda J, Rodríguez-Hernández, Reguera L, del Castillo LF. Porous hexacyanocobaltates(III): Role of the metal on the framework properties. Microporous and Mesoporous Materials. 2007;103:57-71.

430.   Source DSR. STATION 9.3 Material Processing. 2004 [updated 2008; cited 2011 November 14]; Available from: http://www.webarchive.org.uk/wayback/archive/20091018041152/http://www.srs.ac.uk/srs/stations/station9.3.htm.

431.   Source DL. Beamlines I18 - Design Specifications. 2009 [updated 2006; cited 2011 November 14].

432.   Margadonna S, Prassides K, Fitch AN. Large lattice responses in a mixed-valence Prussian blue analogue owing to electronic and spin transitions induced by X-ray irradiation. Angewandte Chemie (International ed in English). 2004;43(46):6316-9.

433.   Strlič M, Cigić Kralj I, Kolar J, de Bruin G, Steemers T. The role of volatile organic compounds in paper degradation. In: Strlič M, Kolar J, editors. Durability of Paper and Writing 2 Book of Abstracts. Ljubljana: National and University Library Ljubljana; 2008. p. 28-9.

434.   Hobaica SC, editor. VOC Testing for Books, Papers and Cellulose Acetate Laminated Documents. Advances in Paper Conservation Research; 2009; London: British Library.

435.   Ramalho O, Dupont A-L, Egasse C, Lattuati-Derieux A. Emission rates of volatile organic compounds from paper. e-Preservation Science. 2009;6:53-9.

436.   Strlič M, Thomas J, Trafela T, Cséfalvayová L, Kralj-Cigić I, Kolar J, et al. The scent of degradation : VOCs as a source of information In: Degrigny C, Cleaver L, editors. Indoor Air Quality in Museums and Archives; Chalon-sur-Saône, France2010.

437.   Gibson LT. Analysing smelly old books. In: Horie CV, editor. Advances in Paper Conservation Research; London: British Library; 2009.

438.   Vorst O, Vos CHRD, Lommen a, Staps RV, Visser RGF, Bino RJ, et al. A non-directed approach to the differential analysis of multiple LC–MS-derived metabolic profiles. Metabolomics. 2005;1(2):169-80.

439.   Verouden MPH, Westerhuis Ja, van der Werf MJ, Smilde AK. Exploring the analysis of structured metabolomics data. Chemometrics and Intelligent Laboratory Systems. 2009;98(1):88-96.

440.   Pohjanen E, Thysell E, Lindberg J, Schuppe-Koistinen I, Moritz T, Jonsson P, et al. Statistical multivariate metabolite profiling for aiding biomarker pattern detection and mechanistic interpretations in GC/MS based metabolomics. Metabolomics. 2006;2(4):257-68.

441.   Jonsson P. A Strategy for Identifying Differences in Large Series of Metabolomic Samples Analyzed by GC/MS. Analytical Chemistry. 2004;76(6):1738-45.

442.   Hansen M, Zhao J. Automated work-flow for processing high-resolution direct infusion electrospray ionization mass spectral fingerprints. 2007;3(1):41-54.

443.   Metabolomics SIo. XCMS Online. 2011 [cited 2011 30 November]; Available from: https://xcmsonline.scripps.edu/.

444.   Xia J. Metaboanalyst a web service for metabolomic data analysis. 2011 [cited 2011 30 November]; Available from: http://www.metaboanalyst.ca.

445.   Dixon SJ, Brereton RG, Soini HA, Novotny MV, Penn DJ. An automated method for peak detection and matching in large gas chromatography-mass spectrometry data sets. Journal of Chemometrics. 2007(January):325-40.

446.   Lange E, Tautenhahn R, Neumann S, Gröpl C. Critical assessment of alignment procedures for LC-MS proteomics and metabolomics measurements. BMC Bioinformatics. 2008;9(375):online

447.   Prince JT. Chromatographic alignment of ESI-LC-MS proteomics data sets by ordered bijective interpolated warping. Analytical Chemistry. 2006;78(17):6140-52.

448.   Dorsten FAV. Assessment of PLSDA cross validation. Metabolomics. 2008:81-9.

449.   NIST. AMDIS. NIST; 2011 [cited 2011 1 December]; Available from: http://chemdata.nist.gov/mass-spc/amdis/.

450.   Carroll A. Metabolome Express. 2011 [cited 2011 1 December]; Available from: https://www.metabolome-express.org.

451.   Kruskal JB, Wish M. Multidimensional Scaling. Beverly Hills: Sage; 1977.

452.   Young FW. Multidimensional Scaling. In: Kotz-Johnson, editor. Encyclopedia of Statistical Sciences: John Wiley & SOns; 1985.

453.   Hammer Ø, Harper D. P A S T PAlaeontological STatistics, Multivariate Statistics. Natural History Museum, University of Oslo; 2011 [cited 2011 September 4, 2011]; documentation of the statistical methods employed by the software PAST].

454.   Jackson D, Chen Y. Robust principal component analysis and outlier detection with ecological data. Environmetrics. 2004;15:129-39.

455.   Wold S. PLS-regression: a basic tool of chemometrics. Chemometrics and Intelligent Laboratory Systems. 2001;58(2):109-30.

456.   Kjeldahl K, Bro R. Some common misunderstandings in chemometrics. Journal of Chemometrics. 2010;24:558-64.

457.   Rubingh CM, Bijlsma S, Derks EPPA, Bobeldijk I, Verheij ER, Kochhar S, et al. Assessing the performance of statistical validation tools for megavariate metabolomics data. 2006;2(2):53-61.

458.   Zupan J, Gasteiger J. Neural Networks in Chemistry and Drug Design. second ed. Chichester: Wiley-VCH; 1999.

459.   Popescu C, Budrugeac P, Wortmann F, Miu L, Demco D, Baias M. Assessment of collagen-based materials which are supports of cultural and historical objects. Polymer Degradation and Stability. 2008;93(5):976-82.

460.   Leclercq S, Milo C, Reineccius G. Effects of cross-linking, capsule wall thickness, and compound hydrophobicity on aroma release from complex coacervate microcapsules. Journal of Agricultural and Food Chemistry. 2009;57(4):1426-32.

461.   Strlič M, Menart E, Kralj Cigić I, de Bruin G, Kolar J, Cassar M. Emission of volatiles and reactive oxygen species during degradation of iron gall ink. Polymer Degradation and Stability. 2010;95:66-71.

462.   Bialecki J, Axe F, Attygalle A. Hydroxycarbonyl anion (m/z 45), a diagnostic marker for alpha-hydroxy carboxylic acids. Journal of Mass Spectrometry. 2009;44(2):252-9.

463.   Strlič M, Kralj Cigić I, Možir A, De Bruin G, Kolar J, Cassar M. The effect of volatile organic compounds and hypoxia on paper degradation. Polymer Degradation and Stability. 2011;96:608-15.

464.   Frankel E. Antioxidant Activity by Headspace Gas Chromatography of Volatile Oxidation Products of ω-6 and ω-3 Polyunsaturated Lipids. Methods in Enzymology. 1999;299:190-201.

465.   van den Berg RA, Rubingh CM, Westerhuis JA, van der Werf MJ, Smilde AK. Metabolomics data exploration guided by prior knowledge. Analytica Chimica Acta. 2009;651:173-81.

466.   Borgatti SP. Multidimensional Scaling. Analytictech; 1997 [cited 2011 September 4, 2011]; Available from: http://www.analytictech.com/borgatti/mds.htm.

467.   Xie Y, Chen F, He J, Zhao J, Wang H. Photoassisted degradation of dyes in the presence of Fe 3+ and H 2 O 2 under visible irradiation. Journal of photochemistry & photobiology A: Chemsitry. 2000;136:235-40.

468.   Wu K, Xie Y, Zhao J, Hidaka H. Photo-Fenton degradation of a dye under visible light irradiation. Journal of Molecular Catalysis A: Chemical. 1999;144:77-84.

469.   Chen F, Xie Y, He J, Zhao J. Photo-Fenton degradation of dye in methanolic solution under both UV and visible irradiation. Journal of Photochemistry and Photobiology A: Chemistry. 2001;138(2):139-46.

470.   Zhang Y-G, Ma L-L, Li J-L, Yu Y. In situ Fenton reagent generated from TiO2/Cu2O composite film: a new way to utilize TiO2 under visible light irradiation. Environmental science & technology. 2007;41(17):6264-9.

471.   Qamar M, Muneer M. A comparative photocatalytic activity of titanium dioxide and zinc oxide by investigating the degradation of vanillin. Desalination. 2009;249:535-40.

472.   Whitmore PM, Pan X, Bailie C. Predicting the fading of objects: identification of fugitive colorants through nondestructive lightfastness measurements. Journal American Institute for Conservation. 1999;38(3):395-409.

473.   Connors-Rowe SA, Morris HR, Whitmore PM. Evaluation of appearance and fading of daylight fluorescent watercolors. Journal of the American Institute for Conservation. 2005;44(2):75-94.

474.   Łojewski T, Thomas J, Gołab R, Kawałko J, Łojewska J. Note: Light ageing with simultaneous colorimetry via fibre optics reflection spectrometry. Review of Scientific Instruments. 2011;82(7):available online.

475.   Salthammer T. Environmental test chambers and cells. In: Salthammer T, Uhde E, editors. Organic Indoor Air Pollutants Occurrence, Measurment, Evaluation. second ed. Weinheim: Wiley-VCH; 2009.

476.   Markes International. Sampling Accessories: FLEC® Emission Cell VOC emissions from materials. 2011 [cited 2011 29 November]; Available from: http://www.markes.com/sampling-accessories/flec-emission-cell.aspx.

477.   Bañares M. Methodology: Combination of in Situ Spectroscopy and Simultaneous Activity Measurements Under Catalytic Reaction Conditions. Catalysis Today. 2005;100(1-2):71-7.

478.   Tinnemans S, Mesu J, Kervinen K, Visser T, Nijhuis T, Beale A, et al. Combining operando techniques in one spectroscopic-reaction cell: New opportunities for elucidating the active site and related reaction mechanism in catalysis. Catalysis Today. 2006;113(1-2):3-15.

479.   Kore Technology. MS-200 Portable Mass Spectrometer. 2005 [cited 2011 28 November]; Available from: http://www.kore.co.uk/ms-200.htm.

480.   Woolfenden E. Standard methods for testing emissions of organic vapours from building products to indoor air. In: Salthammer T, Uhde E, editors. Organic Indoor Air Pollutants Occurrence, Measurment, Evaluation. second ed. Weinheim: Wiley-VCH; 2009.

481.   Clausen PA, Kofeod-Sørensen. Sampling and analysis of SVOCs and POMs in indoor air. In: Salthammer T, Uhde E, editors. Organic Indoor Air Pollutants Occurrence, Measurment, Evaluation. second ed. Weinheim: Wiley-VCH; 2009.

482.   Zhang Y, Mo J. Real-time monitoring of indoor organic compounds. In: Salthammer T, Uhde E, editors. Organic Indoor Air Pollutants Occurrence, Measurment, Evaluation. second ed. Weinheim: Wiley-VCH; 2009.

483.   Sobucki W, Drewniewska-Idziak B. Survey of the Preservation Status of the 19th and 20th Century Collections at the National Library in Warsaw. Restaurator. 2003;24:189-201.

484.   Palm J, Cullhed P. Papierqualität. Restauro. 1988;20:38-43.

485.   Ryhl-Svendsen M, Glastrup J. Acetic acid and formic acid concentrations in the museum environment measured by SPME-GC/MS. Atmospheric Environment. 2002;36(24):3909-16.

486.   Schieweck A, Salthammer T. Indoor pollutants in the museum environment. In: Salthammer T, Uhde E, editors. Organic Indoor Air Pollutants Occurrence, Measurment, Evaluation. second ed. Weinheim: Wiley-VCH; 2009.

487.   Missori M, Righini M. Gelatine sizing and discoloration : A comparative study of optical spectra obtained from ancient and artificially aged modern papers. Optics Communications. 2006;263:289-94.

488.   Strlič M. Heritage Smells! - On the value of gaseous emissions from heritage objects in non-destructive diagnostics. 2011 [cited 2011 28 November]; Available from: http://www.ucl.ac.uk/sustainableheritage/heritagesmells.htm.

489.   Havermans J. Effects of Air Pollutants on the Accelerated Ageing of Cellulose-based Materials. Restaurator. 1995;16:209.

490.   Bukovský V, Trnková M, Nemeček P, Oravec P. Light-induced oxidation of newsprint sheets in a paper block part 1: Colour changes in paper. Restaurator. 2006;27(2):114-30.

491.   Bukovský V, Trnková M, Nemeček P, Oravec P. Light-induced Oxidation of Newsprint Sheets in a Paper Block Part 2: Extent of Degradation Changes. Restaurator. 2006;27(2):200-17.

492.   Tétreault J. Airborne Pollutants in Museums, Galleries, and Archives: Risk Assessment, Control Strategies, and Preservation Management. Ottawa: Canadian Conservation Institute; 2003.

493.   LightCheck. 2008 [cited 2011 28 November]; Available from: http://www.lightcheck.co.uk/.

494.   Townsend JH, Hackney S, editors. The benefits of enclosed and anoxic storage for digital prints. Third Conference on Preservation and Conservation Issues Related to Digital Printing and Digital Photography; 2006; London: Institute of Physics and MATAR Research Centre of the University of the Arts London. .

495.   Anderson G, editor. Reinventing the Museum Historical and Contemporary Perspectives on the Paradigm Shift. Walnut Creek: AltaMira Press; 2004.

496.   Milner C. Who Cares? Conservation in a Contemporary Context. In: Anderson G, editor. Reinventing the Museum Historical and Contemporary Perspectives on the Paradigm Shift. Walnut Creek: AltaMira Press; 2004.

497.   Saunders D, Joyce HT, Woodcock S, editors. Conservation and Access. London: International Institute for Conservation; 2008.

498.   Padfield T, Borchersen K, editors. Museum Microclimates. Contributions to the conference in Copenhagen 19-23 November 2007. Copenhagen: National Museum 2007.

499.   Dahlin E. PROPAINT Improved Protection of Paintings During Exhibition, Storage and Transit, Final Activity Report. EU FP6, 2010 Contract No.: SSPI-044254.

500.   Watts S, Crombie D, Jones S, Yates SA, editors. Museum showcases: specification and reality, costs and benefits. Museum Microclimates; 2007; Copenhagen.

501.   Hackney S, editor. The Evolution of a conservation framing policy at Tate. Museum Microclimates; 2007; Copenhagen.

502.   Ashley-Smith J. Risk Assessment for Object Conservation. Oxford: Butterworth-Heinemann; 1999.

503.   Ford B, Smith N, editors. Lighting guidelines and the lightfastness of Australian indigineous objects at the National Museum of Australia. Cultural Heritage/Cultural Identity – The Role of Conservation XVI ICOM-CC Triennial Conference; 2011; Lisbon: ICOM-CC.

504.   Barański A, Dutka D, Dziembaj R, Konieczna-Molenda A, Łagan JM. Effect of relative humidity on the degradation rate of cellulose. Methodology studies. Restaurator. 2004;25(1):68-74.

505.   Bogaard J, Whitmore PM, editors. Explorations of the role of humidity fluctuations in the deterioration of paper. Works of art on paper: books, documents and photographs: techniques and conservation; 2002 Sep; Baltimore, MD: International Institute for Conservation.

506.   Giles CH, Haslam R, Duff DG. Examination of the cause of the humidity sensitivity of the lightfastness of dyed materials. 1976.

507.   Brown MR. Polyester Film Encapsulation. Washington D.C.: Preservation Office Research Services, Library of Congress; 1980.

508.   Shahani CJ, Harrison G. Spontaneous formation of acids in the natural aging of paper. In: Daniels V, Donnithorne A, Smith P, editors. Works of art on paper: books, documents and photographs: techniques and conservation: contributions to the Baltimore Congress, 2-6 September 2002; London: International Institute for Conservation of Historic and Artistic Works; 2002. p. 189-92.

509.   Hackney S. The development of an anoxic framing system for the display of works of art on paper. The Science of Galleries; 17 February 2005; The British Museum: ICON; 2006.

510.   Ridge J, editor. The Tate brand: its consequences for the care and presentation of Tate collections. The Object in Context; 2006; Munich: IIC.

511.   Italian Ministry for Cultural Heritage and Activities. NET-Heritage. 2011 [cited 2011 1 December]; Available from: http://www.netheritage.eu/index.asp.

512.   Thomas J, Hackney S, Townsend JH. Anoxic framing solutions for display of works of art on paper. Showcases Inside Out; Porto2009.

513.   Nguyen TP, Le Bourg E, Bouvet S, Rottier V. Optimisation of the quality control of cellulosic materials used for the conservation and storage of paper-based cultural heritage, based on the

emissions of volatiles. Cultural Heritage/Cultural Identity – The Role of Conservation XVI ICOM-CC Triennial Conference; Lisbon: ICOM-CC; 2011.

514.	Fournier A. POPART preservation of plastic artefacts in museum collections. 2011 [cited 2011 1 December]; Available from: http://popart.mnhn.fr/.

Appendix A

Paper Samples

Waterleaf Rough (WLR)

Waterleaf NOT/Cold Pressed (WLCP)

Waterleaf Glazed (WLG)

Gelatine Sized Rough (GSR)

Gelatine Sized NOT/Cold Pressed (GSCP)

Gelatine Sized Glazed (GSG)

Appendix B

Anoxia Decision Trees

Should I consider modified atmosphere and/or MC frames for the display/storage for my object?

Is the object in question categorised by your institution as light sensitive?

No

Is the object in question known to be composed of materials that are sensitive to oxidation, humidity changes and/or exogenous pollution?

No

Is the object in question fragile, difficult to clean and/or easily damaged by physical contact?

No

Yes

What is the intended display practice for the object in question?

Long-term/permanent display → Go to long-term display decision tree.

Short-term/temporary display → Go to short-term display decision tree.

Not on display → Go to storage decision tree.

Neither modified atmosphere nor MC treatment are a priority for this object. → Neither modified atmosphere nor MC display/storage are recommended.

My object is on long-term or permanent display.

Has the object been conserved and de-acidified if necessary?

No → Consider conserving the object prior to application of modified atmosphere storage. Acidic paper is a particular concern because it can lead to an accumulation of volatile acids.

Yes

What is the format of the object?

Small to medium format

Large format

Does your budget allow for large format glazing?

Are most of the colorants in your object known?

No → Consider conducting a technical study of the object. The goal of this study can be to identify the primary colorants, but it can be as simple as identifying fugitive colorants *in situ* with a micro-fadeometer.

Yes

Are there fugitive colorants?

The photo-reactivity of a colorant is complex and depends on many factors, but generally if a colorant is fugitive under ambient atmosphere it is undergoing a photo-oxidative process. Note that Some organic colorants can undergo both photo-oxidative and photo-reductive colour change. The presence of oxygen inhibits photo-reductive processes.

Yes

No

In the absence of fugitive colorants, the substrate and binding media must be considered. Most organic materials will benefit from anoxic conditions, but the potential for VOC accumulation must be addressed, this is a particular problem for wool and silk. Care must also be taken to give binding media time to cure and solvents time to evaporate.

Does your object contain colorants that are known to undergo photo reductive fading?

No → Anoxic display is recommended.

Yes

Modified atmosphere and MC treatment require glazing.

Consider other options: timed illumination, curtains/blinds, rotated display.

MC frames are recommended.

Does your object contain a significant proportion of Prussian blue and/or related pigments?

Yes → Faded Prussian blue requires oxygen to revert to its original colour.

Consider low oxygen display, with periodic monitoring for colour change and oxygen depletion.

No

Evaluate the distribution and photo-stability of the colorants in the object. Determine the most fugitive colorants and the colorants that are most "significant" for the visual impact of the object.

Photo-oxidation is a surface phenomenon. At ambient conditions the rate of reaction is not oxygen dependent, and the concentration at which oxygen concentration becomes significant is material dependent. Approximately 5% oxygen has been shown to be a critical level for hand-ground inorganic pigments. At this concentration, cellulosic substrates receive some benefit as do some organic colorants.

Are there fugitive colorants?

1. The most fugitive colorants undergo photo-reductive changes.
2. The most significant colorants undergo photo-reductive changes.
3. The most populous colorants undergo photo-reductive changes.

There are both photo-oxidative and photo-reductive colorants, and representatives of both classes of colorant can be considered significant and/or widely distributed.

1. The most fugitive colorants undergo photo-oxidative changes.
2. The most significant colorants undergo photo-oxidative changes.
3. The most populous colorants undergo photo-oxidative changes.

Anoxic and MC display are possible solutions.

289

My object is on short-term or temporary display.

Has the object been conserved and de-acidified if necessary? → **No** → Consider conserving the object prior to application of modified atmosphere storage. Acidic paper is a particular concern because it can lead to an accumulation of volatile acids.

Yes

Does the object have an individual or interchangeable decorative frame? → **individual**

interchangeable

Compact, multi-object storage (e.g. Boxes, portfolios, plan chests)

What is the storage practice for the objects when not on display?

Photo-oxidation involves both photo-initiation and subsequent "dark reactions". If there is storage space available, and access to the unframed object is not an institutional priority, consider storing the object in its MC or anoxic frame.

In frame

Are most of the colorants in your object known? → **No**

Yes

Does your object contain colorants that are known to undergo photo-reductive fading? → **No**

Yes

Does your object contain a significant proportion of Prussian blue and/or related pigments? → **No**

Yes

Faded Prussian blue requires oxygen to revert to its original colour.

Does the object also contain colorants that undergo photo-oxidative changes? → **No**

Yes

Anoxic display followed by storage in ambient atmosphere is recommended.

Consider conducting a technical study of the object. The goal of this study can be to identify the primary colorants, but it can be as simple as identifying fugitive colorants *in situ* with a micro-fadeometer.

Are there fugitive colorants? → **No**

Yes

The photo-reactivity of a colorant is complex and depends on many factors, but generally if a colorant is fugitive under ambient atmosphere it is undergoing a photo-oxidative process. Note that Some organic colorants can undergo both photo-oxidative and photo-reductive colour change. The presence of oxygen inhibits photo-reductive processes.

In the absence of fugitive colorants, the substrate and binding media must be considered. Anoxia will limit the degradation of most organic materials, including the yellowing of papers. If anoxic frames are used then these objects can be displayed at higher light levels. MC frames offer another solution for micro climate control. In either case the potential for VOC accumulation must be addressed.

Anoxic and MC display are possible solutions.

anoxic display is recommended.

1. The most fugitive colorants undergo photo-oxidative changes.
2. The most significant colorants undergo photo-oxidative changes.
3. The most populous colorants undergo photo-oxidative changes.

1. The most fugitive colorants undergo photo-reductive changes.
2. The most significant colorants undergo photo-reductive changes.
3. The most populous colorants undergo photo-reductive changes.

MC frames are recommended.

Evaluate the distribution and photo-stability of the colorants in the object. Determine the most fugitive colorants and the colorants that are most "significant" for the visual impact of the object.

Are there fugitive colorants? → **No**

Yes

There are both photo-oxidative and photo-reductive colorants, and representatives of both classes of colorant can be considered significant and/or widely distributed.

Photo-oxidation is a surface phenomenon. At ambient conditions the rate of reaction is not oxygen dependent, and the concentration at which oxygen concentration becomes significant is material dependent. Approximately 5% oxygen has been shown to be a critical level for hand ground inorganic pigments. At this concentration cellulosic substrates receive some benefit as do some organic colorants.

Prussian blue and other inorganic pigments that are unstable in anoxia have been found to be stable at approximately 5% oxygen.

Display in 5% oxygen with periodic monitoring for colour change and oxygen depletion is recommended.

290

My object is in storage.

Is the object considered "significant" for the collection? — Yes → Has the object been conserved and de-acidified if necessary? — No → Consider conserving the object prior to application of modified atmosphere storage. Acidic paper is a particular concern because it can lead to an accumulation of volatile acids and autocatalytic degradation.

Is the object considered "significant" for the collection? — No

Has the object been conserved and de-acidified if necessary? — Yes

What is the storage practice for the object in question?

Single object storage system

Compact, multi-object storage (e.g. Boxes, portfolios, plan chests)

Is the object a known endogenous pollutant emitter? — No → Will this object be displayed in the future? — No → Is the object in question prone to auto-oxidative degradation? — No

Is the object a known endogenous pollutant emitter? — Yes

Are most of the colorants in your object known? — Yes / No

Will this object be displayed in the future? — Yes

Is the object in question prone to auto-oxidative degradation? — Yes

In the absence of fugitive colorants, the substrate and binding media must be considered. Anoxia will limit the degradation of most organic materials, including the yellowing of papers. If anoxic frames are used then these objects can be displayed at higher light levels. MC frames offer another solution for micro climate control. In either case the potential for VOC accumulation must be addressed.

Opening and resealing a modified atmosphere storage is an involved process. Consider using a single object storage system for the object.

Accumulation of endogenous pollutants is the primary concern for this object.

Consider conducting a technical study of the object. The goal of this study can be to identify the primary colorants, but it can be as simple as identifying fugitive colorants *in situ* with a micro-fadeometer.

Are there fugitive colorants? — No / Yes

Modified atmosphere storage is not a priority for this object.

Modified atmosphere storage is not a priority for this object.

Modified atmosphere storage is not recommended. Consider other options including resealable MC systems with pollutant sorbents.

Does your object contain colorants that are known to undergo photo reductive fading? — Yes / No

The photo-reactivity of a colorant is complex and depends on many factors, but generally if a colorant is fugitive under ambient atmosphere it is undergoing a photo-oxidative process. Note that some organic colorants can undergo both photo-oxidative and photo-reductive colour changes. The presence of oxygen inhibits photo-reductive processes.

Single object storage in anoxic systems (display frames or hermetically sealed boxes) is a possibility for this object.